Advancements of interventional oncology treatments for early stage hepatocellular carcinoma

Hendriks, P.

ADVANCEMENTS OF INTERVENTIONAL ONCOLOGY TREATMENTS FOR EARLY STAGE HEPATOCELLULAR CARCINOMA

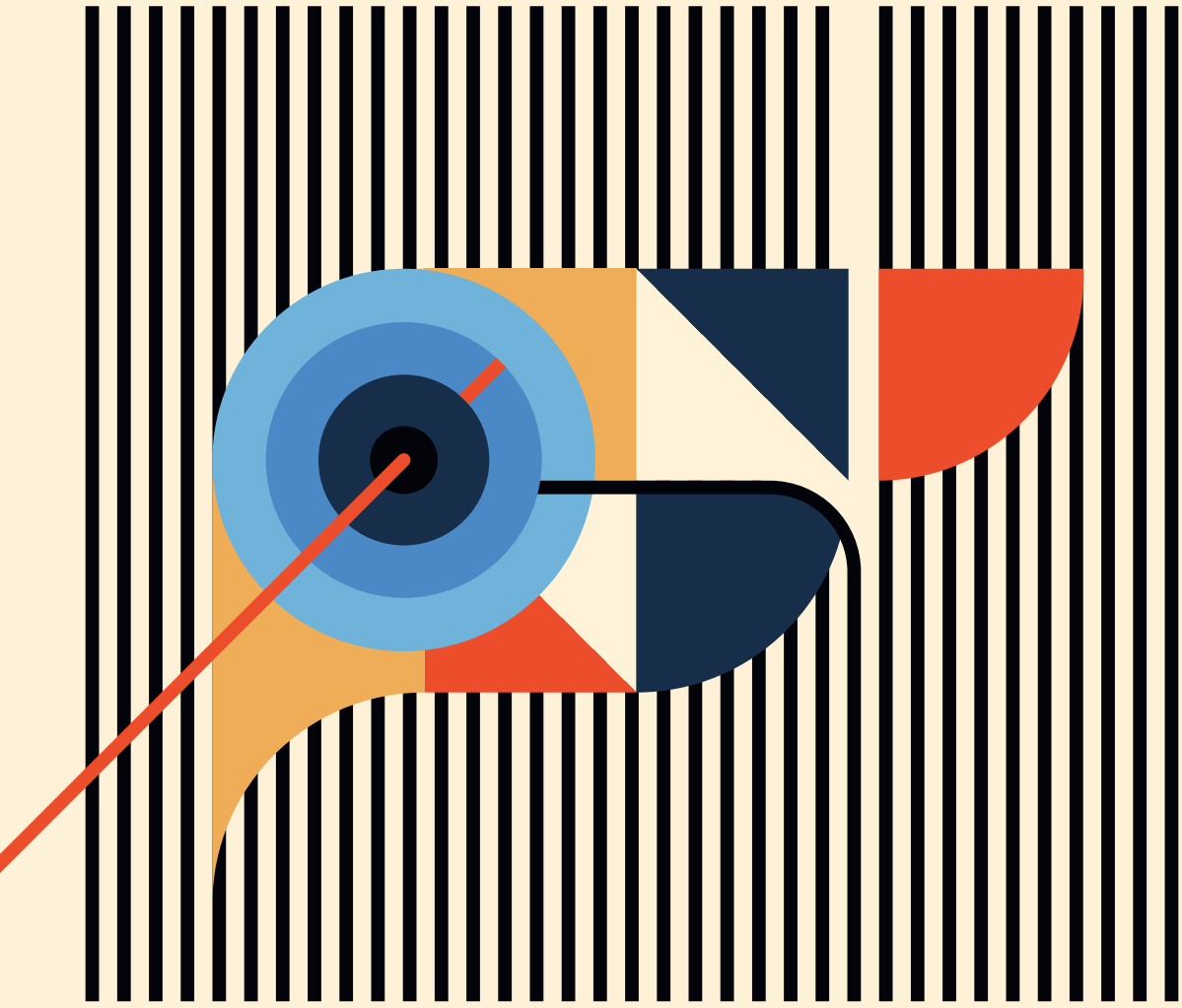

Pim Hendriks

ADVANCEMENTS OF INTERVENTIONAL ONCOLOGY TREATMENTS FOR EARLY STAGE HEPATOCELLULAR CARCINOMA

Pim Hendriks

The clinical studies presented in this thesis were performed at the department of Radiology of the Leiden University Medical Center, Leiden, The Netherlands and financially supported by Health~Holland, Maag-Lever-Darm Stichting (MLDS), Quirem Medical B.V. and Medtronic, Inc.

Publication of this thesis was financially supported by the Dutch Society of Interventional Radiology (NVIR) and Philips.

Cover design by: Stefan Prodanovic
Layout and design: Katie McGonigal | www.persoonlijkproefschrift.nl
Printing: Provided by thesis specialist Ridderprint | www.ridderprint.nl
ISBN: 978-94-6506-161-0

Advancements of interventional oncology treatments for early stage hepatocellular carcinoma

Proefschrift

ter verkrijging van

de graad van doctor aan de Universiteit Leiden,

op gezag van de rector magnificus prof.dr.ir. H. Bijl,

volgens besluit van het college voor promoties

te verdedigen op donderdag 5 september 2024

klokke 14.30 uur

door

Pim Hendriks

geboren te Vianen

in 1994

Promotores

Prof.dr. L.F. de Geus-Oei
Prof.dr. M.J. Coenraad

Co-promotor

dr. M.C. Burgmans

Leden promotiecommissie

Prof.dr. S. Osanto	
Prof.dr. M.G.E.H. Lam	University Medical Center Utrecht
Prof.dr. R. Bale	Medical University of Innsbruck (A)
dr. C.G. Overduin	Radboud University Medical Center, Nijmegen
Prof.dr. B. van Hoek	

TABLE OF CONTENTS

Chapter 1

General introduction and outline of thesis

HEPATOCELLULAR CARCINOMA

Hepatocellular carcinoma (HCC) is the most common primary malignancy of the liver, accounting for 75-80% of all liver cancers [1]. Liver cancer is the sixth most prevalent malignancy worldwide and ranks as the fourth leading cause of cancer-related death [2]. HCC typically arises in the context of chronic liver disease, primarily caused by hepatitis B or C virus infection, alcohol-related liver disease, or metabolic dysfunction-associated liver disease (former non-alcoholic fatty liver disease). Large geographical variation in incidence is observed, with the highest rates reported in Eastern Asia and Sub-Saharan countries and viral hepatitis as the most common etiology. In the Netherlands, the number of new HCC diagnoses in 2021 reached nearly 800, having doubled since 2008 [3], mainly due to an ageing population. Early diagnosis is challenging, as patients often remain asymptomatic until the disease has progressed to an advanced stage with limited treatment options left. However, screening programs for high-risk patients have led to earlier detection and improved outcomes [4].

The staging of HCC in the background of cirrhosis follows the Barcelona Clinic for Liver Cancer (BCLC) criteria [5]. Very early stage HCC (BCLC 0) refers to solitary lesions up to 2 cm. The treatment of choice for BCLC 0 is thermal ablation (TA) with curative intent. Early stage HCC (BCLC A) includes solitary lesions larger than 2 cm or up to 3 lesions of ≤3 cm each, and surgical resection or liver transplantation are generally considered as the treatments of first choice. However, due to portal hypertension caused by cirrhosis, patients may not be eligible for surgical resection. In such cases, depending on lesion size and location, thermal ablation, trans-arterial chemoembolization (TACE), transarterial radioembolization (TARE), or a combination of these therapies can be considered. Intermediate stage patients (BCLC B) have tumor load beyond early stage HCC, remaining confined to the liver. These patients are often treated with trans-arterial or systemic therapy. Patients with extra-hepatic metastases or macrovascular invasion are considered advanced stage (BCLC C) and are, according to the BCLC criteria, eligible for systemic treatment only.

Despite effective HCC treatments, the presence of underlying cirrhosis often leads to development of new intrahepatic lesions elsewhere in the liver [4]. For BCLC A-B patients meeting specific criteria, liver transplantation may be a suitable option [5]. Regardless the risks associated with this major treatment procedure, long-term clinical outcomes are good as it addresses both the underlying liver disease as well as the liver cancer.

Thermal ablation

Over the past decades, TA techniques, such as radiofrequency ablation (RFA) and microwave ablation (MWA), have emerged as effective alternatives to liver surgery. These minimally

invasive treatments are usually performed percutaneously under image guidance [6]. Both RFA and MWA induce tissue heating to at least 55-60 degrees Celsius to necrotize tumor tissue [7]. RFA uses a high-frequency monopolar alternating current leading to resistive heat propagation away from the active tip, resulting in ablation zones up to 4-5 cm. MWA, a more recent technique, employs microwaves to induce oscillation of water molecules for heat induction. Compared to RFA, it relies less on heat conduction, reaches higher temperatures, and is less susceptible to heat sinking by large blood vessels close to the ablation zone. The popularity of MWA has grown due to these advantages, although no significant difference in clinical outcome between the techniques has been reported in literature [8].

Ultrasound, CT or cone-beam CT can all be used for image guidance during needle positioning. While the patient is still under general anestheisa or conscious sedatation, a post-treatment contrast-enhanced CT scan is typically acquired to assess treatment success. In contrast to surgical treatment, technical success after thermal ablation cannot be determined by pathological assessment of the resected specimen. Therefore, a technically successful treatment has been defined as a full ablation of the entire lesion, with a 5 mm safety margin [6]. This margin assessment is usually performed by a side-to-side comparison of pre- and post-ablation cross-sectional images aided by 2D in-plane measurements. Additional ablation may be performed at the discretion of the physician if the margins are deemed insufficient. Despite these efforts the chances of developing local recurrences are generally considered to be higher when compared to surgical resection, for HCC lesions >2 cm [9].

Transarterial radioembolization

TARE is a minimally invasive treatment in which beta radiation-emitting microspheres are delivered trans-arterially to tumor bearing parts of the liver. Since TARE is administered arterially, the treatment makes use of the biological difference in tumor tissue perfusion (mostly arterial) versus parenchymal perfusion (mostly portal venous) [10]. Previous trials in which radioembolization was compared with systemic therapy in BCLC advanced stage HCC did not show overall survival benefit [11], but recent literature has shown that efficacy increases with personalized dosimetry, and beneficial use in earlier stages HCC [12].

Outline of thesis

This thesis aims to evaluate minimally invasive treatments for HCC, with a focus on ‘early stage’ HCC. Patients within this BCLC category are often not eligible for surgical treatment due to underlying liver cirrhosis with portal hypertension. Especially in tumors >3 cm precision ablation and optimized minimally invasive treatments are warranted as these tumors are prone to local recurrence after TA.

PART I of this thesis focuses on reproducibility of TA and ablation margins. *Chapter 2* compares two commercially available MWA devices at different settings in a controlled, ex-vivo environment, evaluating the size and sphericity of their ablation zones. *Chapter 3* presents a systematic review of the available evidence concerning ablation margin quantification in TA, in which recent literature regarding image processing techniques for ablation margin quantification after TA is reviewed. *Chapter 4* is a retrospective study correlating local tumor progression with quantified ablation margins after TA of HCC, using commercially available software based on a non-rigid registration algorithm. *Chapter 5* presents a prospective study evaluating the feasibility of intraprocedural ablation margin quantification using in-house developed software and an optimized pre- and post-ablation CT scanning protocol.

PART II of this thesis explores treatment combinations within early stage HCC. As local recurrence rates after TA increase with lesion size, TA is combined with a transarterial treatment in HCC lesions >3 cm to increase the treatment efficacy. *Chapter 6* evaluates a historic cohort of HCC patients treated with TA and TACE. *Chapter 7* outlines the clinical study protocol of the HORA EST HCC study, in which RFA is combined with adjuvant TARE using holmium-166 microspheres. A dose-escalation study protocol for adjuvant TARE is used to determine the administration dose of holmium-166. The results of this trial are presented in *Chapter 8*.

PART III of this thesis evaluates clinical outcomes of TARE treatment for HCC beyond early stage HCC, where TARE is mainly applied in intermediate or advanced stage HCC. A retrospective cohort of 85 patients in three hospitals was evaluated in respect of clinical outcomes and radioembolization induced liver disease in *Chapter 9*.

Finally, *Chapter 10* provides a summary, general discussion and future perspectives. In *Chapter 11* a Dutch summary can be found.

REFERENCES

[1] Singal AG, Lampertico P, Nahon P. Epidemiology and surveillance for hepatocellular carcinoma: New trends. Journal of Hepatology 2020;72:250-261.

[2] Sung H, Ferlay J, Siegel RL, Laversanne M, Soerjomataram I, Jemal A, et al. Global Cancer Statistics 2020: GLOBOCAN Estimates of Incidence and Mortality Worldwide for 36 Cancers in 185 Countries. CA: A Cancer Journal for Clinicians 2021;71:209-249.

[3] Netherlands Comprehensive Cancer Organization (IKNL). Netherlands Cancer Registry (NCR). [cited 2023 30-07]; Available from: https://iknl.nl/nkr-cijfers

[4] Galle PR, Forner A, Llovet JM, Mazzaferro V, Piscaglia F, Raoul J-L, et al. EASL clinical practice guidelines: management of hepatocellular carcinoma. Journal of hepatology 2018;69:182-236.

[5] Reig M, Forner A, Rimola J, Ferrer-Fàbrega J, Burrel M, Garcia-Criado Á, et al. BCLC strategy for prognosis prediction and treatment recommendation: The 2022 update. J Hepatol 2022;76:681-693.

[6] Crocetti L, de Baére T, Pereira PL, Tarantino FP. CIRSE Standards of Practice on Thermal Ablation of Liver Tumours. Cardiovasc Intervent Radiol 2020;43:951-962.

[7] Ahmed M, Solbiati L, Brace CL, Breen DJ, Callstrom MR, Charboneau JW, et al. Image-guided tumor ablation: standardization of terminology and reporting criteria--a 10-year update. Radiology 2014;273:241-260.

[8] Facciorusso A, Di Maso M, Muscatiello N. Microwave ablation versus radiofrequency ablation for the treatment of hepatocellular carcinoma: A systematic review and meta-analysis. Int J Hyperthermia 2016;32:339-344.

[9] Xu X-L, Liu X-D, Liang M, Luo B-M. Radiofrequency Ablation versus Hepatic Resection for Small Hepatocellular Carcinoma: Systematic Review of Randomized Controlled Trials with Meta-Analysis and Trial Sequential Analysis. Radiology 2018;287:461-472.

[10] Miller FH, Vendrami CL, Gabr A, Horowitz JM, Kelahan LC, Riaz A, et al. Evolution of Radioembolization in Treatment of Hepatocellular Carcinoma: A Pictorial Review. RadioGraphics 2021;41:1802-1818.

[11] Vilgrain V, Pereira H, Assenat E, Guiu B, Ilonca AD, Pageaux G-P, et al. Efficacy and safety of selective internal radiotherapy with yttrium-90 resin microspheres compared with sorafenib in locally advanced and inoperable hepatocellular carcinoma (SARAH): an open-label randomised controlled phase 3 trial. The Lancet Oncology 2017;18:1624-1636.

[12] Salem R, Padia SA, Lam M, Chiesa C, Haste P, Sangro B, et al. Clinical, dosimetric, and reporting considerations for Y-90 glass microspheres in hepatocellular carcinoma: updated 2022 recommendations from an international multidisciplinary working group. Eur J Nucl Med Mol Imaging 2023;50:328-343.

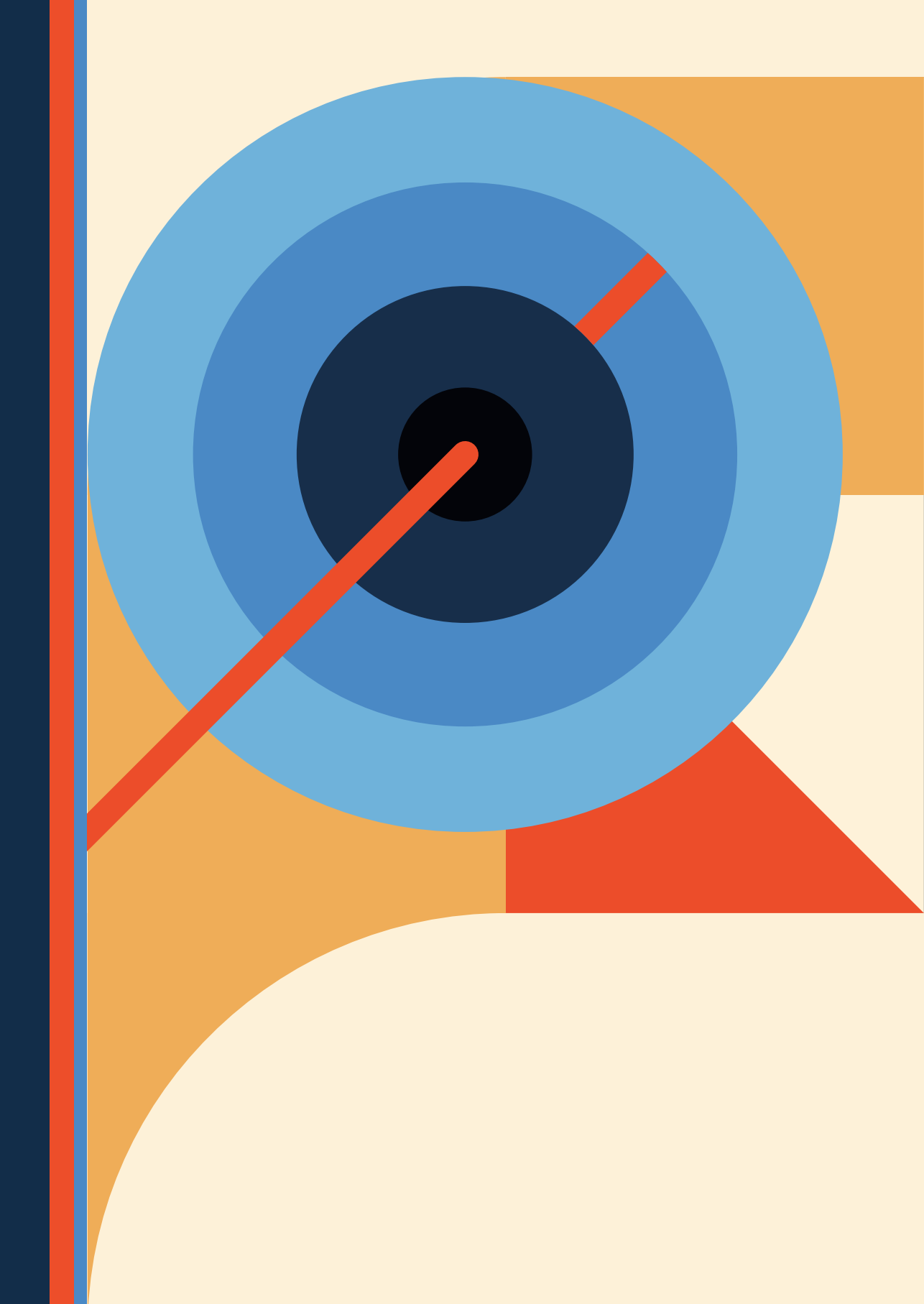

Part 1:

Thermal ablation: reproducibility and ablation margins

Chapter 2

Performance of the Emprint and Amica microwave ablation systems in ex-vivo porcine livers: sphericity and reproducibility versus size

Authors

P. Hendriks, W. E. M. Berkhout, C. I. Kaanen, J. H. Sluijter, I. J. Visser, J. J. van den Dobbelsteen, L. F. de Geus-Oei, A. G. Webb & M. C. Burgmans

Published

CardioVascular and Interventional Radiology, 2021; 44:952–958, *DOI: 10.1007/s00270-020-02742-9*

Supplementary materials

https://doi.org/10.1007/s00270-020-02742-9

ABSTRACT

Purpose To investigate the performance of two microwave ablation (MWA) systems regarding ablation volume, ablation shape and variability.

Materials and methods In this ex-vivo study, the Emprint and Amica MWA systems were used to ablate porcine livers at 4 different settings of time and power (3 and 5 minutes at 60 and 80 Watt). In total, 48 ablations were analysed for ablation size and shape using Vitrea Advanced Visualization software after acquisition of a 7T MRI scan.

Results Emprint ablations were smaller (11,1 vs 21,1 mL $p<0.001$), more spherical (sphericity index of 0.89 vs 0.59 $p<0.001$) and showed less variability than Amica ablations. In both systems, longer ablation time and higher power resulted in significantly larger ablation volumes.

Conclusion Emprint ablations were more spherical and the results showed a lower variability than those of Amica ablations. This comes at the price of smaller ablation volumes.

Keywords: Microwave ablation; Amica; Emprint; Ablation volume; sphericity; variability

INTRODUCTION

Thermal ablation has become a widely accepted treatment modality for liver malignancies. In both primary and secondary liver tumors thermal ablation is an effective, less invasive alternative to surgical resection of small lesions [1, 2]. Radiofrequency ablation (RFA) has been the most widely used thermal ablation technique, but microwave ablation (MWA) has rapidly gained popularity in recent years [3, 4].

Instead of using an electrical current, MWA uses an electromagnetic field at high frequencies that cause dielectric hysteresis, which results in tissue heating [5, 6]. As a result, MWA is associated with higher temperatures, larger ablation zones in a shorter time, and a lower susceptibility to properties of the surrounding tissue, in comparison with RFA [3, 7]. Propagation through (cirrhotic) tissue with a high impedance and heat sink effects in ablations near intrahepatic vessels are therefore less of an issue [6, 7]. Moreover, MWA does not require grounding pads, which reduces the chance of skin burns [8].

Nevertheless, MWA has certain disadvantages. The shape of MWA ablation zones has been described as being elliptical rather than spherical, compared with RFA [5]. Also, the size and shape of the coagulation necrosis tends to be less predictable using MWA [5]. Yet, predictability is of great importance to achieve favourable outcomes.

Local recurrence is the most common adverse event after thermal ablation, but oncological outcomes comparable to surgical resection can be achieved with the use of advanced planning and navigation tools [9, 10], Highly sophisticated navigation software and robot-assistance are now at the hand of interventional radiologists to optimise planning and guide needle placement [11, 12]. These tools make use of modelling techniques for which predictability of ablation shape and volume is a prerequisite. Ablation systems have predefined algorithms to predict the size and shape of the ablation and manufacturers provide reference values for ablations at different settings. In practice however, these theoretical reference values deviate from actual dimensions of the coagulated tissue [13]. These deviations and lack of predictability currently hamper optimal use of treatment planning tools.

New microwave systems have been introduced trying to produce more spherical ablations and to overcome the issue of unpredictability. The Emprint ablation system (Covidien/ Medtronic, Minneapolis, USA) is a new generation microwave system that uses so called thermosphere technology to control the microwave field and length of the microwaves. This techniques combines thermal control by a cooling system that runs to the tip of the antenna with field shape and wavelength control [14]. It is claimed by the vendor that

this new technology allows for more spherical and more predictable ablations. Although retrospective clinical cohort studies provide moderate evidence to these claims, there is a lack of studies comparing this newer ablation system with older generation microwave systems in a controlled setting [13].

To investigate and compare the performances of the Emprint ablation system, we conducted an ex vivo study with standardized needle placement in non-perfused, healthy porcine livers. An ex-vivo study protocol was used to limit the influence of factors unrelated to the design and technology of the MWA systems. In a clinical setting, the geometry of the coagulation necrosis area would also be influenced by factors such as (adjustments in) needle position, hemodynamics and heat-sink, tumor heterogeneity and/or capsule, cirrhosis/fibrosis etcetera. The performance of the Emprint system was compared with the Amica microwave system (HS Hospital Service, Rome, Italy), as this system is widely used and has been studied extensively in both in-vivo as well as ex-vivo studies [13]. The purpose of this experimental study was to investigate and compare the performance of these two systems regarding sphericity, reproducibility and ablation size.

MATERIALS AND METHODS

In this ex-vivo animal study 25 porcine livers were used. The livers were obtained at the abattoir and immediately stored in 0.9% NaCl solution at 5 degrees Celsius.

Microwave ablation systems

The first system used was the Emprint Ablation System with a generator with a maximum of 100W at a frequency of 2.45 GHz. The second system was an Amica system powered by a HS-Amica-Gen (AGN-H-1.0) generator with a maximum output of 140 W, also at a frequency of 2.45 GHz. Both systems use a perfusion cooled antenna and a flexible coaxial cable. A 150 mm 14- and 11-gauge antenna were used for Amica and Emprint, respectively. There was no involvement of both manufacturers in this study.

Ablation protocol

Each porcine liver was divided into four parts, representing the four largest porcine liver lobes (left/right medial and lateral lobes). The lobar size had to exceed the expected ablation area by at least 5 mm on all sides (expected ablation sizes as derived from the manufacturer guidelines). Each liver lobe was positioned in a plastic box, fixated by placing additional plastic bars for an upright position, as shown in the schematic representation in figure 1a.

A horizontal MWA antenna insertion point was chosen at half the height and width of the liver lobe, with a minimal insertion of 60 mm. The antenna positioning is shown in figure 1b. A stable position of the antenna was ensured by fixation of the handle bar during ablation.

For both systems, ablations were performed at 4 different settings; alternating between 3 and 5 minutes of ablation time at both 60 and 80 Watt. An ablation was considered suitable for analysis if the intended ablation time was completed successfully, the ablation did not extend to the surface of the liver and MRI images were free of metal artefacts.

A total of 69 ablations were performed, of which 21 were excluded due to MRI artefacts (n=14), ablation zones that reached the liver surface (n=6), or an error in the cooling system (n=1). Finally, 48 successful ablations were available for analysis: 6 for each setting and for each system.

Assessment of ablation size and geometry

In order to obtain volumetric data on the ablation necrosis, Magnetic Resonance Imaging (MRI) was performed on all ablated liver lobes using a 7 Tesla MRI system (Achieva, Philips Healthcare, Best, The Netherlands) with a quadrature transmit head coil and 32-channel receive coil (Nova Medical). A 3D T1-weighted gradient echo sequences was used with isotropic voxels of 1 mm (repetition time (TR) 4.19 ms, echo time (TE) 1.97 ms, flip angle 7°, field-of-view 200 x 200 x 200 mm, data matrix 200 x 200 x 200, 78% elliptical k-space coverage, radiofrequency spoiling between successive excitations, SENSE factor 2 in left-right direction).

Image processing was performed in Vitrea Advanced Visualization software (Vital Images, Minnetonka, USA) to evaluate the size and shape of each ablation. Ablation size was measured in millilitres (mL) and derived from the images using a semi-automated segmentation tool with adaptive thresholding. The ablation diameter was recorded in three axes, as shown in figure 2: a long axis diameter (LAD) in plane with the needle insertion axis and two orthogonal short axis diameters (SAD). The sphericity index (SI) was defined as the ratio between those diameters $\frac{SAD_1+SAD_2}{2LAD}$. An SI of 1 therefore denotes a perfectly spherical ablation, whereas a lower SI means that the ablation shape is more elliptical. Imaging parameters were acquired blinded from system and settings.

Statistical analysis

The performance of the two MWA systems was statistically analysed in terms of ablation volume and sphericity index. Statistical analyses were performed using IBM SPSS Statistics 25. Descriptive statistics were calculated for the outcomes of the different systems at the different settings, in terms of ablation time and power. The systems were compared using

the unpaired T-test for normal distributed data or the Mann-Whitney U test for non-normally distributed data. Two-way analysis of variance (ANOVA) was conducted to test for differences in ablation volume and sphericity index between different ablation settings within one system. Three-way ANOVA was performed to test for differences in ablation volume and sphericity between both MWA systems in terms of time and power-settings. Normality of data was tested using skewness and kurtosis. Levene's test was used to test for equal variances, and a 95% confidence interval was used.

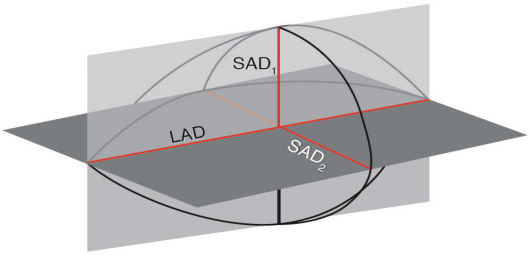

Figure 2 *Short axes diameters (SAD_1 and SAD_2) and long axis diameter (LAD) of the ablation zone.*

RESULTS

An example of the post-ablation liver MRI can be found in figure 3. Table 1 shows the median ablation volume for the 48 ablations. Amica ablations were significantly larger than Emprint ablation ($p<0.001$), with a median ablation volume of 21.1 mL vs 11.1 mL. Figure 4 shows all individual ablation volumes per setting. For all settings, the range of ablation volumes was smaller for Emprint ablations compared to ablations produced with the Amica system (table 1 & figure 4).

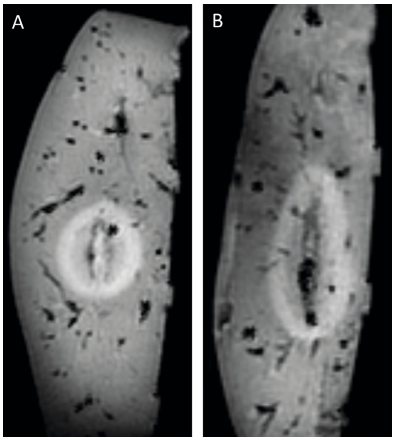

Figure 3 *Sagittal MRI of ex-vivo porcine livers after ablation.* **A:** *Ablation zone after Emprint ablation of 3 minutes at 80W.* **B:** *Ablation zone of Amica ablation of 3 minutes at 80W.*

Table 1 *Ablation volume for each setting and system.*

	Emprint (n = 24)		Amica (n = 24)	
Settings	**Median volume (mL)**	**(Range)**	**Median volume (mL)**	**(Range)**
3 min, 60 W	7.0	(6.1 – 7.5)	15.1	(9.4 - 19.3)
3 min, 80 W	10.3	(7.6 – 12.4)	20.5	(13.4 - 34.7)
5 min, 60 W	13.2	(10.3 – 14.7)	21.7	(17.2 - 32.1)
5 min, 80 W	18.1	(11.5 – 21.5)	31.7	(24.3 - 44.7)
Total	*11.1*	*(6.1 – 21.5)*	*21.1*	*(9.4 - 44.7)*

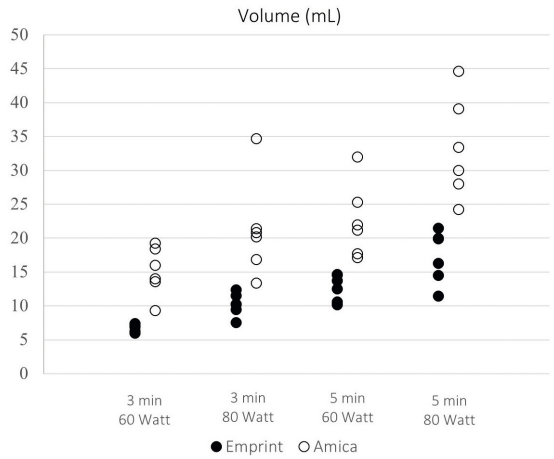

Figure 4 *Each individual ablation volume per setting and system.*

Amica ablation volumes were significantly influenced by both ablation time (p=0.001) and ablation power (p=0.003). No interaction between those factors was revealed in two-way ANOVA analysis. The same results were found for Emprint ablation volume with p-values of p<0.001 for both ablation time and power.

Table 2 shows the median of the long axis and short axes diameters for different ablation settings. All individual measurements are plotted in figure 5. Long axis diameters were non-normally distributed. Mann Whitney U statistics showed that the LAD was significantly larger for Amica ablations (p<0.001). SADs did not significantly differ between the two systems. For all settings, there was a wider range of both LAD and SAD measurements for the Amica system compared to the Emprint system.

The SI of Emprint was significantly higher ($p<0.001$), as can be seen in table 3. Figure 6 shows the SI of each measurement.

In supplementary figure 1 the ablation dimensions are plotted with respect to the manufacturers' reference values.

Table 2 *Median long axis and short axes diameters for each setting and system.*

	Emprint (n = 24)				Amica (n = 24)			
	Long axis diameter (mm)		Short axes diameter (mm)		Long axis diameter (mm)		Short axes diameter (mm)	
Settings	**Median**	**(Range)**	**Median**	**(Range)**	**Median**	**(Range)**	**Median**	**(Range)**
3 min, 60 W	25.4	(21.4 – 27.3)	22.2	(19.4 – 24.8)	45.0	(39.0 – 51.9)	25.4	(19.1 – 28.4)
3 min, 80 W	30.6	(26.7 – 33.3)	25.5	(20.5 – 27.7)	53.1	(49.7 – 71.0)	28.1	(20.2 – 35.8)
5 min, 60 W	30.1	(28.0 – 31.9)	28.2	(24.6 – 31.0)	53.8	(23.4 – 60.5)	29.0	(24.1 – 47.0)
5 min, 80 W	33.9	(30.8 – 34.7)	30.1	(25.7 – 33.3)	57.0	(50.5 – 62.2)	32.9	(25.4 – 41.4)
Total	*30.4*	*(21.4 – 34.7)*	*26.7*	*(19.4 – 33.3)*	*52.5*	*(39.0 – 71.0)*	*28.2*	*(19.1 – 47.0)*

Table 3 *Sphericity index for the Emprint and Amica system at different settings.*

	Emprint (n = 24)		Amica (n = 24)	
Settings	**Mean sphericity index**	**(Range)**	**Mean sphericity index**	**(Range)**
3 min, 60 W	0.90	(0.85 – 1.02)	0.55	(0.52 -0.60)
3 min, 80 W	0.83	(0.75 – 0.97)	0.49	(0.44 – 0.52)
5 min, 60 W	0.93	(0.90 – 0.98)	0.71	(0.44 – 1.57)
5 min, 80 W	0.91	(0.86 – 0.95)	0.59	(0.46 -0.74)
Total	*0.89*	*(0.75 -1.02)*	*0.59*	*(0.44 – 1.57)*

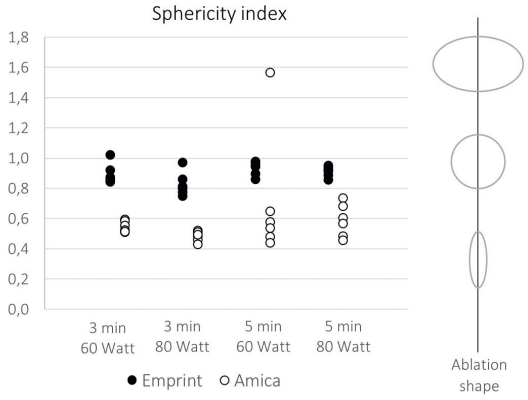

Figure 6 *Sphericity index of the ablation zone for the Emprint and Amica system at different settings.*

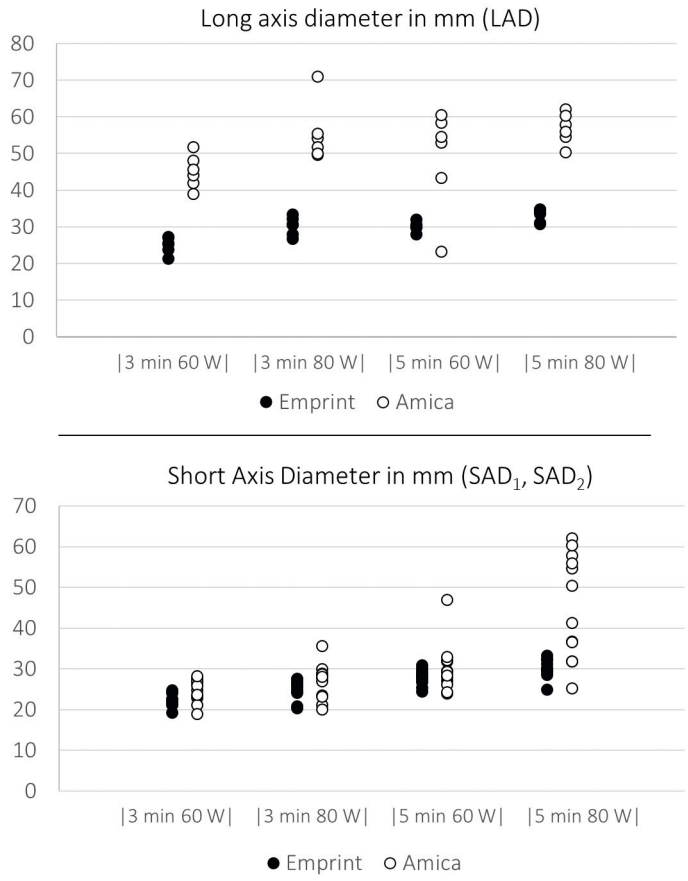

Figure 5 *Ablation axis sizes for all individual ablations per setting and system:* **A***) long axis diameter (LAD) were measured along the MWA antenna and* **B***) short axes diameters (SAD_1 and SAD_2) were measured orthogonal to the LAD.*

DISCUSSION

In this study in ex-vivo porcine livers, the Emprint ablation system created more reproducible ablation zones compared to the Amica system. The variation in repeated measurements for volume, LAD and SAD where smaller for the Emprint ablations. In addition, the Emprint ablation resulted in more consistent spherical ablations. As most liver malignancies tend to be rather spherical, this may be desirable in clinical practice. In larger tumors the Amica system may offer an advantage. Especially due to a larger LAD (mean of 52.5 mm versus 30.4 mm for the Emprint system), Amica ablations were significantly larger. The lower variability and higher sphericity of the Emprint system thus seem to come at the expense of ablations size.

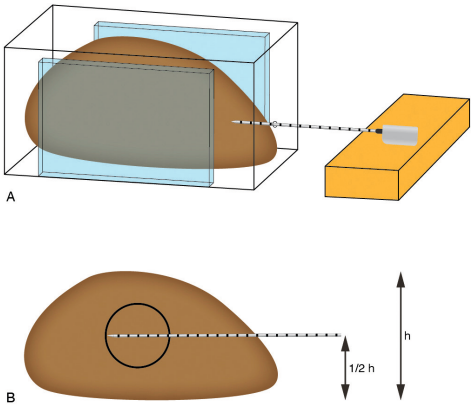

Figure 1 *Experimental ablation setup. The liver lobe is fixated within a plastic container with an antenna placed in the horizontal and vertical center.*

Although no previous results are available for ex-vivo Emprint ablations, our study is consistent with previously published studies with respect to Amica ablations. Amabile et al. performed Amica ablations in an in vivo porcine and ex-vivo bovine study and found sphericity indices comparable to our study: 0.59 and 0.62 for 5 minutes ablation at 60W and 80W, respectively in the in-vivo porcine model. This was 0.70 and 0.72 for the ex-vivo bovine ablations at similar ablation parameters. (compared to 0.71 and 0.59, respectively, in our study) [15]. Also Hoffmann et al. reported similar results to ours for AMICA ablation volume and SAD (22.2 mL and 30.5 mm vs 21.7 mL and 29.0 mm in our study with ablation settings of 5 min at 60 W) [16]. Our ex-vivo findings also match reported clinical outcomes. Vogl et al. retrospectively analysed cross-sectional images of patients that underwent ablation with either an Amica or Emprint system [17]. Similar to our findings, they showed that Amica ablation volumes were larger (51.9 mm^3 vs 33.0 mm^3) and less spherical (SI=0.686 vs. SI=0.865). In another study by Zaidi et al., including 53 patients treated with laparoscopic ablation with the Emprint system, 'roundness indices' were found to be 0.9, 1.0 and 1.1 in three different dimensions [18]. Head to head comparison of the two systems in a controlled environment has not been reported on previously.

The size and shape of ablation necrosis heavily depend on the propagation of heat through tissue. The complexity of heat conductivity can be reduced to the effects evaluated by the bioheat equation, which includes tissue properties, thermal conductivity, the rate at which heat is applied, and the heat loss (e.g. due to heat sink effect) [19]. Tissue properties are of high influence on the transmission of electromagnetic energy, due to their large effect on dielectric permittivity [19]. Porcine liver tissue has been shown to be suitable for simulating microwave energy distribution in healthy or tumorous liver tissue [20]. Earlier simulations

with RFA revealed potential influences of fatty liver tissue on ablation volumes up to 27% and even 36% for cirrhotic liver tissue [21]. In theory, these rates should be lower for MWA than for RFA as MWA is less dependent on heat conductivity. Nevertheless, in practice the unpredictability of MWA systems has been an important limitation with earlier systems. Based on our study, this limitation has partly been overcome with the Emprint thermosphere technology. This makes it a more feasible system to use for precise treatment planning.

Emprint uses thermosphere technology that focuses on creating spherical ablation zones by thermal control, field control and wavelength control [14]. The antenna of Emprint is cooled all the way to the tip, which prevents undesired heating of surrounding tissue and aids in maintenance of a constant field and wavelength despite changing tissue (hydration properties) [22].

A newer Amica generator which has not been used in the current research offers the ability of pulsed ablations, striving for more spherical ablations as well. No results with respect to sphericity were found for this specific new system in literature yet. However, in earlier research the effect of pulsed microwave ablation from another system was described as reaching a similar ablation volumes at lower power, with limited differences in ablation shape when compared to non-pulsed MWA [23].

Despite the ex-vivo character of this study, we chose to obtain our primary volumetric parameters by imaging analysis rather than histological analysis. In this way, we were able to perform accurate volumetric calculations and determine dimensions in a uniform way without risks of tissue deformation during sectioning.

There are several limitations of this study. First of all, ablations were performed in unperfused healthy porcine livers. The performance of the ablation systems used in this study may be different in clinical practice. Secondly, two different systems were used with each their own specifications. Therefore, a head-to-head comparison is not applicable to the full extent i.e. no similar ablation size and volume were expected at similar settings of both systems. For both systems, different needle diameters are available. In this study, only 1 needle diameter was used for each system (14- and 11-gauge antenna were used for Amica and Emprint, respectively). Lastly, only two ablation systems were compared at a limited number of settings. In practice, more combinations in ablation time and power are expected to be used.

In conclusion, the Emprint system with thermosphere technology allows thermal ablation with greater reproducibility and more spherical ablations compared to the Amica system, in this ex-vivo porcine study. This comes at the expense of smaller ablation volumes.

REFERENCES

[1] Van Cutsem E, Cervantes A, Adam R, et al. ESMO consensus guidelines for the management of patients with metastatic colorectal cancer. Annals of Oncology 2016; 27:1386-422.

[2] EASL Clinical Practice Guidelines: Management of hepatocellular carcinoma. Journal of Hepatology 2018; 69:182-236.

[3] Nault J-C, Sutter O, Nahon P, Ganne-Carrié N, Séror O. Percutaneous treatment of hepatocellular carcinoma: State of the art and innovations. Journal of Hepatology 2018; 68:783-97.

[4] Poggi G, Tosoratti N, Montagna B, Picchi C. Microwave ablation of hepatocellular carcinoma. World J Hepatol 2015; 7:2578-89.

[5] Lubner MG, Brace CL, Hinshaw JL, Lee FT. Microwave Tumor Ablation: Mechanism of Action, Clinical Results, and Devices. Journal of Vascular and Interventional Radiology 2010; 21:S192-S203.

[6] Salati U, Barry A, Chou FY, Ma R, Liu DM. State of the ablation nation: a review of ablative therapies for cure in the treatment of hepatocellular carcinoma. Future Oncology 2017; 13:1437-48.

[7] Kim C. Understanding the nuances of microwave ablation for more accurate post-treatment assessment. Future Oncology 2018; 14:1755-64.

[8] Huffman SD, Huffman NP, Lewandowski RJ, Brown DB. Radiofrequency ablation complicated by skin burn. Semin Intervent Radiol 2011; 28:179-82.

[9] Hori T, Nagata K, Hasuike S, et al. Risk factors for the local recurrence of hepatocellular carcinoma after a single session of percutaneous radiofrequency ablation. Journal of Gastroenterology 2003; 38:977-81.

[10] Tanis E, Nordlinger B, Mauer M, et al. Local recurrence rates after radiofrequency ablation or resection of colorectal liver metastases. Analysis of the European Organisation for Research and Treatment of Cancer #40004 and #40983. European journal of cancer (Oxford, England : 1990) 2014; 50:912-9.

[11] Beermann M, Lindeberg J, Engstrand J, et al. 1000 consecutive ablation sessions in the era of computer assisted image guidance - Lessons learned. European journal of radiology open 2019; 6:1-8.

[12] Solbiati M, Muglia R, Goldberg SN, et al. A novel software platform for volumetric assessment of ablation completeness. International Journal of Hyperthermia 2019; 36:336-42.

[13] Ruiter SJS, Heerink WJ, de Jong KP. Liver microwave ablation: a systematic review of various FDA-approved systems. European Radiology 2019; 29:4026-35.

[14] Alonzo M, Bos A, Bennett S, Ferral H. The Emprint™ Ablation System with Thermosphere™ Technology: One of the Newer Next-Generation Microwave Ablation Technologies. Semin Intervent Radiol 2015; 32:335-8.

[15] Amabile C, Ahmed M, Solbiati L, et al. Microwave ablation of primary and secondary liver tumours: ex vivo, in vivo, and clinical characterisation. International Journal of Hyperthermia 2017; 33:34-42.

[16] Hoffmann R, Rempp H, Erhard L, et al. Comparison of four microwave ablation devices: an experimental study in ex vivo bovine liver. Radiology 2013; 268:89-97.

[17] Vogl TJ, Basten LM, Nour-Eldin N-EA, et al. Evaluation of microwave ablation of liver malignancy with enabled constant spatial energy control to achieve a predictable spherical ablation zone. International Journal of Hyperthermia 2018; 34:492-500.

[18] Zaidi N, Okoh A, Yigitbas H, Yazici P, Ali N, Berber E. Laparoscopic microwave thermosphere ablation of malignant liver tumors: An analysis of 53 cases. Journal of surgical oncology 2016; 113:130-4.

[19] Brace CL. Microwave tissue ablation: biophysics, technology, and applications. Crit Rev Biomed Eng 2010; 38:65-78.

[20] Stauffer PR, Rossetto F, Prakash M, Neuman DG, Lee T. Phantom and animal tissues for modelling the electrical properties of human liver. International journal of hyperthermia : the official journal of European Society for Hyperthermic Oncology, North American Hyperthermia Group 2003; 19:89-101.

[21] Deshazer G, Merck D, Hagmann M, Dupuy DE, Prakash P. Physical modeling of microwave ablation zone clinical margin variance. Medical physics 2016; 43:1764-.

[22] Brace CL. Microwave Ablation Technology: What Every User Should Know. Current Problems in Diagnostic Radiology 2009; 38:61-7.

[23] Bedoya M, del Rio AM, Chiang J, Brace CL. Microwave ablation energy delivery: Influence of power pulsing on ablation results in an ex vivo and in vivo liver model. Medical Physics 2014; 41:123301.

Chapter 3

Ablation margin quantification after thermal ablation of malignant liver tumors: how to optimize the procedure? A systematic review of the available evidence.

Authors

*Pim Hendriks**, Fleur Boel*, Timo TM Oosterveer, Alexander Broersen, Lioe-Fee de Geus-Oei, Jouke Dijkstra, Mark C Burgmans

*Shared first authorship

Published

European Journal of Radiology Open, 2023; 11,
DOI: 10.1016/j.ejro.2023.100501

Supplementary materials

https://doi.org/10.1016/j.ejro.2023.100501

ABSTRACT

Introduction To minimize the risk of local tumor progression rates after thermal ablation of liver malignancies, complete tumor ablation with sufficient ablation margins is a prerequisite. This has resulted in ablation margin quantification to become a rapidly evolving field. The aim of this systematic review is to give an overview of the available literature with respect to clinical studies and technical aspects potentially influencing the interpretation and evaluation of ablation margins.

Methods The Medline database was reviewed for studies on radiofrequency and microwave ablation of liver cancer, ablation margins, image processing and tissue shrinkage. Studies included in this systematic review were analyzed for qualitative and quantitative assessment methods of ablation margins, segmentation and co-registration methods, and the potential influence of tissue shrinkage occurring during thermal ablation.

Results 75 articles were included of which 58 were clinical studies. In most clinical studies the aimed minimal ablation margin (MAM) was ≥5 mm. In 10/31 studies, MAM quantification was performed in 3D rather than in three orthogonal image planes. Segmentations were performed either semi-automatically or manually. Rigid and non-rigid co-registration algorithms were used about as often. Tissue shrinkage rates ranged from 7% to 74%.

Conclusions There is a high variability in ablation margin quantification methods. Prospectively obtained data and a validated robust workflow are needed to better understand the clinical value. Interpretation of quantified ablation margins may be influenced by tissue shrinkage, as this may cause underestimation.

Keywords: thermal ablation; RFA; MWA; ablation margin quantification; image co-registration; tissue shrinkage

INTRODUCTION

Thermal ablation is an effective treatment for primary and secondary liver tumors [1-3]. For tumors of limited size (≤2cm) thermal ablation using radiofrequency ablation (RFA) or microwave ablation (MWA) is a first line therapy, particularly in patients with co-morbidity, underlying liver cirrhosis and/or centrally located tumors. Nevertheless, surgical resection is generally considered to be more effective, as thermal ablation is associated with higher local tumor progression (LTP) rates. To minimize the risk of LTP after thermal ablation, complete tumor ablation with sufficient ablation margins is essential. The correlation between ablation margins and LTP was first demonstrated in 2008 by Kei et al. [4]. Later, this was confirmed by other large trials [5-7].

Most commonly, ablation margins after thermal ablation are assessed by side-by-side comparison of pre- and post-ablation cross-sectional images. This method is usually based on visual assessment, i.e. eye-balling, but may be aided by two-dimensional measurements using anatomical landmarks on both scans. The use of software-assisted quantitative assessment of ablation margins has gained interest in literature over the last years [6-9]. Several studies indicate it could contribute to better determine technical success of thermal ablation treatments and estimate the risk of LTP [7-9]. However, there is wide variation in methods used for margin quantification and the optimal method has not yet been established.

Ablation margin quantification is performed using software with specific segmentation and image co-registration algorithms. The co-registration algorithms may differ by design as co-registration can be performed either in a rigid or non-rigid way. In rigid co-registration, the images are registered using only rotation and translation of the images whereas non-rigid co-registration also allows deformation of the images. Besides the differences between rigid and non-rigid co-registration, the co-registration could be performed manually, semi-automatically or fully automatically. Other differences may be with respect to volume of interest selection or usage of landmarks.

Besides the more technical variety among co-registration algorithms, patient and treatment related factors may affect the result of ablation margin quantification. Differences in respiration mode and patient positioning may cause considerable variation in the shape and position of the liver between the pre- and post-ablation scans. Moreover, tissue shrinkage as a direct result of tissue heating possesses an important challenge on ablation margin interpretation [10]. As the ablated tissue tends to shrink during thermal ablation, the ablation margins may be underestimated. Unfortunately, the degree and direction of tissue shrinkage is unpredictable [10].

Quantitative ablation margin assessment holds great promise as a tool to better predict patients at risk for LTP after thermal ablation. The aim of this systematic review is to create an overview of the current evidence with respect to qualitative and quantitative evaluation methods of ablation margins, image processing tools, and the potential influence of tissue shrinkage occurring during thermal ablation.

METHODS

Search strategy

The electronic database Medline was searched on 01/02/2021 for all studies describing "image segmentation", "image registration", "ablation margins", "treatment success" or "tissue shrinkage" during treatment of liver tumors using thermal ablation techniques, i.e. "RFA" or "MWA", since 01/01/2009 as techniques have constantly been improving and the quality of ablation of >12 years old was not considered representative. The full search term used can be found in Appendix A. Articles were sequentially evaluated based on title, abstract and full text for meeting all in- and exclusion criteria. The literature search, study selection, data extraction and study quality assessment were independently conducted by two reviewers (P.H. and F.B.). Any disagreements were resolved in consensus.

Exclusion criteria

Articles were excluded if they did not relate to percutaneous thermal ablation of malignant liver tumors with RFA or MWA; if surgical resection was performed; and if the aim of the article was to evaluate combination therapy with ablation and trans-arterial or systemic therapy. Articles related to liver segmentation or co-registration were excluded if they did not define the segmentation or co-registration method used; and if ultrasound (US), positron emission tomography (PET), or single photon emission computed tomography (SPECT) images were used for image segmentation or co-registration. Articles using hybrid imaging modalities were not excluded if tumor and/or ablation zone segmentation was performed using (contrast-enhanced) CT or MRI. Articles related to evaluation of ablation margins were excluded if they did not provide a definition for technical success or minimal ablation margins. Finally, systematic reviews, reviews, letters to the editor, conference abstracts and full-text articles in other languages than English were excluded. References of systematic reviews and reviews were evaluated for further inclusion of articles missed in the initial search.

Data extraction

For each article, the following information was extracted if present: first author, publication year, journal, study type, imaging modality, tumor type, mean tumor size, number of subjects and tumors, ablation method, software used, intended minimal ablation margin (MAM), LTP

rate, method of MAM determination, segmentation method, co-registration method, other treatment success outcome measures, and validation of segmentation and registration.

RESULTS

The search strategy initially resulted in 215 articles, that were screened by title and abstract (Figure 1). Subsequently, 110 articles were analyzed in full-text for eligibility, resulting in the inclusion of 71 articles. Another 4 articles were included from references of (systematic) reviews. Eventually, a total of 75 articles were included in this review, see Figure 1. Thirty-one articles described a method for determination of technical success or measurement of MAM [5-9, 11-36]. Thirteen articles described segmentation methods for segmentation of the tumor and the ablation zone [8, 9, 22, 31, 37-45]. Twenty-five articles reported on co-registration methods for either pre- and postinterventional image co-registration, or pre- and intraoperative image co-registration [6-9, 12, 24, 26-28, 31, 32, 34, 36, 42, 44-54]. Finally, ten articles evaluated tissue shrinkage due to thermal ablation [10, 55-63].

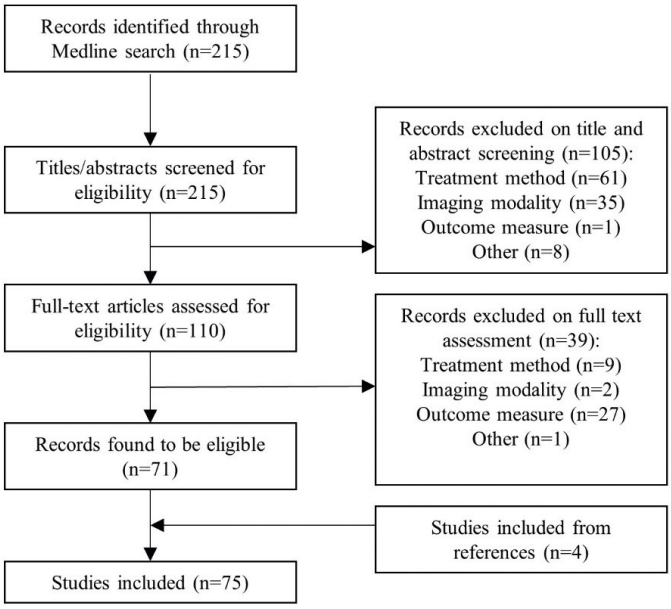

Figure 1: *Overview of the article selection process, specified per step.*

Clinical studies

In total, 58 clinical studies with 4,311 tumors were included in the results. RFA was the ablation method used most frequently and HCC patients (n=3,431 tumors) formed the main population in most studies. Intrahepatic cholangiocarcinoma (n=57) and hepatic metastases

from other primary origin (predominantly colorectal cancer, n=456) were other pathologies included. All studies were performed in a single center and most of them had a retrospective study design. A high variety in population size was found (7-211, median: 36.5). Mean or median lesion sizes were <30 mm for all clinical studies. An overview of all included clinical studies can be found in Table 1.

MAM assessment

In general, three ways of pre- and post-ablation imaging assessment were identified from the results, see Table 2. Analysis with side-by-side projection of pre- and post-scans was performed in 14/31 studies [5, 8, 13-21, 27, 28, 35]. As part of this assessment MAM was determined in the axial plane (n=13) [5, 8, 13, 15-21, 26, 28, 35] or in the coronal and sagittal imaging planes too (n=10) [5, 8, 13, 16, 17, 19, 20, 26, 28, 35]. Manual 2D measurements using anatomical landmarks were performed to quantify the ablation margins in these studies using mostly anatomical landmarks. In 21/31 studies co-registration software for MAM quantification was used [6-9, 11, 12, 22-36]. The software used can further be categorized into a) non-dedicated co-registration software combined with manual measurements (n=17) [6-9, 11, 12, 22, 24-30, 32-34, 36] and b) dedicated MAM quantification software that allows segmentation of tumor and ablation necrosis (n=3) [22, 23, 31].

Euclidian distance measurements were used to quantify the MAM in 3D in case of dedicated MAM quantification software. In non-dedicated co-registration software, either a visual assessment (n=1) [30], in-plane measurements (n=10) [6, 11, 25-30, 33, 34] or 3D MAM measurements (n=6) [7-9, 12, 24, 36] was used.

In all studies, the MAM was expressed as the smallest distance from the tumor boundary to the nearest border of the ablation zone. In general, the intended MAM was ≥5 mm, as can be seen in Table 1. In a few studies additional quantification measures were used, such as the coverage of the tumor by the ablation zone, or the extent that a 5 mm ablation margin was reached in all directions. In 36 studies, the quantified MAM was correlated with the occurrence of LTP. Figure 2 shows the correlation between the intended MAM and the occurrence of LTP. In one study immunohistology of a post-ablation biopsy was correlated with the occurrence of LTP [35].

Segmentation methods

Table 3 describes the different methods used for segmentation of the tumor and ablation zone. Semi-automatic segmentation methods were used in 12/13 studies [8, 9, 22, 31, 37-44] and manual segmentation was used in only one study [45]. Semi-automatic segmentation methods used included edge detection [8, 9, 44], region growing based algorithms [22, 40, 41, 45], and machine learning based algorithms involving classification [39] and clustering

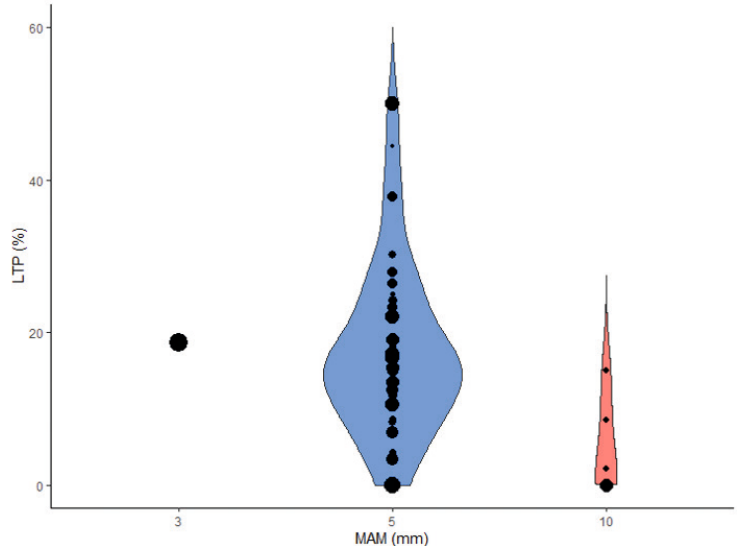

Figure 2: *Violin plot showing the local tumor progression (LTP) rates for different intended minimal ablation margins (MAM). Horizontal width of the plot represents the density of the data along the Y-axis. Each individual dataset is represented as a dot, where larger dots represent studies with more tumors treated*

[37, 38, 42]. In four of these papers in-house segmentation software was used [37-39, 42] and in the other studies commercially available software [8, 9, 22, 31, 40, 41, 43, 44].

The accuracy of segmentation was qualitatively assessed by radiologists in all studies. Quantitative inter- or intra-observer agreement methods were used in eight studies, comparing semi-automatic segmentation with manual segmentation of an observer or the interobserver agreement between manual segmentation of multiple observers. Outcome measures used were the dice similarity coefficient (DSC) [37, 38], volumetric overlap error [39], volume difference [39], average symmetric surface distance [39], root mean square symmetric surface distance [39], maximum symmetric surface distance [39], Lin's concordance correlation coefficient [40, 41], percentage match [42], positive and negative predictivity [42], specificity [42], and Pearson correlation [43].

Registration and MAM quantification software

Table 4 provides an overview of the different software used for co-registration and MAM quantification. CECT-images were used for co-registration in 22/25 studies [6-9, 24, 26-28, 31, 34, 36, 42, 44-46, 48, 50, 51, 53, 54], and MRI-images were used in 10/25 studies [12, 24, 26, 28, 32, 36, 44, 45, 52, 53]. In-house developed software was used in 9/25 studies [12, 42, 46-48, 50, 51, 53, 54].

Rigid co-registration algorithms that only allowed for translation and rotation of images for optimal co-registration were used in 11/25 studies [6, 7, 26, 27, 31, 32, 34, 44, 45, 52, 53]. Reasons for choosing rigid co-registration could be speed, and availability. In 14/25 studies, non-rigid co-registration algorithms were used that also allowed for deformation of the scans to locally optimize the co-registration [8, 9, 12, 24, 28, 31, 36, 42, 46-51, 53, 54]. Reasoning behind the choice of a non-rigid approach were to allow for local liver deformations and to reduce the influence of respiratory motion, adjacent organ movement, heart pulsations and patient positioning. In two studies, both co-registration methods were used [31, 53].

Anatomical landmark placement on the liver surface, hepatic arteries, portal veins and hepatic veins near the tumor were (optionally) used as input parameters in 16/25 different studies [6-9, 24, 26, 32, 34, 36, 44, 45, 47-49, 51, 52]. Placement of anatomical landmarks near the tumor and ablation necrosis was used for local optimization of the image co-registration.

Fully automated co-registration algorithms were used in 6/25 studies [12, 26, 31, 42, 50, 53]. Semi-automatic co-registrations algorithms were used in 14/25 studies [7-9, 24, 32, 34, 36, 45-49, 51, 54]. Manual translation and rotation was possible to adjust the co-registrations in these software packages. Three commercial software packages were used that only allowed for manual co-registration [6, 26, 52]. One software platform was commercially available and dedicated to ablation margin quantification [31].

Quality of co-registration was described in 22/25 studies [6-9, 12, 24, 26, 27, 32, 34, 36, 44, 46-54]. This was qualitatively scored in 12/22 software packages using e.g. a three- or five-points scale [6-9, 24, 32, 34, 36, 44, 45, 49, 52]. Quantitative quality assessment measures included distances between one or multiple pairs of landmarks, and distances between surface areas. Another quantitative quality assessment tool was the use of the Dice similarity coefficient between segmented liver volumes.

Tissue shrinkage

Tissue shrinkage was evaluated using ex vivo bovine or porcine livers [10, 55-60], in vivo porcine livers [61, 62] or pre- and post-ablation imaging of patients with HCC or metastases [63]. In the ex vivo animal models, the liver was divided in test samples, after which ablation was performed using either RFA or MWA. In the in vivo animal model, the ablation was performed in different segments of the liver. The samples consisted of normal liver parenchyma without tumors. Ablation times ranged from 1 minute to 20 minutes, with power settings between 20 and 200 W. Tissue shrinkage was measured through the dimensions of the samples pre- and post-ablation, or the displacement of markers inserted into the tissue sample. Tissue shrinkage was expressed as the contraction ratio, or contraction measured in percentage,

see Table 5. Noteworthy, in the study by Weiss et al. the contraction was expressed as planar strain, which showed tissue expansion for ablation times <10 minutes [59].

In the in vivo human study, measurements were performed using landmarks on both pre- and post-ablation images by two radiologists. A relative ablation zone contraction of 7.11% (+/- 13.3) and 2.39% (+/- 12.7), and tumor contraction of 9.95% (+/- 10.4) and 1.31% (+/- 13.2) were found for MWA and RFA, respectively [63].

DISCUSSION

Ablation margin quantification has been a topic of high interest in literature. In this systematic review, we have evaluated clinical study methodology, MAM quantification software methods, imaging co-registration methods, segmentation methods and tissue shrinkage. In general, a high variety in methodology was found between different studies.

With respect to the clinical studies, a MAM of ≥5 mm was intended mostly, in accordance with ablation guidelines [81]. Although the studies were very heterogeneous, and only limited data were available of studies with an intended MAM of ≥3 mm and ≥10 mm, LTP rates tended to decrease at larger intended MAM.

In studies that aimed at retrospective quantification of the ablation margins, the properties of the ablation margin quantification tools or software were evaluated. The MAM (i.e. smallest distance between outer boundaries of tumor and ablation zone) was the outcome measure used in all studies. Only 3 studies used other additional outcome measures, such as ablation surface area or volumetric data. In a limited number of studies, the MAM could also be quantified in 3D rather than the standard orthogonal image planes. With the emerging field of dedicated ablation margin quantification software and incorporation of ablation margin quantification in clinical trials, it is expected that this more thorough analysis will become the new standard.

Segmentation of tumor and ablation zone plays a major role in objectively quantifying ablation margins. Several segmentation algorithms were used in the included studies, most of them were semi-automatic and based on underlying grey-scale or region-growing algorithms. Multiple methods were used to validate segmentations among different interpreters or against a golden standard. Although the results of these validations are not directly comparable, the overall performance seems good. To be better able to compare the robustness and accuracy of each segmentation tool, a standardized validation method would be needed, despite their specific advantages and disadvantages. The DSC is suitable for comparing two segmentations based on their overlap, but its sensitivity is dependent on

the size of the segmented structure. Besides the technical aspects of segmentation, several clinical implications should be taken into consideration. The size and shape of a tumor may appear differently on arterial and venous phases. Choosing the right scan phase is therefore crucial for obtaining the correct ablation margin. Moreover, for a smooth incorporation in the clinical workflow it is important that segmentation algorithms are fast, accurate and easily correctable.

Image co-registration between pre- and post-ablation imaging is the basis for quantifying distances between boundaries of the tumor and ablation zone. Rigid and non-rigid co-registration techniques were used about as often and most of the co-registration methods included in this systematic review were semi-automatically. Non-rigid co-registration algorithms usually result in visually better outcomes for the entire liver, as deformational differences of the liver between the pre- and post-ablation scans are adjusted for. However, local tissue deformations as a result of thermal ablation may result in inaccurate MAM measurements. Luu et al. proposed to manually penalize local areas with large erroneous non-rigid deformations by enforcing local rigidity [50]. Similarly, Passera et al. replaced these local areas with synthetic patterns to be able to use a non-rigid co-registration approach without the undesired, erroneous deformations in the ablation zone that hamper correct MAM measurements [42]. Locally optimized co-registration between pre- and post-ablation imaging in the tumor region is the main objective. The use of local landmark placement is possible in many co-registration algorithms and may be used for this sake.

To reduce co-registration errors in a clinical setting, the pre- and post-ablation imaging are best obtained during the ablation procedure with the patient in an identical bed position and with a similar inhalation mode. Although thermal ablation could be performed using intravenous sedation, general anesthesia has the advantage of being able to use high-frequency jet ventilation or breath hold [81]. This may help reducing differences in inhalation mode, and therefore co-registration errors. It has yet to be established which scanning protocol and phase is most suitable for accurate and reproducible quantification of ablation margins.

Tissue shrinkage during ablation may be of high influence on the outcome of ablation margin quantification, with substantial tissue shrinkage rates reported in animal studies. As a result of tissue shrinkage, ablation margins may be underestimated. During the follow-up after thermal ablation, the ablation zone may shrink further on imaging [82]. Therefore, ablation margin quantification should be determined based on images acquired directly after treatment. This systematic review only included articles using CECT or MRI for immediate ablation margin evaluation. For clinical purpose, hybrid imaging with PET-CT or PET-MRI may help identifying patients at risk of developing LTP [83]. Besides direct tissue shrinkage

during ablation, local edema around the ablation zone may cause the opposite effect directly surrounding the ablation necrosis, and my influence image co-registration.

The evidence available on the use of ablation margin quantification is currently based on retrospective studies with a high variability in study methodology. Both clinical factors and technical factors, in terms of image acquisition, reconstruction algorithms, and image processing play major roles in the quantification of ablation margins. A better understanding is needed of how these factors affect the outcome, and what combination of factors results in a robust and accurate method of ablation margin quantification. With this standard at hand, the correlation between measured MAM and the occurrence of LTP could ultimately be better understood and incorporated in the standard workflow.

Several prospective clinical trials are currently performed trying to bridge this gap, such as the PROMETHEUS (Netherlands Trial Register NL9713) [84], ACCLAIM (Clinicaltrials.gov: NCT03753789), COVER-ALL (Clinicaltrials.gov: NCT04083378) [85], RFA physics library – PGP (Clinicaltrials.gov: NCT04152343) and IAMCOMPLETE (Clinicaltrials.gov: NCT04123340) trials. Moreover, companies are developing solutions for ablation margin quantification and raising precision e.g. with dedicated ablation margin quantification software [31], ablation needle guidance and integrated ablation margin confirmation software [86], or an ablation system with integrated imaging co-registration and ablation margin verification software [87]. Moreover, the wider application of dual-energy CT and spectral CT may contribute to optimized tumor and ablation zone segmentation [88]. The combination of prospective clinical trials and technological advancements is what is needed to push ablation margin quantification to the next stage.

CONCLUSION

Ablation margin quantification is emerging to become a valuable tool in optimizing minimally invasive treatment of hepatic tumors. This systematic review shows that there is currently a high variability in ablation margin quantification methodology in terms of image co-registration, segmentation methods, and interpretation. Although the method for reaching the maximum precision in a robust way may still be unknown, the correct clinical use and interpretation will be very important as the ultimate goal is to interpret ablation margins at a millimeter level of accuracy. Optimization of scanning protocols, time reduction between pre- and post-ablation scans, and quality assessment of image co-registration are therefore of great importance.

REFERENCES

[1] European Association for the Study of the Liver, EASL Clinical Practice Guidelines: Management of hepatocellular carcinoma, J Hepatol 69(1) (2018) 182-236.

[2] A. Forner, M. Reig, J. Bruix, Hepatocellular carcinoma, Lancet 391(10127) (2018) 1301-1314.

[3] S.K. Roberts, A. Gazzola, J. Lubel, P. Gow, S. Bell, A. Nicoll, A. Dev, M.A. Fink, S. Sood, V. Knight, T. Hong, E. Paul, G. Mishra, A. Majeed, W. Kemp, G. Melbourne Liver, Treatment choice for early-stage hepatocellular carcinoma in real-world practice: impact of treatment stage migration to transarterial chemoembolization and treatment response on survival, Scand J Gastroenterol 53(10-11) (2018) 1368-1375.

[4] S.K. Kei, H. Rhim, D. Choi, W.J. Lee, H.K. Lim, Y.S. Kim, Local tumor progression after radiofrequency ablation of liver tumors: analysis of morphologic pattern and site of recurrence, AJR Am J Roentgenol 190(6) (2008) 1544-51.

[5] X. Wang, C.T. Sofocleous, J.P. Erinjeri, E.N. Petre, M. Gonen, K.G. Do, K.T. Brown, A.M. Covey, L.A. Brody, W. Alago, R.H. Thornton, N.E. Kemeny, S.B. Solomon, Margin size is an independent predictor of local tumor progression after ablation of colon cancer liver metastases, Cardiovasc Intervent Radiol 36(1) (2013) 166-75.

[6] Y.S. Kim, W.J. Lee, H. Rhim, H.K. Lim, D. Choi, J.Y. Lee, The minimal ablative margin of radiofrequency ablation of hepatocellular carcinoma (> 2 and < 5 cm) needed to prevent local tumor progression: 3D quantitative assessment using CT image fusion, AJR Am J Roentgenol 195(3) (2010) 758-65.

[7] G. Laimer, P. Schullian, N. Jaschke, D. Putzer, G. Eberle, A. Alzaga, B. Odisio, R. Bale, Minimal ablative margin (MAM) assessment with image fusion: an independent predictor for local tumor progression in hepatocellular carcinoma after stereotactic radiofrequency ablation, Eur Radiol 30(5) (2020) 2463-2472.

[8] P. Hendriks, W.A. Noortman, T.R. Baetens, A.R. van Erkel, C.S.P. van Rijswijk, R.W. van der Meer, M.J. Coenraad, L.F. de Geus-Oei, C.H. Slump, M.C. Burgmans, Quantitative Volumetric Assessment of Ablative Margins in Hepatocellular Carcinoma: Predicting Local Tumor Progression Using Nonrigid Registration Software, J Oncol 2019 (2019) 4049287.

[9] B.G. Sibinga Mulder, P. Hendriks, T.R. Baetens, A.R. van Erkel, C.S.P. van Rijswijk, R.W. van der Meer, C.J.H. van de Velde, A.L. Vahrmeijer, J.S.D. Mieog, M.C. Burgmans, Quantitative margin assessment of radiofrequency ablation of a solitary colorectal hepatic metastasis using MIRADA RTx on CT scans: a feasibility study, BMC Med Imaging 19(1) (2019) 71.

[10] L. Farina, N. Weiss, Y. Nissenbaum, M. Cavagnaro, V. Lopresto, R. Pinto, N. Tosoratti, C. Amabile, S. Cassarino, S.N. Goldberg, Characterisation of tissue shrinkage during microwave thermal ablation, Int J Hyperthermia 30(7) (2014) 419-28.

[11] M. Abdel-Rehim, M. Ronot, A. Sibert, V. Vilgrain, Assessment of liver ablation using cone beam computed tomography, World J Gastroenterol 21(2) (2015) 517-24.

[12] C. An, Y. Jiang, Z. Huang, Y. Gu, T. Zhang, L. Ma, J. Huang, Assessment of Ablative Margin After Microwave Ablation for Hepatocellular Carcinoma Using Deep Learning-Based Deformable Image Registration, Front Oncol 10 (2020) 573316.

[13] P. Biondetti, E.M. Fumarola, A.M. Ierardi, A. Coppola, G. Gorga, L. Maggi, E. Valconi, S.A. Angileri, G. Carrafiello, Percutaneous US-guided MWA of small liver HCC: predictors of outcome and risk factors for complications from a single center experience, Med Oncol 37(5) (2020) 39.

[14] J.W. Choi, J.M. Lee, D.H. Lee, J.H. Yoon, Y.J. Kim, J.H. Lee, S.J. Yu, E.J. Cho, Radiofrequency ablation using internally cooled wet electrodes in bipolar mode for the treatment of recurrent hepatocellular carcinoma after locoregional treatment: A randomized prospective comparative study, PLoS One 15(9) (2020) e0239733.

[15] K. Fukuda, K. Mori, N. Hasegawa, K. Nasu, K. Ishige, Y. Okamoto, M. Shiigai, M. Abei, M. Minami, I. Hyodo, Safety margin of radiofrequency ablation for hepatocellular carcinoma: a prospective study using magnetic resonance imaging with superparamagnetic iron oxide, Jpn J Radiol 37(7) (2019) 555-563.

[16] J. Iwazawa, S. Ohue, N. Hashimoto, T. Mitani, Ablation margin assessment of liver tumors with intravenous contrast-enhanced C-arm computed tomography, World J Radiol 4(3) (2012) 109-14.

[17] S.M. Kim, S.S. Shin, B.C. Lee, J.W. Kim, S.H. Heo, H.S. Lim, Y.Y. Jeong, Imaging evaluation of ablative margin and index tumor immediately after radiofrequency ablation for hepatocellular carcinoma: comparison between multidetector-row CT and MR imaging, Abdom Radiol (NY) 42(10) (2017) 2527-2537.

[18] Y.H. Koh, J.I. Choi, H.B. Kim, M.J. Kim, Computed tomographic-guided radiofrequency ablation of recurrent or residual hepatocellular carcinomas around retained iodized oil after transarterial chemoembolization, Korean J Radiol 14(5) (2013) 733-42.

[19] T. Motoyama, S. Ogasawara, T. Chiba, T. Higashide, H. Yokota, N. Kanogawa, E. Suzuki, Y. Ooka, A. Tawada, R. Irie, S. Ochi, Y. Masuda, T. Uno, O. Yokosuka, Coronal reformatted CT images contribute to the precise evaluation of the radiofrequency ablative margin for hepatocellular carcinoma, Abdom Imaging 39(2) (2014) 262-8.

[20] Y. Park, D. Choi, H. Rhim, Y.S. Kim, J.Y. Lee, I. Chang, H.K. Lim, C.K. Park, Central lower attenuating lesion in the ablation zone on immediate follow-up CT after percutaneous radiofrequency ablation for hepatocellular carcinoma: incidence and clinical significance, Eur J Radiol 75(3) (2010) 391-6.

[21] K.I. Ringe, F. Wacker, H.J. Raatschen, Is there a need for MRI within 24 hours after CT-guided percutaneous thermoablation of the liver?, Acta Radiol 56(1) (2015) 10-7.

[22] A. Hocquelet, H. Trillaud, N. Frulio, P. Papadopoulos, P. Balageas, C. Salut, M. Meyer, J.F. Blanc, M. Montaudon, B. Denis de Senneville, Three-Dimensional Measurement of Hepatocellular Carcinoma Ablation Zones and Margins for Predicting Local Tumor Progression, J Vasc Interv Radiol 27(7) (2016) 1038-1045 e2.

[23] C. Jiang, B. Liu, S. Chen, Z. Peng, X. Xie, M. Kuang, Safety margin after radiofrequency ablation of hepatocellular carcinoma: precise assessment with a three-dimensional reconstruction technique using CT imaging, Int J Hyperthermia 34(8) (2018) 1135-1141.

[24] A. Kobe, Y. Kindler, E. Klotz, G. Puippe, F. Messmer, H. Alkadhi, T. Pfammatter, Fusion of Preinterventional MR Imaging With Liver Perfusion CT After RFA of Hepatocellular Carcinoma: Early Quantitative Prediction of Local Recurrence, Invest Radiol 56(3) (2021) 188-196.

[25] M. Liao, X. Zhong, J. Zhang, Y. Liu, Z. Zhu, H. Wu, Y. Zeng, J. Huang, Radiofrequency ablation using a 10-mm target margin for small hepatocellular carcinoma in patients with liver cirrhosis: A prospective randomized trial, J Surg Oncol 115(8) (2017) 971-979.

[26] Y. Makino, Y. Imai, T. Igura, M. Hori, K. Fukuda, Y. Sawai, S. Kogita, N. Fujita, T. Takehara, T. Murakami, Comparative evaluation of three-dimensional Gd-EOB-DTPA-enhanced MR fusion imaging with CT fusion imaging in the assessment of treatment effect of radiofrequency ablation of hepatocellular carcinoma, Abdom Imaging 40(1) (2015) 102-11.

[27] Y. Makino, Y. Imai, T. Igura, M. Hori, K. Fukuda, Y. Sawai, S. Kogita, H. Ohama, Y. Matsumoto, M. Nakahara, S. Zushi, M. Kurokawa, K. Isotani, M. Takamura, N. Fujita, T. Murakami, Utility of computed tomography fusion imaging for the evaluation of the ablative margin of radiofrequency ablation for hepatocellular carcinoma and the correlation to local tumor progression, Hepatol Res 43(9) (2013) 950-8.

[28] J. Park, J.M. Lee, D.H. Lee, I. Joo, J.H. Yoon, J.Y. Park, E. Klotz, Value of Nonrigid Registration of Pre-Procedure MR with Post-Procedure CT After Radiofrequency Ablation for Hepatocellular Carcinoma, Cardiovasc Intervent Radiol 40(6) (2017) 873-883.

[29] M. Sakakibara, K. Ohkawa, K. Katayama, K. Imanaka, A. Ishihara, N. Hasegawa, H. Kimura, Three-dimensional registration of images obtained before and after radiofrequency ablation of hepatocellular carcinoma to assess treatment adequacy, AJR Am J Roentgenol 202(5) (2014) W487-95.

[30] S. Shin, J.M. Lee, K.W. Kim, I. Joo, J.K. Han, B.I. Choi, E. Klotz, Postablation assessment using follow-up registration of CT images before and after radiofrequency ablation (RFA): prospective evaluation of midterm therapeutic results of RFA for hepatocellular carcinoma, AJR Am J Roentgenol 203(1) (2014) 70-7.

[31] M. Solbiati, R. Muglia, S.N. Goldberg, T. Ierace, A. Rotilio, K.M. Passera, I. Marre, L. Solbiati, A novel software platform for volumetric assessment of ablation completeness, Int J Hyperthermia 36(1) (2019) 337-343.

[32] N. Takeyama, N. Mizobuchi, M. Sakaki, Y. Shimozuma, J. Munechika, A. Kajiwara, M. Uchikoshi, S. Uozumi, Y. Ohgiya, T. Gokan, Evaluation of hepatocellular carcinoma ablative margins using fused pre- and post-ablation hepatobiliary phase images, Abdom Radiol (NY) 44(3) (2019) 923-935.

[33] P. Tinguely, L. Frehner, A. Lachenmayer, V. Banz, S. Weber, D. Candinas, M.H. Maurer, Stereotactic Image-Guided Microwave Ablation for Malignant Liver Tumors-A Multivariable Accuracy and Efficacy Analysis, Front Oncol 10 (2020) 842.

[34] F. Vandenbroucke, J. Vandemeulebroucke, N. Buls, R.F. Thoeni, J. de Mey, Can tumor coverage evaluated 24 h post-radiofrequency ablation predict local tumor progression of liver metastases?, Int J Comput Assist Radiol Surg 13(12) (2018) 1981-1989.

[35] V.S. Sotirchos, L.M. Petrovic, M. Gönen, D.S. Klimstra, R.K.G. Do, E.N. Petre, A.R. Garcia, A. Barlas, J.P. Erinjeri, K.T. Brown, A.M. Covey, W. Alago, L.A. Brody, R.P. DeMatteo, N.E. Kemeny, S.B. Solomon, K.O. Manova-Todorova, C.T. Sofocleous, Colorectal Cancer Liver Metastases: Biopsy of the Ablation Zone and Margins Can Be Used to Predict Oncologic Outcome, Radiology 280(3) (2016) 949-959.

[36] J.H. Yoon, J.M. Lee, E. Klotz, H. Woo, M.H. Yu, I. Joo, E.S. Lee, J.K. Han, Prediction of Local Tumor Progression after Radiofrequency Ablation (RFA) of Hepatocellular Carcinoma by Assessment of Ablative Margin Using Pre-RFA MRI and Post-RFA CT Registration, Korean J Radiol 19(6) (2018) 1053-1065.

[37] J. Egger, H. Busse, P. Brandmaier, D. Seider, M. Gawlitza, S. Strocka, P. Voglreiter, M. Dokter, M. Hofmann, B. Kainz, X. Chen, A. Hann, P. Boechat, W. Yu, B. Freisleben, T. Alhonnoro, M. Pollari, M. Moche, D. Schmalstieg, RFA-cut: Semi-automatic segmentation of radiofrequency ablation zones with and without needles via optimal s-t-cuts, Annu Int Conf IEEE Eng Med Biol Soc 2015 (2015) 2423-9.

[38] J. Egger, H. Busse, P. Brandmaier, D. Seider, M. Gawlitza, S. Strocka, P. Voglreiter, M. Dokter, M. Hofmann, B. Kainz, A. Hann, X. Chen, T. Alhonnoro, M. Pollari, D. Schmalstieg, M. Moche, Interactive Volumetry Of Liver Ablation Zones, Sci Rep 5 (2015) 15373.

[39] Y. Hame, M. Pollari, Semi-automatic liver tumor segmentation with hidden Markov measure field model and non-parametric distribution estimation, Med Image Anal 16(1) (2012) 140-9.

[40] S. Keil, P. Bruners, L. Ohnsorge, C. Plumhans, F.F. Behrendt, S. Stanzel, M. Suhling, R.W. Gunther, M. Das, A.H. Mahnken, Semiautomated versus manual evaluation of liver metastases treated by radiofrequency ablation, J Vasc Interv Radiol 21(2) (2010) 245-51.

[41] S. Keil, P. Bruners, K. Schiffl, M. Sedlmair, G. Muhlenbruch, R.W. Gunther, M. Das, A.H. Mahnken, Radiofrequency ablation of liver metastases-software-assisted evaluation of the ablation zone in MDCT: tumor-free follow-up versus local recurrent disease, Cardiovasc Intervent Radiol 33(2) (2010) 297-306.

[42] K. Passera, S. Selvaggi, D. Scaramuzza, F. Garbagnati, D. Vergnaghi, L. Mainardi, Radiofrequency ablation of liver tumors: quantitative assessment of tumor coverage through CT image processing, BMC Med Imaging 13 (2013) 3.

[43] V.D. Vo Chieu, F. Wacker, C. Rieder, G.H. Pohler, C. Schumann, H. Ballhausen, K.I. Ringe, Ablation zone geometry after CT-guided hepatic microwave ablation: evaluation of a semi-automatic software and comparison of two different ablation systems, Int J Hyperthermia 37(1) (2020) 533-541.

[44] R.S. Iyer, B.A. Timm, L.M. Mitsumori, O. Kolokythas, Image fusion as a new postprocessing method to evaluate the radiofrequency ablation zone after treatment of malignant liver tumors, J Comput Assist Tomogr 34(2) (2010) 226-8.

[45] E.A. Kaye, F.H. Cornelis, E.N. Petre, N. Tyagi, W. Shady, W. Shi, Z. Zhang, S.B. Solomon, C.T. Sofocleous, J.C. Durack, Volumetric 3D assessment of ablation zones after thermal ablation of colorectal liver metastases to improve prediction of local tumor progression, Eur Radiol 29(5) (2019) 2698-2705.

[46] H. Boulkhrif, H.M. Luu, T. van Walsum, A. Moelker, Accuracy of semi-automated versus manual localisation of liver tumours in CT-guided ablation procedures, Eur Radiol 28(12) (2018) 4978-4984.

[47] G. Gunay, M.H. Luu, A. Moelker, T. van Walsum, S. Klein, Semiautomated registration of pre- and intraoperative CT for image-guided percutaneous liver tumor ablation interventions, Med Phys 44(7) (2017) 3718-3725.

[48] L.M. Gunay G, van Walsum T, Klein S, Semi-automated registration of pre- and intra-operative liver CT for image-guided interventions, Proc. SPIE 9784, Medical Imaging 2016: Image Processing (2016).

[49] K.W. Kim, J.M. Lee, E. Klotz, S.J. Kim, S.H. Kim, J.Y. Kim, J.K. Han, B.I. Choi, Safety margin assessment after radiofrequency ablation of the liver using registration of preprocedure and postprocedure CT images, AJR Am J Roentgenol 196(5) (2011) W565-72.

[50] H.M. Luu, C. Klink, W. Niessen, A. Moelker, T. van Walsum, An automatic registration method for pre- and post-interventional CT images for assessing treatment success in liver RFA treatment, Med Phys 42(9) (2015) 5559-67.

[51] H.M. Luu, C. Klink, W. Niessen, A. Moelker, T. Walsum, Non-Rigid Registration of Liver CT Images for CT-Guided Ablation of Liver Tumors, PLoS One 11(9) (2016) e0161600.

[52] X.L. Wang, K. Li, Z.Z. Su, Z.P. Huang, P. Wang, R.Q. Zheng, Assessment of radiofrequency ablation margin by MRI-MRI image fusion in hepatocellular carcinoma, World J Gastroenterol 21(17) (2015) 5345-51.

[53] D. Wei, S. Ahmad, J. Huo, P. Huang, P.T. Yap, Z. Xue, J. Sun, W. Li, D. Shen, Q. Wang, SLIR: Synthesis, localization, inpainting, and registration for image-guided thermal ablation of liver tumors, Med Image Anal 65 (2020) 101763.

[54] H.M. Luu, A. Moelker, S. Klein, W. Niessen, T. van Walsum, Quantification of nonrigid liver deformation in radiofrequency ablation interventions using image registration, Phys Med Biol 63(17) (2018) 175005.

[55] C. Amabile, L. Farina, V. Lopresto, R. Pinto, S. Cassarino, N. Tosoratti, S.N. Goldberg, M. Cavagnaro, Tissue shrinkage in microwave ablation of liver: an ex vivo predictive model, Int J Hyperthermia 33(1) (2017) 101-109.

[56] C.L. Brace, T.A. Diaz, J.L. Hinshaw, F.T. Lee, Jr., Tissue contraction caused by radiofrequency and microwave ablation: a laboratory study in liver and lung, J Vasc Interv Radiol 21(8) (2010) 1280-6.

[57] D. Liu, C.L. Brace, CT imaging during microwave ablation: analysis of spatial and temporal tissue contraction, Med Phys 41(11) (2014) 113303.

[58] C. Rossmann, E. Garrett-Mayer, F. Rattay, D. Haemmerich, Dynamics of tissue shrinkage during ablative temperature exposures, Physiol Meas 35(1) (2014) 55-67.

[59] N. Weiss, S.N. Goldberg, Y. Nissenbaum, J. Sosna, H. Azhari, Planar strain analysis of liver undergoing microwave thermal ablation using x-ray CT, Med Phys 42(1) (2015) 372-80.

[60] D. Liu, C.L. Brace, Numerical simulation of microwave ablation incorporating tissue contraction based on thermal dose, Phys Med Biol 62(6) (2017) 2070-2086.

[61] K.K. Bressem, J.L. Vahldiek, C. Erxleben, F. Poch, S. Shnaiyen, B. Geyer, K.S. Lehmann, B. Hamm, S.M. Niehues, Exploring Patterns of Dynamic Size Changes of Lesions after Hepatic Microwave Ablation in an In Vivo Porcine Model, Sci Rep 10(1) (2020) 805.

[62] C. Erxleben, S.M. Niehues, B. Geyer, F. Poch, K.K. Bressem, K.S. Lehmann, J.L. Vahldiek, CT-based quantification of short-term tissue shrinkage following hepatic microwave ablation in an in vivo porcine liver model, Acta Radiol 62(1) (2021) 12-18.

[63] J.K. Lee, S. Siripongsakun, S. Bahrami, S.S. Raman, J. Sayre, D.S. Lu, Microwave ablation of liver tumors: degree of tissue contraction as compared to RF ablation, Abdom Radiol (NY) 41(4) (2016) 659-66.

[64] L.P. Beyer, L. Lurken, N. Verloh, M. Haimerl, K. Michalik, J. Schaible, C. Stroszczynski, P. Wiggermann, Stereotactically navigated percutaneous microwave ablation (MWA) compared to conventional MWA: a matched pair analysis, Int J Comput Assist Radiol Surg 13(12) (2018) 1991-1997.

[65] F. Cao, L. Xie, H. Qi, S. Ze, S. Chen, L. Shen, X. Zhang, W. Fan, Melanoma liver metastases with special imaging features on magnetic resonance imaging after microwave ablations: How to evaluate technical efficacy?, J Cancer Res Ther 15(7) (2019) 1501-1507.

[66] D.I. Cha, T.W. Kang, K.D. Song, M.W. Lee, H. Rhim, H.K. Lim, D.H. Sinn, K. Kim, Radiofrequency ablation for subcardiac hepatocellular carcinoma: therapeutic outcomes and risk factors for technical failure, Eur Radiol 29(5) (2019) 2706-2715.

[67] J.W. Choi, J.M. Lee, D.H. Lee, J.H. Yoon, K.S. Suh, J.H. Yoon, Y.J. Kim, J.H. Lee, S.J. Yu, J.K. Han, Switching Monopolar Radiofrequency Ablation Using a Separable Cluster Electrode in Patients with Hepatocellular Carcinoma: A Prospective Study, PLoS One 11(8) (2016) e0161980.

[68] A. El-Gendi, M. El-Shafei, F. Abdel-Aziz, E. Bedewy, Intraoperative ablation for small HCC not amenable for percutaneous radiofrequency ablation in Child A cirrhotic patients, J Gastrointest Surg 17(4) (2013) 712-8.

[69] E.M. Fumarola, A.M. Ierardi, P. Biondetti, A.P. Savoldi, P. Grillo, G. Gorga, A. Coppola, G. Carrafiello, Follow-up of percutaneous microwave (MW) ablation of hepatic lesion: predictive value of CT at 24-h compared with CT at 1 month, Med Oncol 37(5) (2020) 41.

[70] S. Kamei, J. Matsuda, M. Hagihara, A. Kitagawa, Y. Izumi, E. Katsuda, Y. Oshima, S. Ikeda, J. Kimura, T. Ota, T. Kawamura, T. Ishiguchi, Oblique approach for CT-guided liver radiofrequency ablation using multiplanar reformation images in hepatocellular carcinoma, Jpn J Radiol 30(6) (2012) 533-9.

[71] T.W. Kang, H. Rhim, J. Lee, K.D. Song, M.W. Lee, Y.S. Kim, H.K. Lim, K.M. Jang, S.H. Kim, G.Y. Gwak, S.H. Jung, Magnetic resonance imaging with gadoxetic acid for local tumour progression after radiofrequency ablation in patients with hepatocellular carcinoma, Eur Radiol 26(10) (2016) 3437-46.

[72] M.W. Lee, Y.J. Kim, S.W. Park, N.C. Yu, W.H. Choe, S.Y. Kwon, C.H. Lee, Biplane fluoroscopy-guided radiofrequency ablation combined with chemoembolisation for hepatocellular carcinoma: initial experience, Br J Radiol 84(1004) (2011) 691-7.

[73] X. Li, W.J. Fan, L. Zhang, X.P. Zhang, H. Jiang, J.L. Zhang, H. Zhang, CT-guided percutaneous microwave ablation of liver metastases from nasopharyngeal carcinoma, J Vasc Interv Radiol 24(5) (2013) 680-4.

[74] Z.Y. Liu, Z.H. Chang, Z.M. Lu, Q.Y. Guo, Early PET/CT after radiofrequency ablation in colorectal cancer liver metastases: is it useful?, Chin Med J (Engl) 123(13) (2010) 1690-4.

[75] S.I. Park, I.J. Kim, S.J. Lee, M.W. Shin, W.S. Shin, Y.E. Chung, G.M. Kim, M.D. Kim, J.Y. Won, Y. Lee do, J.S. Choi, K.H. Han, Angled Cool-Tip Electrode for Radiofrequency Ablation of Small Superficial Subcapsular Tumors in the Liver: A Feasibility Study, Korean J Radiol 17(5) (2016) 742-9.

[76] A.A. van Tilborg, H.J. Scheffer, K. Nielsen, J.H. van Waesberghe, E.F. Comans, C. van Kuijk, P.M. van den Tol, M.R. Meijerink, Transcatheter CT arterial portography and CT hepatic arteriography for liver tumor visualization during percutaneous ablation, J Vasc Interv Radiol 25(7) (2014) 1101-1111 e4.

[77] V.D. Vo Chieu, T. Werncke, B. Hensen, F. Wacker, K.I. Ringe, CT-Guided Microwave Ablation of Liver Tumors in Anatomically Challenging Locations, Cardiovasc Intervent Radiol 41(10) (2018) 1520-1529.

[78] Y. Yan, Z.Y. Lin, J. Chen, Analysis of imaging-guided thermal ablation puncture routes for tumors of the hepatic caudate lobe, J Cancer Res Ther 16(2) (2020) 258-262.

[79] J.H. Yoon, E.J. Lee, S.S. Cha, S.S. Han, S.J. Choi, J.R. Juhn, M.H. Kim, Y.J. Lee, S.J. Park, Comparison of gadoxetic acid-enhanced MR imaging versus four-phase multi-detector row computed tomography in assessing tumor regression after radiofrequency ablation in subjects with hepatocellular carcinomas, J Vasc Interv Radiol 21(3) (2010) 348-56.

[80] Q. Zhang, X. Li, J. Pan, Z. Wang, Transpulmonary computed tomography-guided radiofrequency ablation of liver neoplasms abutting the diaphragm with multiple bipolar electrodes, Indian J Cancer 52 Suppl 2 (2015) e64-8.

[81] L. Crocetti, T. de Baére, P.L. Pereira, F.P. Tarantino, CIRSE Standards of Practice on Thermal Ablation of Liver Tumours, Cardiovasc Intervent Radiol 43(7) (2020) 951-962.

[82] M. Maas , R. Beets-Tan, J.Y. Gaubert, F. Gomez Munoz, P Habert, L.G. Klompenhouwer, P Vilares Morgado, N Schaefer, F.H. Cornelis, S.B. Solomon, D. Van Der Reijd, J. Ignacio Bilbao. Follow-up after radiological intervention in oncology: ECIO-ESOI evidence and consensus-based recommendations for clinical practice. Insights Imaging 11, 83 (2020).

[83] E.D. McLoney, A.J. Isaacson, P. Keating. The Role of PET Imaging Before, During, and After Percutaneous Hepatic and Pulmonary Tumor Ablation. Semin Intervent Radiol. 2014 Jun;31(2):187-92.

[84] T.T.M. Oosterveer, G.C.M. Van Erp, P. Hendriks, A. Broersen, C.G. overduin, C.S.P. Van Rijswijk, A.R. Van Erkel, R.W. Van Der Meer, M.E. Tushuizen, A. Moelker, M.R. Meijerink, O.M. Van Delden, K.P. De Jong, C. Van Der Leij, M.L.J. smits, T.A.J. Urlings, J.P.B.M. Braak, E. Meershoek-Klein Kranenbarg, B. Van Duijn-De Vreugd, E. Zeijdner, J.J. Goeman, J.J. Fütterer, M.J. Coenraad, J. Dijkstra, M.C. Burgmans. Study Protocol PROMETHEUS: Prospective Multicenter Study to Evaluate the Correlation Between Safety Margin and Local Recurrence After Thermal Ablation Using Image Co-registration in Patients with Hepatocellular Carcinoma, Cardiovasc Intervent Radiol 45 (2022) 606-612.

[85] Y-M. Lin, I. Paolucci, B.M. Anderson, C.S. O'Connor, B.Rigaud, M. Briones-Dimayuga, K.A. Jones, K.K. Brock, B.M. Fellman, B.C. Odisio. Study Protocol COVER-ALL: Clinical Impact of a Volumetric Image Method for Confirming Tumour Coverage with Ablation on Patients with Malignant Liver Lesions. Cardiovasc Intervent Radiol 45 (2022) 1860-1867.

[86] V.M. Banz, M. Baechtold, S. Weber, M. Peterhans, D. Inderbitzin, D. Candinas, Computer planned, image-guided combined resection and ablation for bilobar colorectal liver metastases, World journal of gastroenterology 20(40) (2014) 14992-14996.

[87] N. Vasiniotis Kamarinos, E. Petre, J. Camacho, F. Boas, S. Solomon, C. Sofocleous, Abstract No. 490 Three-dimensional assessment of the ablation zone margins with the Neuwave Ablation Confirmation software: a feasibility study, Journal of Vascular and Interventional Radiology 31(3) (2020) S216.

[88] N.F. Majeed, M. Braschi Amirfarzan, C. Wald, J.R. Wortman. Spectral detector CT applications in advanced liver imaging. Br J Radiol. 2021 Jul 1;94(1123):20201290

Table 1: *Characteristics of all clinical studies included.*

Authors	Study type (Retrospective R, Prospective P)	Ablation method	Tumor Type	Number of patients (tumors)	Tumor size	Intended MAM
Abdel-Rehim M et al. [11]	R	RFA and MWA	HCC (17), CRLM (3), BCLM (1), CCA (2)	23 (23)	Range 8-40 mm	≥5 mm
An C et al. [12]	R	MWA	HCC	141 (141)	Mean 23 mm ± 9 mm	≥5 mm
Beyer LP et al. [64]	R and P	MWA	HCC (20), CRCM (16)	36 (36)	Mean 21.2 mm	-
Biondetti P et al. [13]	R	MWA	HCC	74 (74)	Mean 17.1 mm, range 7 – 30 mm	≥5 mm
Boulkhrif H et al. [46]	R	RFA and MWA	HCC (35), CRLM (16), neuroendocrine (3), gastric (1), BCLM (1)	35 (56)	Mean 20.4 ± 9.4 mm, range 6.1 - 60 mm; median 18.3 mm	-
Cao F et al. [65]	R	MWA	MLM (melanoma liver metastases)	7 (22)	Median 16.37 mm, range 6.66 – 43.72 mm	-
Cha DI et al. [66]	R	RFA	HCC	146 (146)	Median 16 mm, range 7-42 mm	≥5 mm
Choi JW et al. [67]	P	RFA	HCC	79 (98)	Mean 19 ± 7 mm	≥5 mm
Choi JW et al. [14]	P	RFA	HCC	77 (86)	Mean 16.5 mm	≥5 mm
El-Gendi A et al. [68]	P	RFA	HCC	24 (24)	Mean 20.4 ± 4.4 mm	≥10 mm
Fukuda K et al. [15]	P	RFA	HCC	76 (85)	Median 15 mm, range 8 -30 mm	≥10 mm
Fumarola EM et al. [69]	R	MWA	HCC	50 (50)	Mean 17.6 mm, range 7 – 35 mm	-
Hame Y et al. [39]	R	RFA	-	9 (11)	< 5mm	-
Hendriks P et al. [8]	R	RFA	HCC	25 (25)	Median 20 mm, range 12 – 45 mm	≥5 mm
Hocquelet A et al. [22]	R	RFA	HCC	16 (16)	Mean 29 mm	≥5 mm
Iwazawa J et al. [16]	R	RFA	HCC (8), metastatic (4)	12 (12)	Mean 16.3 mm, range 8 – 20 mm	≥5 mm
Iyer RS et al. [44]	R	RFA	HCC (20), metastatic (19)	29 (39)	-	≥10 mm
Jiang C et al. [23]	R	RFA	HCC	134 (159)	Mean 20 ± 9 mm, range 10 – 49 mm	≥5 mm
Kamei S et al. [70]	R	RFA	HCC	19 (22)	Mean 17.5 ± 7.9 mm, range 9 – 34 mm	≥5 mm
Kang TW et al. [71]	R	RFA	HCC	211 (211)	Mean 21 mm	≥5 mm

Table 1: *Characteristics of all clinical studies included.* **(continued)**

Authors	Study type (Retrospective R, Prospective P)	Ablation method	Tumor Type	Number of patients (tumors)	Tumor size	Intended MAM
Kaye EA at al. [45]	R	RFA	CRLM	72 (93)	Mean 18 mm, range 6 - 55 mm	-
Keil S et al. [40]	R	RFA	BCLM (15), CRLM (35)	25 (50)	-	-
Keil S et al.[41]	R	RFA	BCLM (15), CRLM (35)	25 (50)	Mean 23 mm	-
Kim KW et al. [49]	R	RFA	HCC	31 (38)	Mean 19 mm, range 10 – 35 mm	-
Kim SM et al. [17]	P	RFA	HCC	33 (42)	Mean 15.8 ± 5.9, range 7 - 33 mm	-
Kim YS et al. [6]	P	RFA	HCC	103 (110)	Mean 27 ± 6 mm, range 21 – 48 mm	≥5 mm
Kobe A et al. [24]	R	RFA	HCC	39 (43)	Median 16.9 mm, range 14.6 – 22.4 mm	-
Koh YH et al. [18]	R	RFA	HCC	64 (75)	Mean 14.0 ± 4.6 mm, range 10 - 37 mm	≥5 mm
Laimer G et al. [7]	R	RFA	HCC	110 (176)	Mean 25.2 ± 14.9 mm	-
Lee JK et al. [63]	R	RFA and MWA	HCC (49) and metastatic (26)	65 (75)	Range 10 – 65 mm	-
Lee MW et al. [72]	R	RFA	HCC	18 (19)	Mean 25 mm, median 23 mm, range 20 – 42 mm	≥5 mm
Li X et al. [73]	R	MWA	NPC metastases	18 (24)	Maximum diameter of 42 mm	≥5 mm
Liao M et al. [25]	P	RFA	HCC	80 (83)	Mean 24.5 mm	≥5 mm
Liu ZY et al. [74]	P	RFA	CRLM	12 (20)	Mean 28 mm, range 15 – 52 mm	≥5 mm
Makino Y et al. [27]	R	RFA	HCC	85 (94)	Mean 14.0 ± 5.2 mm	-
Makino Y et al. [26]	R	RFA	HCC	67 (92)	Median 12.9 mm, range 4.8 – 41.4 mm	-
Motoyama T et al. [19]	R	RFA	HCC	66 (95)	Median 18 mm, range 7 – 33 mm	≥5 mm
Park J et al. [28]	R	RFA	HCC	178 (178)	Mean 17.3 ± 6.1 mm	-
Park SI et al. [75]	R	RFA	HCC (15), rectosigmoid metastases (1), CCA (1)	15 (17)	Mean 15.68 ± 5.29 mm, range 10 – 26 mm	≥10 mm
Park Y et al. [20]	R	RFA	HCC	146 (167)	Mean 19 mm, median 18 mm, range 8 – 40 mm	≥5 mm

Table 1: *Characteristics of all clinical studies included.* **(continued)**

Authors	Study type (Retrospective R, Prospective P)	Ablation method	Tumor Type	Number of patients (tumors)	Tumor size	Intended MAM
Passera K et al. [42]	R	RFA	HCC (5), metastatic (5)	10 (10)	Range 10-40 mm	-
Ringe KI et al. [21]	R	RFA and MWA		32 (48)	Mean 24 mm, range 9 – 64 mm	-
Sakakibara M et al. [29]	R	RFA	HCC	84 (139)	Mean 13.8 ± 4.6 mm	≥5 mm
Shin S et al. [30]	P	RFA	HCC	150 (150)	Mean 19.5 ± 7.9 mm	≥5 mm
Sibinga Mulder BG et al. [9]	R	RFA	CRLM	29 (29)	Median 22 mm, range 8 – 22 mm	≥5 mm
Solbiati M et al. [31]	R	MWA	HCC	50 (90)	Mean 27 ± 20 mm	≥5 mm
Sotirchos VS et al. [35]	P	RFA	CRLM	47 (67)	Mean 21 mm, range 6 – 43 mm	≥5 mm
Takeyama N et al. [32]	R	RFA	HCC	29 (59)	Mean 11.2 ± 4.4 mm, range 5 – 24 mm	≥3 mm
Van Tilborg AA et al. [76]	R	RFA and MWA	HCC (7), CRLM (29), CCA (2)	20 (38)	Mean 22 mm	≥5 mm
Tinguely P et al. [33]	R	MWA	HCC (174), CRLM (87), NET (17), other (23)	153 (301)	Median 15 mm, IQR 11 - 21 mm	≥5 mm
Vandenbroucke F et al. [34]	R	RFA	CRLM (16), melanoma metastases (3), BCLM (1)	20 (45)	Mean 18.6 mm, median 18 mm, range 6 – 41 mm	-
Vo Chieu VD et al. [77]	R	MWA	HCC/CCA* (97), metastases (77)	94 (174)	Median 19 mm, range 4 – 51 mm	≥5 mm
Vo Chieu VD et al. [43]	R	MWA	HCC (17), CCA (3), metastases (20)	27 (40)	Mean 17.3 ± 6.5 mm, range 6 – 31.5 mm	≥5 mm
Wang XL et al. [52]	R	RFA	HCC	52 (62)	Mean 20 ± 10 mm, range 10 – 31 mm	-
Yan Y et al. [78]	R	RFA and MWA	Primary (7), secondary (7)	12 (14)	Mean 16.6 ± 13.4 mm, range 3 – 45 mm	≥5 mm
Yoon JH et al. [79]	P	RFA	HCC	36 (43)	Mean 24.5 mm, range 20 – 47 mm	≥5 mm
Yoon JH et al. [36]	P	RFA	HCC	68 (88)	Mean 16 mm ± 6 mm, range 6 – 32 mm	≥5 mm
Zhang Q et al. [80]	R	RFA	HCC (29), CCA (1), CRLM (9), OCLM (2), PNET metastases (1)	37 (37)	Mean 26.6 ± 15.1 mm, range 9.1 - 66.7 mm	≥5 mm

*RFA: radiofrequency ablation. MWA: microwave ablation. HCC: hepatocellular carcinoma. CRLM: colorectal liver metastasis. BCLM: breast cancer liver metastasis. CCA: cholangiocarcinoma. GEP-NET: gastroenteropancreatic neuroendocrine tumors. NET: neuroendocrine tumors. NPC: nasopharyngeal carcinoma. OCLM: ovarian cancer liver metastases. PNET: primitive neuroectodermal tumor. MAM: minimal ablative margin. *Not further specified, considered 50% HCC and 50% CCA*

Table 2: *Methodology of ablation margin analysis.*

Article	Modality	Pre- and post-ablation image analysis			MAM measurements			Other treatment success measures	
		Side-to-side	Co-registration software	Ablation margin quantification software	In axial plane	In 3 orthogonal planes	In 3D (oblique angles)	Ablation surface area	Volumetric ablation margin data
Biondetti P et al. [13]	CT and MRI	+	-	-	+	+	-	-	-
Choi JW et al. [14]	CT and MRI	+	-	-	-	-	-	-	-
Fukuda K et al. [15]	CT	+	-	-	+	-	-	-	-
Iwazawa J et al. [16]	CT	+	-	-	+	+	-	-	-
Kim SM et al. [17]	CT and MRI	+	-	-	+	+	-	-	-
Koh YH et al. [18]	CT	+	-	-	+	-	-	-	-
Motoyama T et al. [19]	CT	+	-	-	+	+	-	+	-
Park Y et al. [20]	CT	+	-	-	+	+	-	+	-
Ringe KI et al. [21]	CT and MRI	+	-	-	+	-	-	-	-
Wang X et al. [5]	CT	+	-	-	+	+	-	-	-
Sotirchos et al. [35]	CT	+	-	-	+	+	-	-	-
Abdel-Rehim M et al. [11]	CT and CBCT	-	+	-	+	+	-	-	-
An C et al. [12]	MRI	-	+	-	+	+	+	-	+
Hendriks P et al. [8]	CT	+	+	-	+	+	+	-	-
Kim YS et al. [6]	CT	-	+	-	+	+	-	-	-
Kobe A et al. [24]	CT and MRI	-	+	-	-	-	+	-	+
Laimer G et al. [7]	CT	-	+	-	-	-	+	-	-
Liao M et al. [25]	CT	-	+	-	+	+	-	-	-

Table 2: *Methodology of ablation margin analysis.* **(continued)**

Article	Modality	Pre- and post-ablation image analysis			MAM measurements			Other treatment success measures	
		Side-to-side	Co-registration software	Ablation margin quantification software	In axial plane	In 3 orthogonal planes	In 3D (oblique angles)	Ablation surface area	Volumetric ablation margin data
Makino Y et al. [27]	CT	-	+	-	+	-	-	-	-
Makino Y et al. [26]	CT and MRI	+	+	-	+	+	-	-	-
Park J et al. [28]	CT and MRI	+	+	-	+	+	+	-	-
Sakakibara M et al. [29]	CT and MRI	-	+	-	+	+	-	-	-
Shin S et al. [30]	CT	-	+	-	+	+	-	-	-
Takeyama et al. [32]	MRI	-	+	-	-	-	-	-	-
Tinguely P et al. [33]	CT	-	+	-	-	+	-	-	-
Vandenbroucke F et al. [34]	CT	-	+	-	+	+	-	-	-
Hocquelet A et al. [22]	MRI	-	+	+	-	-	+	+	+
Jiang C et al. [23]	CT	-	+	+	-	-	+	-	-
Sibinga Mulder BG et al. [9]	CT	-	+	-	-	-	+	-	-
Solbiati M et al. [31]	CT	-	+	+	-	-	+	-	+
Yoon JH et al. [36]	CT and MRI	-	+	-	-	-	+	-	-

CT: computed tomography. CBCT: cone-beam computed tomography. MRI: magnetic resonance imaging. MAM: minimal ablation margin.

Table 3: *Specifications of segmentation algorithms used.*

Used in article	Used imaging modality	Commercial software	Used for:	Automation of segmentation	(Semi-) automatic segmentation algorithm used	Evaluation of segmentation	Performance
			T = tumor AZ = ablation zone B = both	M = manual SA = semi-automatic FA = fully automatic			
Egger J et al. [38]	CT	-	AZ	SA	Interactive, graph-based contouring approach with preference for spherically shaped regions.	Dice similarity coefficient (DSC)	DSC = 77.1
Egger J et al. [37]	CT	-	AZ	SA	Interactive, graph-based contouring approach with preference for spherically shaped regions.	Dice similarity coefficient (DSC)	DSC = 77.0
Hame Y et al. [39]	CT	-	T	SA	Non-parametric intensity distribution estimation and hidden Markov measure field model, with application of a spherical shape prior.	Volumetric overlap error (VOE), Volume difference (VD), Symmetric surface distance (SD), Root mean square symmetric volume distance (RD), Maximum symmetric surface distance (MD)	OE= 29.60 ± 5.61 VD= 17.75 ± 11.40 SD= 0.89 ± 0.31 RD= 1.24 ± 0.42 MD= 5.12 ± 2.75
Hendriks P et al. [8]	CT	Mirada RTx	B	SA	Greyscale based delineation tool	Cohen's kappa statistics	K=0.88
Hocquelet A et al. [22]	MRI	ITK-SNAP freeware	B	SA	Region-competition snakes	-	-
Iyer RS et al. [44]	CT and MRI	Adope Photoshop CS v8.0	B	M	Magnetic lasso tool	-	-
Kaye EA et al. [45]	CT and MRI	MIM MEASTRO	B	SA	Seed point based region growing	-	-

Table 3: *Specifications of segmentation algorithms used.* **(continued)**

Used in article	Used imaging modality	Commercial software	Used for:	Automation of segmentation	(Semi-) automatic segmentation algorithm used	Evaluation of segmentation	Performance
			T = tumor AZ = ablation zone B = both	M = manual SA = semi-automatic FA = fully automatic			
Keil S et al. [41]	CT	SyngoCT Oncology, Siemens Healthcare	B	SA	Supervised seeded region growing algorithm	Lin's concordance correlation coefficient for volume (V), CT value (D)	V_{tumor}: 0.98 (0.97 – 0.99) D_{tumor}: 0.90 (0.83 – 0.94) $V_{ablation}$: 0.99 (0.95 – 0.99) $D_{ablation}$: 0.76 (0.62 – 0.85)
Keil S et al. [40]	CT	Syngo Oncology NNWP VE 31 H (Siemens Medical Solutions)	B	SA	Supervised seeded region growing algorithm	Lin's concordance correlation coefficient for volume (V), CT value (D)	V_{tumor}: 0.98 (0.97 – 0.99) D_{tumor}: 0.90 (0.83 – 0.94) $V_{ablation}$: 0.99 (0.98 – 0.99) $D_{ablation}$: 0.76 (0.62 – 0.85)
Passera K et al. [42]	CT	-	B	SA	Clustering based algorithm	Percentage Match (PM), Positive predictivity (PP), Negative predictivity (NP), Specificity (SPEC),	PM_{tumor}: 92% PP_{tumor}: 95% NP_{tumor}: 94% $SPEC_{tumor}$: 96% $PM_{ablation}$: 90% $PP_{ablation}$: 96% $NP_{ablation}$: 93% $SPEC_{ablation}$: 97%

Table 3: *Specifications of segmentation algorithms used.* **(continued)**

Used in article	Used imaging modality	Commercial software	Used for:	Automation of segmentation	(Semi-) automatic segmentation algorithm used	Evaluation of segmentation	Performance
			T = tumor AZ = ablation zone B = both	M = manual SA = semi-automatic FA = fully automatic			
Sibinga Mulder BG et al. [9]	CT	Mirada RTx	B	SA	Greyscale based delineation tool	-	-
Vo Chieu VD et al. [43]	CT	SAFIR (Software Assistant For Interventional Radiology)	AZ	SA	Combined threshold-based and model-based morphological processing.	Pearson correlation	$r_{max\_diameter1}$: 0.715 $r_{max\_diameter2}$: 0.659 $r_{ellipticity}$: 0.707 $r_{volume:}$ 0.978
Solbiati M et al. [31]	CT	Ablation-fit	B	SA		-	-

CT = computed tomography, MRI = magnetic resonance imaging

Table 4: *Specifications of software used for co-registration and ablation margin quantification.*

Name of software	Used in article	Used imaging modality	Commercially available	Dedicated for ablation margin quantification	Co-Registration method	Automation of co-registration	Uses landmarks	Evaluation of co-registration
					R = rigid NR = non-rigid	M = manual SA = semi-automatic FA = fully automatic	+ = landmarks based o = optional - = no landmarks used	
HepaCare	Kobe A et al. [24]	CT/MRI	Prototype	-	NR	(S)A	O	Visual
HepaCare	Kim KW et al. [49]	CT-CT	Prototype	-	NR	(S)A	O	Visual; co-registration error
HepaCare	Yoon JH et al. [36]	CT-MRI	Prototype	-	NR	(S)A	O	Visual
HepaCare 3.0	Park J et al. [28]	CT-MRI	Prototype	-	NR	-	-	-
In house	An C et al. [12]	MRI-MRI	-	-	NR	FA	-	Similarity metric between paired regions
In house	Boulkhrif H et al. [46]	CT-CT	-	-	NR	SA	-	Target co-registration error
In house	Gunay G et al. [48]	CT-CT	-	-	NR	(S)A	O	DICE overlap; Average surface distance
In house	Passera K et al. [42]	CT-CT	-	-	NR	FA	-	-
In house	Wei D. [53]	CT-MRI/CT-CT	-	-	R and NR	FA	-	Dice ratios and target co-registration error
In house	Gunay G et al. [47]	CT-CT	-	-	NR	SA	+	Average surface distance

Table 4: *Specifications of software used for co-registration and ablation margin quantification.* **(continued)**

Name of software	Used in article	Used imaging modality	Commercially available	Dedicated for ablation margin quantification	Co-Registration method	Automation of co-registration	Uses landmarks	Evaluation of co-registration
					R = rigid NR = non-rigid	M = manual SA = semi-automatic FA = fully automatic	+ = landmarks based o = optional - = no landmarks used	
In house	Luu HM et al. [50]	CT-CT	-	-	NR	FA	-	Dice similarity coefficient (DSC), mean surface distance (MSD), mean corresponding difference (MCD) between landmarks.
In house	Luu HM et al. [51]	CT-CT	-	-	NR	SA	O	Dice similarity coefficient (DSC), mean surface distance (MSD), mean corresponding difference (MCD) between landmarks.
In house	Luu HM et al. [54]	CT-CT	-	-	NR	SA	-	Dice Similarity Coefficient
Integrated Registration, GE Healthcare	Makino Y et al. [27]	CT-CT	+	-	R	SA	-	Landmark based co-registration error
Integrated Registration, GE Healthcare	Makino Y et al. [26]	CT-CT/MRI-MRI	+	-	R	M	+	Landmark based co-registration error
Integrated Registration, GE Healthcare	Vandenbroucke F et al. [34]	CT-CT	+	-	R	(S)A	O	Visual

Table 4: *Specifications of software used for co-registration and ablation margin quantification.* **(continued)**

Name of software	Used in article	Used imaging modality	Commercially available	Dedicated for ablation margin quantification	Co-Registration method	Automation of co-registration	Uses landmarks	Evaluation of co-registration
					R = rigid NR = non-rigid	M = manual SA = semi-automatic FA = fully automatic	+ = landmarks based o = optional - = no landmarks used	
MIM MAESTRO	Kaye EA et al. [45]	CT-CT/CT-MRI	+	-	R	SA	O	Visual, co-registration error
Mirada RTx	Hendriks P et al. [8]	CT-CT	+	-	NR	SA	O	Visual
Mirada RTx	Sibinga Mulder BG et al. [9]	CT-CT	+	-	NR	SA	+	Visual
MyLab Twice, Esoate	Wang XL et al. [52]	MRI-MRI	+	-	R	M	+	Visual
Syngo.via VB20A, Siemens Healthineers	Laimer G et al. [7]	CT-CT	+	-	R	(S)A	O	Visual
Virtual Place Advanced Plus version 2.03 (CT workstation)	Kim YS et al. [6]	CT-CT	+	-	R	M	+	Visual
Volume Analyzer Synapse VINCENT, version 5.1, Fujifilm Medical Systems,	Takeyama N et al. [32]	MRI-MRI	+	-	R	(S)A	O	Visual
-	Iyer RS et al. [44]	CT-CT/MRI-MRI	-	-	R	M	+	Visual
Ablation-Fit	Solbiati M et al. [31]	CT-CT	+	+	R and NR	A	-	-

CT= computed tomography, MRI = magnetic resonance imaging

Table 5: *Tissue shrinkage*

Authors	Ablation method	Study subjects (number of tests)	Contraction ratio	Tissue shrinkage [%]
Amabile C et al. [55]	RFA	Ex vivo bovine (n = 6)	0.88 ± 0.05	
	MWA	Ex vivo bovine (n = 4)	Radial: 0.83 Longitudinal: 0.82	Radial: 20.5 Longitudinal: 22.5
Brace CL et al. [56]	RFA	Ex-vivo porcine (n = 20)		In 1 diameter: 15
	MWA	Ex-vivo porcine (n = 8)		In 1 diameter: 30
Bressem KK et al. [61]	MWA	In-vivo porcine (n = 10)		4
Erxleben C et al. [62]	MWA	In-vivo porcine (n = 19)		1-12
Farina L et al. [10]	MWA	Ex-vivo bovine Ex-vivo turkey muscle (total: n = 119)		28-74
Lee JK et al. [63]	MWA	In-vivo human (n = 31)	Absolute ablation zone: 2.45 ± 0.47 Absolute tumor: 2.37 ± 0.28 mm	
	RFA	In-vivo human (n = 44)	Absolute ablation zone: 0.94 ± 0.38 mm Absolute tumor: 0.55 ± 0.26 mm	
Liu D et al. [57]	MWA	Ex-vivo bovine (n = 6)		Radial: 10 Longitudinal: 20 Volumetric:40
Liu D et al. [60]	MWA	Ex-vivo porcine (n = 16)		Radial: 11-35
Rossmann C et al. [58]	RFA	Ex-vivo porcine (n = 35)		12.3 – 21.7
Weiss N et al. [59]	MWA	Ex-vivo porcine (n = 16)	Planar strain: 10 min: 0.97 ± 0.02 1,2,3, 6 min: all >1	

RFA = radiofrequency ablation, MWA = microwave ablation

Chapter 4

Quantitative volumetric assessment of ablative margins in hepatocellular carcinoma: Predicting local tumor progression using non-rigid registration software

Authors

P. Hendriks, W. A. Noortman, T. R. Baetens, A. R. van Erkel, C. S. P. van Rijswijk, R. W. van der Meer, M. J. Coenraad, L. F. de Geus-Oei, C. H. Slump, and M. C. Burgmans

Published

Journal of Oncology, 2019, *DOI: 10.1155/2019/4049287*

ABSTRACT

Purpose After radiofrequency ablation (RFA) of hepatocellular carcinoma (HCC), pre- and post-interventional contrast-enhanced CT (CECT) images are usually qualitatively interpreted to determine technical success, by eye-balling. The objective of this study was to evaluate the feasibility of quantitative assessment, using a non-rigid CT-CT co-registration algorithm.

Materials and Methods 25 patients treated with RFA for HCC between 2009 and 2014 were retrospectively included. Semi-automated co-registration of pre- and post-treatment CECT was performed independently by two radiologists. In scans with a reliable registration, the tumor and ablation area were delineated to identify the side and size of narrowest RFA margin. In addition, qualitative assessment was performed independently by two other radiologists to determine technical success, and the anatomical side and size of narrowest margin. Interobserver agreement rates were determined for both methods and the outcomes were compared with occurrence of local tumor progression (LTP).

Results CT-CT co-registration was technically feasible in 18/25 patients with almost perfect inter-observer agreement for quantitative analysis (κ=0.88). The inter-observer agreement for qualitative RFA margin analysis was κ=0.64. Using quantitative assessment, negative ablative margins were found in 12/18 patients, with LTP occurring in 8 of these patients. In the remaining 6 patients, quantitative analysis demonstrated complete tumor ablation and no LTP occurred.

Conclusion Feasibility of quantitative RFA margin assessment using non-rigid co-registration of pre- and post-ablation CT is limited, but appears to be a valuable tool in predicting LTP in HCC patients (p=0.013).

Key words: Radiofrequency ablation; ablative margins; hepatocellular carcinoma; local tumor progression; non-rigid co-registration

INTRODUCTION

Radiofrequency ablation (RFA) has been recognized as first line treatment for very early stage hepatocellular carcinoma (HCC) (lesion diameter <2 cm), and is used as treatment for unresectable early stage HCC (solitary lesion, or a maximum of 3 lesions with a diameter ≤3 cm each), according to the Barcelona Clinic for Liver Cancer (BCLC) staging system [1, 2]. As a result of the implementation of surveillance in high-risk populations, diagnosis of BCLC very early- or early stage HCC is now feasible in up to 60% of all new HCC cases in developed countries [3]. This makes RFA an increasingly used treatment modality. Recurrence rates for RFA in very early stage HCC patients are comparable to those after surgical treatment [1]. However, higher recurrence rates are found in patients treated for larger HCC lesions [4-6].

After RFA treatment, two types of intrahepatic recurrences may occur. Local tumor progression (LTP) is found in up to 50% of ablations [7], and is known to be associated with insufficient ablative margin, large tumor size, blood vessels in the direct proximity of the tumor, and adhesion of viable tumor cells to the RFA electrodes [8]. Distant intrahepatic recurrence is related more to systemic parameters, such as the presence of vascular invasion, multifocal disease, elevated alpha-fetoprotein blood levels, and hepatitis C viral infection [9].

The preferred treatment for early-stage HCC is surgical resection. However, many patients are not eligible for this treatment, due to cirrhosis with portal hypertension, unfavorable tumor location, and/or comorbidities [1, 10]. Thermal ablation is considered as the treatment of choice for unresectable early-stage HCC. Distant intrahepatic recurrence rates after resection and ablation are similar, but LTP rates are higher after ablation and negatively affect overall survival [4-6, 11]. To improve the results of RFA in unresectable early stage HCC, a reduction of LTP rates appears to be crucial.

Histological confirmation of total tumor necrosis after RFA is not possible. In many centers, the current workflow involves qualitative assessment of RFA margins by scrolling through pre- and post-interventional images, separately. Technical success is considered when a predefined amount of energy is successfully delivered to the tumor, and complete tumor coverage with sufficient ablative margins is confirmed on contrast-enhanced computed tomography (CECT) [8]. In general, an ablative margin of >5 mm, or ideally 10 mm, is recommended [8]. These values are rather arbitrarily derived from surgical standards, and supported by some studies [10-12]. However, the evidence is limited, and no standardized way of ablative margin assessment is currently available.

Supportive ablation verification software has gained interest. However, at this moment, software dedicated to quantitative ablation margin assessment is lacking and available

software has not been validated in large patient cohorts. Merging of pre- and post-ablation scans can be performed using either non-rigid or rigid co-registration software. Non-rigid co-registration algorithms allow more degrees of freedom in the transformation to fit a scan better onto another. Besides global linear transformations, like translation and rotation, the algorithm may e.g. use radial basis functions or other free form deformation models that allow for local warping of the image to find a better registration. Mirada RTx (Mirada Medical Ltd., Oxford, UK) is a software application developed for radiation therapy treatment planning, that uses non-rigid registration of medical image datasets including computed tomography (CT) and magnetic resonance imaging (MRI). This software was used in this study.

The primary objective of this study was to assess the feasibility of quantitative three dimensional (3D)- margin assessment after non-rigid CT-CT co-registration of pre- and post-interventional imaging, using Mirada RTx. Secondary objectives were to compare quantitative ablative margin assessment with the current workflow of qualitative assessment, and to assess whether quantitative assessment allows prediction of local tumor progression.

METHODOLOGY

Patients

All patients that were consecutively treated with RFA for de novo HCC between January 2009 and March 2014 (n=79) in our institution were identified retrospectively. The diagnosis of HCC was based on either histology or radiological findings according to European Association for the Study of the Liver (EASL) criteria (arterial enhancing lesion >1 cm with washout on the late phase on CT or MRI). Exclusion criteria were: multifocal disease (n=27), surgical approach (n=4), adjuvant trans-arterial chemoembolization (TACE) (n=7), lateral patient positioning on the post-ablation scan (n=11) and extensive metal artifacts caused by in-vivo RFA probes (n=5). Finally, 25 patients were included in this study. Baseline characteristics of this cohort are shown in Table 1. Pre- and post-ablation multi-phase CECT scans with an arterial and portal-venous phase were available for all patients.

RFA procedure

Percutaneous RFA procedures were performed under general anesthesia, and with image guidance of ultrasound and/or CT. Based on tumor size and availability, one of the single electrode RFA systems (3 cm exposed tip Cooltip (Covidien Ltd., Gosport Hamspire, United Kingdom) or StarBurst XL (AngioDynamics, Amsterdam, Netherlands)), or multiple electrode RFA system (3 or 4 cm exposed tip Cooltip with switch control system (Covidien Ltd.)) was used. The ablation time was set 12 minutes for single Cooltip electrode, and 16 minutes for the multiple Cooltip electrodes. Temperature-based ablation was performed with the StarBurst XL electrode.

Table 1 *Patient characteristics of analyzed patients*

		n	
total		25	
age	mean (SD)	62,1	11.8
sex	male	20	80.0%
	female	5	20.0%
Cirrhosis presence	yes	25	100.0%
	no	0	0.0%
Ascites presence	yes	7	28.0%
	no	18	72.0%
Etiology	Hepatitis B	2	8.0%
	Hepatitis C	8	32.0%
	Alcohol abuse	15	60.0%
	NASH	2	8.0%
	Cryptogenic	1	4.0%
ECOG	0	24	96.0%
	1	1	4.0%
Child-Pugh	A	12	48.0%
	B	13	52.0%
	C	0	0.0%
BCLC	very early	10	40.0%
	early	15	60.0%
lesion size (mm)	median (range)	20	12-45
year of RFA	2009-2011	10	31.3%
	2012-2014	15	46.9%

NASH = Non-alcoholic steatohepatitis, ECOG = Eastern Cooperative Oncology Group, BCLC = Barcelona Clinic for Liver Cancer, RFA = Radiofrequency ablation. More etiological factors could be present in one patient.

Immediately after ablation, a CECT of the liver was performed on a 16-slice spiral CT (Aquillion-16, Toshiba, Tokyo, Japan) with the settings: 120 kV, rotation 0.5 s, 16×1 mm scanning. Dose weight dependent Ultravist 370 contrast agent, or Xenetex 350 contrast agent was used with a 15 seconds and 75 seconds delay after bolus triggering for arterial and portal venous phase, respectively. Consequently, the CECT scans were qualitatively evaluated for technical success. The ablation was considered technically successful if the coagulation area fully encompassed the tumor in the absence of residual tumor enhancement. This assessment was done by visual comparison of the tumor location on preprocedural CT and area of necrosis on the postprocedural CT ('eye-balling'), and 2D measurements.

Follow-up

All patients underwent blood tests (including alpha-fetoprotein), and CECT every three months after treatment. Upon discretion of the referring physician or interventional radiologist, multiphase MRI was used instead of CECT. Liver explants of patients that underwent an orthotopic liver transplantation (OLTx) were pathologically examined for local tumor progression. The median follow-up time was 9,5 months.

Scoring

CT-CT registration and delineation of the tumor volume and RFA ablation volume were performed in Mirada RTx software. Two radiologists independently performed the CT-CT co-registration and delineation of the tumor and RFA ablation volume, while being blinded for follow-up information. CT-CT co-registration was performed using a semi-automated non-rigid registration. Manual alterations were possible by rotation and translation of a scan, or with use of a rigid landmark algorithm. The registration performance was graded on a 5-points scale (1 = completely unreliable co-registration, 2 = suboptimal co-registration, 3 = sufficient quality of co-registration, but not accurate enough for measurements in mm, 4 =good co-registration, 5 =perfect co-registration). Patients with co-registration performances of 1-3 were excluded from further analysis.

A greyscale-based semi-automatic delineation tool was used with manual adjustments for segmentation of the tumor and ablation volume. RFA margins were quantitatively assessed in a fused image window. The narrowest margin (in mm), as well as the anatomical location of the narrowest margin or largest tumor residue was determined. Inter-observer agreement was determined for the categorical assessment of margin size (1: negative, 2: 0 to 5 mm, or 3: ≥5 mm). A 'negative' margin was defined as: tumor extending beyond the boundaries of the ablation zone on the overlay of pre- and post-ablation CT. This would not necessarily mean that the tumor was incompletely ablated. The ablation may have caused tissue shrinkage and as a result the ablation area may be smaller than the tumor even when the tumor was completely ablated. The side of LTP occurrence was correlated with the side of the minimal ablative margin or largest tumor residual. A comparison of patient characteristics between those with and without LTP was performed.

Two other radiologists independently repeated the qualitative assessment of the pre- and post-ablation scans for technical success, and determined categorical ablative margins (1: negative, 2: 0 to 5 mm, or 3: ≥5 mm), while being blinded for follow-up information. Also, the anatomical side of narrowest margin was recorded. Inter-observer agreement was determined for technical success and margin size. In both the quantitative and the qualitative assessment, a consensus re-evaluation took place by the two radiologists for determining technical success for cases they initially disagreed on.

Statistics

Inter-observer agreement was determined with use of unweighted Cohen's Kappa statistics. A κ of 0 meant that the agreement was similar to chance, whereas a κ of 1 meant perfect agreement [13].

Continuous data were analyzed with the independent t-test and categorical data with the chi-square test. SPSS version 23.0 was used to perform the data analysis, and a significance interval of 5% was used. Boxplots were created using GraphPad Prism 5 (GraphPad Software, San Diego, California, USA).

RESULTS

Patients

The co-registration quality of pre- and post-ablation scans was rated ≤3 in 7/25 (28.0%) patients, who were therefore excluded for further analysis. Table 2 shows all patient and tumor characteristics of the 18 remaining cases that were technically feasible for quantitative analysis.

Scoring

The inter-observer agreement for *quantitative* assessment with use of CT-CT co-registration and delineation was almost perfect, with a κ of 0.88 (SE: 0.12 and p <0.01). Categorical agreement on the minimal margin size (negative, 0 to 5 mm, or ≥5 mm) was similar with a κ of 0.88 (SE: 0.12 and p <0.01). A consensus re-evaluation of one case lead to agreement on technical success that the radiologists initially disagreed on.

The inter-observer agreement of two radiologists who *qualitatively* assessed the ablative margins was moderate: 0.64 (SE: 0.33 and p< 0.01). Agreement on categorical margin assessment was very poor (negative, 0 to 5 mm, or ≥5 mm) with a κ of 0.24 (SE of 0.28 and p= 0.16). Consensus was reached between the observers on technical success for two cases that they initially disagreed on, for further analysis.

Local tumor progression rate

In 8 out of 18 patients (44.4%), LTP was found, either radiologically (5/8), or histologically after OLTx (3/8). In 1 (5.6%) patient, distant intrahepatic recurrence was found. Out of the 10 (55.6%) patients who did not develop recurrence, 3 underwent OLTx within 1 year after RFA (average 9.3 months).

Table 2 *Patient characteristics of patients technically feasible for quantitative analysis*

		Total		No LTP		LTP		
		n		n		n		*p-value*
Total		**18**		10		8		
Age	mean (SD)		**64.9 (9.0)**		66.1 (10.7)		63.4 (6.5)	*0.538*
Sex	male	**14**	**77.8%**	7	70.0%	7	87.5%	*0.375*
	female	**4**	**22.2%**	3	30.0%	1	12.5%	
Cirrhosis presence	yes	**18**	**100.0%**	10	100.0%	8	100.0%	
	no	**0**	**0.0%**	0	0.0%	0	0.0%	
Ascites presence	yes	**5**	**27.8%**	3	30.0%	2	25.0%	*0.814*
	no	**13**	**72.2%**	7	70.0%	6	75.0%	
Etiology	Hepatitis B	**0**		0		0		
	Hepatitis C	**4**		2		2		*0.800*
	Alcohol abuse	**5**		2		3		*0.410*
	NASH	**2**		2		0		*0.180*
	Cryptogenic	**1**		0		1		*0.250*
ECOG	0	**17**	**94.4%**	10	100.0%	7	87.5%	*0.250*
	1	**1**	**5.6%**	0	0.0%	1	12.5%	
Child-Pugh	A	**9**	**50.0%**	5	50.0%	4	50.0%	*1.000*
	B	**9**	**50.0%**	5	50.0%	4	50.0%	
BCLC	very early	**6**	**33.3%**	3	30.0%	3	37.5%	*0.737*
	early	**12**	**66.7%**	7	70.0%	5	62.5%	
lesion size	median in mm (range)		**22 (12-27)**		22 (12-27)		22 (16-25)	
OLTx <18 months	yes	**6**	**33.3%**	3	30.0%	3	37.5%	*0.737*
	no	**12**	**66.7%**	7	70.0%	5	62.5%	
Distant intrahepatic	yes	**1**	**5.6%**	1	10.0%	0	0.0%	*0.357*
Recurrence	no	**17**	**94.4%**	9	90.0%	8	100.0%	
RFA on Target	yes	**6**	**33.3%**	6	60.0%	0	0.0%	*0.013*
Quantitative assessment	no	**12**	**66.7%**	4	40.0%	8	100.0%	
RFA on Target	yes	**16**	**88.9%**	10	100.0%	6	75.0%	*0.094*
Qualitative assessment	no	**2**	**11.1%**	0		2	25.0%	
year of RFA	2009-2011	**7**	**38.9%**	2	20.0%	5	62.5%	*0.066*
	2012-2014	**11**	**61.1%**	8	80.0%	3	37.5%	

NASH = Non-alcoholic steatohepatitis, ECOG = Eastern Cooperative Oncology Group, BCLC = Barcelona Clinic for Liver Cancer, RFA = Radiofrequency ablation. More etiological factors could be present in one patient.

Differences in patient and tumor characteristics were analyzed between patients who developed LTP (n=8) and patients who did not (n=10). No significant differences were found in patient and tumor characteristics between the groups.

Based on the *quantitative* analysis, RFA necrosis fully encompassed the tumor in 6/18 (33.3%) of all patients, with a mean margin of 0.91 mm (SD: 1.11 range: 0-3 mm). In none of these patients, LTP was found. Out of the other 12 patients, 8 (66,7%) developed LTP (5 cases of LTP were identified radiologically, and 3 cases of LTP were pathologically proven after OLTx). LTP was associated with insufficient ablative margins, with a p-value of 0.013. All patients who developed local tumor progression, did so at (one of) the anatomical side(s) with a negative ablative margin. An example of the entire work-up and occurrence of local recurrence at a negative ablative margin is shown in Figure 1.

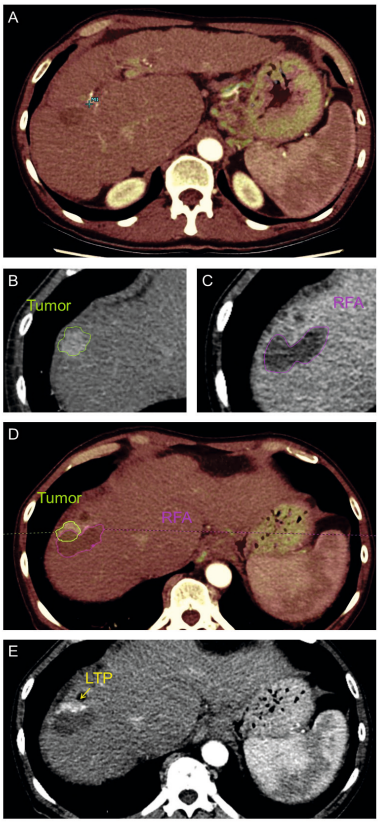

Figure 1 *Image analysis protocol.* **A:** *registration (overlay) of pre-interventional and post-interventional CT scans.* **B:** *Semi-automatic delineation of tumor volume.* **C:** *Semi-automatic delineation of RFA volume.* **D:** *Image fusion plane: margin analysis by overlaying pre- and post interventional imaging.* **E:** *Follow-up scan with local tumor progression.*

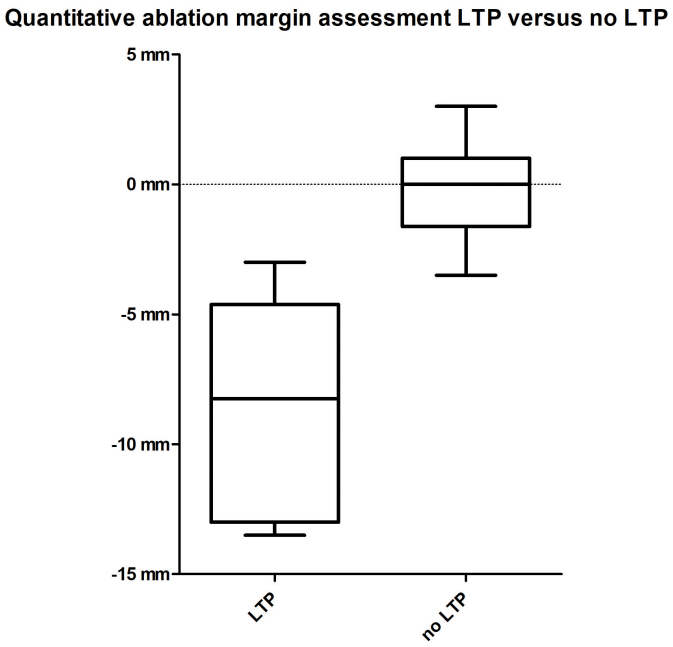

Figure 2 *Boxplot of quantitative ablative margin size for patients with and without local tumor progression (LTP).*

The average minimal ablative margin in all cases was -6,38 mm (SD: 4.64). The ablative margin size significantly correlated to the occurrence of LTP with a p-value of 0.001. The mean ablative margin of patients who developed LTP was -8.44 mm (SD: 4.27), and -0.30 mm (SD: 2.00) for patients who did not, as can be seen in Figure 2.

Based on the qualitative analysis, 16/18 (88.9%) ablation areas fully encompassed the tumor. Yet, 6 of these patients (42.9%) developed LTP during FU. In 2 (11.1%) patients, the observers concluded that the ablation zone did not completely cover the tumor; these two patients did develop LTP.

One patient developed intrahepatic distant metastatic disease within 18 months after treatment. This was a patient with a fully ablated initial tumor with no LTP.

DISCUSSION

In this retrospective pilot study, quantitative ablative margin assessment using MIRADA RTx software was feasible only in selected patients, as in 7 out of 25 patients the performance of co-registration was insufficient. However, high inter-observer agreement rates were found for quantitative assessment in the remaining 18 patients. LTP occurrence correlated with

negative margin sizes with a p = 0.013, indicating a predictive value of quantitative margin assessment.

A disadvantage of minimally invasive HCC treatments is that no pathological confirmation of treatment success can be obtained. The chance on treatment success is generally thought to increase when aiming at safety margins of 5 or 10 mm, to overcome potential heat-transduction variations caused by factors such as heat-sink, tumor heterogeneity, and liver parenchyma fibrosis or cirrhosis. It is challenging to accurately assess the actual ablative margins. The results of this study indicate that conventional qualitative assessment is prone to overestimation of the obtained ablative margins. Only 2 out of 8 patients who developed LTP were identified qualitatively, whereas all 8 patients were identified using quantitative assessment.

Other studies have addressed the potential of quantitative assessment of ablation margins. A rigid registration algorithm was used in the largest study, by Kim et al. [12]. They analyzed 110 HCC tumors, and found a cut-off value of >3 mm as a minimal ablation safety margin. Remarkably, in only 3/110 (2.7%) ablations, the target of 5 mm safety margin was actually met. Smaller studies used a non-rigid registration algorithm similar to ours. In a retrospective study in 31 patients with HCC, non-rigid registration of pre- and post-ablation CT scans using HepaCare software (Siemens, Germany) was feasible with an inter-observer agreement comparable to our findings [14]. In another small cohort study, correlation between margin size and LTP was evaluated in a heterogeneous cohort with different tumor types [15]. In this study, no inter-observer agreement analysis was performed. To our knowledge, the current study has been the first study in which both the feasibility of using a non-rigid registration algorithm, and the correlation between margin size and LTP was reviewed, in a homogeneous HCC population.

As the liver is a deformable organ, a non-rigid registration seems to be more fit for reliable registration. The MIRADA RTx software used in this pilot study is not dedicated for the quantification of ablation margins, but has the tools necessary for delineation and non-rigid registration. For future research, the software should be adopted with the purpose to optimize registration of pre- and post-ablation scans. Adding a step for selecting the liver as volume of interest in which optimal registration should be strived for, may increase the registration success for the purpose of ablation margin measurements.

In the quantitative assessment, none of the patients with a fully ablated tumor developed LTP. Even in those cases where no safety margin was found. However, tissue shrinks during ablation, which influences the quantification of safety margins [16-18]. A 0 mm ablative margin on post-RFA imaging may therefore denote a fully ablated tumor with a few millimeter

of margin, as a result of tissue shrinkage. To be fully able of interpreting treatment success without pathological confirmation, a better understanding in heat conduction and tissue shrinkage would be necessary, as the latter seems to occur in an inhomogeneous, and unpredictable way [16]. Quantification of ablative margins therefore remains arbitrary, as it may not reflect the actual distance between the boundary of the initial tumor and the boundary of the ablation area. To use the software as a decision support tool during ablation procedures, prospective studies in larger patient cohorts are needed to determine the risk of recurrence for different ablation margins, and to set a standard for the optimal ablation margin.

The LTP-rate of 44.4% in this study is comparable to studies with a similar patient population. In a large randomized study that included 701 patients treated with RFA, the HEAT III study, tumor progression rates of 53.3% were found after treatment with RFA in a population with slightly more unfavorable patient and tumor characteristics [19].

The main limitations of this study are its retrospective design and low sample size. Although the initial cohort consisted of 79 patients, only 25 patients were included, of which18 patients were assessable for the final analysis. The majority of patients were excluded for this pilot study to prevent potential bias in follow-up data. Secondary exclusion (7/25 included patients) due to unfeasible registration could potentially be reduced by performing a CT scan immediately before and after the ablation. To optimize co-registration of the CT scans, the scan should be acquired with the patient in an identical position, and during a similar inhalation mode or with use of high-jet ventilation.

Clinically, LTP is not the most valuable outcome measure. This study was designed as pilot study to evaluate software that assesses the completeness of a local treatment. Therefore, LTP was chosen as most relevant parameter for this study rather than survival.

CONCLUSION

Feasibility of co-registration of pre- and post-ablation CT images using Mirada RTx software was found for selected patients (18/25), as difference in position and shape of the liver may hamper reliable image co-registration. For patients in whom co-registration is feasible, the interobserver agreement is high, confirming the robustness of this method. Compared to qualitative assessment, quantitative assessment of ablative margins allows better prediction of LTP and may thus be a better method to determine technical success. To increase the feasibility of CT-CT co-registration as a method to determine the end-point of ablation, there is a need for optimized scanning protocols and dedicated software Prospective studies in larger patient cohorts are needed to better determine the risk of recurrence for different ablation margins and to define a cut-off value for the optimal margin.

REFERENCES

[1] Forner A, Llovet JM, Bruix J. Hepatocellular carcinoma. The Lancet 2012; 379:1245-55.

[2] Livraghi T, Meloni F, Di Stasi M, et al. Sustained complete response and complications rates after radiofrequency ablation of very early hepatocellular carcinoma in cirrhosis: Is resection still the treatment of choice? Hepatology (Baltimore, Md) 2008; 47:82-9.

[3] EASL–EORTC Clinical Practice Guidelines: Management of hepatocellular carcinoma. European Journal of Cancer 2012; 48:599-641.

[4] Lin SM, Lin CJ, Lin CC, Hsu CW, Chen YC. Randomised controlled trial comparing percutaneous radiofrequency thermal ablation, percutaneous ethanol injection, and percutaneous acetic acid injection to treat hepatocellular carcinoma of 3 cm or less. Gut 2005; 54:1151-6.

[5] Morimoto M, Numata K, Kondou M, Nozaki A, Morita S, Tanaka K. Midterm outcomes in patients with intermediate-sized hepatocellular carcinoma: a randomized controlled trial for determining the efficacy of radiofrequency ablation combined with transcatheter arterial chemoembolization. Cancer 2010; 116:5452-60.

[6] Hänsler J, Frieser M, Tietz V, et al. Percutaneous radiofrequency ablation of liver tumors using multiple saline-perfused electrodes. J Vasc Interv Radiol 2007; 18:405-10.

[7] Hori T, Nagata K, Hasuike S, et al. Risk factors for the local recurrence of hepatocellular carcinoma after a single session of percutaneous radiofrequency ablation. Journal of Gastroenterology 2003; 38:977-81.

[8] Crocetti L, de Baere T, Lencioni R. Quality Improvement Guidelines for Radiofrequency Ablation of Liver Tumours. CardioVascular and Interventional Radiology 2010; 33:11-7.

[9] Colecchia A, Schiumerini R, Cucchetti A, et al. Prognostic factors for hepatocellular carcinoma recurrence. World Journal of Gastroenterology : WJG 2014; 20:5935-50.

[10] Nakazawa T, Kokubu S, Shibuya A, et al. Radiofrequency ablation of hepatocellular carcinoma: correlation between local tumor progression after ablation and ablative margin. AJR American journal of roentgenology 2007; 188:480-8.

[11] Liao M, Zhong X, Zhang J, et al. Radiofrequency ablation using a 10-mm target margin for small hepatocellular carcinoma in patients with liver cirrhosis: A prospective randomized trial. Journal of surgical oncology 2017; 115:971-9.

[12] Kim YS, Lee WJ, Rhim H, Lim HK, Choi D, Lee JY. The minimal ablative margin of radiofrequency ablation of hepatocellular carcinoma (> 2 and < 5 cm) needed to prevent local tumor progression: 3D quantitative assessment using CT image fusion. AJR American journal of roentgenology 2010; 195:758-65.

[13] Viera AJ, Garrett JM. Understanding interobserver agreement: the kappa statistic. Family medicine 2005; 37:360-3.

[14] Kim KW, Lee JM, Klotz E, et al. Safety Margin Assessment After Radiofrequency Ablation of the Liver Using Registration of Preprocedure and Postprocedure CT Images. American Journal of Roentgenology 2011; 196:W565-W72.

[15] Tani S, Tatli S, Hata N, et al. Three-dimensional quantitative assessment of ablation margins based on registration of pre- and post-procedural MRI and distance map. International journal of computer assisted radiology and surgery 2016; 11:1133-42.

[16] Farina L, Weiss N, Nissenbaum Y, et al. Characterisation of tissue shrinkage during microwave thermal ablation. International Journal of Hyperthermia 2014; 30:419-28.

[17] Rossmann C, Garrett-Mayer E, Rattay F, Haemmerich D. Dynamics of tissue shrinkage during ablative temperature exposures. Physiological measurement 2014; 35:55-67.

[18] Brace CL, Diaz TA, Hinshaw JL, Lee FT, Jr. Tissue contraction caused by radiofrequency and microwave ablation: a laboratory study in liver and lung. J Vasc Interv Radiol 2010; 21:1280-6.

[19] Tak WY, Lin S-M, Wang Y, et al. Phase III HEAT Study Adding Lyso-Thermosensitive Liposomal Doxorubicin to Radiofrequency Ablation in Patients With Unresectable Hepatocellular Carcinoma Lesions. Clinical Cancer Research 2018; 24.

Chapter 5

Intraprocedural assessment of ablation margins using computed tomography co-registration in hepatocellular carcinoma treatment with percutaneous ablation: IAMCOMPLETE study

Authors

Pim Hendriks, Kiki M van Dijk, Bas Boekestijn, Alexander Broersen, Jacoba J van Duijn-de Vreugd, Minneke J Coenraad, Maarten E Tushuizen, Arian R van Erkel, Rutger W van der Meer, Catharina SP van Rijswijk, Jouke Dijkstra, Lioe-Fee de Geus-Oei, Mark C Burgmans

Published

Diagnostic and Interventional Imaging, 2023, 105(2):57-64, DOI: 10.1016/j.diii.2023.07.002

ABSTRACT

Objective To determine the feasibility of ablation margin quantification using a standardized scanning protocol during thermal ablation (TA) of hepatocellular carcinoma (HCC) lesions, and a rigid registration algorithm. Secondary objectives included to determine the inter- and intra-observer variability of tumor segmentation and quantification of the minimal ablation margin (MAM),.

Materials and Methods Twenty patients (male: n=13; age: 67.1 years ± 10.8 [SD] (range: 49.1-81.1 years)) undergoing thermal ablation for HCC were included. All patients underwent contrast enhanced CT scans (CECT) under general anesthesia directly before and after TA, with preoxygenated breath hold. The scans were analyzed by radiologists using rigid registration software. Registration was deemed feasible if accurate rigid co-registration could be obtained. Inter- and intra-observer rates of tumor segmentation and MAM quantification were determined. MAM values were correlated with local tumor progression (LTP) after 1 year follow up.

Results Co-registration of pre- and post-ablation images was feasible in 80% of patients and 83.4% of lesions. Mean Dice similarity coefficient for inter- and intra-observer variability of tumor segmentation were 0.815 and 0.830, respectively. Mean MAM was 0.63 ± 3.589 mm [SD] (range: -6.26-6.65). LTP occurred in four patients. The mean MAM-value for patients that developed LTP was -4.00 mm, as compared to 0.727 mm for patients who did not develop LTP.

Conclusion Ablation margin quantification is feasible using a standardized scanning protocol. Interpretation of MAM was hampered by the occurrence of tissue shrinkage during TA. Further validation in a larger cohort should lead to meaningful cut-off values for technical success of TA.

Key words: Thermal ablation; Hepatocellular Carcinoma; Ablation margin; Image processing; Computed Tomography; Treatment outcome

INTRODUCTION

Hepatocellular carcinoma (HCC) represents the sixth most common malignancy worldwide and the fourth most common cause of cancer-related mortality. It occurs predominantly in patients with chronic liver disease, in particular cirrhosis [1]. Thermal ablation (TA) is an effective treatment for small HCC lesions and considered the preferred modality for very early stage HCC according to the Barcelona Clinic for Liver Cancer (BCLC) guidelines [2]. For solitary lesions ≤2 cm, the effectiveness is equal to that of surgery but at a lower risk of complications [3-6]. For lesions ≥2 cm surgical resection remains the preferred treatment as local tumor progression (LTP) is more prevalent after thermal ablation with relative risk ratios found up to 1.42 [7].

The most common causes of LTP are insufficient heat propagation resulting in remaining viable tumor tissue at the peripheral parts of the tumor, heat sink due to bordering intrahepatic blood vessels, and the presence of satellite nodules [8]. In order to minimize the risk of LTP after TA, it is generally recommended to achieve a minimal ablation margin (MAM) of ≥5 mm encompassing the tumor [9, 10]. After tumor ablation a contrast enhanced computed tomography (CECT) is acquired to determine whether complete tumor necrosis with sufficient MAM has been achieved. The evaluation is usually based on a qualitative visual interpretation of side-to-side positioned diagnostic imaging and post-ablation CECT, assisted by 2D in-plane measurements using anatomical landmarks.

In an attempt to identify patients at risk of developing LTP, software-assisted ablation margin assessment has found to be a promising tool [11-17]. Such a software tool objectifies the MAM by using co-registration of diagnostic and post-ablation imaging. By segmenting the tumor on the diagnostic scan and the ablation zone on the post-ablation CECT, a three-dimensional volumetric analysis can be performed to determine the MAM after coregistration of the images. Multiple retrospective studies have found a correlation between software-assisted ablation margins and the occurrence of LTP [11-14].

Although software-assisted MAM determination is promising, no standardized or widely validated workflow has been described yet. Co-registration of preprocedural diagnostic images with a post-ablation CECT may result in registration errors as a result of differences in patient positioning, inhalation mode and imaging modality [11]. Moreover, tumor growth in the time interval between diagnostic imaging and TA may cause overestimation of the MAM. Lastly, little is known about the robustness of the co-registration process. Dissimilarities between different operators may occur while segmenting or registering medical images. We hypothesize that standardized acquisition of pre- and post-ablation images contributes to the efficacy of software-assisted ablation margin quantification.

The objective of this study is to investigate the feasibility of ablation margin quantification using a standardized scanning protocol and a rigid registration algorithm. The standardized scanning protocol involves a dual phase CECT acquired during apnea before and after ablation. Secondary objectives were to investigate inter- and intra-observer variability, the time need for CT-CT co-registration, and the correlation between ablation margins and local recurrence.

METHODS

The IAMCOMPLETE study was a prospective, single-arm, single center phase II feasibility study. The study protocol was approved by the institutional medical ethical board, and informed consent was obtained from all patients. The study is registered with number NCT04123340.

Patients

Twenty patients who underwent TA for HCC were recruited for this pilot study. Eligibility for TA and study participation of all patients were discussed in a multidisciplinary tumor board meeting. Inclusion criteria were (very) early stage HCC according to the BCLC staging system (solitary lesion ≤5 cm or a maximum of 3 lesions of ≤3 cm each), general eligibility for percutaneous TA and age of ≥18 years. HCC was diagnosed according to European Association for the Study of the Liver (EASL) guidelines based on histology or The Liver Imaging Reporting and Data System (LI-RADS) imaging characteristics on CT or magnetic resonance imaging (MRI) [18, 19]. Exclusion criteria were an estimated glomerular filtration rate (eGFR) of <30 ml/min/1.73 m^2, morbid obesity (body mass index ≥40) or any pulmonary condition that would be a contraindication to prolonged apnea, Child Pugh C liver cirrhosis, extrahepatic metastasis and uncorrectable coagulopathy. Baseline patient and tumor characteristics were pseudonymized and stored in an encrypted database.

Thermal ablation procedure

Thermal ablation was performed using either radiofrequency ablation (RFA) or microwave ablation (MWA). RFA was performed using Medtronic Cool-tip (single 3 or 4 cm needles, 3 x 3 cm or 3 x 4 cm needles) with up to 6 needle positions and MWA using Medtronic Emprint with thermosphere technology. Factors influencing the choice of ablation technique and settings included tumor size, tumor location, bordering blood vessels and operator preference. Needle positioning was performed using ultrasound guidance, ultrasound-CT/MRI fusion (General Electric LOGIC E9, General Electric, Boston, USA) or CT-guidance.

Scanning protocol

All TA procedures were performed under general anesthesia in a procedure room with a Canon Aquilion-One CT-scanner. Prior to ablation, a CECT was acquired using a patient weight dependent bolus of iodinated contrast agent 350 mg I/ mL (Xenetix 350, Guerbet, Villepinte, France). The full contrast protocol can be found in supplementary table 1. Pre-oxygenated apnea was used while scanning by disconnection of the ventilation tube just before intravenous administration of the contrast agent. CT images were acquired using Sure Start bolus tracking at the descending aorta with a 10 and 50 seconds delay for arterial and venous phase, respectively.

Immediately after TA a second CECT was acquired using the same scan protocol. This CECT was used by the performing interventional radiologist to determine whether technical success was achieved. The ablation was considered successful when the interventional radiologist estimated that a safety margin of >5 mm was obtained based on a qualitative interpretation of the pre- and post-ablation imaging. The quantitative assessment was performed after the procedure and was not used to determine the technical success per-procedurally.

Follow-up

Study participants were followed for one year after TA. The follow-up schedule was similar to all regular TA patients and consisted of blood testing (including alpha-fetoprotein) at 6 weeks after the procedure, complemented with imaging using CECT or MRI every 3-4 months. Adverse events were graded according to the common terminology criteria for adverse events (CTCAE) 5.0 [20].

Software-assisted ablation margin quantification

Two teams performed the software-assisted ablation margin assessment, consisting of a researcher (PH, KMvD) and an a radiologist with 8 or 20 years of experience in abdominal radiology (BB, MCB). In-house built “deLIVERed” software was used, which uses an open-source Elastix-based registration algorithm, which is implemented in MeVisLab [21, 22]. Axial 1 mm slices were used for all analyses.

A schematic overview of the software assisted workflow can be found in Figure 1. In *step 1)* semi-automatic segmentation of the liver volume on the pre-ablation scan is performed to create a “liver mask” as region of interest for image registration. Manual tumor volume segmentation was performed by segmenting the tumor contour on every axial slice. *Step 2)* consisted of a semi-automatic rigid registration of pre- and post-ablation CECT. This step was aided by a projection of the “liver mask” on the post-ablation CECT. After initializing the starting position of the scans onto each other (i.e. dragging the liver mask onto the liver

Table 1 *Characteristics of 20 patients with hepatocellular carcinoma*

		n	
Total		20	
Age	mean ± SD (range)	67.1	± 10.8 (49.4-81.1)
Sex	male	13	65%
	female	7	35%
Cirrhosis	yes	17	85%
	no	3	15%
Etiology of cirrhosis	Hepatitis B	1	6%
	Hepatitis C	1	6%
	Alcohol abuse	14	82%
	NASH	1	6%
Child-Pugh	A	12	88%
	B	5	12%
BCLC	very early	8	40%
	early	10	50%
	intermediate	2	10%
Diagnostic imaging	CT	9	45%
	MRI	11	55%
Prior HCC treatment	none	11	60%
	surgical resection	1	5%
	RFA	4	20%
	TACE	4	20%
Number of lesions	1	13	70%
	2	5	20%
	3	1	5%
	4	0	0%
	5	1	5%
Lesion size (mm)	mean ± SD (range)	18.8	± 7.34 (8-38)
Ablation technique	RFA	7	35%
	MWA	13	65%

HCC = hepatocellular carcinoma, NASH = Non-alcoholic steatohepatitis, BCLC = Barcelona Clinic for Liver Cancer, CT = computed tomography, MRI = magnetic resonance imaging, RFA = radiofrequency ablation, MWA = microwave ablation, TACE = trans-arterial chemoembolization.

in the post-ablation CECT), the automatic rigid registration algorithm is used. This result could be refined with help of anatomical landmarks or manual adjustments by means of translation and rotation. Local optimized registration was strived for in the region of the tumor and ablation zone. *Step 3)* was to semi-automatically define the “liver mask” on the

post-ablation CECT and to semi-automatically segment the ablation necrosis on the post-ablation CECT. This was done by manual segmentation of the ablation zone on multiple slices and interpolation between these contours on intermediate slices. *Step 4)* was to transform the contours and registration into a 3D model that was saved as a mesh structure in a Visualization ToolKit (VTK) file. This file was then quantitatively analyzed using Paraview 5.10.0 software. A lookup table (LUT) was created in which the MAM, i.e. the shortest distance between the tumor surface and ablation necrosis surface, was stored. The exported LUT was used for further statistical analysis. All steps were repeated for every tumor. The segmented liver mask on post-ablation scans ensured the MAM to always represent the shortest distance from pre-ablation tumor segmentation to post-ablation viable liver tissue, in accordance with the methodology of Sandu et al. (2021) [13].

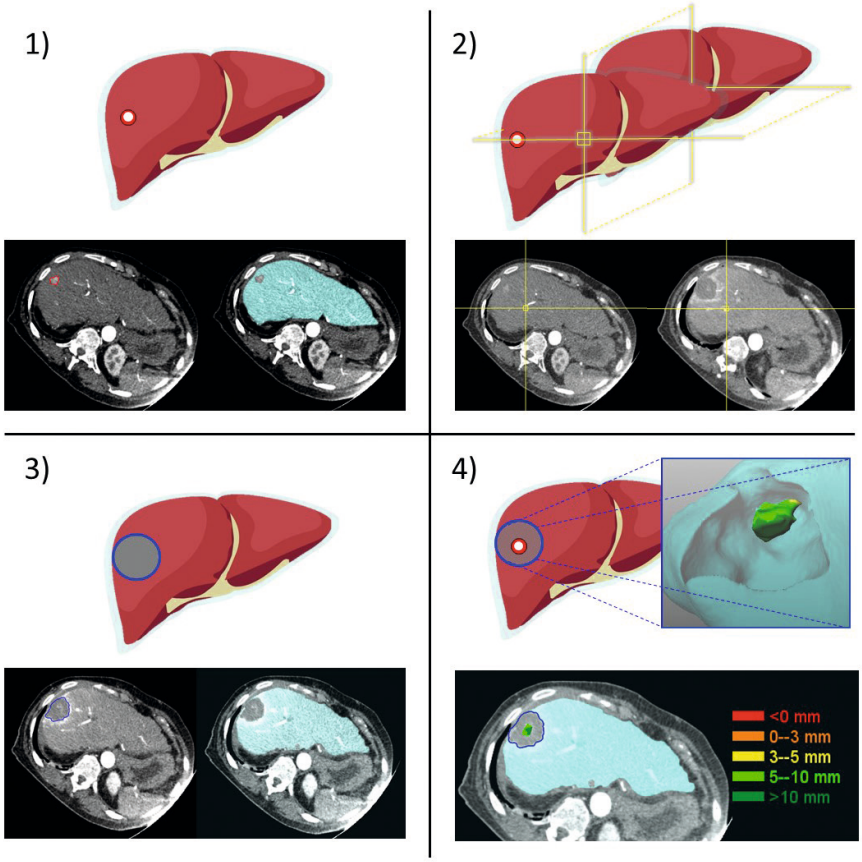

Figure 1 *Software assisted ablation margin quantification.* **1:** *Semi-automatic segmentation of the liver and manual segmentation of the liver tumor.* **2:** *Semi-automatic grey-scale based rigid registration of pre- and post-ablation CT scans.* **3:** *Semi-automatic segmentation of the ablation zone.* **4:** *Analysis of quantified ablation margins.*

Analyses

MAM quantification using the previously described workflow was performed for each tumor separately in both scan phases. Moreover, all MAM quantifications were repeated by both teams to determine intra-observer variability. The anatomical tumor side of the MAM was captured. A minimal time interval of 2 weeks between the two analyses was taken into account. The time needed to complete several steps of the workflow was captured: liver segmentation, tumor segmentation, co-registration and post-ablation image analysis. For inter-observer variability, the second analyses of both teams were used.

End points

The primary endpoint of this study was met if CT-CT co-registration was feasible in ≥80% of all patients. This parameter was objectified using a 5-points scale. (Quality of registration: 1 = ”poor”, 2 = “insufficient”, 3 = ”moderate”, 4 = ”good”, 5 = ”perfect”). In case of disagreement between the two teams, a consensus reading was performed. At a score of 4 or 5, the registration was considered feasible and well enough to pursue ablation margin quantification.

Secondary endpoints of this study were inter- and intra-observer agreement rates for tumor delineation and MAM measurement. The MAM is defined as the single shortest distance between the tumor volume on and ablation volume. In this study the tumor volume segmented from the pre-ablation CECT and the ablation volume segmented from the post-ablation CECT are co-registered to botain the MAM using three-dimensional, software -assisted analysis (see section 2.5). The inter- and intra-observer agreement rates were expressed as volumetric Dice similarity coefficient (vDSC) and degree of similarity (DoS) within a two-pixel range (Figure 2). The values from vDSC and DoS range from 0 to 1, meaning no spatial overlap and perfect agreement, respectively [23]. In general values 0.6-0.8 are considered substantial overlap and 0.8-1.0 are considered almost perfect overlap, as they are derived from Kappa statistics [24]. For each lesion a single MAM value is determined as average value of the 2nd measurements of both teams, in the arterial phase. For lesions that were invisible in the arterial phase, the portal venous scan phase was used. These single MAM-values were expressed in a Bland-Altman plot.

All follow-up scans of patients developing LTP or intrahepatic metastases were double read by two radiologists with 8 and 20 years of experience in abdominal radiology (BB, MCB). In case of disagreement, consensus was reached on the anatomical orientation of LTP with respect to the tumor necrosis. This anatomical orientation was correlated to the anatomical orientation of the MAM.

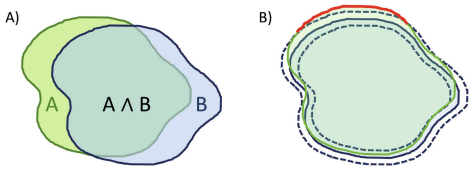

Figure 2 *Inter- and intra-observer variability outcome measures of tumor segmentation.* **A:** *shows the volumetric Dice Similarity Coefficient (vDSC), which is calculated by dividing the overlapping volume of two segmented volumes by the non-overlapping parts of these volumes.* **B:** *shows the degree of similarity (DoS) within 2 voxel distance between two segmentations. Dashed blue lines represent 2 voxel distance of the blue segmentation and the green segmentation exceeds this margin for approximately 20% at the top border (in red).*

Statistics

Numerical data were expressed as mean ± standard deviations and ranges. Categorical data were expressed as numbers and proportions. Analyses were performed using Rstudio 1.4.1106. No comparative statistics were used. Inter- and intra-observer variability were analyzed using a Bland-Altman plot. Mean MAM-values of the two observers were plotted in box-plots and expressed as median with inter quartile ranges. the intraclass correlation coefficient (ICC) for inter-observer variability was determined [25].

RESULTS

Informed consent was obtained from 23 patients of whom 20 patients were treated according to the study protocol, see the flowchart in Figure 3. Reasons for preliminary exclusion were lack of histopathological confirmation of HCC after a combined biopsy and TA procedure for a LI-RADS-4 lesion (n=1) [19], disease progression to Child-Pugh C liver cirrhosis (n=1) or to intermediate HCC (n=1) within a maximum of 6 weeks waiting time. Table 1 shows the baseline characteristics of the patients analyzed. A total of 20 patients with 31 HCC lesions were included with an average lesion diameter of 18.8 ± 7.34 mm [SD] (range: 8-38 mm). Eight patients underwent prior HCC treatment before inclusion in this study.

Thirteen patients were treated with MWA and seven patients with RFA. TA was deemed successful with sufficient ablation margins in 30/31 ablations by discretion of the treating physician based on side-to-side reading of pre- and post-ablation CECT. In those patients, no additional ablation was performed. In one patient a CTCAE 5.0 grade 3 bleeding occurred that led to preliminary termination of the procedure. In this patient additional TA was performed in a second treatment. Other adverse events were CTCAE 5.0 grade 3: post-procedural pleural effusion (n=1), grade 2: hematoma formation (n=2), grade 2: postprocedural pain (n=2), grade 2: postprocedural fever (n=1), and grade 1: iatrogenic vascular thrombosis of a segmental vessel leading to segmental liver infarction (n=1).

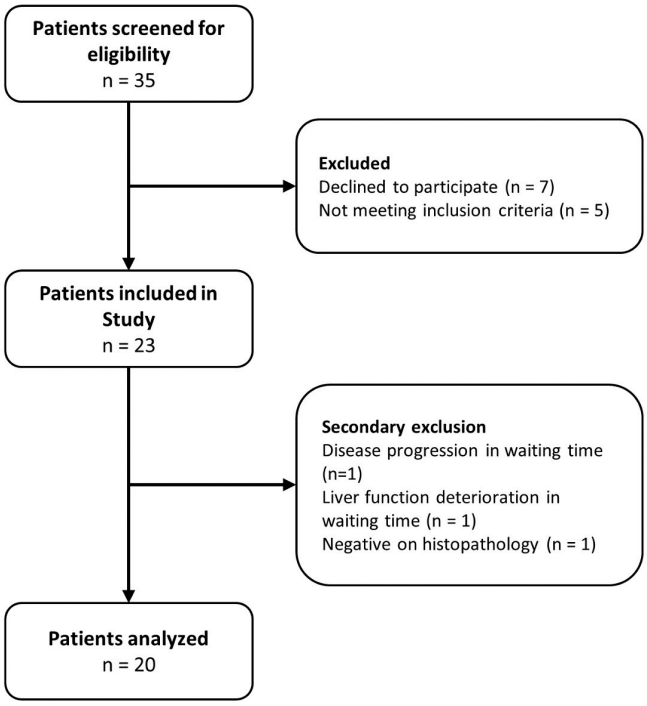

Figure 3 *Flowchart of the study population.*

Figure 4 shows two examples of MAM quantification. Table 2 shows per lesion characteristics and ablation margin quantification parameters. Out of 31 lesions, 18 lesions were visible in both scan phases and 11 lesions were visible in one scan phase. Two solitary lesions in two different patients were not visible on both scan phases and therefore infeasible for analysis. These lesions were targeted by fusion of ultrasound images with diagnostic MRI. The total time for tumor segmentation, scan registration and ablation zone segmentation was 19:31 ± 6:39 min [SD] (range: 07:36-36:01). vDSC rates of inter- and intra-observer variability for tumor segmentation were 0.815 ± 0.069 [SD] (range: 0.660-0.930) and 0.830 ± 0.073 [SD] (range: 0.512-0.930), respectively. The mean MAM was 0.63 ± 3.59 mm [SD] (range: -7.57-10.67). For individual lesions that were visible in both scan phases, a mean volumetric difference of 31.8% between both scan phases was found. However, there was no uniformity in whether delineation in arterial or portal-venous phase resulted in a larger tumor volume.

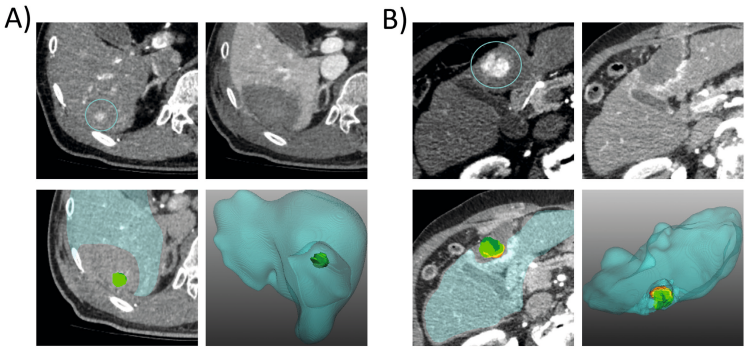

Figure 4 *Two examples of minimal ablation margin quantification of thermal ablation of hepatocellular carcinoma lesions, using in-house built software.* **A:** *Small lesion is segment 6 of the liver with an ablation zone of >5 mm.* **B:** *large lesion in segment 4 of the liver with 0 mm of minimal ablation margin.*

Table 2 *Ablation margin quantification parameters*

		n	
Number of lesions	total	31	
Visibility in scan phase	arterial only	5	16.1%
	portal venous only	6	19.4%
	both	18	58.1%
	invisible	2	6.5%
		time in mm:ss ± SD (range)	
Time duration delineation	tumor	04:28 ± 01:57 (01:13-11:00)	
	ablation zone	04:06 ± 01:53 (01:16-11:29)	
	registration	06:55 ± 03:38 (01:44-19:12)	
	total	19:31 ± 06:39 (07:36-36:01)	
		vDSC ± SD (range)	*DoS ± SD (range)*
Inter-observer variability tumor delineation	arterial phase	0.816 ± 0.085 (0.608-0.910)	0.782 ± 0.161 (0.454-0.997)
	portal venous phase	0.811 ± 0.087 (0.580-0.930)	0.780 ± 0.163 (0.379-0.959)
	total	0.815 ± 0.069 (0.660-0.930)	0.781 ± 0.140 (0.536-0.978)
Intra-observer variability tumor delineation	arterial phase	0.823 ± 0.061 (0.665-0.920)	0.840 ± 0.088 (0.653-0.979)
	portal venous phase	0.837 ± 0.085 (0.512-0.930)	0.815 ± 0.143 (0.526-0.982)
	total	0.830 ± 0.073 (0.512-0.930)	0.828 ± 0.120 (0.526-0.982)
		mm ± SD (range)	
Minimal ablation margin	arterial phase	0.728 ± 3.349 (-5.834-6.203)	
	portal venous phase	0.554 ± 3.749 (-7.567-10.666)	
	total	0.626 ± 3.589 (-7.567-10.666)	

Numerical variables are expressed as mean ± SD (range).
vDSC= volumetric Dice similarity coefficient. DoS=Degree of similarity (chances of two delineations to overlap within a 2 voxel distance).

As mentioned before, 2 lesions in 2 patients were invisible on both scan phases, making them infeasible for ablation margin quantification. In another 3 lesions in 2 patients, the registration quality was insufficient (with scores of 3/5, 3/5 and 2/5) to accurately quantify the ablation margins, resulting in a total feasibility of 26/31 (83.9%) lesions in 16/20 (80%) patients. For the feasible lesions, the Bland-Altman plots in Figure 5 show the inter- and intra-observer agreement of ablation margin quantification. The mean absolute error between two observers was 2.15 ± 2.12 mm [SD] (range:0.39-10.45) with an intraclass correlation coefficient of 0.794 (CI: 0.594 – 0.895).

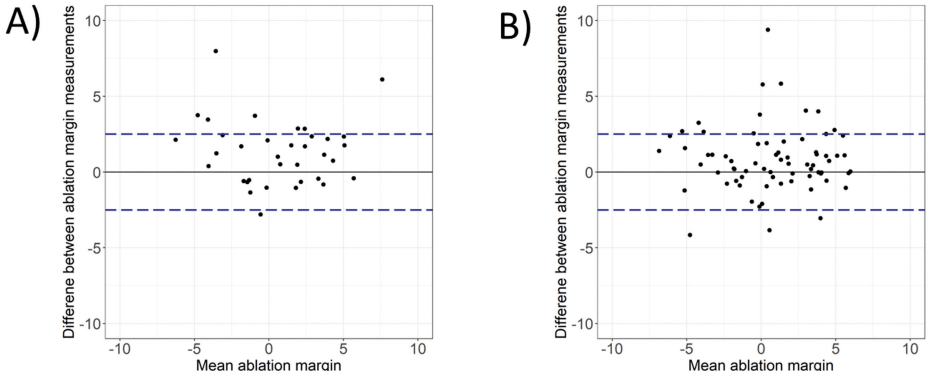

Figure 5 *Bland-Altman plots for* **A:** *inter-observer variability and* **B:** *intra-observer variability of ablation margin quantification. X-axis shows the mean of the two measurements of quantified ablation margins and the Y-axis shows the difference between the two measurements. The blue dashed lines depict the mean inter-observer difference of 2.5 mm.*

Four patients developed LTP in one of the ablated tumors. This included the single patient in whom the thermal ablation was technically unsuccessful but terminated due to a bleeding. In one patient, the tumor was invisible on US and pre-ablation CECT. This lesion was targeted using fusion navigation of US and diagnostic MRI. The mean MAM of the other two lesions that developed LTP was -4.00 mm, compared to an overall mean MAM of 0.626 ± 3.589 mm [SD] (range: -6.26-6.65), as can be seen in Figure 6. Noteworthy, three patients who developed LTP were treated for recurrent HCC as part of this study. Moreover, three lesions were peripherally located in the liver dome. Six patients developed new HCC lesions elsewhere in the liver. None of the patients with a MAM >0 mm developed LTP. In the group of patients with a MAM <0 mm, 2/9 (22%) patients developed LTP.

DISCUSSION

Quantitative margin analysis using co-registration imaging is a promising method to assess technical success of liver tumor ablation and has the potential to be superior to visual

qualitative assessment [11-14]. Our study demonstrates that a standardized imaging protocol with intraprocedural pre- and post-ablation CT under general anesthesia with preoxygenated breath hold allows accurate image co-registration. We found a feasibility for accurate co-registration of pre- and post- ablation CECT scans in 80% of patients and 83.9% of all lesions treated, using a standardized scanning protocol.

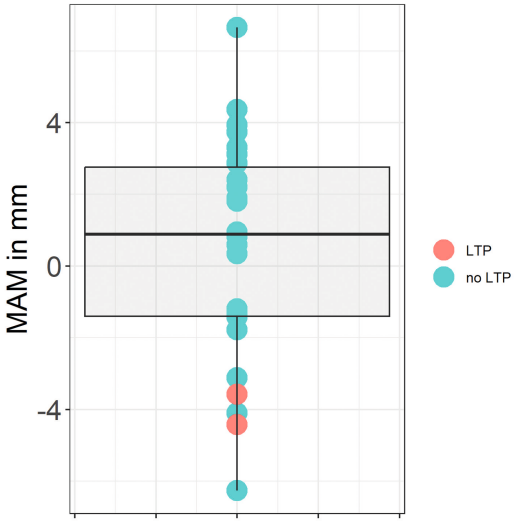

Figure 6 *Boxplot of minimal ablation margins (MAM) for ablated lesions that developed local tumor progression (LTP) (n=2) vs casus that did not develop LTP (n=26).*

In previous retrospective studies on ablation margin quantification, exclusion rates up to 40% were reported, when co-registration of diagnostic CECT or MRI with post-ablation CECT was used [11, 14, 26, 27]. Reasons for inaccurate co-registration in these studies included differences in the position and shape of the liver as a result of differences in patient positioning and breathing mode, and motion artefacts. In studies that did use intraprocedural pre- and post-ablation CECT, feasibility rates similar to our study were found, after selection of well demarcated lesions [12, 28]. Standardization of pre- and post-ablation CECT protocols thus seem to contribute to the feasibility of ablation margin quantification.

As secondary endpoints, we investigated inter- and intra-observer variability of segmentation of the tumor. Reproducibility of segmentation is a prerequisite for accurate quantitative ablation margin analysis. High inter- and intra-observer vDSC rates for tumor segmentation 0.815 ± 0.069 [SD] (range: 0.660-0.930) and 0.830 ± 0.073 [SD] (range: 0.512-0.930) were found, respectively. Although the vDSC is an objective measure of volumetric overlap, it is less sensitive in larger volumes [29]. The DoS within a 2-voxel distance contributes to an objective measure for inter- and intra-observer agreement, as it is volume independent. With DoS

values of 0.781 ± 0.140 [SD] (range: 0.536-0.978) and 0.828 ± 0.120 [SD] (range: 0.526-0.982) at a voxel size of 0.71x0.71x1 mm, high inter- and intra-observer agreement rates were found. In a recent systematic review on ablation margin quantification of Minier et al. only limited studies evaluated inter- and intra-operator characteristics of segmentation or MAM quantification [30]. Most studies used Kappa statistics, and therefore categorized the outcome measure to <0 mm, 0-5 mm and >5 mm. Values ranged from 0.68 to >0.95. Kim et al. reported a Kappa of 0.71 for inter-observer agreement of HCC delineation resulting in a few recommendations for optimization, which were partly implemented in our study (small slice thickness <3 mm, respiratory motion restriction, multiphasic CT, consensus meeting for overcoming discrepancies) [31]. In a study of Hocquelet et al. to ablation margin quantification on MRI, high DSC values of >0.9 were found for each lesion, using MRI scans with larger voxel sizes [32]. We found a mean difference in tumor volume of 31% between segmentations of the same tumor in arterial phase and portal venous phase. This is an important factor to take into account when interpreting the result of quantitative margin analysis. Several factors may influence the volumetric measurements when segmenting a tumor, such as CT level and window settings, as demonstrated by Van Hoe et al [33]. Other factors that may influence tumor segmentation are the timing of image acquisition, contrast volume and contrast load. Optimized scan timing, standardized CT level and window settings, target segmentation training, and consensus reading may contribute to the robustness of the workflow [34].

In our study, a mean MAM of 0.626 ± 3.589 mm [SD] (range: -6.26-6.65) was found, with 36.5% of all MAM quantifications being <0 mm. This was considerably lower than the intended ablation margin of at least 5 mm. Despite the limited ablation margin, the LTP rates were in concordance with those of earlier studies in similar populations [35, 36]. Other studies on quantitative ablation margin analyses also found margins that were considerably lower than 5 mm [12-14]. Although a MAM of >5 mm is associated with good clinical outcomes, this may often not be achieved in practice. Previous studies reported a MAM > 5 mm in only 2.7% (Kim et al. 2010) and 37.5% (Laimer et al. 2020) of lesions where they used software-assisted ablation margin quantification [12, 14]. In a study of Shin et al. (2014) the overestimation of qualitative interpretation of ablation was shown as the number of patients requiring additional TA increased from 12/150 to 35/150 after introducing software-assisted quantification of MAM with a threshold of 2 mm. In our study, LTP occurred in only 2/9 with a quantified MAM < 0 mm. There may be several explanations for this. Experimental studies have demonstrated that considerable tissue shrinkage may occur during ablation [37, 38]. As a result of the contraction of the ablated tissue, the volume of the ablation zone may be smaller than the tumor volume as determined on the pre-procedural scan, even in a patient in whom the tumor was completely ablated with sufficient margins. Tissue shrinkage may vary considerably depending on individual patient and tumor characteristics, as well as the thermal ablation equipment and settings. Also, it occurs non-uniform over time and

asymmetrical [39]. Moreover, the software may incorrectly calculate a negative MAM as a result of errors in image co-registration or segmentation of the tumor and/or ablation zone. In fact, our study demonstrates that segmentation is subject to inter- and intra-observer variability, and may be discordant between arterial and portal venous phase. Future research should focus on methods to further reduce such variability to increase reliability and reproducibility of ablation margin quantification, preferably with fast, reliable and fully automated co-registration and segmentation. It is important to stress that a negative MAM does not necessarily mean that a tumor was incompletely ablated as it is only investigated as a predictive factor. On the other hand, none of the patients in our study with a positive MAM-value developed LTP, and a positive MAM value should of course be aimed for.

In this study, a rigid registration algorithm was used for performing quantitative margin assessment. Previous research showed that non-rigid deformations may be present in the liver, especially caused by breathing motion differences [30, 40]. Non-rigid registration allows for transformation and scaling of images rather than just translation and rotation to reach an optimal registration [41]. Since the process of thermal ablation actually causes local deformation of the tissue, nonrigid algorithms should be restricted in order not to overcompensate for local deformations [42]. Using the standardized intraprocedural scanning protocol with ventilation tube disconnection, the main reason for large deformation (breathing motion and positioning artifacts) were prevented and fast rigid registration with high accuracy was feasible.

Limitations of this feasibility study were the limited number of included patients, the retrospective use of ablation margin quantification software and the limited number of events, which brings limitations to statistical analysis on the MAM results. Despite these limitations we have been able to prospectively demonstrate a feasible pipeline for robust ablation margin quantification. In contrast, a recent study by Schaible et al. objectified the limitations of qualitative ablation margin assessment as they found an ICC of 0.377 for inter-observer agreement. In our study to quantitative ablation margin assessment, the ICC was 0.794 and a mean inter-observer difference of 2.15 mm was found [43].

Results of liver tumor ablation have improved significantly over the last decade and quantitative margin analysis is a promising tool to further increase efficacy of TA. Ultimately, standardized MAM values should be correlated to LTP. Besides MAM values, other volumetric outcome values for identifying patients at risk of developing LTP were demonstrated by Laimer et al. [44]. Current prospective trials are performed to validate quantitative margin analysis in large clinical studies and increase knowledge on the relation between MAM and LTP: PROMETHEUS and COVER-ALL for HCC [45, 46], and the ACCLAIM trial for colorectal liver metastases (NCT05265169).

In conclusion, ablation margin quantification after TA of HCC was found to be feasible by implementing a standardized scanning protocol consisting of pre- and post-ablation CECT under breath hold by disconnection of the ventilation tube under general anesthesia. High inter- and intra-observer agreement rates were found for lesion delineation. LTP seemed to be associated with low MAM-values (<0 mm), but this should further be studied in larger cohort trials.

TRIAL REGISTRATION

Clinicaltrials.gov identifier: NCT04123340

REFERENCES

[1] Forner A, Reig M, Bruix J. Hepatocellular carcinoma. Lancet 2018; 391:1301-14.

[2] Reig M, Forner A, Rimola J, Ferrer-Fàbrega J, Burrel M, Garcia-Criado Á, et al. BCLC strategy for prognosis prediction and treatment recommendation: The 2022 update. J Hepatol 2022; 76:681-93.

[3] Cho YK, Kim JK, Kim WT, Chung JW. Hepatic resection versus radiofrequency ablation for very early stage hepatocellular carcinoma: A Markov model analysis. Hepatology 2010; 51:1284-90.

[4] Cucchetti A, Piscaglia F, Cescon M, Colecchia A, Ercolani G, Bolondi L, et al. Cost-effectiveness of hepatic resection versus percutaneous radiofrequency ablation for early hepatocellular carcinoma. J Hepatol 2013; 59:300-7.

[5] Izumi N, Hasegawa K, Nishioka Y, Takayama T, Yamanaka N, Kudo M, et al. A multicenter randomized controlled trial to evaluate the efficacy of surgery vs. radiofrequency ablation for small hepatocellular carcinoma (SURF trial). J Clin Oncol 2019; 37:4002-.

[6] Doyle A, Gorgen A, Muaddi H, Aravinthan AD, Issachar A, Mironov O, et al. Outcomes of radiofrequency ablation as first-line therapy for hepatocellular carcinoma less than 3 cm in potentially transplantable patients. J Hepatol 2019; 70:866-73.

[7] Xu X-L, Liu X-D, Liang M, Luo B-M. Radiofrequency Ablation versus Hepatic Resection for Small Hepatocellular Carcinoma: Systematic Review of Randomized Controlled Trials with Meta-Analysis and Trial Sequential Analysis. Radiology 2018; 287:461-72.

[8] Habibollahi P, Sheth RA, Cressman ENK. Histological Correlation for Radiofrequency and Microwave Ablation in the Local Control of Hepatocellular Carcinoma (HCC) before Liver Transplantation: A Comprehensive Review. Cancers (Basel) 2021; 13:104.

[9] Crocetti L, de Baére T, Pereira PL, Tarantino FP. CIRSE Standards of Practice on Thermal Ablation of Liver Tumours. Cardiovasc Intervent Radiol 2020; 43:951-62.

[10] Nakazawa T, Kokubu S, Shibuya A, Ono K, Watanabe M, Hidaka H, et al. Radiofrequency Ablation of Hepatocellular Carcinoma: Correlation Between Local Tumor Progression After Ablation and Ablative Margin. AJR Am J Roentgenol 2007; 188:480-8.

[11] Hendriks P, Noortman WA, Baetens TR, van Erkel AR, van Rijswijk CSP, van der Meer RW, et al. Quantitative Volumetric Assessment of Ablative Margins in Hepatocellular Carcinoma: Predicting Local Tumor Progression Using Nonrigid Registration Software. J Oncol 2019; 2019:4049287.

[12] Laimer G, Schullian P, Jaschke N, Putzer D, Eberle G, Alzaga A, et al. Minimal ablative margin (MAM) assessment with image fusion: an independent predictor for local tumor progression in hepatocellular carcinoma after stereotactic radiofrequency ablation. Eur Radiol 2020; 30:2463-72.

[13] Sandu R-M, Paolucci I, Ruiter SJS, Sznitman R, de Jong KP, Freedman J, et al. Volumetric Quantitative Ablation Margins for Assessment of Ablation Completeness in Thermal Ablation of Liver Tumors. Front Oncol 2021; 11.

[14] Kim Y-s, Lee WJ, Rhim H, Lim HK, Choi D, Lee JY. The Minimal Ablative Margin of Radiofrequency Ablation of Hepatocellular Carcinoma (> 2 and < 5 cm) Needed to Prevent Local Tumor Progression: 3D Quantitative Assessment Using CT Image Fusion. AJR Am J Roentgenol 2010; 195:758-65.

[15] Takeyama N, Mizobuchi N, Sakaki M, Shimozuma Y, Munechika J, Kajiwara A, et al. Evaluation of hepatocellular carcinoma ablative margins using fused pre- and post-ablation hepatobiliary phase images. Abdom Radiol 2019; 44:923-35.

[16] Tomonari A, Tsuji K, Yamazaki H, Aoki H, Kang J-H, Kodama Y, et al. Feasibility of fused imaging for the evaluation of radiofrequency ablative margin for hepatocellular carcinoma. Hepatol Res 2013; 43:728-34.

[17] An C, Jiang Y, Huang Z, Gu Y, Zhang T, Ma L, et al. Assessment of Ablative Margin After Microwave Ablation for Hepatocellular Carcinoma Using Deep Learning-Based Deformable Image Registration. Front Oncol 2020; 10.

[18] European Association for the Study of the Liver. EASL Clinical Practice Guidelines: Management of hepatocellular carcinoma. J Hepatology 2018; 69:182-236.

[19] Chernyak V, Fowler KJ, Kamaya A, Kielar AZ, Elsayes KM, Bashir MR, et al. Liver Imaging Reporting and Data System (LI-RADS) Version 2018: Imaging of Hepatocellular Carcinoma in At-Risk Patients. Radiology 2018; 289:816-30.

[20] Freites-Martinez A, Santana N, Arias-Santiago S, Viera A. Using the Common Terminology Criteria for Adverse Events (CTCAE - Version 5.0) to Evaluate the Severity of Adverse Events of Anticancer Therapies. Actas Dermosifiliogr (Engl Ed) 2021; 112:90-2.

[21] Shamonin D, Bron E, Lelieveldt B, Smits M, Klein S, Staring M. Fast Parallel Image Registration on CPU and GPU for Diagnostic Classification of Alzheimer's Disease. Front Neuroinform 2014; 7.

[22] Klein S, Staring M, Murphy K, Viergever MA, Pluim JPW. elastix: A Toolbox for Intensity-Based Medical Image Registration. IEEE Trans Med Imaging 2010; 29:196-205.

[23] Zou KH, Warfield SK, Bharatha A, Tempany CM, Kaus MR, Haker SJ, et al. Statistical validation of image segmentation quality based on a spatial overlap index. Academic radiology 2004; 11:178-89.

[24] McHugh ML. Interrater reliability: the kappa statistic. Biochem Med (Zagreb) 2012; 22:276-82.

[25] Benchoufi M, Matzner-Lober E, Molinari N, Jannot AS, Soyer P. Interobserver agreement issues in radiology. Diagn Interv Imaging 2020; 101:639-41.

[26] Sibinga Mulder BG, Hendriks P, Baetens TR, van Erkel AR, van Rijswijk CSP, van der Meer RW, et al. Quantitative margin assessment of radiofrequency ablation of a solitary colorectal hepatic metastasis using MIRADA RTx on CT scans: a feasibility study. BMC Med Imaging 2019; 19:71.

[27] Faber RA, Burghout KST, Bijlstra OD, Hendriks P, van Erp GCM, Broersen A, et al. Three-dimensional quantitative margin assessment in patients with colorectal liver metastases treated with percutaneous thermal ablation using semi-automatic rigid MRI/CECT-CECT co-registration. Eur J Radiol 2022; 156:110552.

[28] Ruiter SJS, Tinguely P, Paolucci I, Engstrand J, Candinas D, Weber S, et al. 3D Quantitative Ablation Margins for Prediction of Ablation Site Recurrence After Stereotactic Image-Guided Microwave Ablation of Colorectal Liver Metastases: A Multicenter Study. Front Oncol 2021; 11:757167.

[29] Lohmann P, Stavrinou P, Lipke K, Bauer EK, Ceccon G, Werner J-M, et al. FET PET reveals considerable spatial differences in tumour burden compared to conventional MRI in newly diagnosed glioblastoma. Eur J Nucl Med Mol Imaging 2019; 46:591-602.

[30] Minier C, Hermida M, Allimant C, Escal L, Pierredon-Foulongne M-A, Belgour A, et al. Software-based assessment of tumor margins after percutaneous thermal ablation of liver tumors: A systematic review. Diagn Interv Imaging 2022; 103:240-50.

[31] Kim YS, Kim JW, Yoon WS, Kang MK, Lee IJ, Kim TH, et al. Interobserver variability in gross tumor volume delineation for hepatocellular carcinoma. Strahlenther Onkol 2016; 192:714-21.

[32] Hocquelet A, Trillaud H, Frulio N, Papadopoulos P, Balageas P, Salut C, et al. Three-Dimensional Measurement of Hepatocellular Carcinoma Ablation Zones and Margins for Predicting Local Tumor Progression. J Vasc Interv Radiol 2016; 27:1038-45.e2.

[33] Van Hoe L, Haven F, Bellon E, Baert AL, Bosmans H, Feron M, et al. Factors Influencing the Accuracy of Volume Measurements in Spiral CT: A Phantom Study. J Comput Assist Tomogr 1997; 21.

[34] Eriksen JG, Salembier C, Rivera S, De Bari B, Berger D, Mantello G, et al. Four years with FALCON – An ESTRO educational project: Achievements and perspectives. Radiother Oncol 2014; 112:145-9.

[35] Burgmans MC, Too CW, Fiocco M, Kerbert AJC, Lo RHG, Schaapman JJ, et al. Differences in Patient Characteristics and Midterm Outcome Between Asian and European Patients Treated with Radiofrequency Ablation for Hepatocellular Carcinoma. Cardiovasc Intervent Radiol 2016; 39:1708-15.

[36] Huang J, Huang W, Guo Y, Cai M, Zhou J, Lin L, et al. Risk Factors, Patterns, and Long-Term Survival of Recurrence After Radiofrequency Ablation With or Without Transarterial Chemoembolization for Hepatocellular Carcinoma. Front Oncol 2021; 11.

[37] Brace CL, Diaz TA, Hinshaw JL, Lee FT, Jr. Tissue contraction caused by radiofrequency and microwave ablation: a laboratory study in liver and lung. J Vasc Interv Radiol 2010; 21:1280-6.

[38] Rossmann C, Garrett-Mayer E, Rattay F, Haemmerich D. Dynamics of tissue shrinkage during ablative temperature exposures. Physiol Meas 2014; 35:55-67.

[39] Farina L, Weiss N, Nissenbaum Y, Cavagnaro M, Lopresto V, Pinto R, et al. Characterisation of tissue shrinkage during microwave thermal ablation. Int J Hyperthermia 2014; 30:419-28.

[40] Luu HM, Moelker A, Klein S, Niessen W, van Walsum T. Quantification of nonrigid liver deformation in radiofrequency ablation interventions using image registration. Phys Med Biol 2018; 63:175005.

[41] Crum WR, Hartkens T, Hill DLG. Non-rigid image registration: theory and practice. Br J Radiol 2004; 77:S140-S53.

[42] Dong C, Chen Y-w, Seki T, Inoguchi R, Lin C-L, Han X-h. Non-rigid image registration with anatomical structure constraint for assessing locoregional therapy of hepatocellular carcinoma. Comput Med Imaging Graph 2015; 45:75-83.

[43] Schaible J, Pregler B, Bäumler W, Einspieler I, Jung EM, Stroszczynski C, et al. Safety margin assessment after microwave ablation of liver tumors: inter- and intrareader variability. Radiol Oncol 2020; 54:57-61.

[44] Laimer G, Jaschke N, Schullian P, Putzer D, Eberle G, Solbiati M, et al. Volumetric assessment of the periablational safety margin after thermal ablation of colorectal liver metastases. Eur Radiol 2021; 31:6489-99.

[45] Oosterveer TTM, van Erp GCM, Hendriks P, Broersen A, Overduin CG, van Rijswijk CSP, et al. Study Protocol PROMETHEUS: Prospective Multicenter Study to Evaluate the Correlation Between Safety Margin and Local Recurrence After Thermal Ablation Using Image Co-registration in Patients with Hepatocellular Carcinoma. Cardiovasc Intervent Radiol 2022; 45:606-12.

[46] Lin Y-M, Paolucci I, Anderson BM, O'Connor CS, Rigaud B, Briones-Dimayuga M, et al. Study Protocol COVER-ALL: Clinical Impact of a Volumetric Image Method for Confirming Tumour Coverage with Ablation on Patients with Malignant Liver Lesions. Cardiovasc Intervent Radiol 2022.

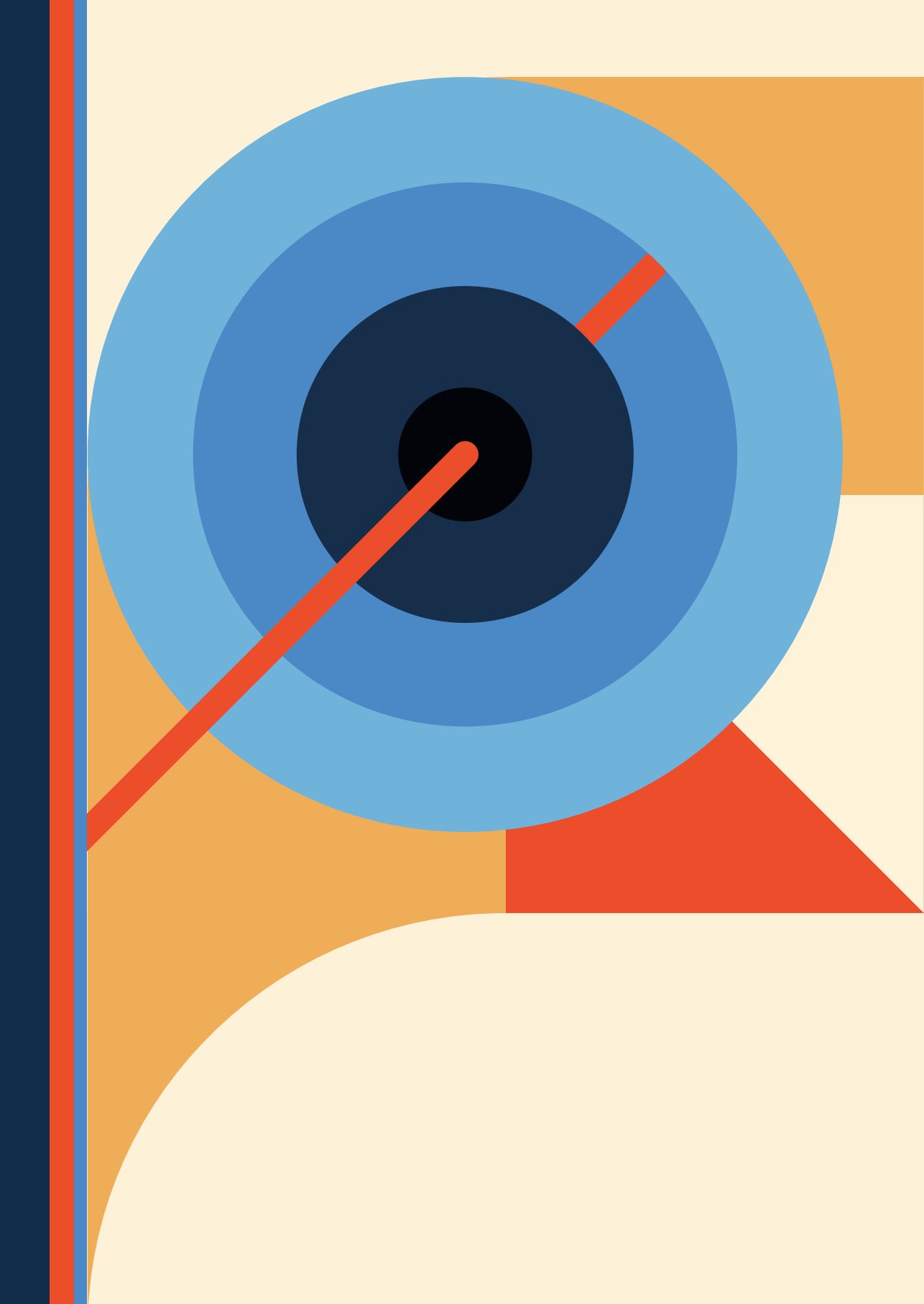

Part 2:

Combined treatment regimens for early stage HCC

Chapter 6

Thermal ablation combined with transarterial chemoembolization for hepatocellular carcinoma: what is the right treatment sequence?

Authors

P. Hendriks, D.R. Sudiono, J.J. Schaapman, M.J. Coenraad, M.E. Tushuizen, R.B. Takkenberg, T.T.M. Oosterveer, L.F. de Geus-Oei, O.M. van Delden, M.C. Burgmans

Published

European Journal of Radiology, 2021; *144, DOI: 0.1016/j.ejrad.2021.110006*

ABSTRACT

Background The combination treatment regimen of thermal ablation (TA) and transarterial chemoembolization (TACE) has gained a place in treatment of hepatocellular carcinoma (HCC) lesions > 3 cm unsuitable for surgery. Despite a high heterogeneity in the currently used treatment protocols, the pooled results of combined treatments seem to outperform those of TA or TACE alone. TACE preceding TA has been studied extensively, while results of the reverse treatment sequence are lacking. In this retrospective cohort study we compared the two treatment sequences.

Patients and Methods 38 patients (median age: 68.5 yrs (range 40-84), male: 34, liver cirrhosis: 33, early stage HCC: 21, intermediate stage HCC: 17) were included in two tertiary referral centers, of whom 27 were treated with TA and adjuvant TACE (TA+TACE). The other 11 patients received TA with neoadjuvant TACE (TACE+TA). Overall survival (OS), time to progression (TTP) and local tumor progression (LTP) free survival were determined for the entire cohort and compared between the two treatment sequences.

Results The median OS of all patients was 52.7 months and the median time to LTP was 11.5 months (censored for liver transplantation). No differences were found with respect to OS between the two treatment sequences. Median time to LTP for TACE+TA was 23.6 months and 8.1 months for TA+TACE (p=0.19).

Discussion No statistical differences were found for OS, TTP and time to LTP between patients treated with TA combined with neoadjuvant or adjuvant TACE.

Keywords: hepatocellular carcinoma; chemoembolization; drug eluting bead; thermal ablation; radiofrequency ablation; microwave ablation; oncology; interventional radiology

INTRODUCTION

Thermal ablation (TA) is an established treatment for hepatocellular carcinoma (HCC) and considered treatment of choice in HCC lesions <2 cm, as local tumor progression (LTP) rates are comparable to those after surgical resection [1]. Surgical resection remains the treatment of first choice in larger lesions due to better local control, but carries a high risk of complications, especially in patients with cirrhosis and portal hypertension [2]. In patients who are not suitable candidates for surgical resection, TA or transarterial chemoembolization (TACE) are considered alternative therapies, depending on the tumor characteristics, tumor location, liver function, portal hypertension, performance status [3].

In order to decrease LTP rates after TA treatments of HCC lesions > 3 cm, Lencioni et al. published a first pilot study on the combination of TA with adjuvant TACE (TA+TACE) in 2008 [4]. Subsequent studies most commonly used the reversed sequence of neoadjuvant TACE before TA (TACE+TA) and confirmed the potential benefit of the combined therapy [5, 6]. Over the last decade, the treatment combination has been adopted in many clinical practices. The latest European and American guidelines on HCC management mention the potential benefit of combining TA with TACE for larger lesions, although large phase III trials and validation in western patient populations are lacking [7, 8].

A meta-analysis was published on the combined treatment effect of TACE+TA vs. TA alone [9]. The authors included 8 studies in which 648 patients were evaluated and significantly better hazard ratios with respect to overall survival (OS) and recurrence free survival were found. Most of the included studies were cohort studies, but the results were also confirmed by a randomized controlled trial from China [10]. Although the evidence for the use of combined TA and TACE treatment in either sequence is growing, treatment schedules are currently heterogeneous and unconcise in the optimal interval between TA and TACE. Moreover, there is a paucity of studies directly comparing the treatment sequences.

In 2009, the combined treatment regimen was adopted in our clinical practices. Adjuvant TACE after TA was the initial treatment sequence. This was later changed to neoadjuvant TACE prior to TA, due to growing clinical evidence for that treatment sequence. In this retrospective cohort study we compared the effectiveness of both treatment regimens in terms of local tumor control, time to progression (TTP) and OS.

METHODOLOGY

Patients

This was a retrospective cohort study performed in two academic tertiary referral centers. Between January 2009 and April 2020, 38 patients were treated with a combination of TA and TACE and had a minimum follow up duration of one year. All patients had de novo unresectable HCC, diagnosed in accordance with the European Association for the Study of the Liver (EASL) guidelines [7]. Consensus on combined treatment with TACE and TA was reached in multidisciplinary tumor board meetings for all patients, attended by at least a hepatologist, surgeon, (interventional) radiologist, pathologist and oncologist. The preferred treatment order was changed from adjuvant TACE to neoadjuvant TACE prior to TA in 2015 in both centres.

Selection criteria for undergoing the treatments included a Child-Pugh classification of A or B and Eastern Cooperation Oncology Group (ECOG) performance status of <2. Ineligibility criteria were radiologic evidence of vascular invasion into portal/hepatic vein branches, extrahepatic metastases, severe liver dysfunction (Child-Pugh C), significant and uncorrectable coagulopathy (International Normalized Ratio (INR) >1.7, platelet count $<50^{*}10^{9}/mm^{3}$).

Thermal ablation

Percutaneous TA was performed under general anesthesia with image guidance using ultrasound and/or CT. Three different radiofrequency ablation (RFA) systems were used throughout the study period, of which two were single electrode systems (3cm exposed tip Covidien (Medtronic Covidien, Fridley, Minessota, USA) and StarBurst XL (Angiodynamics, Amsterdam, The Netherlands)) and one multiple electrodes switch-control system (3 or 4 cm exposed Cooltip (Covidien)). Two microwave ablation (MWA) systems were used: Amica (HS Hospital Service, Rome, Italy) and Emprint (Covidien/Medtronic, Minneapolis, USA). Immediate intraprocedural post-ablation contrast-enhanced computed tomography (CECT) was performed on a 16 or 64 slice spiral CT-scanner. Technical success was defined as 'complete coverage of the tumor by the ablation necrosis as assessed by juxta-positioning of pre- and procedural cross-sectional images and absence of tumor enhancement on the immediate post-ablation CECT'. Immediate re-ablation was performed when no technical success was reached at the first attempt.

Transarterial chemoembolization

Using a transfemoral approach, selective angiography was performed of the common, lobar and (sub)segmental hepatic arteries. Contrast-enhanced cone-beam computed tomography (CBCT) was performed in most patients to assess the local vascular tumor supply (XperCT,

Philips Healthcare, Best, The Netherlands). Catheter positions were chosen as selective as possible and 100-300 µm and 300-500 µm DC Beads were used, loaded with a maximum of 75 mg of doxorubicin per vial (Boston Scientific, Natick, Massachusetts, USA) and up to 150 mg of doxorubicin per patient. In early years of this study, both 100-300 µm and 300-500 µm were used. The treatment protocol was later changed to 100-300 µm beads only, as evidence came available that smaller beads penetrate more distally and may thus cause more extensive tumor necrosis. Endpoints for the treatment were arterial flow stasis or the total infusion of DC Beads with up to 150 mg of doxorubicin. Hepatic angiography was performed immediately after embolization and technical success was defined as the successful delivery of the DC Beads with absence of tumor blush on the last angiogram.

Follow-up

Imaging was performed 6 weeks after TA and then continued every 3 months until untreatable disease or death, using dynamic gadolinium enhanced magnetic resonance imaging (GE-MRI) or CECT. In one centre, FU was reduced to every 6 months after 2 years of complete remission. Local tumor progression (LTP) was defined as the presence of tumor enhancement on a follow-up scan within or directly bordering the treated tumor. LTP was distinguished from distant intrahepatic recurrence or extrahepatic metastatic disease. Included patients had at least one year follow-up. Patients were followed until death, last follow-up or the end of the study (08-2021).

Outcomes

Effectivity was evaluated as Time to LTP, TTP of any kind (LTP, intrahepatic metastases or distant metastases) and OS. Complications were evaluated according to the Common Terminology Criteria for Adverse Effects (CTCAE) version 5.0.

Statistical analysis

Statistical analyses were performed using RStudio 1.4.1106. Continuous variables were compared using an unpaired t-test for normally distributed, continuous variables and Mann-Whitney U for non-normally distributed data. The Chi-square test was used to compare categorical variables.

Univariate and multivariate Cox's proportional hazards models were used to evaluate the predictive factors of survival. The factors age, sex, cirrhosis, ECOG score, Child-Pugh score, number of lesions, lesion size, BCLC stage, treatment order, and liver transplantation after treatment were evaluated. Factors with a p-value <0.2 in the univariate analyses were considered to be potential predictors of survival and were further analysed in the multivariate analysis.

Survival analyses for OS, TTP and time to LTP were performed using Kaplan Meier estimates. Starting point was set at the date of treatment completion. Censoring was applied in comparative survival analyses to patients that underwent liver transplantation, and in all Kaplan-Meier analyses for cases that were lost to follow up. Moreover, survival was censored for patients who were still alive at the closeout date. Differences in OS, TTP and LTP free survival were tested for using the log-rank test. P-values of < 0.05 were considered statistically significant.

RESULTS

Baseline characteristics

Baseline characteristics of all patients are shown in Table 1. In total 38 patients were included with a median age of 68.5 years old, of which 34 were male. Underlying liver cirrhosis was found in 33 patients, all with Child-Pugh A cirrhosis. Most patients had 1 lesion (n=21), 15 patients had 2 lesions and 2 patients had 3 lesions. The median tumor size of the largest lesion was 40 mm (range: 21 mm – 69 mm). An example of both treatment sequences can be found in Figure 1.

Statistically significant differences between the two cohorts of different treatment sequences were found with respect to Child-Pugh score (higher for patients treated with neoadjuvant TACE, $p<0.001$), lesion size (larger for patients treated with adjuvant TACE, $p = 0.034$), the use

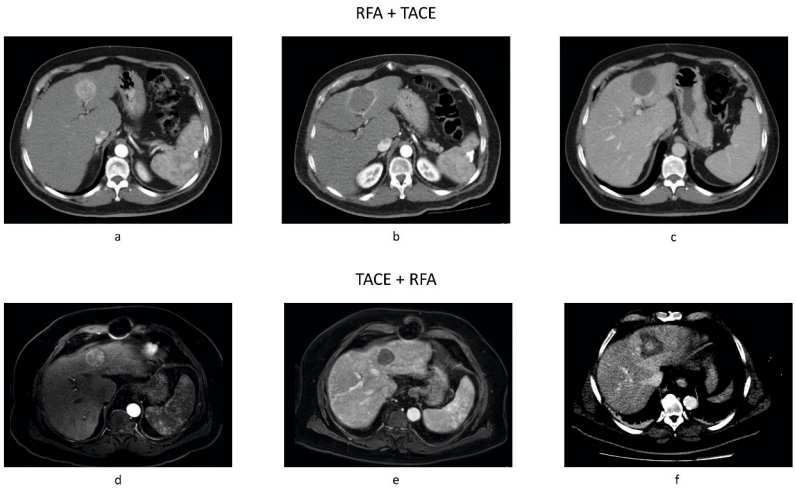

Figure 1 *Two cases of patients treated with different treatment sequences. Adjuvant TACE was used in the first case (***A:** *diagnostic CT,* **B:** *post-ablation CT,* **C:** *post TACE CT) Neoadjuvant TACE was used in the second case (***D:** *pre-treatment gadolinium-enhanced MRI in arterial phase,* **E:** *pre-treatment gadolinium-enhanced MRI in portal venous phase,* **F:** *post-treatment CT scan)*

of TARE as consecutive treatment (used more often in patients treated with adjuvant TACE) and year of treatment (the treatment sequence changed from adjuvant TACE to neoadjuvant TACE). All details can be found in Table 1. Data on the TACE particle size were missing in 5 patients. In 5 patients, both small sized (100-300 µm) and larger sized (300-500 µm) particles were used.

Cox proportional hazards model

Table 2 shows the results of the univariate and multivariate analysis for survival. BCLC stage and liver transplantation were the only covariates that showed a p-value <0.2 in the univariate analysis. After multivariate analysis, only liver transplantation contributed significantly to survival with a Hazard Ratio of 0.05 (CI 95%: 0.01 – 0.27) and p-value of <0.001.

Treatment outcome

Technical success of TA and TACE was achieved in all patients. Two out of 38 patients were lost to follow-up. The median survival was 52.7 months for all patients. Figure 2 demonstrates the corresponding Kaplan-Meier curve. The 1-year, 2-year, 3-year, 4 year and 5-year OS are respectively 86.5%, 62.3.1%, 55.5%, 51.2% and 47.0%.

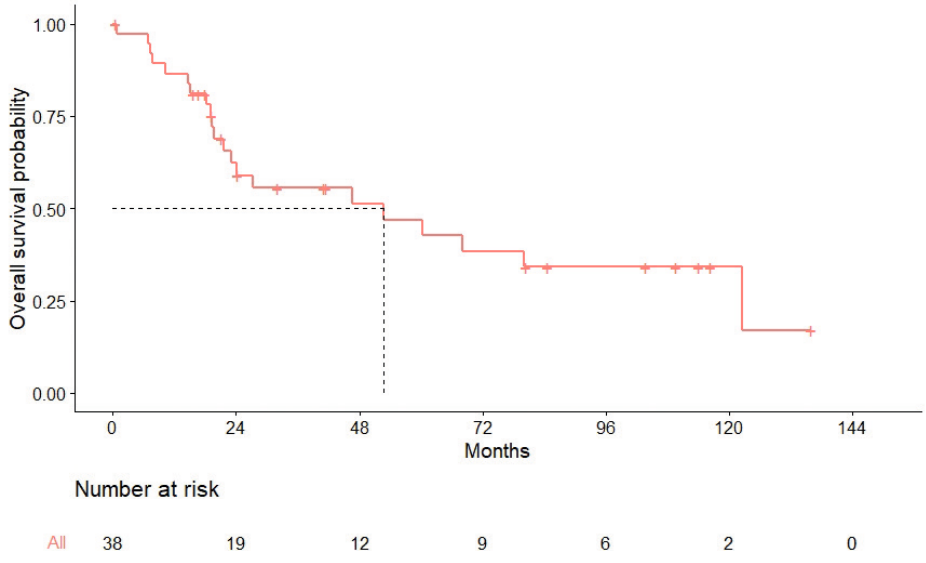

Figure 2 *Kaplan-Meier overall survival function of all patients treated with combined TA+TACE.*

Table 1 *Patient characteristics of analyzed patients*

		Total		*TA+TACE*		*TACE+TA*		*p-value*
Total		38		27		11		
Age (years)	median (range)	68.5	*(40-84)*	65	*(40-84)*	70	(54-78)	*0.351*
Sex	male	34	*89.5%*	23	*85.2%*	11	100%	*0.238*
Center	Center 1	31	*81.6%*	23	*85.2%*	8	72.7%	*0.370*
	Center 2	7	*18.4%*	4	*14.8%*	3	27.3%	
Cirrhosis	yes	33	*86.8%*	22	*81.5%*	10	90.1%	*0.429*
Etiology of cirrhosis*	Hepatitis B	4		4		0		
	Hepatitis C	11		6		5		
	Alcoholic liver disease	16		11		5		
	NASH	6		3		2		
	Other	3		3		0		
Child-Pugh	A5	22	*66.7%*	18	*81.8%*	4	36.4%	*<0.001**
	A6	11	*33.3%*	4	*18.2%*	7	63.6%	
ECOG score	0	33	*86.8%*	23	*85.2%*	10	90.9%	*0.636*
	1	5	*13.2%*	4	*14.8%*	1	9.1%	
BCLC stage	early	21	*55.3%*	13	*48.1%*	8	72.7%	*0.167*
	intermediate	17	*44.7%*	14	*51.9%*	3	27.3%	
Number of lesions	1	21	*55.3%*	13	*48.1%*	8	72.7%	*0.216*
	2	15	*39.4%*	13	*48.1%*	2	18.2%	
	3	2	*5.3%*	1	*3.8%*	1	9.1%	
Size largest lesion (mm)	median (range)	40	*(21-69)*	43	*(30-69)*	37	(21-55)	*0.034**
Type of TA	RFA	33	*86.8%*	25	*92.6%*	8	73.7%	*0.100*

Table 1 *Patient characteristics of analyzed patients* **(continued)**

		Total		*TA+TACE*		*TACE+TA*		*p-value*
	MWA	5	*23.2%*	2	*7.4%*	3	27.3%	
Size TACE particles	100-300 µm	32		25		7		
	300-500 µm	6		5		1		
	Unknown	5		2		3		
Dose of doxorubicin (mg)	median (range)	50	*(25-100)*	50	*(25-100)*	67.5	(25-100)	*0.510*
Consecutive treatments	Thermal ablation	15	*39.5%*	12	*44.4%*	3	27.3%	*0.272*
	Liver transplantation	12	*31.6%*	10	*37.0%*	2	18.2%	*0.231*
	TACE	11	*28.9%*	8	*29.6%*	3	27.3%	*0.334*
	TARE	3	*7.9%*	3	*11.1%*	0	-	*<0.001**
	Sorafenib	9	*23.7%*	8	*29.6%*	1	*9.1%*	*0.237*
Year of treatment	2009-2014	25	*65.8%*	24	*88.9%*	1	*9.1%*	*<0.001**
	2015-2020	13	*34.2%*	3	*11.1%*	10	*90.9%*	

*NASH = Non-alcoholic steatohepatitis, ECOG = Eastern Cooperative Oncology Group, BCLC = Barcelona Clinic for Liver Cancer, TA = Thermal ablation, RFA = Radiofrequency ablation, MWA = Microwave ablation, TACE = Trans arterial chemoembolization, TARE = Trans arterial radioembolization. *More etiological factors could apply to one patient. *Statistically significant*

Table 2 *Univariate and multivariate analysis for survival*

	Univariate		Multivariate	
	HR (95% CI)	*p-value*	HR (95% CI)	*p-value*
Age	1.03 (0.99 – 1.07)	*0.178*		
Sex	0.98 (0.28 – 3.46)	*0.976*		
Cirrhosis	1.15 (0.33 – 4.03)	*0.830*		
ECOG score	1.75 (0.39 – 7.85)	*0.466*		
BCLC stage	0.54 (0.21 – 1.36)	*0.190*	1.65 (0.59 – 4.61)	*0.337*
Child Pugh	1.79 (0.67 – 4.82)	*0.246*		
Number of Lesions	0.65 (0.30 – 1.39)	*0.264*		
Lesion size	1.02 (0.99 – 1.05)	*0.239*		
Treatment sequence	1.24 (0.44 – 3.52)	*0.684*		
Liver transplantation	0.07 (0.01 – 0.31)	*<0.001*	0.05 (0.01 – 0.27)	*<0.001*

HR = hazard ratio, CI = confide interval, ECOG = eastern cooperative oncology group, BCLC = Barcelona clinic for liver cancer

Disease progression occurred in 28/38 patients with a median TTP of 4.8 months. LTP occurred in 20/38 patients. Median time to LTP was 11.5 months. Figure 3 shows the corresponding TTP and time to LTP curves, censored for liver transplantation.

Treatment sequence

Adjuvant TACE was performed after TA in 27/38 patients with an average interval of 3.52 days (SD = 6.81). In the other 11 patients, patients first underwent neoadjuvant TACE followed by TA with an average interval of 30.73 days (SD= 25.15). OS curves were similar between those groups (p=0.68). Median TTP was 12.8 months for TACE+TA and 2.8 months for TA+TACE (p = 0.30). Time to LTP was 23.6 months for TACE+TA and 8.1 months for TA+TACE (p = 0.19) The corresponding Kaplan-Meier curves can be found in Figure 4.

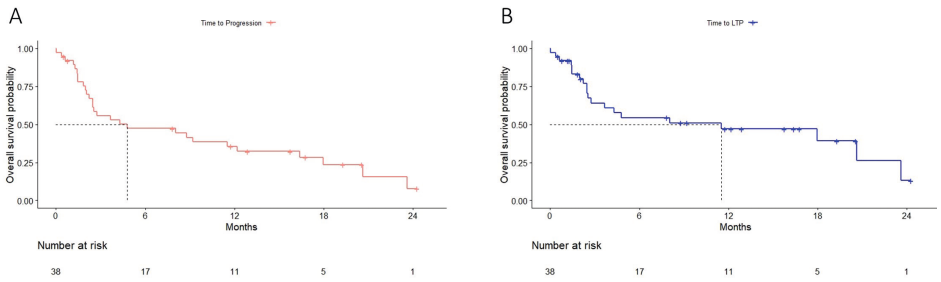

Figure 3 A: *Kaplan-Meier analysis of the TTP, censored for liver transplantation.* **B:** *Kaplan-Meier analysis of the Time to LTP, censored for liver transplantation*

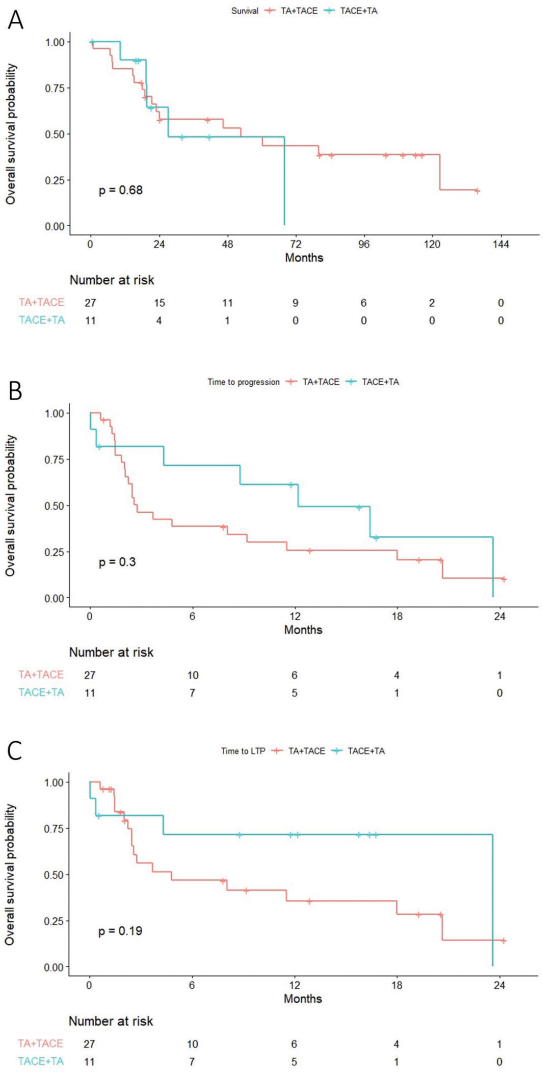

Figure 4 *Kaplan-Meier curves of differences between treatment sequences TA+TACE (orange) and TACE+-TA (turquoise).* **A:** *overall survival.* **B:** *Time to progression.* **C:** *Time to local tumor progression.*

Complications

One grade CTCAE 5.0 grade 5 complication occurred. In a patient who was treated for a large (47 mm) HCC lesion in the liver dome. This procedure was complicated by a right sided pneumothorax for which a chest tube was inserted. The next day, super selective TACE was performed. Five days later, the patient developed sepsis as a result of E. Coli peritonitis. Despite treatment with percutaneous drainage and antibiotics, the patient died 23 days after TA as a result of sepsis and hepatorenal syndrome. Two patients developed a liver abscess days after ablation, which were successfully treated with percutaneous drainage and antibiotics (CTCAE 5.0 grade 3 and 4). Moreover 6 complications were graded 1 or 2 (mostly post-TACE symptoms). All grade 2-5 complications (n=6) were reported in patients who underwent adjuvant TACE.

Consecutive treatments

Liver transplantation was performed in 12/38 patients treated with the combined regimen of TA and TACE. The median time to transplantation was 419 days (range: 183-1373 days). In one transplanted patient, recurrent disease was found 3 years after transplantation. No disease progression was found in all other transplanted patients. Details on all other consecutive treatments can be found in Table 1.

DISCUSSION

In this retrospective cohort study, we evaluated the effect of combined TA and TACE treatment on OS, TTP and time to LTP. In the multivariate analysis of survival, only liver transplantation as consecutive treatment turned out to be an independent covariate. In the Kaplan-Meier analysis, median time to LTP was 23.6 months for TACE+TA and 8.1 months for TA+TACE (p=0.19). No statistical difference was found between the groups, but local tumor control can be considered a goal itself as combined TA and TACE can be used as bridging therapy to liver transplantation [11].

The median OS of 52.7 months corresponds to expected OS for early and intermediate stage HCC patients according to the BCLC criteria [3]. Table 3 shows an overview of clinical trials studying the TA+TACE treatment combinations with respect to treatment protocol and clinical outcomes. Our results are in general comparable to those of other clinical studies. Very limited data are available on the combination of TA followed by TACE. One clinical study was found comparing TA+TACE with TACE+TA by El Dorry et al and they found median disease-free survival of 17.1 months for TACE+TA vs 23.2 months for TA+TACE (p>0.05) [12]. These results confirm our results as no statistical differences were found. Uncensored, the TTP in our study was 14.2 months, which is slightly lower than in the study by El Dorry et al.

As shown in Table 3, considerable heterogeneity exist between the treatment protocols in the various studies. Besides the sequence of both treatments, variability exists in patient selection, interval between the treatments, type of ablation (RFA and/or MWA) and type of TACE (conventional TACE (cTACE) or drug-eluting bead TACE (DEB-TACE)). Most clinical evidence is available for the use of TACE+TA. The rationale for this treatment sequence is that TACE causes vessel occlusion and reduced tumor perfusion, potentially resulting in volume reduction, reduction of 'heat-sink' and larger ablation zones [13]. A less studied alternative is TA+TACE. TA causes hyperemia in the liver parenchyma surrounding the area of coagulation necrosis and this hyperemia is utilized to target residual tumor cells or satellite lesions. It is hypothesized that by performing TACE within several days after TA, the hyperemia will cause preferential flow and high uptake of chemo-embolic drugs in the tissue surrounding the ablation. Furthermore, insufficiently heated tumor tissue may have reduced cell resistance to drugs used in TACE [13]

In our study, RFA and MWA were used interchangeably. The available literature indicates that OS is comparable between the two techniques, but differences between RFA and MWA may affect the combinational effect when ablation is combined with TACE [14-17]. Compared to RFA, MWA is less susceptible to heat-sink and tissue perfusion. This may reduce the added value of TACE in a neoadjuvant setting. Also, ablation times are shorter with MWA and intratumoral temperatures tend to be higher. Both factors would potentially influence the degree of hyperemia that occurs in the surrounding liver parenchyma after ablation. This may potentially reduce the efficacy of TACE in an adjuvant setting [14-17].

With respect to TACE technique, patients in our study underwent TACE with drug eluting beads (DEB-TACE) rather than conventional TACE (cTACE). After cTACE, lipiodol causes visualization of the targeted lesion on a non-contrast CT-scan, which may help needle positioning when TA is performed after TACE. Although limited evidence suggests DEB-TACE may yield better local control when used as single therapy [18, 19], the influence of different TACE techniques when combined with TA has not been studied. Further research is warranted to determine how synergy between TA and TACE is best achieved.

The main limitations of this study are its limited number of included patients and its retrospective nature. Comparative analysis to a matching group from our own institutions was not performed as the selection criteria for the combined treatment regimen was distinctly different from patients undergoing either TA or TACE only. Instead, we chose to validate our results with evidence available from other studies to TA and TACE combined treatments and to perform a comparative analysis within our own cohort only between the treatment sequences. Comparison between the two groups was hampered by the low number of patients, in particular in the TA+TACE group.

Table 3 *Overview of treatment regimens and clinical outcomes of previous studies. All survival data are in months. OS = Overall survival, PFS = Progression free survival, TTP = Time to progression, RFA = radiofrequency ablation, MWA = microwave ablation, DEB-TACE = drug-eluting beads transarterial chemoembolization, cTACE = conventional transarterial chemoembolization.*

Article	Lesion size	Treatment	Interval	Overall Survival (OS in %)			Progression Free Survival (PFS in %)			Median/ Mean OS	Median/ Mean TTP
				1 year	2 year	3 year	1 year	2 year	3 year		
Lencioni et al. [4]	5.0 cm (3.3-7.0)	RFA + DEB-TACE	<24 hours	-	-	-	-	-	-	-	-
Sheta et al. [17]	4.2-5.6 4.8-5.6	RFA + cTACE MWA + cTACE	same session same session	-	-	-	-	-	-	-	-
Wang et al. [20]	1.5-10 cm	RFA + cTACE	1-2 months	83.1	55.7	43.7	-	-	-	-	-
El Dorry et al. [12]	-	RFA + TACE* TACE* + RFA	same session same session	100 85	74 64	-	-	-	-	-	23.2 17.1
Lin et al. [21]	3-5 cm	TACE* + RFA	1 week	90.6	72	53.1	75	50	34	-	-
Peng et al. [10]	<7 cm	cTACE + RFA	<2 weeks	92.6	66.6	-	79.4	60.6	-	-	-
Morimoto et al. [22]	3.1-5.0 cm	cTACE + RFA	same day	100	93	93	67	19	-	-	-
Shibata et al. [23]	0.8-3.0 cm	cTACE + RFA	1 week	100	100	84.8	85.6	82.4	82.4	-	-
Yan et al. [24]	1.1-15.6	cTACE + RFA	1-14 days	-	-	-	-	-	-	46	28
Zhang et al [25]	3.75 (SD: 1.21)	DEB-TACE + RFA	1-2 weeks	97.5	84.7	66.1	75	51.7	35.4	-	-
Liu et al. [26]	<5 cm	cTACE + RFA	7-15 days	76.2	-	37.1	43.2	-	18	27.6	9.1
Sun et al. [27]	<7 cm	cTACE + RFA	1 week	94.4	-	70.8	76.4	-	37.1	-	-
Abdelaziz et al. [15]	4.6 +/- 1.9 cm 4.2 +/- 1.9 cm	cTACE + RFA cTACE + MWA	<2 weeks <2 weeks	-	-	-	73.1 83.3	40.6 64.7	16.2 64.7	-	-
Zhu et al. [28]	2.7 (2.1-4.8)	DEB-TACE + RFA	1-3 months	-	-	-	-	-	-	12.5	8.8

**Type of TACE not specified*

CONCLUSION

There is growing evidence for the combined treatment regimen of TA and TACE for HCC lesions >3 cm. The vast majority of clinical evidence is available on TACE as a neoadjuvant treatment to TA. Our retrospective clinical data contributes to this field as we have compared the two treatment sequences in a western cohort. No difference in OS or LTP was found between the TA with adjuvant TACE and TA with neoadjuvant TACE groups.

REFERENCES

[1] Livraghi T, Meloni F, Di Stasi M, et al. Sustained complete response and complications rates after radiofrequency ablation of very early hepatocellular carcinoma in cirrhosis: Is resection still the treatment of choice? 2008; 47:82-9.

[2] R, Crocetti L. Local-Regional Treatment of Hepatocellular Carcinoma. 2012; 262:43-58.

[3] Forner A, Reig M, Bruix J. Hepatocellular carcinoma. The Lancet 2018; 391:1301-14.

[4] Lencioni R, Crocetti L, Petruzzi P, et al. Doxorubicin-eluting bead-enhanced radiofrequency ablation of hepatocellular carcinoma: A pilot clinical study. Journal of Hepatology 2008; 49:217-22.

[5] Yin X, Zhang L, Wang YH, et al. Transcatheter arterial chemoembolization combined with radiofrequency ablation delays tumor progression and prolongs overall survival in patients with intermediate (BCLC B) hepatocellular carcinoma. BMC cancer 2014; 14:849.

[6] Yamanaka T, Yamakado K, Takaki H, et al. Ablative zone size created by radiofrequency ablation with and without chemoembolization in small hepatocellular carcinomas. Japanese journal of radiology 2012; 30:553-9.

[7] Galle PR, Forner A, Llovet JM, et al. EASL Clinical Practice Guidelines: Management of hepatocellular carcinoma. Journal of Hepatology 2018; 69:182-236.

[8] Heimbach JK, Kulik LM, Finn RS, et al. AASLD guidelines for the treatment of hepatocellular carcinoma. Hepatology 2018; 67:358-80.

[9 Chen QW, Ying HF, Gao S, et al. Radiofrequency ablation plus chemoembolization versus radiofrequency ablation alone for hepatocellular carcinoma: A systematic review and meta-analysis. Clinics and research in hepatology and gastroenterology 2016; 40:309-14.

[10] Peng Z-W, Zhang Y-J, Chen M-S, et al. Radiofrequency Ablation With or Without Transcatheter Arterial Chemoembolization in the Treatment of Hepatocellular Carcinoma: A Prospective Randomized Trial. Journal of Clinical Oncology 2012; 31:426-32.

[11] Mazzaferro V, Llovet JM, Miceli R, et al. Predicting survival after liver transplantation in patients with hepatocellular carcinoma beyond the Milan criteria: a retrospective, exploratory analysis. The Lancet Oncology 2009; 10:35-43.

[12] El Dorry AK, Shaker MK, El-Fouly NF, et al. Effectiveness of combined therapy radiofrequency ablation/transarterial chemoembolization versus transarterial chemoembolization/radiofrequency ablation on management of hepatocellular carcinoma. European journal of gastroenterology & hepatology 2020.

[13] Iezzi R, Pompili M, Posa A, Coppola G, Gasbarrini A, Bonomo L. Combined locoregional treatment of patients with hepatocellular carcinoma: State of the art. World journal of gastroenterology 2016; 22:1935-42.

[14] Vasnani R, Ginsburg M, Ahmed O, et al. Radiofrequency and microwave ablation in combination with transarterial chemoembolization induce equivalent histopathologic coagulation necrosis in hepatocellular carcinoma patients bridged to liver transplantation. Hepatobiliary surgery and nutrition 2016; 5:225-33.

[15] Abdelaziz AO, Abdelmaksoud AH, Nabeel MM, et al. Transarterial Chemoembolization Combined with Either Radiofrequency or Microwave Ablation in Management of Hepatocellular Carcinoma. Asian Pacific journal of cancer prevention : APJCP 2017; 18:189-94.

[16] Thornton LM, Cabrera R, Kapp M, Lazarowicz M, Vogel JD, Toskich BB. Radiofrequency vs Microwave Ablation After Neoadjuvant Transarterial Bland and Drug-Eluting Microsphere Chembolization for the Treatment of Hepatocellular Carcinoma. Current problems in diagnostic radiology 2017; 46:402-9.

[17] Sheta E, El-Kalla F, El-Gharib M, et al. Comparison of single-session transarterial chemoembolization combined with microwave ablation or radiofrequency ablation in the treatment of hepatocellular carcinoma: a randomized-controlled study. European journal of gastroenterology & hepatology 2016; 28:1198-203.

[18] Wen P, Chen SD, Wang JR, Zeng YH. Comparison of Treatment Response and Survival Profiles Between Drug-Eluting Bead Transarterial Chemoembolization and Conventional Transarterial Chemoembolization in Chinese Hepatocellular Carcinoma Patients: A Prospective Cohort Study. Oncology research 2019; 27:583-92.

[19] Liu YS, Lin CY, Chuang MT, et al. Five-year outcome of conventional and drug-eluting transcatheter arterial chemoembolization in patients with hepatocellular carcinoma. BMC Gastroenterol 2018; 18:124.

[20] Wang YH, Liu JF, Li F, et al. Radiofrequency ablation combined with transarterial chemoembolization for unresectable primary liver cancer. Chinese medical journal 2009; 122:889-94.

[21] Lin JJ, Wu W, Jiang XF, Jin XJ, Lu LJ, Bao LW. [Clinical outcomes of radiofrequency ablation combined with transcatheter arterial chemoembolization for the treatment of hepatocellular carcinoma: a single-center experience]. Zhonghua zhong liu za zhi [Chinese journal of oncology] 2013; 35:144-7.

[22] Morimoto M, Numata K, Kondou M, Nozaki A, Morita S, Tanaka K. Midterm outcomes in patients with intermediate-sized hepatocellular carcinoma. Cancer 2010; 116:5452-60.

[23] Shibata T, Isoda H, Hirokawa Y, Arizono S, Shimada K, Togashi K. Small Hepatocellular Carcinoma: Is Radiofrequency Ablation Combined with Transcatheter Arterial Chemoembolization More Effective than Radiofrequency Ablation Alone for Treatment? Radiology 2009; 252:905-13.

[24] Yan L, Ren Y, Qian K, et al. Sequential transarterial chemoembolization and early radiofrequency ablation improves clinical outcomes for early-intermediate hepatocellular carcinoma in a 10-year single-center comparative study. BMC Gastroenterology 2021; 21:182.

[25] Zhang Y, Zhang MW, Fan XX, et al. Drug-eluting beads transarterial chemoembolization sequentially combined with radiofrequency ablation in the treatment of untreated and recurrent hepatocellular carcinoma. World journal of gastrointestinal surgery 2020; 12:355-68.

[26] Liu W, Xu H, Ying X, et al. Radiofrequency Ablation (RFA) Combined with Transcatheter Arterial Chemoembolization (TACE) for Patients with Medium-to-Large Hepatocellular Carcinoma: A Retrospective Analysis of Long-Term Outcome. Medical science monitor : international medical journal of experimental and clinical research 2020; 26:e923263.

[27] Sun Y, Ji S, Ji H, Liu L, Li C. Clinical efficacy analysis of transcatheter arterial chemoembolization (TACE) combined with radiofrequency ablation (RFA) in primary liver cancer and recurrent liver cancer. Journal of BUON : official journal of the Balkan Union of Oncology 2019; 24:1402-7.

[28] Zhu D, Yuan D, Wang Z, Chen S. Efficacy of drug-eluting bead transarterial chemoembolization (DEB-TACE) combined with radiofrequency ablation versus DEB-TACE alone in Chinese hepatocellular carcinoma patients. Medicine 2019; 98:e15682.

Chapter 7

Study protocol: Adjuvant holmium-166 radioembolization after radiofrequency ablation in early-stage hepatocellular carcinoma patients: a dose-finding study (HORA EST HCC trial)

Authors

Pim Hendriks, Daphne D. D. Rietbergen, Arian R. van Erkel, Minneke J. Coenraad, Mark J. Arntz, Roel J. Bennink, Andries E. Braat, A. Stijn L. P. Crobach, Otto M. van Delden, Tom van der Hulle, Heinz-Josef Klümpen, Rutger W. van der Meer, J. Frank W. Nijsen, Carla S. P. van Rijswijk, Joey Roosen, Bastian N. Ruijter, Frits Smit, Mette K. Stam, R. Bart Takkenberg, Maarten E. Tushuizen, Floris H. P. van Velden, Lioe-Fee de Geus-Oei, Mark C. Burgmans

On behalf of: Dutch Hepatocellular Cholangiocarcinoma Group

Published

CardioVascular and Interventional Radiology, 2022; 45:1057-1063,
DOI: 10.1007/s00270-022-03162-7

Supplementary materials

https://doi.org/10.1007/s00270-022-03162-7

ABSTRACT

Purpose To investigate the biodistribution of holmium-166 microspheres (^{166}Ho-MS) when administered after radiofrequency ablation (RFA) of early-stage hepatocellular carcinoma (HCC). The aim is to establish a perfused liver administration dose that results in a tumoricidal dose of holmium-166 on the hyperaemic zone around the ablation necrosis (i.e. target volume).

Materials and Methods Multicentre, prospective, dose-escalation study in HCC patients with a solitary lesion 2-5 cm, or a maximum of 3 lesions of ≤3 cm each. The day after RFA patients undergo angiography and cone-beam CT (CBCT) with (super)selective infusion of technetium-99m labelled microalbumin aggregates (^{99m}Tc-MAA). The perfused liver volume is segmented from the CBCT and ^{166}Ho-MS is administered to this treatment volume 5-10 days later. The dose of holmium-166 is escalated in a maximum of 3 patient cohorts (60 Gy, 90 Gy and 120 Gy) until the endpoint is reached. SPECT/CT is used to determine the biodistribution of holmium-166. The endpoint is met when a dose of ≥120 Gy has been reached on the target volume in 9/10 patients of a cohort. Secondary endpoints include toxicity, local recurrence, disease-free and overall survival.

Discussion This study aims to find the optimal administration dose of adjuvant radioembolization with ^{166}Ho-MS after RFA. Ultimately, the goal is to bring the efficacy of thermal ablation up to par with surgical resection for early stage HCC patients.

Key words: Hepatocellular carcinoma; early stage HCC; Thermal ablation; Radiofrequency ablation; Radioembolization; holmium-166; TARE

INTRODUCTION

Thermal ablation (TA) has proven to be an effective treatment for hepatocellular carcinoma (HCC) and it has become the treatment of first choice in solitary lesions up to 2 cm owing to its equal effectiveness and lower complication rate compared with surgical resection [1]. In patients with a preserved liver function and larger solitary, or up to 3 HCC lesions of ≤3 cm, surgical resection remains the preferred treatment modality [1, 2], as it yields a better oncological outcome [3-5]. Yet, surgical resection is often contraindicated due to liver cirrhosis with portal hypertension, deranged liver function, comorbidity or an unfavourable tumour localization [1].

Efforts to prevent tumour recurrence are key to improve the long-term prognosis of HCC patients treated with TA. Recent systematic reviews show that the chance of developing local tumour progression (LTP) is higher after TA compared to surgical resection, especially in the treatment of lesions >3 cm [4, 5]. Causes for higher LTP rates in larger tumours are a) insufficient heat generation or propagation at the peripheral parts of the tumour, b) viable satellite nodules found in the direct proximity of the main tumour, and c) the 'heat-sink effect' near medium to large blood vessels. Regardless of the cause, local recurrence after TA is most commonly seen at the periphery of, or in close proximity to the main tumour [6].

External beam radiation therapy is widely used as an adjuvant therapy to surgery in different types of cancer, but is infrequently used to treat liver cancer, as the liver has a low tolerability to it and liver cirrhosis further reduces this tolerability [7, 8]. Preclinical studies identified potential benefits of combined radiofrequency ablation (RFA) and radiation-based therapy too [9-12]. Potential causes for synergy between RFA and radiation-based therapy include the sensitization of viable tumour cells to subsequent radiation owing to the increased oxygenation resulting from hyperaemia, like in hyperbaric radiotherapy [13]. Another possible synergetic result may be a radiation-induced inhibition of repair and recovery and increased free radical formation, as observed in animal tumour models with RFA and transarterial chemoembolization (TACE) [14]. Transarterial radioembolization (TARE) provides an alternative way of delivering adjuvant radiation therapy by means of radioactive microspheres that are administered selectively in the hepatic artery using a high tumour dose and a low toxicity to the healthy liver parenchyma [15, 16].

RFA induces hyperaemia in a marginal zone around the area of ablation necrosis [17]. This hyperaemic zone encompasses the area in which viable residual tumour cells or satellite nodules may reside. When TARE is administered shortly after RFA, it is hypothesized that the hyperaemia can be used to deliver a large amount of holmium-166 microspheres (^{166}Ho-MS) to this marginal zone with the aim of decreasing the chance of LTP. The objective of this study

is to find the necessary administrated dose of ^{166}Ho-MS that yields a dose of ≥120 Gy to the hyperaemic zone (target volume).

METHODS

This is a multicentre, open-label, non-randomized, phase I dose-escalation study of the use of adjuvant TARE after RFA in HCC patients with a solitary lesion of 2-5 cm, or a maximum of 3 lesions of ≤3 cm each. Leiden University Medical Center is the sponsor of the study. The trial will be executed in 3 academic hospitals (see supplementary table 1).

Eligibility criteria

A full list of in- and exclusion criteria can be found in table 1. Patients with BCLC early stage HCC (A) are eligible if they have a solitary lesion of 2-5 cm or a maximum of 3 lesions of ≤3 cm each, and if surgical resection would not be the treatment of first choice as decided upon by the multidisciplinary tumour board. General contraindication criteria for RFA and TARE are used [1, 2]. Additional exclusion criteria where: a) a treatment volume (i.e. area exposed to radiation) exceeding 50% of the total liver volume. b) creatinine clearance rate <30 mL/min.

Interventions

A schematic overview of the study procedure can be found in figure 1. RFA is performed under general anaesthesia or deep sedation using single or three 3 or 4 cm exposed tip multi-electrode Cooltip RFA probes with switch-control system (Medtronic Inc, Dublin, Ireland). A contrast enhanced computed tomography (CECT) scan is performed on a 64-slice Aquilion CT-scanner (Canon, Tochigi, Japan) immediately after ablation and additional ablation is performed in the same session when residual tumour tissue is identified on this scan.

Table 1. *List of in- and exclusion criteria.*

Inclusion criteria	Exclusion criteria
• Informed consent • Age > 18 years • Single HCC lesion with diameter of ≥ 2-5cm or up to three lesions with each lesion measuring no more than 3cm • HCC diagnosis is based on histology or non-invasive imaging criteria according to EORTC-EASL guidelines • Child Pugh A or B ≤7 • (HCC-unrelated) ECOG performance status ≤ 2 • Bilirubin < 2mg/dL • ASAT < 5x upper limit of normal • ALAT < 5x upper limit of normal • Thrombocytes ≥ 50 X 10^9/L	• Tumour location precluding percutaneous RFA • Treatment volume >50% of total liver volume, based on CBCT images • Vascular tumour invasion or extrahepatic metastasis • Hemihepatectomy • Severe comorbidity (e.g. cardiovascular disease, diabetes with nephropathy, active infections) • Uncorrectable coagulopathy • Large arterio-portovenous shunt • Previous radiotherapy to the liver • Surgical hepatico-enterostomy • Hepatic resection with placement of surgical clips that may cause artefacts on MRI • Incompetent/ mentally disabled • Pregnancy, inadequate anticonception • Lung shunt fraction > 20% • Creatinine clearance <30 mL/min/1.73m^2

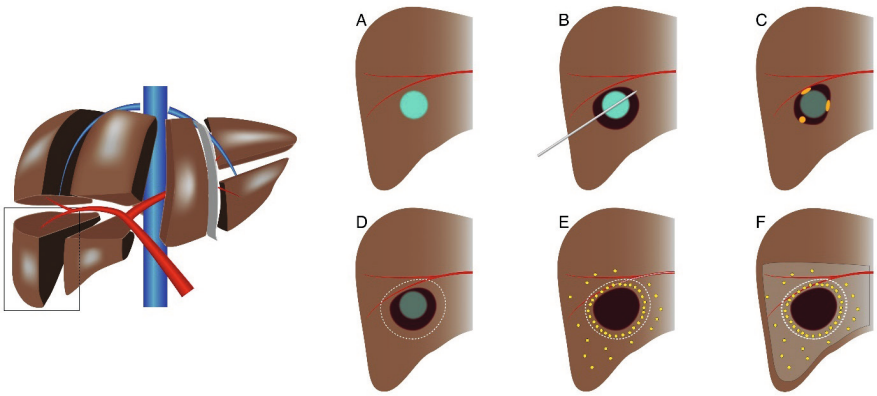

Figure 1. *Schematic drawings of the study procedure.* **A:** *HCC lesion of 2-5 cm.* **B:** *Thermal ablation of HCC lesion.* **C:** *Potential sites of LTP due to heat-sink effect, impaired heat propagation or satellite nodules.* **D:** *Target zone for adjuvant TARE.* **E:** *Deposition of ^{166}Ho-MS with preferential flow of microspheres to the hyperaemic zone surrounding the ablation area.* **F:** *Perfused liver volume after ^{166}Ho-MS TARE (i.e. treatment volume).*

On the second day, angiography and administration of 150 MBq of ^{99m}Technetium-labeled macro albumin aggregate (^{99m}Tc-MAA) is performed with a single photon emission/ computed tomography (SPECT/CT) scan directly after the procedure on a Symbia T6 or Symbia Intevo (Siemens Healthineers, Erlangen, Germany) or Discovery 670 Pro (GE Healthcare, Boston, Massachusetts, USA). Prior to injection a contrast enhanced cone-beam CT (CBCT) is performed to verify the treatment volume, and potassium perchlorate was given to patients [19]. Hepatico-enteric anastomoses are coiled if necessary. Using a Progreat 2.4F or 2.7F microcatheter (Terumo corporation, Tokyo, Japan), catheter position(s) is/are chosen as selectively as possible for ^{99m}Tc-MAA-injection. Multiple catheter positions may be used to ensure adjuvant treatment of the entire hyperaemic zone(s) after ablation. The SPECT/CT scan is used to rule out lung shunting >20%.

On day 5-10 after RFA, TARE with ^{166}Ho-MS QuiremSpheres (Quirem Medical B.V., Deventer, the Netherlands) is performed. The administration activity of holmium-166 (AHo-166) is calculated using the following equation [20]:

$$A_{Ho-166} = Perfused\ Liver\ Dose\ [Gy] * W_i\ [kg] * 63\ [MBq/J]$$

Depending of the cohort, patients are treated with 60, 90 or 120 Gy to the treated liver segments. The weight of the treated volume (w_i) is determined by the treatment volume as segmented from the CBCT, determined using IntelliSpace software. (Philips Healthcare, Eindhoven, The Netherlands), using an anticipated tissue density of 1.00 g/cm^3. The catheter position for Ho-166 injection is verified by fluoroscopic and CBCT imaging prior to infusion.

Post-treatment SPECT/CT is performed the day after TARE for dosimetry purposes. Moreover, magnetic resonance imaging (MRI) is acquired between RFA and TARE, and after Ho-166 treatment. T2* sequences are acquired on a 1.5T Ingenia MRI system (Philips Healthcare, Eindhoven, The Netherlands) or 3T Magnetom Skyra (Siemens Healthineers, Erlangen, Germany) for post-treatment dosimetry purpose, by subtracting these scans, making use of the paramagnetic properties of Ho-166 [20-22].

A participant's timeline of the two hospitalizations can be found in figure 2.

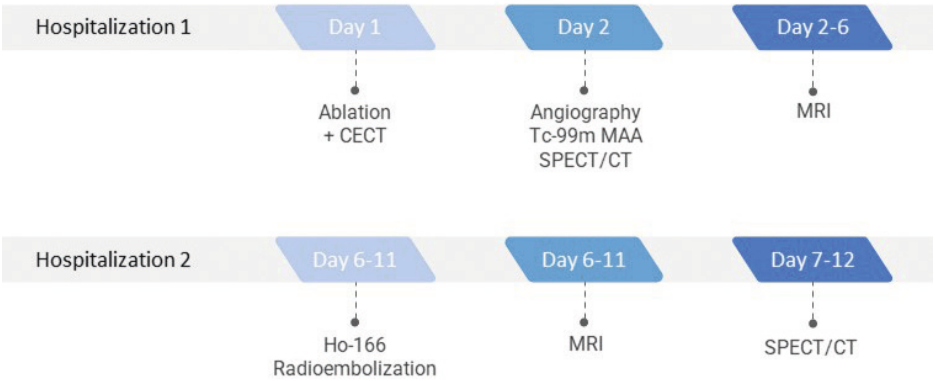

Figure 2. *Participants timeline of the treatment period. After the angiography procedure and the acquisition of the Tc-99m MAA SPECT/CT, the dose calculation was performed and ^{166}Ho-MS were ordered.*

Follow-up

Patients are followed for 12 months after treatment. The follow-up is performed according to regular HCC treatment regimen. Imaging follow up will be performed by CECT or MRI at 6 weeks and 3 months after treatment and then every 3 months. Clinical assessment and biochemical liver function tests are performed at 2 weeks, 6 weeks and 3 months and continued synchronized with imaging. Adverse events will be categorized according to common terminology criteria for adverse events (CTCAE) 4.0 [23]. Serious adverse events will be immediately reported to the ethical board upon notification.

Outcomes

Different small cohorts are exposed to 60 Gy, 90 Gy or 120 Gy to the treated liver volume. The primary endpoint of this study is to find the treatment volume dose that results in a dose of ≥120 Gy to the target volume in 9/10 patients, based on post-treatment SPECT scan. The hyperaemic zone encompassing the ablation necrosis (or necroses) is considered the target volume and generally anticipated to be a 1 cm rim around the ablation necrosis/necroses. Segmentation of the treatment and target volumes in the post-treatment SPECT scan is

performed using Xeleris workstation version 4.0 (GE Healthcare, Boston, Massachusetts, USA). The study consists of a maximum of 3 cohorts (treatment volume doses of 60 Gy, 90 Gy and 120 Gy), depending on when the final endpoint is met. If the second patient within one cohort fails to meet ≥120 Gy on the target volume, the study endpoint of 9/10 patients fails and the cohort is closed. Consecutive patients are then treated with a higher dose as part of the following cohort.

Secondary endpoints include toxicity according to CTCAE 4.0, disease-free and overall survival.

Sample size

No sample size calculations were performed as this is a phase I feasibility study. A minimum of 10 patients will be recruited when ≥9/10 patients will meet the end point of 120 Gy to the target volume at a treatment dose volume dose of 60 Gy. A maximum of 30 patients will be recruited as there are maximally 3 cohorts in this study with a maximum of 10 patients in each cohort.

Data

The obtained CBCT, SPECT/CT and MRI scans will be pseudonymized and stored in an encrypted folder accessible only to the PI and study coordinator. Pseudonymized patient baseline, study and follow-up data are stored in an encrypted database by Castor EDC (Castor, Amsterdam, The Netherlands). Data will be subject to data monitoring every year.

DISCUSSION

This is the first clinical trial in which TARE is investigated as adjuvant therapy after TA in patients with HCC. Advancements in tumour targeting, treatment planning and evaluation have led to increased efficacy of TA with clinical studies reporting local recurrence rates comparable to surgery even for tumours >2 cm [24]. Nevertheless, in larger clinical trials these findings have not been confirmed and surgical resection remains the recommendation for solitary HCC lesions >2 cm in the recently published update of the BCLC system [25]. The task that lies ahead for interventional radiologists is to bring the efficacy of thermal ablation up to par with that of surgical resection.

The combination of TA with either systemic therapy or transarterial therapy has been investigated in different studies. In the STORM trial, no difference was found in median recurrence free survival between patients treated with adjuvant sorafenib or placebo [26]. Currently, several trials combining thermal ablation with molecular or immuno-therapy are ongoing [27]. The most widely investigated combination therapy is that of TA and TACE.

Superiority of TACE-RFA compared with RFA with respect to LTP after treatment of lesions >2 cm was found in a recent meta-analysis [28]. Nevertheless, validation in a western cohort is lacking and it is not recommended in the European guidelines. Furthermore, there is a lack of consensus on how the two therapies are best combined with respect to sequence, interval and embolic agent [29].

Over recent years, radiation segmentectomy has received attention as an alternative to thermal ablation. In the LEGACY study, patients with a solitary HCC up to 8 cm were treated with a high dose of yttrium-90. The results of this trial were promising, since a high local control rate was found, which led to the acceptance of radiation segmentectomy as a treatment for patients that are not a candidate for resection or ablation [30]. Limitations of the LEGACY study are that this was a retrospective study and mean tumour size was only 2.7 cm. Prospective comparative studies are warranted before radiation segmentectomy can be further implemented in clinical practise.

Our study investigates the combination of TA and TARE. This is a first-in-man study to investigate the biodistribution of ^{166}Ho-MS when administrated shortly after RFA. The data will be used in future prospective studies investigating the efficacy of combined thermal ablation and TARE, with the long term objective to bring the efficacy of TA up to par with surgical resection for HCC >2cm.

With respect to TA, the current protocol only permits the use of RFA. Microwave ablation (MWA) may have technological advantages over RFA, but yet similar outcomes are found [31]. In order to minimize variability in technique and materials, it was chosen to perform all TA procedures with RFA and with the same system. Furthermore, (pre-)clinical work on the combination of TA and radionuclide therapy has so far only been performed with RFA [9-12].

In this study, TARE is used as an adjuvant rather than as a neoadjuvant therapy. In this way, TARE can be used to target the marginal zone that corresponds to the area where LTP is most commonly seen after TA. When TARE is performed shortly after the ablation, a preferential flow of ^{166}Ho-MS to the hyperaemic volume is expected. This principle has also been utilized in studies investigating TA with adjuvant TACE the next day. In our study, the interval between TA and TARE ranges between 5-10 days, which is mainly due to logistical reasons. Every patient receives an individualized treatment dose and the microspheres need to be prepared in a nuclear facility prior to administration. There is sufficient evidence though, that the aforementioned hyperaemia persists during the first weeks and sometimes even months [32].

In this study, ^{166}Ho-MS were used rather than yttrium-90. Holmium-166 offers specific advantages as it emits gamma radiation at 81 keV besides the therapeutical beta particles, allowing for quantitative SPECT. Moreover, due to its paramagnetic properties, post-treatment dosimetry can also be performed using MRI. Data from the HEPAR 1 study were used to determine the dose for the first patient cohort, i.e. patients treated with a treatment volume dose of 60 Gy [33]. In the HEPAR 1 study, an administrated dose of 60 Gy was established as the maximal tolerated for patients with multiple liver metastases. A dose escalation to a maximum of 120 Gy is expected to be safe, as no more than 50% of the non-tumorous liver parenchyma will be exposed to radiation and only patients with a preserved liver function are allowed to participate in the study. The treatment volume is calculated using CBCT images as these provide the best insight in the vascular territories of tumour-feeding arteries. No data were available on the dose-response relationship for holmium-166 radioembolization at the time the study was designed. A target dose of 120 Gy was chosen in close consultation with Quirem Medical B.V. (producer of ^{166}Ho-MS). Although well aware of the potential differences in radiobiology between yttrium-90 and holmium-166, this was based on earlier ^{166}Ho-MS cases and based on yttrium-90 therapy standards, prior to more recently published dose-response evaluation studies. Several studies investigating ^{166}Ho-MS are currently on-going, including the HEPAR PRIMARY trial. Those studies are expected to provide further insight in the dose-response relationship of holmium-166.

As an exploratory end-point, MRI-based dosimetry will be performed. Yet, to determine the absorbed dose on the target volume and to determine the primary end-point of the study, SPECT/CT imaging will be used. SPECT/CT will be able to give an estimate of the absorbed radiation dose, but due to the limited spatial resolution it will be difficult to determine the precise border of the target volume. The thickness of the hyperaemic zone, i.e. target volume, will be measured on the post-ablation diagnostic CT and CBCT images. In general, a rim of 1 cm around the ablation zone will be considered as the target volume as most satellite tumours reside within 1 cm from the primary tumour [34].

The TARE work-up is performed with ^{99m}Tc-MAA in this study whereas Ho-166 specific work-up could also be performed with Ho-166 scout dose [35]. At the time of the initial study design, Ho-166 scout dose was not commercially available yet. Moreover, since the work-up was only used for ruling out high lung-shunt fractions rather than partition model based dosing, ^{99m}Tc-MAA was deemed sufficient.

The goal of the current trial is to study the feasibility and dosimetry of TARE as adjuvant treatment after TA for HCC patients. In this trial, all early stage patients with a solitary tumour of 2-5 cm or a maximum of 3 tumours of ≤3 cm each can be included, while this study focuses on the proof of concept of combining the treatments. In future trials, further specification of

patient characteristics should be defined to identify which patients potentially benefit most from this treatment combination. Moreover, these trials should reveal the potential clinical benefit of this new treatment combination in terms of disease-free and overall survival.

TRIAL REGISTRATION

Clinicaltrials.gov identifier: NCT03437382.

REFERENCES

[1] Galle PR, Forner A, Llovet JM, et al. EASL Clinical Practice Guidelines: Management of hepatocellular carcinoma. Journal of Hepatology 2018; 69:182-236.

[2] Forner A, Reig M, Bruix J. Hepatocellular carcinoma. The Lancet 2018; 391:1301-14.

[3] Weis S, Franke A, Mössner J, Jakobsen JC, Schoppmeyer K. Radiofrequency (thermal) ablation versus no intervention or other interventions for hepatocellular carcinoma. The Cochrane database of systematic reviews 2013:Cd003046.

[4] Xu X-L, Liu X-D, Liang M, Luo B-M. Radiofrequency Ablation versus Hepatic Resection for Small Hepatocellular Carcinoma: Systematic Review of Randomized Controlled Trials with Meta-Analysis and Trial Sequential Analysis. Radiology 2017; 287:461-72.

[5] Shin SW, Ahn KS, Kim SW, Kim T-S, Kim YH, Kang KJ. Liver Resection Versus Local Ablation Therapies for Hepatocellular Carcinoma Within the Milan Criteria: A Systematic Review and Meta-analysis. Annals of Surgery 2021; 273.

[6] Habibollahi P, Sheth RA, Cressman ENK. Histological Correlation for Radiofrequency and Microwave Ablation in the Local Control of Hepatocellular Carcinoma (HCC) before Liver Transplantation: A Comprehensive Review. Cancers 2021; 13.

[7] Dawson LA, Guha C. Hepatocellular Carcinoma: Radiation Therapy. The Cancer Journal 2008; 14.

[8] Cheng JC, Wu JK, Lee PC, et al. Biologic susceptibility of hepatocellular carcinoma patients treated with radiotherapy to radiation-induced liver disease. International journal of radiation oncology, biology, physics 2004; 60:1502-9.

[9] Solazzo S, Mertyna P, Peddi H, Ahmed M, Horkan C, Nahum Goldberg S. RF ablation with adjuvant therapy: Comparison of external beam radiation and liposomal doxorubicin on ablation efficacy in an animal tumor model. International Journal of Hyperthermia 2008; 24:560-7.

[10] Horkan C, Dalal K, Coderre JA, et al. Reduced tumor growth with combined radiofrequency ablation and radiation therapy in a rat breast tumor model. Radiology 2005; 235:81-8.

[11] Lin ZY, Chen J, Deng XF. Treatment of hepatocellular carcinoma adjacent to large blood vessels using 1.5T MRI-guided percutaneous radiofrequency ablation combined with iodine-125 radioactive seed implantation. Eur J Radiol 2012; 81:3079-83.

[12] Chen K, Chen G, Wang H, et al. Increased survival in hepatocellular carcinoma with iodine-125 implantation plus radiofrequency ablation: a prospective randomized controlled trial. Journal of hepatology 2014; 61:1304-11.

[13] Mayer R, Hamilton-Farrell MR, van der Kleij AJ, et al. Hyperbaric oxygen and radiotherapy. Strahlentherapie und Onkologie : Organ der Deutschen Rontgengesellschaft [et al] 2005; 181:113-23.

[14] Solazzo SA, Ahmed M, Schor-Bardach R, et al. Liposomal doxorubicin increases radiofrequency ablation-induced tumor destruction by increasing cellular oxidative and nitrative stress and accelerating apoptotic pathways. Radiology 2010; 255:62-74.

[15] Riaz A, Gates VL, Atassi B, et al. Radiation segmentectomy: a novel approach to increase safety and efficacy of radioembolization. International journal of radiation oncology, biology, physics 2011; 79:163-71.

[16] Roosen J, Klaassen NJM, Westlund Gotby LEL, et al. To 1000 Gy and back again: a systematic review on dose-response evaluation in selective internal radiation therapy for primary and secondary liver cancer. European journal of nuclear medicine and molecular imaging 2021.

[17] Park M-h, Rhim H, Kim Y-s, Choi D, Lim HK, Lee WJ. Spectrum of CT Findings after Radiofrequency Ablation of Hepatic Tumors. RadioGraphics 2008; 28:379-90.

[18] Lau WY, Leung WT, Ho S, et al. Treatment of inoperable hepatocellular carcinoma with intrahepatic arterial yttrium-90 microspheres: a phase I and II study. British journal of cancer 1994; 70:994-9.

[19] Sabet A, Ahmadzadehfar H, Muckle M, et al. Significance of oral administration of sodium perchlorate in planning liver-directed radioembolization. Journal of nuclear medicine : official publication, Society of Nuclear Medicine 2011; 52:1063-7.

[20] Smits ML, Elschot M, van den Bosch MA, et al. In vivo dosimetry based on SPECT and MR imaging of 166Ho-microspheres for treatment of liver malignancies. Journal of nuclear medicine : official publication, Society of Nuclear Medicine 2013; 54:2093-100.

[21] van de Maat GH, Seevinck PR, Bos C, Bakker CJG. Quantification of holmium-166 loaded microspheres: Estimating high local concentrations using a conventional multiple gradient echo sequence with S0-fitting. 2012; 35:1453-61.

[22] Roosen J, Arntz MJ, Janssen MJR, et al. Development of an MRI-Guided Approach to Selective Internal Radiation Therapy Using Holmium-166 Microspheres. 2021; 13:5462.

[23] USA NIH National Cancer Institute. Common Terminology Criteria in Adverse Events, version 4.0 (CTCAE 4.0).

[24] Ng KKC, Chok KSH, Chan ACY, et al. Randomized clinical trial of hepatic resection versus radiofrequency ablation for early-stage hepatocellular carcinoma. British Journal of Surgery 2017; 104:1775-84.

[25] Reig M, Forner A, Rimola J, et al. BCLC strategy for prognosis prediction and treatment recommendation: The 2022 update. Journal of hepatology.

[26] Bruix J, Takayama T, Mazzaferro V, et al. Adjuvant sorafenib for hepatocellular carcinoma after resection or ablation (STORM): a phase 3, randomised, double-blind, placebo-controlled trial. The Lancet Oncology 2015; 16:1344-54.

[27] Bo XW, Sun LP, Yu SY, Xu HX. Thermal ablation and immunotherapy for hepatocellular carcinoma: Recent advances and future directions. World journal of gastrointestinal oncology 2021; 13:1397-411.

[28] Cao S, Zou Y, Lyu T, et al. Long-term outcomes of combined transarterial chemoembolization and radiofrequency ablation versus RFA monotherapy for single hepatocellular carcinoma ≤3 cm: emphasis on local tumor progression. International Journal of Hyperthermia 2022; 39:1-7.

[29] Hendriks P, Sudiono DR, Schaapman JJ, et al. Thermal ablation combined with transarterial chemoembolization for hepatocellular carcinoma: What is the right treatment sequence? European Journal of Radiology 2021; 144:110006.

[30] Salem R, Johnson GE, Kim E, et al. Yttrium-90 Radioembolization for the Treatment of Solitary, Unresectable HCC: The LEGACY Study. Hepatology (Baltimore, Md) 2021; 74:2342-52.

[31] Poulou LS, Botsa E, Thanou I, Ziakas PD, Thanos L. Percutaneous microwave ablation vs radiofrequency ablation in the treatment of hepatocellular carcinoma. World J Hepatol 2015; 7:1054-63.

[32] Kasper H-U, Bangard C, Gossmann A, Dienes HP, Stippel DL. Pathomorphological changes after radiofrequency ablation in the liver. Pathology International 2010; 60:149-55.

[33] Smits MLJ, Nijsen JFW, van den Bosch MAAJ, et al. Holmium-166 radioembolisation in patients with unresectable, chemorefractory liver metastases (HEPAR trial): a phase 1, dose-escalation study. The Lancet Oncology 2012; 13:1025-34.

[34] Okusaka T, Okada S, Ueno H, et al. Satellite lesions in patients with small hepatocellular carcinoma with reference to clinicopathologic features. Cancer 2002; 95:1931-7.

[35] Smits MLJ, Dassen MG, Prince JF, et al. The superior predictive value of (166)Ho-scout compared with (99m)Tc-macroaggregated albumin prior to (166)Ho-microspheres radioembolization in patients with liver metastases. European journal of nuclear medicine and molecular imaging 2020; 47:798-806.

Chapter 8

Adjuvant holmium-166 radioembolization after radiofrequency ablation in early-stage hepatocellular carcinoma patients: a dose-finding study (HORA EST HCC trial)

Authors

Pim Hendriks, Daphne D. D. Rietbergen, Arian R. van Erkel, Minneke J. Coenraad, Mark J. Arntz, Roel J. Bennink, Andries E. Braat, A. Stijn L. P. Crobach, Otto M. van Delden, Petra Dibbets-Schneider, Tom van der Hulle, Heinz-Josef Klümpen, Rutger W. van der Meer, J. Frank W. Nijsen, Carla S. P. van Rijswijk, Joey Roosen, Bastian N. Ruijter, Frits Smit, Mette K. Stam, R. Bart Takkenberg, Maarten E. Tushuizen, Floris H. P. van Velden, Lioe-Fee de Geus-Oei, Mark C. Burgmans

On behalf of: Dutch Hepatocellular Cholangiocarcinoma Group

Published

European Journal of Nuclear Medicine and Molecular Imaging, 2024; 51:2085-2097, *DOI: 10.1007/s00259-024-06630-z*

ABSTRACT

Purpose The aim of this study was to investigate the biodistribution of (super-)selective trans-arterial radioembolization (TARE) with holmium-166 microspheres (^{166}Ho-MS), when administered as adjuvant therapy after RFA of HCC 2-5 cm. The objective was to establish a treatment volume absorbed dose that results in an absorbed dose of ≥120 Gy on the hyperemic zone around the ablation necrosis (i.e. target volume).

Methods In this multicenter, prospective dose-escalation study in BCLC early stage HCC patients with lesions 2-5 cm, RFA was followed by (super-)selective infusion of ^{166}Ho-MS on day 5-10 after RFA. Dose distribution within the treatment volume was based on SPECT-CT. Cohorts of up to 10 patients were treated with an incremental dose (60 Gy, 90 Gy, 120 Gy) of ^{166}Ho-MS to the treatment volume. The primary endpoint was to obtain a target volume dose of ≥120 Gy in 9/10 patients within a cohort.

Results Twelve patients were treated (male 10; median age: 66.5 years (IQR: [64.3-71.7])) with a median tumor diameter of 2.7 cm (IQR: [2.1-4.0]). At a treatment volume absorbed dose of 90 Gy, the primary end point was met with a median absorbed target volume dose of 138 Gy (IQR: [127-145]). No local recurrences were found within one year follow up.

Conclusion Adjuvant (super-)selective infusion of ^{166}Ho-MS after RFA for the treatment of HCC can be administered safely at a dose of 90 Gy to the treatment volume while reaching a dose of ≥120 Gy to the target volume, and may be a favorable adjuvant therapy for HCC lesions 2-5 cm.

Key words: Hepatocellular carcinoma; Radiofrequency ablation; Trans-arterial radioembolization; holmium-166; adjuvant therapy; dose-escalation study

INTRODUCTION

In the management of hepatocellular carcinoma (HCC), thermal ablation (TA) has become the preferred curative treatment for lesions up to 2 cm, owing to its equal effectiveness and lower complication rate compared to surgical techniques [1, 2]. For larger tumors, surgical resection is generally regarded as the recommended treatment, provided that liver function is preserved [1-7]. Nevertheless, most patients are not eligible for surgery due to the presence of underlying liver cirrhosis induced portal hypertension, impaired liver function, other comorbidity and/or an unfavorable tumor location [1]. As a result, these patients are often treated with TA or trans-arterial therapies, such as trans-arterial chemoembolization (TACE) or trans-arterial radioembolization (TARE) [1, 2].

The risk of developing local recurrence after TA is generally considered to be higher than after surgical resection, especially for lesions >3 cm [5, 6, 8]. Local recurrences are mainly caused by a) insufficient heat propagation during thermal ablation, b) heat sink effect in case of tumors with a bordering intrahepatic vessel, or c) the presence of viable satellite nodules. Most recurrences are found in the periphery of, or in close proximity to the treated tumor [9].

In order to reduce local recurrence rates after TA of larger lesions (>3 cm), the combined treatment of TA with TACE has been studied previously. Although the combined treatment may improve survival as compared to TA alone, superiority over surgical treatment has not been proven [10, 11]. Preclinical studies identified potential benefits of combined radiofrequency ablation (RFA) and radiation-based therapies [12-15]. However, the liver has a low tolerability to external beam radiation therapy [16, 17]. TARE provides a selective way of delivering high doses of radiation therapy to a tumor while saving healthy parenchyma [18, 19] and may work synergistically with RFA when the two therapies are combined.

Since RFA induces hyperemia around the ablation zone [20], this reactive viable liver parenchyma corresponds to the volume where residual tumor cells or satellite nodules are most likely to reside, if present [9]. We hypothesized that this hyperemic effect can be used to deliver a high absorbed dose of holmium-166 microspheres (^{166}Ho-MS) to the tissue directly bordering the ablated tissue with the aim of decreasing chances of developing local recurrences. Early studies on TARE dosimetry reported on higher response rates in patients who received ≥120 Gy of yttrium-90 (^{90}Y) monotherapy on their nonresectable HCC, compared to patients who received a lower absorbed dose [21]. The primary objective of this prospective study was to find the treatment volume absorbed dose of ^{166}Ho-MS that yields an absorbed dose of ≥120 Gy to the hyperemic zone (target volume). Secondary objectives were to investigate safety and efficacy of this adjuvant therapy.

MATERIALS AND METHODS

Design

The HORA EST HCC study (NCT03437382) was a multicenter (3 tertiary referral centers for HCC), open-label, non-randomized phase Ib dose-escalation study to the use of adjuvant TARE after RFA in patients with Barcelona Clinic for Liver cancer (BCLC) early stage HCC (A) lesions of 2-5 cm [2]. The study protocol was approved by the local Medical Ethics Committee and was performed in accordance with good clinical practice and the declaration of Helsinki. All participants provided written informed consent. The full study protocol has been published earlier, in accordance with good research practice [22].

Patients

Eligible patients were those with BCLC early stage HCC (A) with a solitary lesion of 2-5 cm or with up to 3 lesions of ≤3 cm and at least one lesion >2 cm, in whom surgical resection was not the treatment of first choice upon decision by the multidisciplinary tumor board. Main inclusion criteria were age of ≥18 years old, Child Pugh (CP) A or B ≤7, an Eastern Cooperative Oncology Group (ECOG) performance status of 0 or 1, an estimated TARE treatment volume ≤50% of the total liver volume, no prior hemi-hepatectomy or radiation therapy, and a creatinine clearance rate ≥30 mL/min. A list of all in- and exclusion criteria can be found in table 1.

Table 1 *Inclusion and exclusion criteria*

Inclusion Criteria	Exclusion criteria
• Informed consent • Age >18 year • Single HCC lesion with diameter of ≥2-5cm or up to three lesions with each lesion measuring no more than 3cm • HCC diagnosis is based on histology or non-invasive imaging criteria according to EORTC-EASL guidelines • Child Pugh A or B ≤7 • (HCC-unrelated) ECOG performance status ≤2 • Bilirubin <2mg/dL • ASAT <5x upper limit of normal • ALAT <5x upper limit of normal • Thrombocytes ≥50 X 10^9/L	• Tumor location precluding percutaneous RFA • Treatment volume >50% of total liver • Vascular tumor invasion or extrahepatic metastasis • Prior hemi-hepatectomy • Severe comorbidity (e.g. cardiovascular disease, diabetes with nephropathy, active infections) • Uncorrectable coagulopathy • Large arterio-portal venous shunting • Previous radiotherapy to the liver • Surgical hepatico-enterostomy • Hepatic resection with placement of surgical clips that may cause artefacts on MRI • Incapability to give informed consent due to mental disorder • Pregnancy, inadequate anticonception • Lung shunt fraction >20% • Creatinine clearance <30 mL/min/1.73m^2

Study procedures

A schematic overview of the study procedures can be found in Figure 1. On the first day of treatment, ultrasound or CT guided RFA was performed under general anesthesia using 3x3 or 3x4 cm exposed tip multi-electrode Cool-tip™ RFA system, electrodes and switching controller (Medtronic Inc, Dublin, Ireland). Immediately after RFA, a contrast enhanced computed tomography (CECT) scan was performed on a 64-slice Aquilion CT-scanner (Canon, Tochigi, Japan) and an additional ablation was acquired in the same session in case residual viable tumor tissue was identified on this scan.

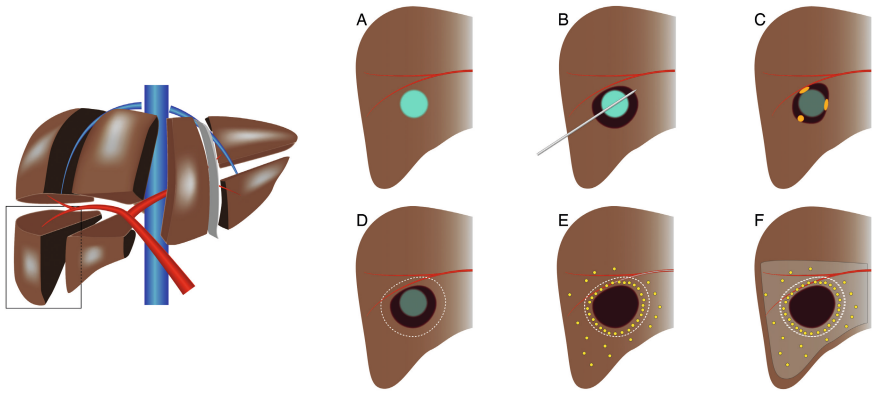

Figure 1 *Schematic drawings of the study procedure.* **A:** *HCC lesion of 2-5 cm.* **B:** *Thermal ablation of HCC lesion.* **C:** *Potential sites of local recurrences due to impaired heat propagation, heat-sink effect, or satellite nodules.* **D:** *Target volume for adjuvant TARE.* **E:** *Deposition of ^{166}Ho-MS with preferential flow of microspheres to the hyperemic zone surrounding the ablated tissue (i.e. target volume).* **F:** *Liver volume infused with ^{166}Ho-MS TARE (i.e. treatment volume) [22].*

On day two, an angiography procedure was performed to selectively catheterize the hepatic arteries with vascular supply to the hyperemic tissue using a Progreat 2.4F or 2.7F microcatheter (Terumo corporation, Tokyo, Japan). Catheter position(s) were chosen as selectively as possible and were verified by contrast enhanced cone-beam CT (CBCT). Next, 150 MBq of technetium-99m labeled macroaggregated albumin ([^{99m}Tc]Tc-MAA) was injected. The treatment volume was defined as the volume exposed to radiation, based on CBCT [23]. This would include both the hyperemic zone (i.e. target volume) and a limited volume of normal liver parenchyma (i.e. non-target volume). A single photon emission computed tomography (SPECT-CT) scan was acquired directly after the angiography procedure on a Symbia T6 or Symbia Intevo (Siemens Healthineers, Erlangen, Germany) or Discovery 670 Pro (GE Healthcare, Boston, Massachusetts, USA).

On day 5-10 after RFA, TARE with infusion of ^{166}Ho-MS QuiremSpheres (Quirem Medical B.V., Deventer, the Netherlands) was performed during a second hospitalization. Prior to ^{166}Ho-MS injection, the catheter position was verified using fluoroscopy and CBCT to ensure that spheres would be injected at the identical location as the [^{99m}Tc]Tc-MAA. The total activity administered was calculated using the following equation [24]:

$$A_{Ho-166} = Treatment\ volume\ dose\ [Gy] * M_i\ [kg] * 63\ [MBq/J]$$

The treatment volume was segmented from the contrast enhanced CBCT and a tissue density of 1.00 g/mL was used to determine the mass of the treatment volume (M_i). One day after TARE (day 6-11), a post-treatment SPECT-CT was acquired for post-treatment dosimetry purposes. These SPECT images were acquired with a medium energy general purpose collimator. A total of 90 projections over a circular 360° orbit were acquired on a 128x128 matrix with an overall scanning time of 27 min (18 s per projection). Projections were recorded in the 81 keV (15% width) photopeak window. An additional energy window centered at 118 keV (12% width) was used to correct for bremsstrahlung and higher energy gamma emissions. Planar scintigraphy was used to calculate lung shunting. In addition to this SPECT-scan, MRI was performed before and after TARE to allow MRI-based quantification of ^{166}Ho-MS. The MRI-images were acquired on a 1.5T scanner (Ingenia, Philips Healthcare, Best, The Netherlands) and included an MGRE sequence with 10 subsequent echoes (TE1: 1.06 ms, ΔTE: 1.38 ms, TR: 149 ms, flip angle: 33°, in-plane resolution: 2 × 2 mm2, slice thickness: 4 mm, FOV: 384 × 384 mm2).

Follow-up

All patients were followed for 12 months which included imaging using CECT or dynamic MRI of the liver and chest at 6 weeks and 3 months after treatment, and every three months thereafter. Clinical assessment and biochemical liver function tests were performed at week 2 and simultaneous with all moments of imaging.

Endpoints

The primary endpoint of this study was to find the treatment volume absorbed dose that resulted in an absorbed dose of ≥120 Gy to the target volume in 9/10 patients within a cohort, based on post-treatment SPECT-CT. The target volume was defined as the hyperemic zone encompassing the ablated tissue and generally anticipated to be a 1 cm rim around the ablated tissue. Manual segmentation of the treatment and target volumes in the post-treatment SPECT scan was performed using Xeleris workstation version 4.0 (GE Healthcare, Boston, Massachusetts, USA). The non-target volume dose was defined as the treatment volume subtracted by the target volume. Post-treatment MRI dosimetry was performed using Q-Suite 2.0 software (Quirem Medical B.V. Deventer, The Netherlands).

In the first cohort, a dose of 60 Gy was administered to the treatment volume. If a second patient within a cohort failed to reach an absorbed dose of ≥120 Gy to the target volume, the dose was escalated to 90 Gy to the treatment volume in subsequent patients (cohort 2), and could ultimately be escalated to 120 Gy (cohort 3). The design of this study was based on the assumption that microspheres would preferentially flow to the hyperemic zone around the ablation zone (i.e. target volume) rather than to the normal parenchyma (i.e. non-target volume) within the treatment volume. If the ratio of microsphere accumulation in the target volume versus normal non-target volume would be high, a low amount of radioactivity to the treatment volume (cohort 1) would be sufficient to reach an absorbed dose of ≥120 Gy to the target volume. If there would be an even distribution of microspheres between the target volume and non-target volume a treatment volume absorbed dose of 120 Gy (cohort 3) would be needed to meet the study endpoint. Per cohort at least 2 patients were treated and no further dose escalation was performed when the final endpoint was met of an absorbed dose of ≥120 Gy to the target volume in 9/10 patients. The sample size of this study was thus determined to be a minimum of 10 and a maximum of 30 patients.

Secondary endpoints included toxicity, local tumor recurrence rates, progression-free survival (PFS) and overall survival (OS) at 6 months and at 1 year. Adverse events were categorized according to Common Terminology Criteria for Adverse Events (CTCAE) 4.0 [25]. Local recurrences were defined as appearance at follow-up of foci of untreated disease in tumors that were previously considered to be completely ablated, in concordance with the CIRSE Standards of practice guideline [26].

MRI-based quantification of ^{166}Ho-MS was investigated as an exploratory endpoint.

Statistical analysis

Descriptive statistics and outcomes were calculated by medians and interquartile ranges (IQR) for continuous variables, and frequencies and percentages per category for categorical variables. Local recurrence free survival, PFS, and OS rates at 6 months and 12 months follow-up were calculated. Patients that underwent liver transplantation were censored in the survival statistics. Statistical analyses were performed using RStudio 1.4.1106.

RESULTS

Patients

Informed consent was obtained from 20 patients between April 2018 and March 2021. Twelve of these patients completed the treatment regimen, as can be seen in Figure 2. Reasons for exclusion were: withdrawal from the study (n=3), progression beyond BCLC early stage HCC in the time between inclusion and treatment (n=1), CTCAE grade 3 complication after

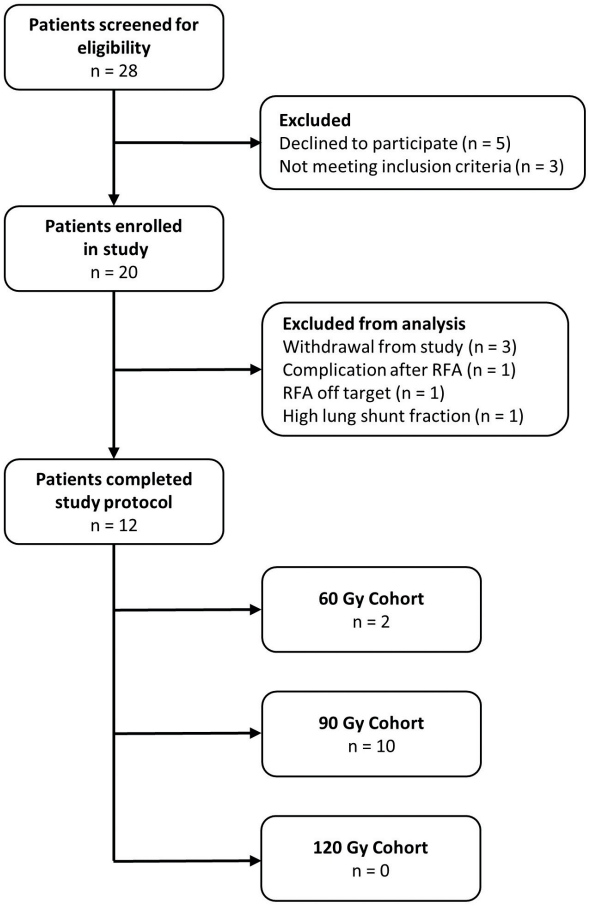

Figure 2 *Flowchart of the study population.*

RFA (n=1), RFA off target (n=1), high lung shunt fraction (n=1), and incomplete administration of ^{166}Ho-MS (n=1). Baseline characteristics of all 12 treated patients are shown in Table 2. The population consisted of more males (n=10) than females (n=2) and most patients had underlying Child Pugh A liver cirrhosis (n=10).

Treatment

A patient case example is given in Figure 3. Treatment characteristics can be found in Table 3. All ablations were performed with a multiprobe approach. Three out of sixteen lesions in two out of twelve patients were treated with RFA only as the tumor diameter was <2 cm. In those patients, only the larger lesion(s) (>2 cm) were treated with adjuvant TARE after RFA. Most ^{166}Ho-MS infusions were performed (sub-)segmental or bi-segmental, and one infusion was performed lobar. The median treatment volume was 360 mL, IQR: [270 - 394] and the median administered activity of ^{166}Ho was 1.79 GBq IQR: [1.45 – 2.23].

Table 2 *Patient characteristics of analyzed patients*

		n	
Total		12	
Age	median [IQR]	66.5	[64.3 - 71.7]
Sex	male	10	83%
	female	2	17%
Liver parenchyma status	Child-Pugh A cirrhosis	10	83%
	fibrosis	2	17%
Etiology of cirrhosis	hepatitis B	4	40%
	alcohol induced	6	60%
BCLC stage	early	12	100%
Prior HCC treatment	none	11	
	TA	1	
Number of study lesions *	1	11	92%
	2	1	8%
Tumor location (Couinaud segments)	Segment 3	1	
	Segment 4	2	
	Segment 5	1	
	Segment 6	2	
	Segment 7	6	
	Segment 8	1	
Size (mm) of study lesions*	median [IQR]	27	[21 - 40]

**3 lesions in 2 patients were treated with TA only in the same treatment session. All three lesions were <15 mm and therefore not eligible for TARE after TA.*
HCC = hepatocellular carcinoma, BCLC = Barcelona Clinic for Liver Cancer, TA = thermal ablation, TACE = trans-arterial chemoembolization.

Primary end-point

The first two patients were treated with a dose of 60 Gy on the treatment volume. Figure 4 shows the dose distribution per patient. Although a preferential dose accumulation in the target volume was found in the first two patients, the absorbed target volume doses were 89 Gy and 93 Gy, respectively. As the end point of ≥ 120 Gy to the target volume was not met, the dose was escalated to 90 Gy to the treatment volume. In 9/10 patients in the 90 Gy cohort, a mean target volume dose of ≥120 Gy was met. In this cohort the median absorbed target volume dose was 138 Gy, IQR: [127 – 145] and the median absorbed non-target volume dose was 67 Gy, IQR: [54 – 75], as can be seen in Figure 4. As the primary endpoint was met, the inclusion was closed and the recommended treatment volume absorbed dose was set at 90 Gy.

Table 3 *Treatment characteristics*

		n	
RFA probes used	Multiprobe 3x3 cm	5	
	Multiprobe 3x4 cm	3	
	Multiprobe 6x3 cm	2	
	Multiprobe 6x4 cm	2	
Modality used for needle placement	CT	2	
	Ultrasound	10	
Angiography: catheter position	(sub-)segmental	2	
	bi-segmental	9	
	lobar	1	
Treatment volume (mL)	Median [IQR]	360	[270 – 394]
Target volume (mL)	Median [IQR]	88	[69 – 128]
Lung shunt fraction (%)	Median [IQR]	4.6	[2.2 - 6.55]
Dose to treatment volume	60 Gy	2	
	90 Gy	10	
	120 Gy	0	
Administered activity of ^{166}Ho (GBq)	Median [IQR]	1.79	[1.45 - 2.23]

RFA = radiofrequency ablation, CT = computed tomography, ^{166}Ho = holmium-166, mL = milliliter, GBq = Giga-becquerel, Gy = gray.

Toxicity

One patient was readmitted to the hospital on the third day after radioembolization because of fever. Ultrasound and CECT demonstrated abscess formation within the ablated tissue that was treated with percutaneous drainage (CTCAE 4.0 grade 3 infection). Other reported adverse events were grade 1-2 nausea (n=3) and grade 1 fatigue (n=4).

Efficacy

Two patients underwent liver transplantation at 7.5 and 8.0 months after treatment. They were both local recurrence free before liver transplantation. All other ten patients were also free of local recurrences within 12 months after treatment. Three patients developed new HCC lesions elsewhere in the liver, at 4.6, 5.5 and 5.6 months. Therefore, PFS was 75% at 6 months and 75% at 1 year. Two patients died, one as a result of decompensated liver cirrhosis and one following bacterial sepsis after liver transplantation. This resulted in an OS of 92% at 6 months and 83% at 1 year. Figure 5 shows an example of histological confirmation of ^{166}Ho-MS accumulation surrounding the fibrotic and central necrotic tissue.

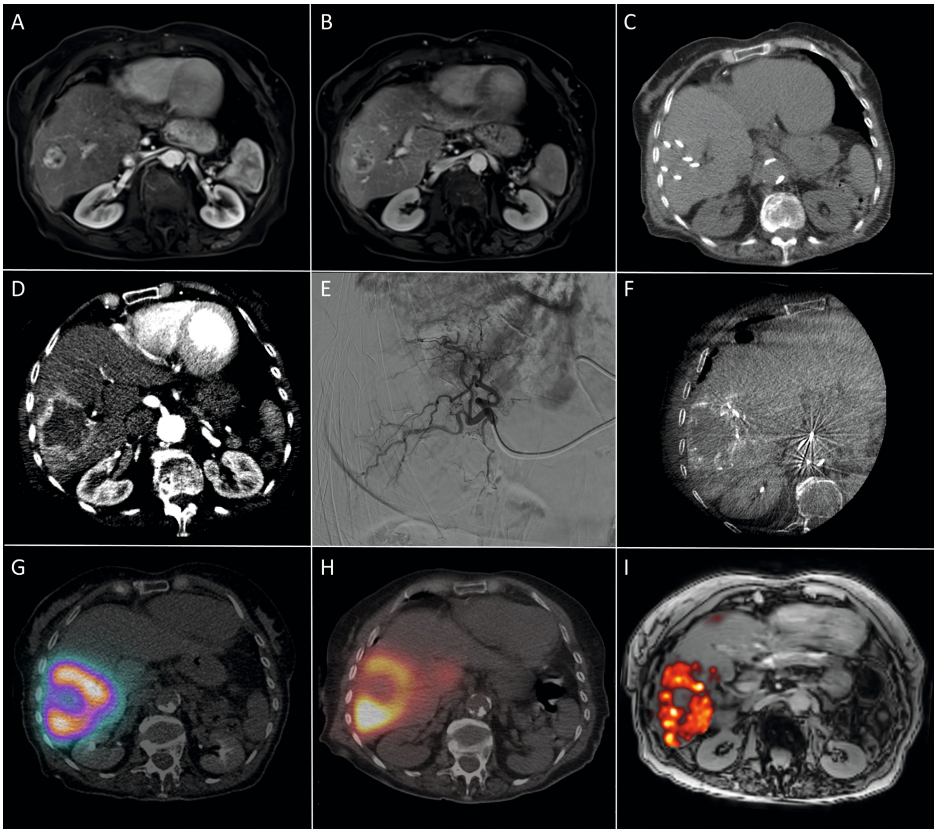

Figure 3 *HORA EST HCC treatment sequence:* **A:** *Arterial scan phase of diagnostic MRI showing a hypervascular HCC lesion of 31 mm in the liver.* **B:** *Portal venous scan phase of MRI showing central wash-out in the HCC lesion.* **C:** *Intraprocedural CT after placement of six cooled-tip RFA needles with 3 cm exposed tip.* **D:** *Intraprocedural contrast enhanced CT scan in arterial phase showing hyperemia around the ablation zone on post-ablation CECT.* **E:** *Super-selective catheterization of hepatic arteries with vascular supply to the target volume.* **F:** *CBCT of the treatment volume with an identical catheter position as in E.* **G:** *SPECT-CT of [^{99m}Tc]Tc-MAA dose distribution used for dose planning.* **H:** *SPECT-CT of ^{166}Ho-MS distribution.* **I:** *MRI-based dosimetry of ^{166}Ho-MS distribution.*

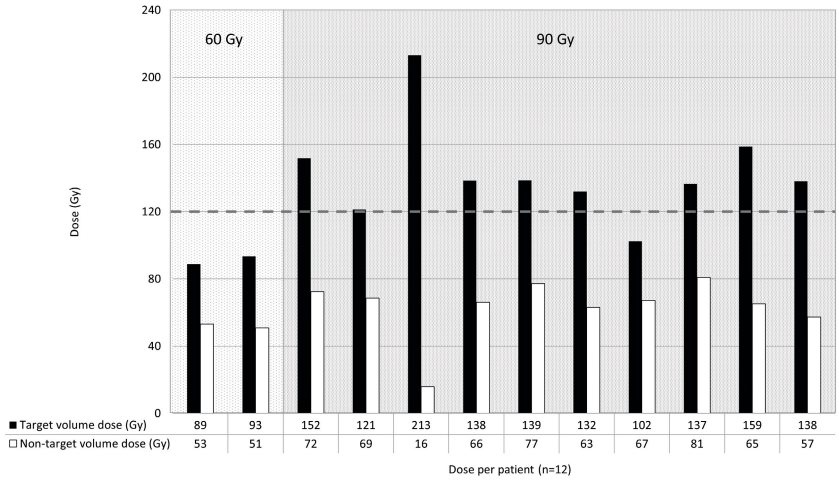

Figure 4 *Dose distribution per patient within treatment volume, based on SPECT imaging. The bars in black represent the mean absorbed dose on the target volume directly surrounding the ablation volume per patient. The cut-off point of an absorbed target volume dose of ≥ 120 Gy is indicated by the horizontal dashed line. The bars in white show the absorbed dose to the non-target volume within the treatment volume. The first two patients were treated with 60 Gy to the treatment volume, whereas the other patients were treated with 90 Gy to the treatment volume. The median ratio of target volume dose vs non-target volume dose was 1.97 (IQR: [1.75 – 2.17]).*

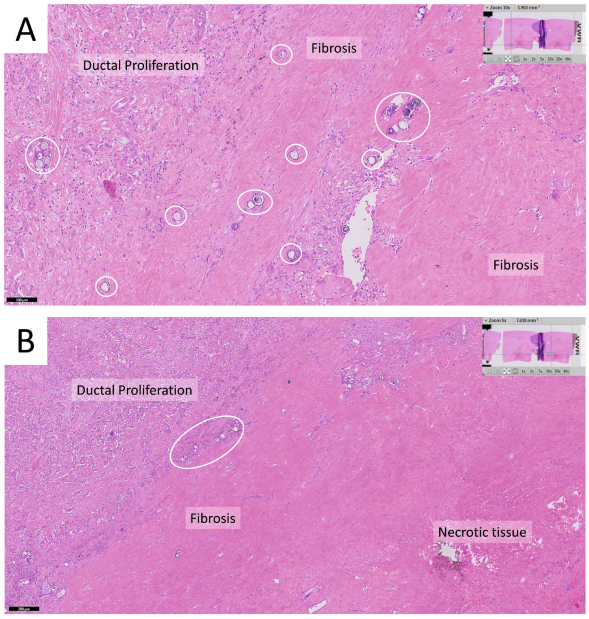

Figure 5 *Histology of explanted liver treated with radiofrequency ablation and adjuvant ^{166}Ho TARE. Digitalized histology using Ultra Fast Scanner (Philips Healthcare, Best, The Netherlands) with a magnitude of 40x* **A:** *Zoom: 10x. Transition from liver tissue with ductal proliferation to fibrosis with marked depositions of ^{166}Ho-MS.* **B:** *zoom 5x. Overview of transition from ductal proliferation to necrotic tissue with marked ^{166}Ho-MS.*

DISCUSSION

In this multi-center, single arm study we prospectively evaluated the feasibility of adjuvant TARE after RFA in BCLC early stage HCC 2-5 cm. The results show that an absorbed dose of >120 Gy of ^{166}Ho-MS on the target volume around the ablation zone could be reached at an administered dose of 90 Gy to the treatment volume. The median target volume dose was about twice as high as the median dose to the non-target parenchyma, confirming our hypothesis that hyperemia induced by RFA can be utilized to deposit ^{166}Ho-MS in a peripheral zone surrounding the ablation volume. The safety profile of the combined treatment was in concordance with the safety of RFA or TARE mono-therapy, or combined RFA and TACE. Only one CTCAE grade 4 complication occurred in 12 patients (8.3%) and no grade 5 complications were observed [27-29]. Within one year after treatment no local recurrences developed, three patients developed recurrent HCC elsewhere in the liver and two patients died. Treatment efficacy and safety profile should be further validated in a larger cohort.

Many patients with larger HCC lesions are not eligible to surgical resection due to comorbidities, cirrhosis with portal hypertension, or insufficient future liver remnant volume. TA is an alternative treatment, but a large diameter is an important risk factor of local recurrence [6, 8]. In the continuous search towards better treatment outcomes and extended bridging to liver transplantation, several treatment combinations of TA with other locoregional or systemic therapies have been investigated. The STORM trial investigated adjuvant sorafenib after surgery or TA, but failed to prove benefit in terms of time to progression free and overall survival [30]. Another widely studied combined treatment regimen is TA with (neo)adjuvant TACE. Several trials in Asian populations have indicated superiority of combined TA and TACE over TA alone [31, 32], but the combination therapy has not been adopted in the EASL, AASL or BCLC guidelines [1, 2, 7]. The different studies have methodological limitations and there is a considerable variation between the trials in technique and treatment sequence [33-35]. Furthermore, superiority of the combination therapy over surgical resection has not been proven [11, 33]. To our knowledge this is the first study to combine TA with TARE.

Technical advancements have led to the adoption of TA as the preferred treatment of HCC <2 cm a decade ago [2, 36]. Similarly, recent advancements in patient selection and optimized patient-tailored dosing have resulted in a place for TARE in the recent BCLC update [2]. The LEGACY and RASER studies reported promising results of radiation segmentectomy in patients with (very) early stage HCC patients with a mean lesion diameter of 2.7 cm and median lesion diameter of 2.1 cm, respectively [37, 38]. These results indicate high local control rates to be achievable using radiation segmentectomy, although results were not superior to those that may be achieved with TA. Further prospective validation is needed

in larger trials and in patients with larger lesions. Ultimately, the role of TARE in HCC is to be further clarified for different indications.

In this trial only RFA was used as ablation modality. In this way the treatment regimen was kept as homogeneous as possible. Moreover, preclinical work combining TA with radiation-based therapies were only performed with RFA [12-15]. However, over the last years, the use of microwave ablation (MWA) has increased. MWA may have some technological advancements over RFA, but similar outcomes have been found [39]. As hyperemia around the ablation zone is seen after MWA similarly to RFA, it is expected that a similar ^{166}Ho-MS dose distribution can be achieved when TARE is performed following MWA [40-42].

^{166}Ho-MS were used for radioembolization in this study rather than ^{90}Y TARE. ^{166}Ho has advantages in terms of imaging as it emits direct gamma radiation at 81 keV. Moreover, the paramagnetic property of ^{166}Ho allows for MRI-based post TARE dosimetry [24, 43]. The study endpoint was determined using SPECT-based dosimetry, and MRI-based quantification of ^{166}Ho-MS was used as an exploratory endpoint. Unfortunately, reliable quantitative MRI-based dosimetry was unfeasible in many patients as a result of breathing and movement artifacts. MRI scans were obtained shortly after the RFA and TARE procedures, and many patients experienced discomfort and as a result had difficulty lying still and maintaining breath holds. [^{99m}Tc]Tc-MAA was used for the scout procedure. Despite the potential benefits of ^{166}Ho scout dose in terms of intrahepatic treatment dose distribution mimicking, ^{166}Ho scout dose was not yet available by the time of study design [44]. In the current study however, standard volume-based dosimetry was used based on CBCT, so this would not have affected dose planning

The current study has several limitations. First, the sample size is small and therefore no definite conclusions can be drawn on the efficacy. Nevertheless, the absence of local recurrences in all study patients within 1 year after treatment suggest that the efficacy of the combination therapy is high. Second, despite of meeting the primary end point at an administered dose of 90 Gy, a substantial variety in ratio of target volume dose versus non-target volume dose between individual patients was observed. This ratio depends on various factors, such as degree of hyperemia, catheter position, occurrence of vascular stasis during injection and the ratio target volume versus treatment volume. In the 90 Gy cohort an absorbed target volume dose of ≥120 Gy was not reached in one patient. As a result of a very selective catheter position in this patient the target volume constituted >50 % of the treatment volume. In patients where the ratio between target volume and treatment volume ratio is very high, an administered dose higher than 90 Gy to the treatment volume may be required. Clearly, in the theoretical case that the target volume constitutes 100% of the treatment volume, TARE with a dose of 90 Gy would not be sufficient. For future

studies, a volume-dependent administration dose planning could help to individualize treatment planning. Another limitation of this study is the complexity of the treatment regimen. For patients this meant undergoing a second treatment, including four additional imaging examinations (2x MRI and 2x SPECT/CT), and an additional hospitalization. This was considered burdensome by some patients, and therefore a reason not to participate in this trial.

Since the initial plans of this study originate from 2017, less was known on (^{166}Ho) TARE dosimetry, and the 120 Gy cut-off was mainly chosen based on initial ^{90}Y research [21]. Treatment volume absorbed doses of the several cohorts were based on a phase I ^{166}Ho-MS dose escalation 'study (HEPAR trial), in which a whole liver dose of 60 Gy was considered safe [45]. Recently, the first efficacy evidence for ^{166}Ho-MS in HCC was demonstrated in the HEPAR Primary study [28]. At a treatment volume absorbed dose of 50 Gy in an average of 54% of the total liver volume, partial or complete responses were seen in patients receiving an average absorbed dose of 210 Gy on their lesions versus 116 Gy in patients with progressive disease [28]. Since hyperemic tissue surrounding the ablation zone is targeted in our study rather than (large) lesions, these tumor dose values cannot be directly compared to the 138 Gy absorbed target volume dose found in our study. Nevertheless, taking into account the recent advancements of safe radiation segmentectomy procedures, and the fact that a tumor absorbed dose of 210 Gy did show a higher level of tissue necrotization when compared to an absorbed dose of 116 Gy in the HEPAR primary study, investigating higher dosing of ^{166}Ho-MS as adjuvant treatment after thermal ablation seems to be justified. Especially when a small treatment volume is treated that mainly consists of the target volume, a higher dose than in the current trail should be chosen. In light of recent segmentectomy studies [37, 38, 46], recommendations with ^{90}Y [47], and the HEPAR primary trial [28], the treatment volume absorbed dose may be as high as about 200 Gy. For patients with a larger treatment volume (for example due to multiple ablations or a more centrally located tumor), a treatment volume absorbed dose of 90 Gy remains recommended to limit the absorbed radiation dose to the liver parenchyma. Our study provides insight in the biodistribution of ^{166}Ho-MS after TA with an average target volume vs non-target volume ratio of 2:1. This may help to determine the optimal dose in each individual patient, while taking into account the risk of radiation induced liver disease in patients with a larger treatment volume.

The median tumor diameter in this study was 2.7 cm. Patients with a tumor diameter of ≥2 cm were eligible for inclusion in this dose finding study. It may be questionable whether adjuvant TARE will be cost-effective in patients with a tumor < 3 cm. Future studies investigating effectivity of thermal ablation with adjuvant TARE are more likely to be positive when larger tumors are recruited.

Moreover, in a future study, the feasibility of combined TA and TARE in a single procedure could be explored. Owing to the low dose of ^{166}Ho-MS used in this treatment regimen, the chance of introducing a substantial radiation dose to the lung parenchyma is extremely low. Moreover, as a result of super-selective catheterization and the use of CBCT prior to infusion of ^{166}Ho-MS, the chance of other extrahepatic deposition is small as well. Especially since combined Angio-CT systems are increasingly being used, the combined treatment could be performed in a single session with high precision [48]. The current proposed treatment protocol is promising for the locoregional treatment of HCC lesions 2-5 cm that are at higher risk of local recurrences. Further research into subtypes of HCC or identification of satellite nodules may contribute to identifying patients who potentially benefit most of the combined treatment regimen.

CONCLUSION

Selective radioembolization with ^{166}Ho-MS can be used safely as an adjuvant treatment in early stage HCC 2-5 cm. Hyperemia induced by TA can be utilized to deliver a high radiation dose to the target volume while limiting the dose to the normal liver parenchyma. A treatment volume absorbed dose of 90 Gy is safe and sufficient to deliver a tumoricidal absorbed radiation dose of at least 120 Gy to the target volume.

TRIAL REGISTRATION

Clinicaltrials.gov identifier: NCT03437382.

REFERENCES

[1] Galle PR, Forner A, Llovet JM, Mazzaferro V, Piscaglia F, Raoul J-L, et al. EASL Clinical Practice Guidelines: Management of hepatocellular carcinoma. Journal of Hepatology 2018;69:182-236.

[2] Reig M, Forner A, Rimola J, Ferrer-Fábrega J, Burrel M, Garcia-Criado Á, et al. BCLC strategy for prognosis prediction and treatment recommendation: The 2022 update. Journal of hepatology.

[3] Forner A, Reig M, Bruix J. Hepatocellular carcinoma. The Lancet 2018;391:1301-1314.

[4] Weis S, Franke A, Mössner J, Jakobsen JC, Schoppmeyer K. Radiofrequency (thermal) ablation versus no intervention or other interventions for hepatocellular carcinoma. The Cochrane database of systematic reviews 2013:Cd003046.

[5] Xu X-L, Liu X-D, Liang M, Luo B-M. Radiofrequency Ablation versus Hepatic Resection for Small Hepatocellular Carcinoma: Systematic Review of Randomized Controlled Trials with Meta-Analysis and Trial Sequential Analysis. Radiology 2017;287:461-472.

[6] Shin SW, Ahn KS, Kim SW, Kim T-S, Kim YH, Kang KJ. Liver Resection Versus Local Ablation Therapies for Hepatocellular Carcinoma Within the Milan Criteria: A Systematic Review and Meta-analysis. Annals of Surgery 2021;273.

[7] Heimbach JK, Kulik LM, Finn RS, Sirlin CB, Abecassis MM, Roberts LR, et al. AASLD guidelines for the treatment of hepatocellular carcinoma. Hepatology (Baltimore, Md) 2018;67:358-380.

[8] Burgmans MC, Too CW, Fiocco M, Kerbert AJC, Lo RHG, Schaapman JJ, et al. Differences in Patient Characteristics and Midterm Outcome Between Asian and European Patients Treated with Radiofrequency Ablation for Hepatocellular Carcinoma. CardioVascular and Interventional Radiology 2016;39:1708-1715.

[9] Habibollahi P, Sheth RA, Cressman ENK. Histological Correlation for Radiofrequency and Microwave Ablation in the Local Control of Hepatocellular Carcinoma (HCC) before Liver Transplantation: A Comprehensive Review. Cancers 2021;13.

[10] Cao S, Zou Y, Lyu T, Fan Z, Guan H, Song L, et al. Long-term outcomes of combined transarterial chemoembolization and radiofrequency ablation versus RFA monotherapy for single hepatocellular carcinoma ≤3 cm: emphasis on local tumor progression. International Journal of Hyperthermia 2022;39:1-7.

[11] Lin C-W, Chen Y-S, Lo G-H, Hsu Y-C, Hsu C-C, Wu T-C, et al. Comparison of overall survival on surgical resection versus transarterial chemoembolization with or without radiofrequency ablation in intermediate stage hepatocellular carcinoma: a propensity score matching analysis. BMC Gastroenterology 2020;20:99.

[12] Solazzo S, Mertyna P, Peddi H, Ahmed M, Horkan C, Nahum Goldberg S. RF ablation with adjuvant therapy: Comparison of external beam radiation and liposomal doxorubicin on ablation efficacy in an animal tumor model. International Journal of Hyperthermia 2008;24:560-567.

[13] Horkan C, Dalal K, Coderre JA, Kiger JL, Dupuy DE, Signoretti S, et al. Reduced tumor growth with combined radiofrequency ablation and radiation therapy in a rat breast tumor model. Radiology 2005;235:81-88.

[14] Lin ZY, Chen J, Deng XF. Treatment of hepatocellular carcinoma adjacent to large blood vessels using 1.5T MRI-guided percutaneous radiofrequency ablation combined with iodine-125 radioactive seed implantation. Eur J Radiol 2012;81:3079-3083.

[15] Chen K, Chen G, Wang H, Li H, Xiao J, Duan X, et al. Increased survival in hepatocellular carcinoma with iodine-125 implantation plus radiofrequency ablation: a prospective randomized controlled trial. Journal of hepatology 2014;61:1304-1311.

[16] Dawson LA, Guha C. Hepatocellular Carcinoma: Radiation Therapy. The Cancer Journal 2008;14.

[17] Cheng JC, Wu JK, Lee PC, Liu HS, Jian JJ, Lin YM, et al. Biologic susceptibility of hepatocellular carcinoma patients treated with radiotherapy to radiation-induced liver disease. International journal of radiation oncology, biology, physics 2004;60:1502-1509.

[18] Riaz A, Gates VL, Atassi B, Lewandowski RJ, Mulcahy MF, Ryu RK, et al. Radiation segmentectomy: a novel approach to increase safety and efficacy of radioembolization. International journal of radiation oncology, biology, physics 2011;79:163-171.

[19] Roosen J, Klaassen NJM, Westlund Gotby LEL, Overduin CG, Verheij M, Konijnenberg MW, et al. To 1000 Gy and back again: a systematic review on dose-response evaluation in selective internal radiation therapy for primary and secondary liver cancer. European journal of nuclear medicine and molecular imaging 2021.

[20] Park M-h, Rhim H, Kim Y-s, Choi D, Lim HK, Lee WJ. Spectrum of CT Findings after Radiofrequency Ablation of Hepatic Tumors. RadioGraphics 2008;28:379-390.

[21] Lau WY, Leung WT, Ho S, Leung NW, Chan M, Lin J, et al. Treatment of inoperable hepatocellular carcinoma with intrahepatic arterial yttrium-90 microspheres: a phase I and II study. British journal of cancer 1994;70:994-999.

[22] Hendriks P, Rietbergen DDD, van Erkel AR, Coenraad MJ, Arntz MJ, Bennink RJ, et al. Study Protocol: Adjuvant Holmium-166 Radioembolization After Radiofrequency Ablation in Early-Stage Hepatocellular Carcinoma Patients—A Dose-Finding Study (HORA EST HCC Trial). CardioVascular and Interventional Radiology 2022;45:1057-1063.

[23] Sabet A, Ahmadzadehfar H, Muckle M, Haslerud T, Wilhelm K, Biersack HJ, et al. Significance of oral administration of sodium perchlorate in planning liver-directed radioembolization. Journal of nuclear medicine : official publication, Society of Nuclear Medicine 2011;52:1063-1067.

[24] Smits ML, Elschot M, van den Bosch MA, van de Maat GH, van het Schip AD, Zonnenberg BA, et al. In vivo dosimetry based on SPECT and MR imaging of 166Ho-microspheres for treatment of liver malignancies. Journal of nuclear medicine : official publication, Society of Nuclear Medicine 2013;54:2093-2100.

[25] USA NIH National Cancer Institute. Common Terminology Criteria in Adverse Events, version 4.0 (CTCAE 4.0). [cited; Available from: https://ctep.cancer.gov/protocoldevelopment/electronic_applications/ctc.htm

[26] Crocetti L, de Baére T, Pereira PL, Tarantino FP. CIRSE Standards of Practice on Thermal Ablation of Liver Tumours. CardioVascular and Interventional Radiology 2020;43:951-962.

[27] Kong WT, Zhang WW, Qiu YD, Zhou T, Qiu JL, Zhang W, et al. Major complications after radiofrequency ablation for liver tumors: analysis of 255 patients. World J Gastroenterol 2009;15:2651-2656.

[28] Reinders MTM, van Erpecum KJ, Smits MLJ, Braat AJAT, Bruijne Jd, Bruijnen R, et al. Safety and Efficacy of 166Ho Radioembolization in Hepatocellular Carcinoma: The HEPAR Primary Study. Journal of Nuclear Medicine 2022;63:1891.

[29] Liu W, Xu H, Ying X, Zhang D, Lai L, Wang L, et al. Radiofrequency Ablation (RFA) Combined with Transcatheter Arterial Chemoembolization (TACE) for Patients with Medium-to-Large Hepatocellular Carcinoma: A Retrospective Analysis of Long-Term Outcome. Med Sci Monit 2020;26:e923263.

[30] Bruix J, Takayama T, Mazzaferro V, Chau GY, Yang J, Kudo M, et al. Adjuvant sorafenib for hepatocellular carcinoma after resection or ablation (STORM): a phase 3, randomised, double-blind, placebo-controlled trial. The Lancet Oncology 2015;16:1344-1354.

[31] Yin X, Zhang L, Wang Y-H, Zhang B-H, Gan Y-H, Ge N-L, et al. Transcatheter arterial chemoembolization combined with radiofrequency ablation delays tumor progression and prolongs overall survival in patients with intermediate (BCLC B) hepatocellular carcinoma. BMC Cancer 2014;14:849.

[32] Yamanaka T, Yamakado K, Takaki H, Nakatsuka A, Shiraki K, Hasegawa H, et al. Ablative zone size created by radiofrequency ablation with and without chemoembolization in small hepatocellular carcinomas. Japanese Journal of Radiology 2012;30:553-559.

[33] Hendriks P, Sudiono DR, Schaapman JJ, Coenraad MJ, Tushuizen ME, Takkenberg RB, et al. Thermal ablation combined with transarterial chemoembolization for hepatocellular carcinoma: What is the right treatment sequence? European Journal of Radiology 2021;144:110006.

[34] Chen Q-W, Ying H-F, Gao S, Shen Y-H, Meng Z-Q, Chen H, et al. Radiofrequency ablation plus chemoembolization versus radiofrequency ablation alone for hepatocellular carcinoma: A systematic review and meta-analysis. Clinics and Research in Hepatology and Gastroenterology 2016;40:309-314.

[35] Peng Z-W, Zhang Y-J, Chen M-S, Xu L, Liang H-H, Lin X-J, et al. Radiofrequency ablation with or without transcatheter arterial chemoembolization in the treatment of hepatocellular carcinoma: a prospective randomized trial. Journal of clinical oncology 2013;31:426-432.

[36] Ng KKC, Chok KSH, Chan ACY, Cheung TT, Wong TCL, Fung JYY, et al. Randomized clinical trial of hepatic resection versus radiofrequency ablation for early-stage hepatocellular carcinoma. British Journal of Surgery 2017;104:1775-1784.

[37] Salem R, Johnson GE, Kim E, Riaz A, Bishay V, Boucher E, et al. Yttrium-90 Radioembolization for the Treatment of Solitary, Unresectable HCC: The LEGACY Study. Hepatology (Baltimore, Md) 2021;74:2342-2352.

[38] Kim E, Sher A, Abboud G, Schwartz M, Facciuto M, Tabrizian P, et al. Radiation segmentectomy for curative intent of unresectable very early to early stage hepatocellular carcinoma (RASER): a single-centre, single-arm study. The Lancet Gastroenterology & Hepatology 2022;7:843-850.

[39] Poulou LS, Botsa E, Thanou I, Ziakas PD, Thanos L. Percutaneous microwave ablation vs radiofrequency ablation in the treatment of hepatocellular carcinoma. World J Hepatol 2015;7:1054-1063.

[40] Carrafiello G, Laganà D, Mangini M, Fontana F, Dionigi G, Boni L, et al. Microwave tumors ablation: Principles, clinical applications and review of preliminary experiences. International Journal of Surgery 2008;6:S65-S69.

[41] Giorgio A, Gatti P, Montesarchio L, Merola MG, Amendola F, Calvanese A, et al. Microwave Ablation in Intermediate Hepatocellular Carcinoma in Cirrhosis: An Italian Multicenter Prospective Study. J Clin Transl Hepatol 2018;6:251-257.

[42] Vogl TJ, Nour-Eldin NA, Hammerstingl RM, Panahi B, Naguib NNN. Microwave Ablation (MWA): Basics, Technique and Results in Primary and Metastatic Liver Neoplasms - Review Article. Rofo 2017;189:1055-1066.

[43] Roosen J, van Wijk MWM, Westlund Gotby LEL, Arntz MJ, Janssen MJR, Lobeek D, et al. Improving MRI-based dosimetry for holmium-166 transarterial radioembolization using a nonrigid image registration for voxelwise ΔR_2^* calculation. Medical Physics 2023;50:935-946.

[44] Smits MLJ, Dassen MG, Prince JF, Braat A, Beijst C, Bruijnen RCG, et al. The superior predictive value of (166)Ho-scout compared with (99m)Tc-macroaggregated albumin prior to (166)Ho-microspheres radioembolization in patients with liver metastases. European journal of nuclear medicine and molecular imaging 2020;47:798-806.

[45] Smits MLJ, Nijsen JFW, van den Bosch MAAJ, Lam MGEH, Vente MAD, Mali WPTM, et al. Holmium-166 radioembolisation in patients with unresectable, chemorefractory liver metastases (HEPAR trial): a phase 1, dose-escalation study. The Lancet Oncology 2012;13:1025-1034.

[46] Lewandowski RJ, Gabr A, Abouchaleh N, Ali R, Al Asadi A, Mora RA, et al. Radiation Segmentectomy: Potential Curative Therapy for Early Hepatocellular Carcinoma. Radiology 2018;287:1050-1058.

[47] Salem R, Padia SA, Lam M, Chiesa C, Haste P, Sangro B, et al. Clinical, dosimetric, and reporting considerations for Y-90 glass microspheres in hepatocellular carcinoma: updated 2022 recommendations from an international multidisciplinary working group. European journal of nuclear medicine and molecular imaging 2023;50:328-343.

[48] Taiji R, Lin EY, Lin Y-M, Yevich S, Avritscher R, Sheth RA, et al. Combined Angio-CT Systems: A Roadmap Tool for Precision Therapy in Interventional Oncology. Radiology: Imaging Cancer 2021;3:e210039.

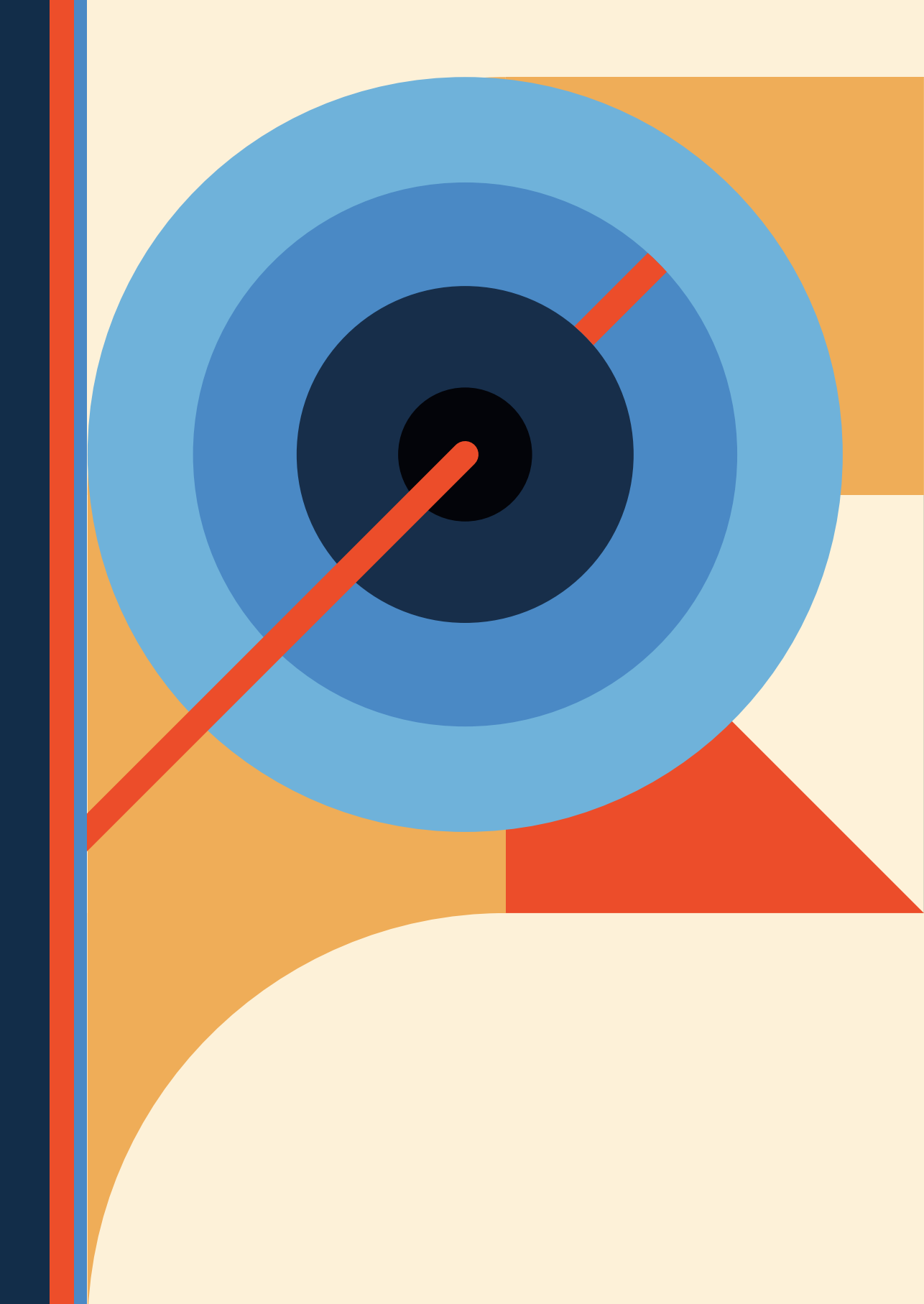

Part 3:

Radioembolization beyond early stage HCC

Chapter 9

Liver Decompensation as Late Complication in HCC Patients with Long-Term Response following Selective Internal Radiation Therapy

Authors

Diederick J. van Doorn, *Pim Hendriks**, Mark C. Burgmans, Daphne D. D. Rietbergen, Minneke J. Coenraad, Otto M. van Delden, Roel J. Bennink, Tim A. Labeur, Heinz-Josef Klümpen, Ferry A. L. M. Eskens, Adriaan Moelker, Erik Vegt, Dave Sprengers, Nahid Mostafavi, Jan Ijzermans and R. Bart Takkenberg

**Second author*

Publised

Cancers, 2021; 13, *DOI: 10.3390/cancers13215427*

Supplementary materials

https://doi.org/10.3390/cancers13215427

ABSTRACT

Selective internal radiation therapy (SIRT) is used as a treatment for hepatocellular carcinoma (HCC). The aim of this study was to assess long-term liver-related complications of SIRT in patients who had not developed radioembolization-induced liver disease (REILD). The primary outcome was the percentage of patients without REILD that developed Child-Pugh (CP) ≥ B7 liver decompensation after SIRT. The secondary outcomes were overall survival (OS) and tumor response. These data were compared with a matched cohort of patients treated with sorafenib. Eighty-five patients were included, of whom 16 developed REILD. Of the remaining 69 patients, 38 developed liver decompensation CP ≥ B7. The median OS was 18 months. In patients without REILD, the median OS in patients with CP ≥ B7 was significantly shorter compared to those without CP ≥ B7; 16 vs. 31 months. In the case-matched analysis, the median OS was significantly longer in SIRT-treated patients; 16 vs. 8 months in sorafenib. Liver decompensation CP ≥ B7 occurred significantly more in SIRT when compared to sorafenib; 62% vs. 27%. The ALBI score was an independent predictor of liver decompensation (OR 0.07) and OS (HR 2.83). After SIRT, liver decompensation CP ≥ B7 often developed as a late complication in HCC patients and was associated with a shorter OS. The ALBI score was predictive of CP ≥ B7 liver decompensation and the OS, and this may be a valuable marker for patient selection for SIRT.

Keywords: hepatocellular carcinoma; selective internal radiation therapy; long-term response; liver decompensation; overlal survival

INTRODUCTION

Hepatocellular carcinoma (HCC) is the sixth most common type of cancer worldwide [1]. Staging of HCC follows the Barcelona clinic liver cancer (BCLC) staging system. In this classification, the disease is divided into (very) early-stage (BCLC 0/A), intermediatestage (BCLC B), advanced-stage (BCLC C) and end-stage disease (BCLC D) [2]. The standard of care for patients with BCLC stage B HCC is transarterial chemoembolization (TACE). Guidelines recommend systemic therapy in patients with BCLC stage C HCC [3]. International guidelines advise that selective internal radiotherapy (SIRT) may be considered for BCLC stage B HCC in patients in whom TACE is not an option (i.e., beyond TACE) or BCLC stage C HCC with macrovascular invasion and without distant metastases [4,5]. SIRT is a form of brachytherapy, which uses microspheres loaded with beta-emitting isotopes, usually yttrium-90 (^{90}Y) or in alternative cases holmium-166 (166Ho) [6]. These microspheres are delivered to the tumor using intra-arterial injection in (branches of) the hepatic artery. Although proven safe, SIRT has not yet reached a well-defined place in the treatment algorithm of HCC [4,5]. Two randomized controlled trials, SIRveNIB and SARAH, showed that SIRT has a higher objective response rate compared to sorafenib, but with no impact on overall survival (OS) [7,8]. These studies showed a median OS of 17 months for patients with BCLC stage B HCC and 10 to 12 months for patients with BCLC stage C HCC treated with SIRT [9–12]. Furthermore, another trial (SORAMIC) showed that the addition of SIRT to sorafenib did not lead to a significant improvement in OS, with a median OS of 12 months in the SIRT plus sorafenib arm, compared to 11 months in the sorafenib monotherapy arm [13].

One severe complication of SIRT is radioembolization-induced liver disease (REILD), which is defined as a symptomatic deterioration of the liver function, developing between two weeks and four months after SIRT, in the absence of tumor progression or biliary tract obstruction. In previous studies, the incidence of REILD ranged from 0 to 31% [14]. There are only a few small studies that have reported on the long-term liver-related outcome after SIRT. These studies revealed that SIRT was associated with hepatic volume changes, liver fibrosis, portal hypertension and an increase in splenic volume. These effects usually have their onset 4–20 weeks after SIRT and continue to develop over time [15,16]. The damage to non-tumorous liver parenchyma resulting in loss of liver function, progression of cirrhosis or liver failure might negatively impact survival outcomes in patients with HCC.

In this study, we aimed to assess the long-term liver-related complications (deterioration of liver function, progression of liver cirrhosis or portal hypertension) in patients with BCLC stage B HCC who were not eligible for TACE or patients with BCLC stage C HCC confined to the liver with macrovascular invasion, who were treated with SIRT and did not develop REILD. We aimed to identify predictors of these liver-related complications.

METHODS

Study population

All patients diagnosed with HCC according to the EASL guidelines, and considered eligible for treatment with SIRT by the local multidisciplinary tumor board for primary liver cancer at three university medical centers (Amsterdam University Medical Center (Amsterdam UMC), Leiden University Medical Center (LUMC) and Erasmus Medical Center Rotterdam (Erasmus MC)) between 2011 and 2019 were included in the study screening. Patients were diagnosed in accordance with international guidelines by radiological criteria, or when cirrhosis was not present, by histology [4,5]. Diagnosis was made by multi-phase computed tomography (CT) or dynamic contrast-enhanced magnetic resonance imaging (MRI) and all patients were discussed at a multidisciplinary meeting with surgeons, medical oncologists, gastroenterologists, (interventional) radiologists and nuclear medicine physicians.

The aim of this study was to assess the long-term liver-related complications in patients receiving SIRT who did not develop REILD, and to identify predictors of the treatment outcome. Patients were divided in two different cohorts. The first cohort included all patients treated with SIRT (total cohort). In the second cohort (study cohort), patients who died or developed REILD within four months after SIRT were excluded (shown in Figure 1).

The data were collected from electronic patient records after permission was gained from the local ethics committees of each participating center to waive the necessity of written informed consent for this retrospective study.

Case-matched cohort analysis was performed with a cohort (n = 300) of patients treated with sorafenib between January 2007 and December 2016 in the Amsterdam UMC and Erasmus MC. These patients were analyzed in a retrospective study, which was published earlier [17].

Data collection

Patients were identified using the code for pre-SIRT workup, which could be captured from the electronic patient record (EPD). In the case of consecutive SIRT sessions in one patient, the data were collected from the first session onwards. Patients' clinical, radiological, nuclear medicine and laboratory data were manually extracted from their medical files, as were all relevant SIRT data. The collected data consisted of patient baseline characteristics, disease etiology and previous treatments. Baseline laboratory results, together with imaging, clinical data and tumor characteristics, were obtained prior to SIRT. Child-Pugh (CP), model for end-stage liver disease (MELD) (pre-2016) and albumin-bilirubin (ALBI) scores were calculated for each patient.

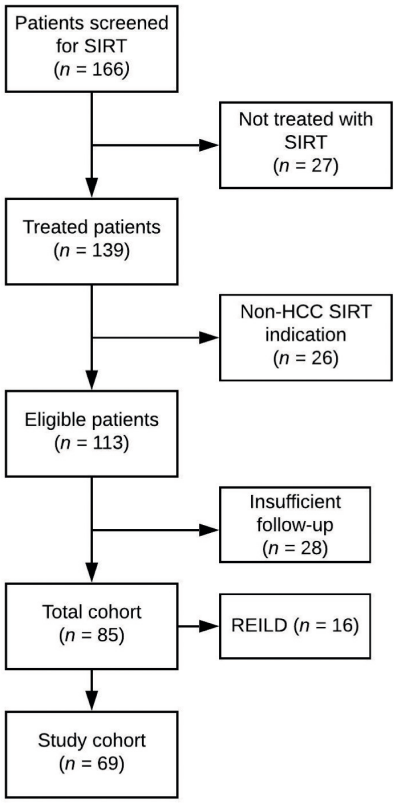

Figure 1 *Inclusion flowchart. SIRT: Selective Internal Radiation Therapy; Non-HCC: Patients who underwent SIRT for clinical indications other than hepatocellular carcinoma; REILD: Radioembolization-induced liver disease.*

Treatment details of SIRT such as the dosage, segments treated, tumor response and treatment-related adverse events (AEs) were collected. Follow-up data consisted of laboratory assessments and imaging results obtained six weeks, three months, six months, nine months and one year after SIRT. In the case of survival longer than one year, the liver-related outcome was observed until decompensation, loss to follow-up or death. All data were anonymized, coded and entered into an online database management system (Castor EDC).

Outcome measures

The primary outcome was the percentage of patients without REILD that developed CP score ≥ B7 liver decompensation four months or more after SIRT. The Common Terminology Criteria for Adverse Events (CTCAE) recently released version 4.0 of its definitions, including chronic hepatotoxicity.

Even though it is a complete and precise criterion describing hepatotoxicity, it lacks a cumulative scoring system. We, therefore, chose CP ≥ B7 as the endpoint as it correlates most with CTCAE grade ≥ 3 liver toxicity and due to its wide application by clinicians.

REILD was defined as a symptomatic post-radioembolization deterioration in the ability of the liver to maintain its (normal or preprocedural) synthetic, excretory and detoxifying functions, characterized by the onset of jaundice, new onset or increase in ascites, hyperbilirubinemia and hypoalbuminemia developing at least two weeks and no later than four months after RE, which could not be explained by either tumor progression or biliary tract obstruction [12]. Long-term liver-related complications were defined as clinical or biochemical presentation of liver decompensation that occurred at the first follow-up after the defined four months after SIRT. Liver decompensation was scored according to the CP classification, whereby decompensation was considered in case of a CP B7 or higher when initially CP A. Other scoring and used definitions of criteria are summarized in the supplementary text.

The secondary outcomes were OS, tumor response and time to progression (TTP). For OS, the date of the first SIRT until the date of death for any reason was used, or censored on the last known date to be alive. TTP was defined as the date of SIRT until radiological disease progression. Patients without progression were censored on the last date of follow-up. Radiological response evaluation was performed every three months using the Response Evaluation Criteria in Solid Tumors (RECIST 1.1) [18]. For analysis for the cause of death, patients were categorized into four groups: tumor-related death, liver-related death, combined (i.e., liver plus tumor-related) cause or other/unknown cause. Death was considered tumor-related in the case of a progressive disease without the occurrence of liver decompensation. Death was considered liver-related in the case of liver decompensation without documentation of tumor progression, and combined in the case of liver decompensation and progressive disease. Patients' last available follow-up results were clustered and analyzed.

For the comparison of OS between the SIRT-treated patients and the matched sorafenib treated patients, two separate propensity-matched analyses were done: one for all patients after treatment (including patients who developed REILD) and one for all patients who received a minimum of four months of sorafenib versus patients who did not develop REILD. For comparison between SIRT and sorafenib in terms of liver decompensation, grade 3-4 liver toxicity according to the CTCAE in the sorafenib cohort was compared with the occurrence of liver decompensation (CP ≥ B7) in the SIRT cohort. Patient and matching characteristics of the matched cohorts are shown in supplementary Tables S1–S4.

Statistical analysis

Continuous variables were reported as the mean with standard deviation (SD), or where appropriate, as the median with interquartile range. Categorical variables were reported as absolute values with percentages. For comparison of baseline and follow-up data, a paired T-test was used in the case of normally distributed data. In the case of non-normally distributed data, a Wilcoxon signed rank test was used. For comparison between groups, a Mann-Whitney U-test was used when appropriate. When comparing categorical data, 2 × 2 contingency tables were created and analyzed with the appropriate test, which was either the Pearson's chi-square or Fisher's exact test.

For OS and TTP estimates, comparison and figures, the Kaplan-Meier method was used and log-rank tests were performed, and Cox proportional hazard regression analysis was used to calculate hazard ratios (HRs). Cox proportional hazard regression and logistic regression were used to assess the association between different baseline variables/predictors and survival or liver decompensation, respectively.

For comparison of OS and occurrence of liver decompensation between patients treated with sorafenib and SIRT, propensity score matching was performed to create maximally balanced groups. For OS, the total cohort of SIRT patients was matched with sorafenib patients. For long-term liver-related complications, the long-term survival cohort of SIRT patients was matched with sorafenib patients treated with sorafenib for at least four months. Matching was done using the optimal method, focusing on minimizing the average absolute distance between all pairs based on sex, age, cirrhosis, CP score, portal hypertension, liver confined disease and BCLC classification, in a ratio of 1:1. Standardized mean differences (SMD) of each covariate were used to determine whether matching improved balance. Matching was performed separately for each outcome (OS in the total cohort of treated patients, and occurrence of liver decompensation), for optimal comparability.

A two-sided p value < 0.05 was considered statically significant. Statistical analyses were performed using SPSS statistics (version 26.0; IBM Corp. Armonk, NY: IBM Corp.). Propensity analyses were performed using the MatchIt package in R (version 3.6.1, https://cran.r-project.org/ (accessed on 15 August 2021))

RESULTS

Patient characteristics

For this analysis, 85 patients treated with SIRT between June 2011 and March 2019 were identified, who comprised the total cohort. Sixteen patients (19%) developed significant liver toxicity within four months after SIRT, meeting the REILD criteria. No patient developed

decompensation due to tumor progression or biliary tract obstruction. The remaining 69 (81%) patients were included in the study cohort. The baseline characteristics for both cohorts, as well as the tumor and previous treatment characteristics, are summarized in Table 1.

Table 1 *Baseline, treatment and previous treatment characteristics of patients treated with SIRT.*

Baseline Characteristics	Total Cohort (*n* = 85)	Study Cohort (*n* = 69)	REILD (*n* = 16)
Mean age in years (SD)	67.7 (8.5)	68.1 (8.4)	66.3 (9.4)
Sex, *n* (%)			
Male	73 (86)	61 (88)	12 (75)
Female	12 (14)	8 (12)	4 (25)
Comorbidities, *n* (%)			
None	27 (32)	25 (36)	2 (13)
Cardiovascular	30 (35)	22 (32)	8 (50)
Diabetes mellitus	32 (38)	24 (35)	8 (50)
Other	16 (19)	11 (16)	5 (31)
Etiology of liver disease, *n* (%)			
Alcohol	37 (44)	30 (44)	7 (44)
Hep B	10 (12)	8 (12)	2 (13)
Hep C	16 (19)	13 (19)	3 (19)
NAFLD	10 (12)	8 (12)	2 (13)
Unknown	10 (12)	7 (10)	3 (19)
Other	7 (8)	6 (9)	1 (6)
None	3 (4)	3 (4)	0 (0)
Cirrhosis, *n* (%)	62 (73)	49 (71)	13 (81)
Mean ALBI score (SD)	−2.7 (0.39)	−2.8 (0.37)	−2.6 (0.44)
ALBI grade, *n* (%)			
1	55 (65)	46 (67)	9 (56)
2	30 (35)	23 (33)	7 (44)
CP score, *n* (%)			
A5	73 (86)	61 (88)	12 (75)
A6	10 (12)	6 (9)	4 (25)
B7	2 (3)	2 (3)	0 (0)
Ascites, *n* (%)	9 (13)	9 (13)	0 (0)
Clinically irrelevant	6 (67)	6 (67)	N.A.
Mild	2 (22)	2 (22)	N.A.
Moderate-severe	1 (11)	1 (11)	N.A.
Portal hypertension, *n* (%)	42 (49)	31 (45)	11 (69)
MVI, *n* (%)	29 (34)	23 (33)	6 (38)
Tumor thrombus	26 (90)	21 (91)	5 (83)

Table 1 *Baseline, treatment and previous treatment characteristics of patients treated with SIRT.*
(continued)

Baseline Characteristics	Total Cohort (*n* = 85)	Study Cohort (*n* = 69)	REILD (*n* = 16)
Extra-hepatic metastasis, *n* (%)	6 (7)	6 (9)	0 (0)
	BCLC stage, *n* (%)		
A	1 (1)	1 (1)	0 (0)
B	52 (61)	43 (62)	9 (56)
C	32 (38)	25 (36)	7 (44)
Prior treatment, *n* (%)	34 (40)	28 (41)	10 (63)
Resection	7 (8)	6 (9)	1 (6)
RFA	13 (15)	12 (17)	1 (6)
MWA	2 (2)	2 (3)	0 (0)
TACE	16 (19)	13 (19)	3 (19)
Sorafenib	6 (7)	5 (7)	1 (6)

BCLC: Barcelona clinic liver cancer; CP: Child-Pugh; Hep: hepatitis virus; MVI: macro vascular involvement; MWA: microwave ablation; N.A.: not applicable; NAFLD: non-alcoholic fatty liver disease; RFA: radio frequent ablation; SD: standard deviation; TACE: transarterial chemo embolization; TARE: transarterial radioembolization.

Total cohort (all patients who received SIRT)

For the total cohort of 85 patients, the most common HCC etiology was alcohol (44%), followed by hepatitis C virus infection (19%) and hepatitis B virus infection (12%). Sixty-two patients (73%) had underlying liver cirrhosis, of whom 59 patients (95%) had CP A5 or A6. Forty-two patients (49%) had portal hypertension at the baseline. Nine patients (13%) had ascites on imaging, of whom three patients (33%) had clinically relevant ascites. At the baseline, patients had a median MELD score of 8 and a mean ALBI score of −2.7. Translated into ALBI grades, this accounted for 55 patients (65%) with ALBI grade 1 and 30 patients (35%) with ALBI grade 2.

At the time of SIRT, 34 patients (40%) had received any other prior treatment, mostly TACE (19%), radiofrequency ablation or microwave ablation (17%). At the baseline, 52 patients (61%) had BCLC stage B HCC. Of the 85 patients who had been treated with SIRT, 8 had received whole liver treatment, 63 lobar treatment (of whom 19 with an additional segmental treatment in the contralateral lobe) and 14 segmental treatment. Patients treated with SIRT received a median activity of 1930 MBq ^{90}Y (range 500–7200 MBq). There was no relation between the total dose and long-term complication rate.

Study cohort (Patients who received SIRT who did not develop REILD)

In the study cohort, after a median follow-up of 30 months (95% confidence interval (CI) 18–41), 38/69 patients (55%) developed liver decompensation CP ≥ B7 (shown in Table 2). From these 38 patients, 23 (61%) had hyperbilirubinemia, 31 (82%) had hypoalbuminemia, 7

(18%) experienced an episode of hepatic encephalopathy and 35 patients (92%) had newly onset ascites, of whom 30 (86%) required intervention. At the end of follow-up, for the CP score, a signed-rank test indicated that the follow-up CP (median = 7) was significantly higher than at the baseline (median = 5) ($Z = 30.0$, $p < 0.001$). For the MELD score, a signed-rank test indicated that the follow-up MELD (median = 12) was significantly higher than at the baseline (median = 8) ($Z = 26.0$, $p < 0.001$). For the ALBI score, a paired T-test showed a significant increase of the ALBI score at the follow-up when compared to the baseline (baseline mean = −2.8, SD 0.37; follow-up mean = −2.1, SD: 0.73; conditions $t(63) = -9.6$, $p < 0.001$) (shown in Figure 2).

Table 2 *Outcome summary of patients treated with SIRT.*

Variable	Deceased Patients *n* = 45	Alive Patients *n* = 22
Survival after SIRT, median (95% CI) (months)	15 (95% CI 9.6–20.4)	20 (95% CI 16.8–23.3)
Cause of death, *n* (%)		
Tumor related	5 (11)	N.A.
Liver related	10 (22)	N.A.
Combined	18 (40)	N.A.
Unknown/Other	12 (27)	N.A.
At last follow-up		
Presence of progression, *n* (%)		
Yes	34 (76)	11 (50)
No	11 (24)	10 (45)
Missing	0 (0)	1 (5)
Time to progression, median (95% CI) (months)	6.0 (95% CI 5.6–6.4)	9.0 (95% CI 4.3–13.7)
Tumor response at last FU, *n* (%)		
Complete response	2 (4)	3 (14)
Partial response	9 (20)	4 (18)
Stable disease	4 (9)	8 (36)
Progressive disease	25 (56)	4 (18)
Could not be determined	3 (7)	3 (14)
Missing	2 (4)	0 (0)
Child-Pugh score at last FU, *n* (%)		
A5	5 (11)	10 (45)
A6	3 (7)	1 (5)
B7	6 (13)	5 (23)
B8	7 (16)	1 (5)
B9	8 (18)	1 (5)
C10	7 (16)	0 (0)
C11	1 (2)	0 (0)
C12	2 (4)	0 (0)

Variable	Deceased Patients *n* = 45	Alive Patients *n* = 22
Missing	6 (13)	4 (18)
ALBI score at last FU, median (range)	−1.56 (−3.51–−0.10)	−2.47 (−3.44–−1.71)
ALBI grade at last FU, *n* (%)		
1	8 (18)	9 (41)
2	24 (53)	10 (46)
3	11 (24)	0 (0)
Missing	2 (4)	3 (14)
MELD at last FU, median (range)	14.50 (6–27)	8 (6–24)
Decompensation at last FU, *n* (%)		
Yes	31 (69)	7 (32)
No	8 (18)	11 (50)
Missing	6 (13)	4 (18)
Presence of ascites at last FU, *n* (%)		
Yes	29 (64)	6 (27)
No	13 (29)	16 (73)
Missing	3 (7)	0 (0)
Relevance of ascites at last FU, *n* (%)		
Clinically irrelevant	5 (17)	0 (0)
Mild	10 (34)	4 (67)
Moderate-severe	14 (48)	2 (33)

ALBI: albumin-bilirubin; 95% CI: 95% confidence interval; FU: follow-up; MELD: model for end-stage liver disease; N.A.: not applicable.

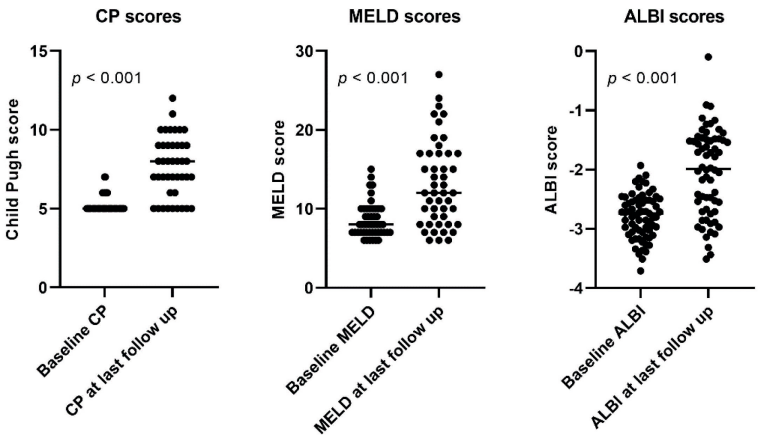

Figure 2 *Liver function scores at baseline compared to last follow-up after SIRT in the study cohort. ALBI: albumin-bilirubin; CP: Child Pugh; MELD: model for end-stage liver disease.*

The presence of liver cirrhosis at the baseline was significantly associated with liver decompensation at the last follow-up after SIRT (odds ratio (OR) of 4.0 (95% CI 1.2–13.2, p = 0.018)) (shown in Table 3). Furthermore, a lower ALBI score at the baseline was also significantly associated with a better outcome, with an OR of 0.074 per point of absolute increase (i.e., more negative ALBI score) (95% CI 0.012–0.475, p = 0.006) (shown in Table 3). After multivariate analysis, the ALBI score remained an independent predictor of liver decompensation at the last follow-up (OR of 0.114 (95% CI 0.016–0.824, p = 0.031)), making it the only predictor that showed a significant correlation with liver decompensation at last follow-up.

Table 3 *Odds ratios for liver decompensation after SIRT (study cohort).*

Variable	Odds Ratio	*n*	95% CI	*p*-Value
Sex	0.178	59	0.031–1.015	$p = 0.085$
Age	0.987	59	0.927–1.051	$p = 0.688$
Cirrhosis at baseline	**4.026**	**59**	**1.230 –13.178**	$\mathbf{p = 0.018}$
Ascites at baseline	4.516	59	0.516–39.529	$p = 0.238$
Portal hypertension at baseline	2.222	59	0.733–6.733	$p = 0.154$
MELD score	0.981	42	0.630–1.261	$p = 0.515$
ALBI score	**0.074**	**59**	**0.012 –0.475**	$\mathbf{p = 0.006}$

ALBI: albumin-bilirubin; 95% CI: 95% confidence interval; FIB-4: fibrosis-4; MELD: model for end-stage liver disease. p < 0.05 are printed in bold.

Treatment and tumor response

During follow-up, 46 patients (67%) had tumor progression. At the last follow-up, 5 patients had a complete response (7%), 13 (19%) had a partial response, 13 (19%) had a stable disease and 30 (43%) had a progressive disease (shown in Table 2). In six patients (9%) the response could not be determined, and in two patients (3%) data were missing. The median TTP was not significantly different between patients who had liver decompensation at the last follow-up (six months (95% CI 4.6–7.4)) and patients who did not decompose at the last follow-up (six months 95% CI 4.4–7.6) (p = 0.899). In addition, there was no difference in the ^{90}Y activity between patients who decomposed at the last follow-up and those who did not (p = 0.820).

Overall survival

The median OS in the total cohort of SIRT-treated patients was 18 months (95% CI 14–22). In the study cohort, 45/69 patients (65%) had died after a median follow-up of 30 months (95% CI 18–41). The median OS in this study cohort was 19 months (95% CI 17–21) (shown in Figure 3a). Of these 45 patients, four (9%) died due to tumor-related complications without any signs of liver dysfunction. Ten patients (22%) died due to liver-related complications, such as liver failure or varices bleeding, without signs of tumor progression at the time of

the last follow-up. Eighteen patients (40%) died with tumor progression in combination with liver decompensation. There was no significant difference in OS between patients who died due to liver-related complications (median OS 12 months, 95% CI 5–19) and patients who died with tumor progression at the end of the follow-up (median OS 15 months (95% CI 7–22); p = 0.752).

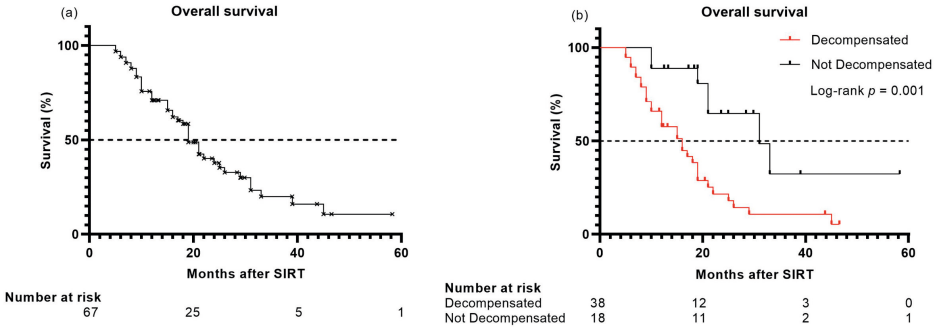

Figure 3 *(a) Overall survival (study cohort); and (b) Overall survival (study cohort) in patients who developed liver decompensation compared with patients who did not develop liver decompensation at last follow-up.*

For patients who developed liver decompensation (n = 38), the median OS was 16 months (95% CI 11–21), which was significantly shorter compared to the OS in patients who did not develop liver decompensation (median OS 31 months (95% CI 19–43); p = 0.001) (shown in Figure 3b). The ALBI score was an independent predictor of OS (HR 2.83; 95% CI 1.43–5.60; p = 0.003).

Propensity matched analysis of survival in SIRT versus sorafenib

In total, 76 matched patients were included in both groups. The patient characteristics of the matched cohorts are shown in supplementary Tables S1–S4. After a median follow-up of 30 months from their start of treatment, SIRT-treated patients showed a significantly longer median OS (16 months; 95% CI 12–21) compared to patients treated with sorafenib (median OS eight months; 95% CI 6–12; p = 0.0027) (shown in Figure 4). Patients who underwent SIRT showed a median progression-free survival (PFS) of nine months (95% CI 6–12). Patients who were treated with sorafenib had a shorter PFS (six months; 95% CI 2–9). However, the difference in PFS was not significant when comparing the two treatment modalities (p = 0.14).

Long-term liver decompensation: SIRT matched with sorafenib

In unmatched cohorts, the occurrence of liver decompensation in patients treated with SIRT was 55%, and in patients treated with sorafenib for at least four consecutive months was 22%. Secondary analysis was performed on the matched cohorts. Patients treated with SIRT

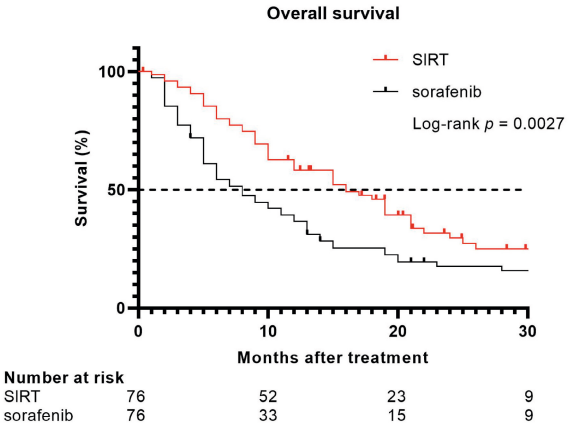

Figure 4 *Overall survival in all patients treated with SIRT matched with patients treated with sorafenib.*

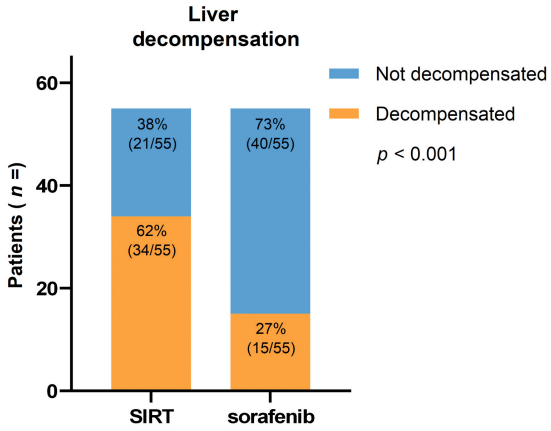

Figure 5 *Number of patients with liver decompensation at last follow-up, where SIRT is compared with a matched cohort of patients treated with sorafenib.*

and sorafenib were matched for comparison of the occurrence of liver decompensation. Ten patients with missing values in the SIRT cohort were excluded from this analysis, which showed higher occurrence of liver decompensation in patients treated with SIRT. Liver decompensation occurred significantly more often in patients who were treated with SIRT (62%) compared to patients treated with sorafenib (27%) (35% difference; 95% CI 0.28–0.57; p < 0.001; shown in Figure 5).

DISCUSSION

This study aimed to assess the long-term liver-related complications in patients with BCLC B and C HCC who were treated with SIRT and did not develop REILD within the first four months after SIRT. We hypothesized that despite better response rates with fewer short-term side effects, the long-term liver-related toxicity of SIRT would be more pronounced when compared to that of other treatment modalities such as sorafenib. This would then explain the lack of benefit for OS as reported previously [11–13]. In this retrospective analysis, we found that in patients who did not develop REILD after SIRT, still more than half (55%) developed liver decompensation CP ≥ B7. Decompensation was associated with a significantly shorter OS compared to patients with preserved liver function. Liver decompensation occurred significantly more often after SIRT compared to matched patients treated with sorafenib (SIRT 62% vs. sorafenib 27%). Despite these liver-related complications, OS after SIRT was significantly longer than after sorafenib when patients did not develop REILD. The ALBI score was predictive of long-term liver-related complications as well as OS.

More patients experienced liver decompensation after SIRT during long-term follow-up as compared to patients treated with sorafenib. Several studies showed that the function of treated liver parenchyma declined after SIRT, with a variable compensatory increase of liver volume in the non-treated part [19]. However, a recent study from our group showed that this volume-increased non-treated part was unable to compensate for the loss of liver function in the treated part [19]. The most probable explanation would be that the untreated liver segments possess insufficient reserve capacity to (fully) compensate for the loss of function from treated liver segments. This phenomenon would be even greater in patients with HCC, who mostly have liver cirrhosis, and thus have a worse regenerative capacity of the liver to begin with [20]. It could also imply that SIRT results in significant damage to the non-tumorous liver parenchyma in the treated (and also untreated) regions. REILD is acknowledged as an acute liver injury due to radiation, and yet our current findings and prior studies have shown that delayed effects of SIRT may result in long-term liver toxicity as well. It seems that the definition of REILD falls short regarding the timeframe it has to occur in. It is clear that REILD is a problem where hepatocyte regeneration no longer occurs as a collateral effect of radiation, up to a point where liver decompensation develops. This can happen within four months, but also beyond that timeframe. This might explain why patients who have better liver function at the baseline have a better outcome. In this study, the ALBI score was identified as an independent predictor at the baseline, which showed a correlation with long-term liver decompensation as well as OS. ALBI was first described in 2015, and offers a simple and objective method of assessing the liver function in patients with HCC [21]. The model has been validated in more than 46,000 patients [22]. Lower ALBI scores were prognostic of less liver decompensation and better OS, independent of Child-

Pugh scores. This could be a valuable model by which to select patients who are candidates for SIRT in the future. A recent study endorses the finding that SIRT can have a negative impact on liver function and correlates to the ALBI score [23]. Therefore, further analyses of cut-off values for the ALBI score are recommended, as well as validation in a larger cohort.

This study showed that the OS in patients treated with SIRT was significantly longer than in patients treated with sorafenib. This is in contrast with the current literature, which does not report a survival benefit of SIRT compared to systemic treatment in large phase-three trials [7,8]. However, earlier mentioned studies do suggest a survival benefit for patients treated with SIRT [9–12]. The SARAH trial gave us the inspiration to further investigate the relationship of dosage of ^{90}Y, survival and response for patients treated with SIRT [24]. This study shows that optimization of the tumor dosage of ^{90}Y is associated with better overall survival. In line with this study, more recent hypotheses are focusing on patient and tumor characteristics, and adjusting the treatment in accordance (i.e., higher dosage of ^{90}Y on smaller segments whilst sparing liver function due to less damage to healthy liver parenchyma), which can lead to a better response and survival benefit.

Still, the most obvious explanation for the difference between the outcome of the phase-three trials and our study could be that, in this study, patients with less advanced disease were included. In the SARAH trial, with only 28% of patients with BCLC B HCC and 68% with BCLC stage C HCC, the median OS after SIRT was eight months. In this current analysis, 54% of patients had BCLC B HCC, which likewise explains the better results. In the SIRveNIB study 51% of patients had BCLC C HCC, but still the median OS after SIRT only reached 8.8 months. Another difference between the studies that could explain the difference in OS is that, for example, in the SIRveNIB study, patients with underlying hepatitis B (51%) or C (14%) as the etiology for HCC were dominant, whereas our study involved mostly alcohol-related HCCs. Furthermore, although the objective response rates after SIRT in the SARAH and SIRveNIB trials were significantly higher compared to those after sorafenib, the observation that the OS was not different could also be the result of the here described long-term complications after SIRT. Although CP classification was not different between the SIRT and sorafenib cohorts, it is plausible that in this real-life cohort, patients with better-preserved liver function were included, which could be reflected in a lower ALBI score, and therefore, longer survival. Unfortunately, the SARAH and SIRveNIB trials did not report ALBI scores. Of course, comparing SIRT with sorafenib retrospectively is prone to various kinds of bias, primarily related to patient selection. Matching patients for tumor specific criteria such as BCLC may compensate for some of these differences, but will not compensate for all potential differences between the two groups.

This study also has several limitations, most importantly its retrospective design, with some inherent drawbacks, such as the lack of availability of important data. Another limitation is the observer or investigator bias that could be the case in radiological assessment of tumor response. This is particularly difficult in patients treated with SIRT since the radiation-induced changes in liver parenchyma impede objective response evaluation according to tumor size or contrast-enhancement. Furthermore, the radiological tumor response after SIRT can be delayed, or due to tumor necrosis and edema, show initial pseudo progression followed by stable or responsive disease afterwards [25].

CONCLUSIONS

In conclusion, this is the first study to report the long-term liver-related outcome after SIRT in patients with HCC, and this study assessed the largest cohort of patients treated with SIRT to date with this endpoint in mind. Patients with intermediate- or advanced stage HCC treated with SIRT have a substantial risk of developing liver decompensation, both in the short term (19% developed REILD) and in the longer term (>six months). Liver decompensation after SIRT is associated with shorter OS. Despite this risk, the survival of patients treated with SIRT who did not develop REILD was significantly better than matched patients treated with sorafenib. This suggests that, in well-selected patients, SIRT has a potential survival benefit over sorafenib. The ALBI score was predictive of both liver decompensation and OS and thus could be a valuable marker for patient selection.

REFERENCES

[1] Bray F, Ferlay J, Soerjomataram I, et al. Global cancer statistics 2018: GLOBOCAN estimates of incidence and mortality worldwide for 36 cancers in 185 countries. CA: A Cancer Journal for Clinicians 2018;68:394-424.

[2] Bruix J, Reig M, Sherman M. Evidence-Based Diagnosis, Staging, and Treatment of Patients With Hepatocellular Carcinoma. Gastroenterology 2016;150:835-53.

[3] Kudo M, Finn RS, Qin S, et al. Lenvatinib versus sorafenib in first-line treatment of patients with unresectable hepatocellular carcinoma: a randomised phase 3 non-inferiority trial. Lancet 2018;391:1163-1173.

[4] Heimbach JK, Kulik LM, Finn RS, et al. AASLD guidelines for the treatment of hepatocellular carcinoma. Hepatology 2018;67:358-380.

[5] EASL Clinical Practice Guidelines: Management of hepatocellular carcinoma. J Hepatol 2018;69:182-236.

[6] Sundram FX, Buscombe JR. Selective internal radiation therapy for liver tumours. Clin Med (Lond) 2017;17:449-453.

[7] Vilgrain V, Pereira H, Assenat E, et al. Efficacy and safety of selective internal radiotherapy with yttrium-90 resin microspheres compared with sorafenib in locally advanced and inoperable hepatocellular carcinoma (SARAH): an open-label randomised controlled phase 3 trial. Lancet Oncol 2017;18:1624-1636.

[8] Chow PKH, Gandhi M, Tan SB, et al. SIRveNIB: Selective Internal Radiation Therapy Versus Sorafenib in Asia-Pacific Patients With Hepatocellular Carcinoma. J Clin Oncol 2018;36:1913-1921.

[9] Mazzaferro V, Sposito C, Bhoori S, et al. Yttrium-90 radioembolization for intermediate-advanced hepatocellular carcinoma: a phase 2 study. Hepatology 2013;57:1826-37.

[10] Salem R, Lewandowski RJ, Mulcahy MF, et al. Radioembolization for hepatocellular carcinoma using Yttrium-90 microspheres: a comprehensive report of long-term outcomes. Gastroenterology 2010;138:52-64.

[11] Sangro B, Carpanese L, Cianni R, et al. Survival after yttrium-90 resin microsphere radioembolization of hepatocellular carcinoma across Barcelona clinic liver cancer stages: a European evaluation. Hepatology 2011;54:868-78.

[12] Hilgard P, Hamami M, Fouly AE, et al. Radioembolization with yttrium-90 glass microspheres in hepatocellular carcinoma: European experience on safety and long-term survival. Hepatology 2010;52:1741-9.

[13] Ricke J, Klümpen HJ, Amthauer H, et al. Impact of combined selective internal radiation therapy and sorafenib on survival in advanced hepatocellular carcinoma. J Hepatol 2019;71:1164-1174.

[14] Braat MN, van Erpecum KJ, Zonnenberg BA, et al. Radioembolization-induced liver disease: a systematic review. Eur J Gastroenterol Hepatol 2017;29:144-152.

[15] Jakobs TF, Saleem S, Atassi B, et al. Fibrosis, portal hypertension, and hepatic volume changes induced by intra-arterial radiotherapy with 90yttrium microspheres. Dig Dis Sci 2008;53:2556-63.

[16] Fernandez-Ros N, Silva N, Bilbao JI, et al. Partial liver volume radioembolization induces hypertrophy in the spared hemiliver and no major signs of portal hypertension. HPB (Oxford) 2014;16:243-9.

[17] Labeur TA, van Vugt JLA, Ten Cate DWG, et al. Body Composition Is an Independent Predictor of Outcome in Patients with Hepatocellular Carcinoma Treated with Sorafenib. Liver Cancer 2019;8:255-270.

[18] Therasse P, Arbuck SG, Eisenhauer EA, et al. New guidelines to evaluate the response to treatment in solid tumors. European Organization for Research and Treatment of Cancer, National Cancer Institute of the United States, National Cancer Institute of Canada. J Natl Cancer Inst 2000;92:205-16.

[19] Van der Velden, S.; Braat, M.N.G.J.A.; Labeur, T.A.; Scholten, M.V.; van Delden, O.M.; Bennink, R.J.; de Jong, H.W.A.M.; Lam, M.G.E.H. A Pilot Study on Hepatobiliary Scintigraphy to Monitor Regional Liver Function in (90)Y Radioembolization. J. Nucl. Med. 2019, 60, 1430–1436.

[20] Bennink, R.J.; Tulchinsky, M.; de Graaf, W.; Kadry, Z.; van Gulik, T.M. Liver Function Testing with Nuclear Medicine Techniques Is Coming of Age. Semin. Nucl. Med. 2012, 42, 124–137.

[21]. Johnson, P.J.; Berhane, S.; Kagebayashi, C.; Satomura, S.; Teng, M.; Reeves, H.L.; O'Beirne, J.; Fox, R.; Skowronska, A.; Palmer, D.; et al. Assessment of Liver Function in Patients With Hepatocellular Carcinoma: A New Evidence-Based Approach—The ALBI Grade. J. Clin. Oncol. 2015, 33, 550–558.

[22] Hiraoka, A.; Michitaka, K.; Kumada, T.; Izumi, N.; Kadoya, M.; Kokudo, N.; Kubo, S.; Matsuyama, Y.; Nakashima, O.; Sakamoto, M.; et al. Validation and Potential of Albumin-Bilirubin Grade and Prognostication in a Nationwide Survey of 46,681 Hepatocellular Carcinoma Patients in Japan: The Need for a More Detailed Evaluation of Hepatic Function. Liver Cancer. 2017, 6, 325–336.

[23] Ricke, J.; Schinner, R.; Seidensticker, M.; Gasbarrini, A.; van Delden, O.M.; Amthauer, H.; Peynircioglu, B.; Bargellini, I.; Iezzi, R.; De Toni, E.N.; et al. Liver function after combined selective internal radiation therapy or sorafenib monotherapy in advanced hepatocellular carcinoma. J. Hepatol. 2021, in press.

[24] Hermann, A.-L.; Dieudonné, A.; Ronot, M.; Sanchez, M.; Pereira, H.; Chatellier, G.; Garin, E.; Castera, L.; Lebtahi, R.; Vilgrain, V.; et al. Relationship of Tumor Radiation–absorbed Dose to Survival and Response in Hepatocellular Carcinoma Treated with Transarterial Radioembolization with 90Y in the SARAH Study. Radiology 2020, 296, 673–684.

[25] Salem, M.E.; Jain, N.; Dyson, G.; Taylor, S.; El-Refai, S.M.; Choi, M.; Shields, A.F.; Critchfield, J.; Philip, P.A. Radiographic parameters in predicting outcome of patients with hepatocellular carcinoma treated with yttrium-90 microsphere radioembolization. ISRN Oncol. 2013, 15, 538376.

Chapter 10

Summary, general discussion and future perspectives

SUMMARY

Hepatocellular carcinoma (HCC) is witnessing a rise in its incidence, predominantly attributable to the aging population. The implementation of screening programs among high-risk populations has led to improved detection in an early phase. However, since the underlying liver cirrhosis remains incurable, the cause of tumor genesis is not being addressed, and a risk of developing new intrahepatic lesions after initial treatment remains present. Accurate minimally invasive treatment of Barcelona Clinic Liver Cancer (BCLC) early stage disease therefore serves two main purposes. First, it aims to offer an equally efficacious alternative to surgical resection for patients unable to undergo surgery due to portal hypertension caused by the underlying cirrhosis. Secondly, these interventions strive for optimal local control of the disease, while extending the window of opportunity for potential liver transplantation in eligible patients. This thesis contributes to pushing the boundaries for patient tailored and optimal minimally invasive management of early stage HCC.

Part 1 of this thesis focusses on the optimization of thermal ablation (TA) techniques, with the ultimate goal of enhancing their effectiveness in the treatment of early stage HCC lesions >2 cm. In *Part 2*, minimally invasive combination therapies are studied, tailored for early stage HCC lesions of 2 - 5 cm. Lastly, *Part 3* is directed to the long term outcomes after trans-arterial radioembolization (TARE) treatment for HCC.

Part 1: Thermal ablation: reproducibility and ablation margins

In *Chapter 2,* a comparative assessment of two commercially available microwave ablation (MWA) systems was conducted, focusing on the dimensions and sphericity of the ablation zones. These experiments were carried out in ex-vivo porcine liver specimens. Analysis of the ablation zones using high-field MRI showed differences in ablation size and sphericity between the two MWA systems at similar ablation settings. Notably, the Emprint ablation system demonstrated more uniform and predictable ablation zones across repeated measurements. Consistency in the size and shape of ablation zones is of high importance in the context of treatment planning and, ultimately, the prevention of local recurrences.

The confirmation of technical success is of great value in averting local recurrences. *Chapter 3* provides a comprehensive overview of the existing literature on ablation margin quantification methods. A total of 75 studies were included in a systematic review, 58 of which being clinical trials. In most clinical trials, target ablation margins were set at ≥ 5 mm, which is in accordance with clinical practice guidelines. Among all studies, 21 used co-registration software for minimal ablation margin (MAM) quantification. Both rigid and non-rigid registration techniques were utilized almost equally, whilst most applications incorporated semi-automatic segmentation tools. Furthermore, ten studies that explored

tissue shrinkage after TA were included, revealing a considerable variation in their findings. It is important to note that the vast majority of evidence is derived from retrospective data analysis. There is need for prospective data concerning ablation margin quantification and its correlation with local recurrences.

In *Chapter 4* commercially available non-rigid registration software was used for retrospective ablation margin quantification in 25 patients who had undergone TA of HCC lesion(s). In 7 of these patients, registration quality between diagnostic and post-ablation imaging was insufficient for quantitative analysis of ablation margins. Local recurrences were observed in eight out of the 18 remaining patients with a median follow-up time of 9.5 months. The results indicated that negative ablation margins strongly correlated with the occurrence of local tumor progression, as the average minimal ablation margin was -8.44 mm (SD 4.27) in patients who developed local recurrences, against -0.30 mm (SD: 2.00) in patients who did not. Interestingly, all patients with an ablation margin >0 mm did not develop local recurrent disease. The findings indicate that tissue shrinkage after ablation is an important factor to take into account, since not all patients with negative ablation margins developed local recurrences. It is important to stress the low eligibility to the study of the initial cohort (25/78 patients), due to its retrospective nature and differences in patient positioning between diagnostic and post-ablation imaging. To surpass the limitations faced in the retrospective study, the IAMCOMPLETE study protocol was designed, which incorporates a standardized pre- and post-ablation scanning protocol.

Chapter 5 describes the results of the prospective IAMCOMPLETE study, in which feasibility of rigid co-registration and ablation margin quantification was analyzed. In a study cohort of 20 patients (male: 13; mean age : 67.1 ± 10.8 [SD]; Child-Pugh A: n=12, B: n=8; BCLC stages very early: n=8, early: n=12, intermediate: n=2) , pre- and post- ablation contrast enhanced CT scans were acquired under general anesthesia and with a pre-oxygenated breath hold. This approach yielded a successful image registration in 16/20 patients (80%) and in 84% of all tumors. High inter- and intra-observer agreement rates for tumor segmentation were found, with a dice similarity coefficient of 0.815 and 0.830, respectively. The average MAM was 0.63 mm (SD: 3.589). Noteworthy, an average MAM of -4.0 mm was found in the two cases in which local recurrences developed and margins of the ablation procedure could be quantified. In this study the potential influence of tissue shrinkage was also suspected, since only 2/9 lesions with a negative MAM developed local recurrent HCC within one year.

Part 2: Combined treatment regimens for early stage HCC

Chapter 6 presents the findings of a retrospective cohort study on the combined treatment approach involving TA and transarterial chemoembolization (TACE) in 38 patients (male: n=34; median age 68.5 (range: 40-84); liver cirrhosis: n=33; BCLC early stage HCC: n=21,

intermediate stage: n=17, adjuvant TACE: n=27, neoadjuvant TACE: n=11). In this study the clinical outcomes in terms of overall survival (OS), time to progression (TTP), and local tumor progression (LTP) of both neoadjuvant and adjuvant use of TACE were examined. The median time to LTP was 23.6 months among patients subjected to neoadjuvant TACE whereas the median time to LTP in those treated with adjuvant TACE was 8.1 months ($p = 0.19$). Although no significant results were found, the trend suggests a better local control was obtained in patients treated with neoadjuvant TACE. This is in line with the current most common application of combined TACE and TA as described in literature. The median OS was 52.7 months for the entire cohort and no statistically significant differences between adjuvant and neoadjuvant TACE were found.

The HORA EST HCC study protocol is introduced in *Chapter 7*. In this multicenter, dose escalation cohort study, patients with HCC lesions of 2-5 cm underwent a combined treatment regimen involving TA and adjuvant holmium-166 (^{166}Ho) TARE. The hypothesis of this study was that hyperemia occurs in the direct proximity after ablation, which would allow for preferential accumulation of TARE using holmium-166 microspheres. The primary objective of this trial was to determine the optimal radiation dose to the treatment volume, ensuring a tissue absorbed radiation dose of 120 Gy to the target volume, encompassing the immediate periphery of the ablation zone.

In *Chapter 8* the results of the HORA EST HCC study are presented. In this prospective trial, 12 patients were treated with TA and holmium-166 TARE (male: 10; median age: 66.5 (IQR [64.3-71.7]); median tumor diameter: 2.7 cm (IQR [2.1-4.0])) A preferential accumulation of ^{166}Ho microspheres was observed within the target volume. After 2 patients had received 60 Gy of ^{166}Ho to the treatment volume the dose was escalated to 90 Gy for subsequent patients. The study ascertained that a treatment volume dose of 90 Gy was required to achieve the desired absorbed dose of 120 Gy within the target volume (median absorbed dose: 138 Gy (IQR: [127-145])). Remarkably, none of the 12 patients who underwent this treatment protocol developed local recurrences within 1 year of follow up, highlighting its promising efficacy in preventing tumor recurrence.

Part 3: TARE beyond early stage HCC

Chapter 9 describes the long-term results after TARE in a multi-center cohort comprising three academic medical centers, focusing on the long-term liver-related complications of TARE in patients who had not developed TARE induced liver disease (REILD). In total, 85 patients were included, 16 of whom developed REILD. Of the remaining 69 patients, 38 developed liver decompensation with Child-Pugh ≥ B7. A significant difference in OS was found between patients who developed REILD versus patients who did not; 16 vs 31 months respectively. In comparison to a matched control group of patients who underwent systemic

treatment with sorafenib, a higher incidence of liver decompensation was observed as late complication after TARE; 62% vs 27%. Nevertheless, it is worth noting that the OS after TARE was significantly longer than after sorafenib; 16 vs 8 months. Notably, the Albumin-Bilirubin (ALBI) score emerged as an independent predictive factor for the development of liver decompensation and OS.

GENERAL DISCUSSION AND FUTURE PERSPECTIVES

The role of interventional oncology has grown tremendously over the last decade, which has led to it being a fully accepted and integrated discipline in oncologic care pathways [1]. Interventional oncology often offers effective, minimally invasive local therapies with low complication rates and shorter hospital stays [2]. This provides clear advantages over surgery and systemic therapies, as both are related with a high burden on the individual patient as well as healthcare costs. The increased use of interventional oncology is reflected in all recent HCC guidelines. TA is the treatment of choice in HCC lesions <2 cm, as the oncological outcomes are equal to those of surgery but at lower complication rates and costs [3, 4]. In the recent update of the Barcelona Clinic Liver Cancer (BCLC) staging system trans-arterial therapies, such as trans-arterial chemoembolization (TACE) and TARE, are recognized as effective alternative regimens for early stage HCC patients not eligible for surgery or ablation. Also in more advanced stages, TACE and TARE have been recognized as effective palliative treatments. Continuous technological advancement and the execution of larger and well-designed clinical trials studying the effect of treatment improvements, as well as head-to-head comparisons with other therapies, ameliorate and may further define the position of these therapies.

Thermal ablation

TA is the main treatment modality that has been discussed in this thesis. Advancements in treatment techniques have led to adoption of TA as first line treatment for HCC lesions <2 cm. For larger lesions, there is a clinically unmet need for a validated tool or technique that reduces the risk of local recurrences, that hampers further implementation in HCC guidelines. The workflow of TA consists of several steps, as can be seen in figure 1. Each step allows for the use of different techniques that could influence the treatment outcome of TA.

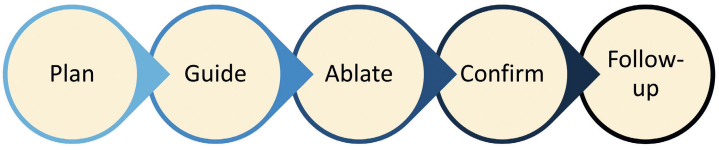

Figure 1 *Workflow of TA.*

Consistency in ablation zone sizes is of great importance for accurate treatment planning. Chapter 2 of this thesis presented the potential variety observed in ablation zones created by two different MWA systems, and even by a single ablation system in repeated measurements. The findings of this study reflect clinical practice, as ablation zone sizes and shapes can highly vary among patients. There are computational models that predict ablation zone sizes and shapes, while taking into account patient- and tissue specific factors [5]. Although the

use of these models would be very helpful, the research is currently in a premature phase and needs further development and validation before it can be used in clinical practice for treatment planning.

Image guidance can be provided by ultrasound, fusion of ultrasound-CT or ultrasound-MR, CT with intravenous contrast, CT with direct contrast agent infusion in the hepatic artery, and cone-beam CT. The image guiding modality should be chosen that provides the highest level of control over the needle position in respect to the tumor location, which can differ per treatment. Besides different imaging modalities, advanced needle guidance systems are currently available, for instance using optical or electromagnetic tracking, or even robotic assistance [6]. These systems contribute to the standardization of the procedure, which often translates to low tumor recurrence rates [7-9]. Moreover, as it increases reproducibility, those systems could contribute to shorter learning curves [10].

Confirmation of treatment success has been the most investigated topic in this thesis. Key in defining technical success of TA is the verification of ablation margins by using registration of pre- and post-ablation images, as has been demonstrated in *Chapters 4 and 5*. Besides the research presented in this thesis, multiple other articles have demonstrated poor reproducibility of eyeballing on pre-and post-ablation scans in the assessment of technical success, and the potential of quantifying the MAM [11, 12]. Interestingly, introducing a more objectified way to quantify a treatment outcome goes hand in hand with introducing the quantification paradox. By being able to measure an outcome, a complex problem is reduced to a single value, which is analyzed in terms of accuracy. In ablation margin quantification, the level of treatment success is often reflected by the smallest distance between a single point on a tumor surface and its closest border of an ablation zone: the MAM. This single value may be influenced by factors such as accuracy of tumor segmentation and image registration, but also factors such as liver deformation or tissue shrinkage during ablation, as can be read in *Chapter 5.* Further research should focus on advanced algorithms that allow for image registration with highest accuracy, and to different quantitative outcome measure that correlate mostly with treatment outcome. This research would be of great importance for further advancing TA practice. However, bringing an image registration tool to clinical practice today would enable a shift from side-by-side eyeballing to an overlay of images, which is likely to directly impact patient care. Although mostly supported by retrospective data, literature is unambiguous in the finding that image registration would improve the assessment of technical treatment success [13].

Prospective clinical trials are necessary to further prove the benefit of ablation margin quantification in clinical practice. Ideally, a cut-off minimal ablation zone value would be found that correlates with a low risk of local tumor recurrence. This requires a robust analysis

workflow that needs optimization of pre- and post ablation imaging protocols for accurate and automatic segmentation of tumor and ablation zone [14]. Moreover, image registration of pre- and post ablation images should further be optimized, which should probably be (partly) AI powered and use a combination of rigid and non-rigid registration [14, 15]. Large clinical trials are needed, such as the PROMETHEUS study which is coordinated by the LUMC, to further investigate how quantitative ablation margin values correlate to treatment outcome. [16, 17].

The growing role of real world data studies, such as CIEMAR and IMAGIO [18], and large clinical trials in the field of TA could create large datasets of TA imaging and patient data. By using large data sets for the training of AI models, a more patient tailored treatment approach could be developed. Depending on patient and tumor specific factors, the a priori probability of local recurrence after treatment varies among patients. Besides the lesion size and ablation margins obtained, treatment of recurrent cancer, perivascular tumor localizations, non-smooth tumor surfaces, high alpha-fetoprotein levels and higher Child-Pugh liver cirrhosis status are associated with more aggressive recurrences [19]. Further personalization of TA treatment therefore seems needed, although limited literature on this topic is currently available. Future research could learn from large data sets and answer questions like: *Do different tumor subtypes require different ablation margins? Do all TA patients need the same follow-up protocol? Could peri-procedural imaging protocols be optimized for better delineation of HCC lesions with non-smooth tumor borders? Is it possible to simulate the ablation zone pre-procedurally based on patient-specific parameters? Which patients would benefit most from (neo)adjuvant treatment?*

TARE

TARE has had a bumpy ride in making its way to clinical practice guidelines of HCC, and may be the best example to emphasize the value of the patient-tailored use of a minimally invasive treatment. After failing to meet superiority over the multi-kinase inhibitor sorafenib for advanced HCC (SARAH and SIRveNIB trials), the expectations for this treatment may have been tempered. However, since the first correlation of tumor absorbed radiation dose with treatment outcome was found, a large research field developed in terms of personalized dosimetry, with studies describing treatments with tumor absorbed doses of over hundreds of grays [20]. In a retrospective analysis of the SARAH trail, the predicted absorbed tumor dose at time of the Tc-99m labeled aggregated macro-albumin (^{99m}Tc-MAA) SPECT/CT scan during the work-up procedure turned out to be the only independent predictor of survival: 14.1 months in patients receiving >100 Gy ^{90}Y to the tumor vs 6.1 months in patients receiving a lower tumor dose [21]. Recently, it was prospectively confirmed in the DOSISPHERE-01 trial that personalized dosimetry yielded a higher objective response rate in patients targeted ≥205 Gy of glass microspheres to the tumors [22].

Over the last few years, clinical guidelines have been developed demonstrating the use of TARE for different applications: radiation segmentectomy for smaller lesions, lobectomy procedures for larger lesions and to induce hypertrophy of the future liver remnant prior to hemi-hepatectomy, and whole liver treatment [23]. In general, the trend has shifted more to the use of TARE in limited parts of the liver for intermediate or early stage HCC rather than whole liver treatment in advanced stages. This is in line with the findings of *Chapter 9* of this thesis, which discusses the late onset of liver decompensation after the use of TARE in a population with mainly intermediate and advanced stage HCC. In line with the findings of this study, more papers describe the ALBI score as early predictor of liver decompensation onset after TARE [24, 25]. Since better systemic treatment options, such as combined atezolizumab and bevacizumab, are now available, patient selection for TARE in more advanced disease stages is of even greater importance. This emphasizes the role of treatment planning based on the scout procedure. In general, selective catheterization of the tumor(s) and leaving a part of the liver untreated is a prerequisite for a successful therapy. The ^{99m}Tc-MAA scout procedure should demonstrate sufficient dose accumulation in the tumors that enable a high tumor dose while limiting the dose to the healthy liver parenchyma. This also means that a patient with an insufficient tumor absorbed dose as predicted by the SPECT-CT scan after the ^{99m}Tc-MAA-procedure should be brought back to the tumor board meeting to reconsider the choice of therapy. Future research could contribute to this decision by further defining threshold values that predict successful or unsuccessful treatment for the different radioembolization products and treatment approaches. Moreover, a patient tailored work up currently requires information from diagnostic imaging, SPECT/CT, and cone-beam CT. The development of a scout procedure with PET-tracer would allow for a contrast enhanced PET/CT scan with optimal image registration between anatomical and nuclear imaging at a superior resolution. Especially in challenging cases, this would contribute to improved dose planning and thus to treatment outcome.

In the HORA EST HCC trial, TARE has been used as adjuvant therapy after TA. Since the design of that study, the RASER and LEGACY studies have demonstrated high efficacy of TARE segmentectomy in equally sized lesions with local control rates similar to those after TA [26, 27]. These findings have led to the positioning of TARE as therapy for early stage HCC lesions ≤8 cm in the BCLC guidelines for patients ineligible to surgery or TA [28]. Despite the promising results so far, superiority over TA or surgical resection for these patients has not been investigated. Years of combined TA with TACE did not lead to full adoption in clinical guidelines, despite several studies that were performed. In *Chapter 8* the results of the HORA EST HCC trial showed that ^{166}Ho microspheres could be delivered in high concentrations to the area at risk for tumor recurrences after TA. Future research should focus on how to incorporate the excellent results of high dosed radiation segmentectomy in the combined treatment regimen of TA and TARE to further reduce local recurrence rates. The current

protocol could be altered in such way that small treatment volumes receive a higher average radiation dose than larger treatment volumes. Moreover, since the individual treatment outcomes of TA and TARE have improved over time, one could debate whether a combined treatment regimen in tumors <3 cm would be (cost-)effective. Therefore, inclusion criteria should shift from 2-5 cm to 3-6 cm lesions.

CONCLUSION

Early stage HCC remains a complex field with numerous sophisticated treatment options. Consequently, a 'one size fits all' approach is unlikely to be applicable. On the one hand conducting extensive studies with harmonized treatment protocols is crucial for head-to-head comparisons of outcomes within patient cohorts. At the same time, this wealth of data is essential for developing a nuanced understanding of which patients would benefit most from what treatment on an individual level. We should be aware not to treat all TA patients with an adjuvant treatment in order to prevent one tumor recurrence, which could have been predicted on by better use of imaging parameters and patient data.

Historically, progress in cancer therapy has been marked by incremental advancements rather than a quest for a singular "magic bullet" solution. The introduction of groundbreaking anti-cancer drugs or surgical techniques has often been met with initial enthusiasm, only to reveal limitations in their effectiveness over time. Nevertheless, these individual therapies have made meaningful contributions to the treatment of cancer patients. Interventional oncology is a relatively young field that experiences rapid and successive technological advancements. It is only logical to expect the growth and developments of the field to continue, playing a pivotal role in addressing future healthcare challenges, which is particularly relevant in the context of a healthcare system under pressure of an aging population and limited resources.

REFERENCES

[1] Kim HS, Chapiro J, Geschwind J-FH. From the Guest Editor: Interventional Oncology: The Fourth Pillar of Oncology. The Cancer Journal 2016;22.

[2] Iezzi R, Gangi A, Posa A, Pua U, Liang P, Santos E, et al. Emerging Indications for Interventional Oncology: Expert Discussion on New Locoregional Treatments. Cancers (Basel) 2023;15.

[3] Cucchetti A, Piscaglia F, Cescon M, Colecchia A, Ercolani G, Bolondi L, et al. Cost-effectiveness of hepatic resection versus percutaneous radiofrequency ablation for early hepatocellular carcinoma. J Hepatol 2013;59:300-307.

[4] Livraghi T, Meloni F, Di Stasi M, Rolle E, Solbiati L, Tinelli C, et al. Sustained complete response and complications rates after radiofrequency ablation of very early hepatocellular carcinoma in cirrhosis: Is resection still the treatment of choice? Hepatology 2008;47:82-89.

[5] van Erp GCM, Hendriks P, Broersen A, Verhagen CAM, Gholamiankhah F, Dijkstra J, et al. Computational Modeling of Thermal Ablation Zones in the Liver: A Systematic Review. Cancers 2023;15:5684.

[6] de Baère T, Roux C, Deschamps F, Tselikas L, Guiu B. Evaluation of a New CT-Guided Robotic System for Percutaneous Needle Insertion for Thermal Ablation of Liver Tumors: A Prospective Pilot Study. CardioVascular and Interventional Radiology 2022;45:1701-1709.

[7] Laimer G, Schullian P, Bale R. Stereotactic Thermal Ablation of Liver Tumors: 3D Planning, Multiple Needle Approach, and Intraprocedural Image Fusion Are the Key to Success-A Narrative Review. Biology (Basel) 2021;10.

[8] Smits MLJ, Bruijnen RCG, Tetteroo P, Vonken E-jPA, Meijerink MR, Hagendoorn J, et al. Hepatic Arteriography and C-Arm CT-Guided Ablation (HepACAGA) to Improve Tumor Visualization, Navigation and Margin Confirmation in Percutaneous Liver Tumor Ablation. CardioVascular and Interventional Radiology 2023;46:1365-1374.

[9] Beermann M, Lindeberg J, Engstrand J, Galmén K, Karlgren S, Stillström D, et al. 1000 consecutive ablation sessions in the era of computer assisted image guidance - Lessons learned. Eur J Radiol Open 2019;6:1-8.

[10] Wallach D, Toporek G, Weber S, Bale R, Widmann G. Comparison of freehand-navigated and aiming device-navigated targeting of liver lesions. Int J Med Robot 2014;10:35-43.

[11] Laimer G, Schullian P, Jaschke N, Putzer D, Eberle G, Alzaga A, et al. Minimal ablative margin (MAM) assessment with image fusion: an independent predictor for local tumor progression in hepatocellular carcinoma after stereotactic radiofrequency ablation. European Radiology 2020;30:2463-2472.

[12] Kim YS, Lee WJ, Rhim H, Lim HK, Choi D, Lee JY. The minimal ablative margin of radiofrequency ablation of hepatocellular carcinoma (> 2 and < 5 cm) needed to prevent local tumor progression: 3D quantitative assessment using CT image fusion. AJR Am J Roentgenol 2010;195:758-765.

[13] Minier C, Hermida M, Allimant C, Escal L, Pierredon-Foulongne M-A, Belgour A, et al. Software-based assessment of tumor margins after percutaneous thermal ablation of liver tumors: A systematic review. Diagnostic and Interventional Imaging 2022;103:240-250.

[14] Survarachakan S, Prasad PJR, Naseem R, Pérez de Frutos J, Kumar RP, Langø T, et al. Deep learning for image-based liver analysis — A comprehensive review focusing on malignant lesions. Artificial Intelligence in Medicine 2022;130:102331.

[15] Berbís MA, Paulano Godino F, Royuela Del Val J, Alcalá Mata L, Luna A. Clinical impact of artificial intelligence-based solutions on imaging of the pancreas and liver. World J Gastroenterol 2023;29:1427-1445.

[16] Oosterveer TTM, van Erp GCM, Hendriks P, Broersen A, Overduin CG, van Rijswijk CSP, et al. Study Protocol PROMETHEUS: Prospective Multicenter Study to Evaluate the Correlation Between Safety Margin and Local Recurrence After Thermal Ablation Using Image Co-registration in Patients with Hepatocellular Carcinoma. Cardiovasc Intervent Radiol 2022;45:606-612.

[17] Lin YM, Paolucci I, Anderson BM, O'Connor CS, Rigaud B, Briones-Dimayuga M, et al. Study Protocol COVER-ALL: Clinical Impact of a Volumetric Image Method for Confirming Tumour Coverage with Ablation on Patients with Malignant Liver Lesions. Cardiovasc Intervent Radiol 2022;45:1860-1867.

[18] Pereira PL, Bale R, Fretland ÅA, Goldberg SN, Helmberger T, Meijerink MR, et al. Local Tumour Control Following Microwave Ablation: Protocol for the Prospective Observational CIEMAR Study. CardioVascular and Interventional Radiology 2023.

[19] Huang J, Huang W, Guo Y, Cai M, Zhou J, Lin L, et al. Risk Factors, Patterns, and Long-Term Survival of Recurrence After Radiofrequency Ablation With or Without Transarterial Chemoembolization for Hepatocellular Carcinoma. Front Oncol 2021;11:638428.

[20] Roosen J, Klaassen NJM, Westlund Gotby LEL, Overduin CG, Verheij M, Konijnenberg MW, et al. To 1000 Gy and back again: a systematic review on dose-response evaluation in selective internal radiation therapy for primary and secondary liver cancer. Eur J Nucl Med Mol Imaging 2021;48:3776-3790.

[21] Hermann A-L, Dieudonné A, Ronot M, Sanchez M, Pereira H, Chatellier G, et al. Relationship of Tumor Radiation–absorbed Dose to Survival and Response in Hepatocellular Carcinoma Treated with Transarterial Radioembolization with 90Y in the SARAH Study. Radiology 2020;296:673-684.

[22] Garin E, Tselikas L, Guiu B, Chalaye J, Edeline J, de Baere T, et al. Personalised versus standard dosimetry approach of selective internal radiation therapy in patients with locally advanced hepatocellular carcinoma (DOSISPHERE-01): a randomised, multicentre, open-label phase 2 trial. The Lancet Gastroenterology & Hepatology 2021;6:17-29.

[23] Salem R, Padia SA, Lam M, Chiesa C, Haste P, Sangro B, et al. Clinical, dosimetric, and reporting considerations for Y-90 glass microspheres in hepatocellular carcinoma: updated 2022 recommendations from an international multidisciplinary working group. Eur J Nucl Med Mol Imaging 2023;50:328-343.

[24] Lescure C, Estrade F, Pedrono M, Campillo-Gimenez B, Le Sourd S, Pracht M, et al. ALBI Score Is a Strong Predictor of Toxicity Following SIRT for Hepatocellular Carcinoma. Cancers (Basel) 2021;13.

[25] Mohammadi H, Abuodeh Y, Jin W, Frakes J, Friedman M, Biebel B, et al. Using the Albumin-Bilirubin (ALBI) grade as a prognostic marker for radioembolization of hepatocellular carcinoma. J Gastrointest Oncol 2018;9:840-846.

[26] Salem R, Johnson GE, Kim E, Riaz A, Bishay V, Boucher E, et al. Yttrium-90 Radioembolization for the Treatment of Solitary, Unresectable HCC: The LEGACY Study. Hepatology 2021;74:2342-2352.

[27] Kim E, Sher A, Abboud G, Schwartz M, Facciuto M, Tabrizian P, et al. Radiation segmentectomy for curative intent of unresectable very early to early stage hepatocellular carcinoma (RASER): a single-centre, single-arm study. The Lancet Gastroenterology & Hepatology 2022;7:843-850.

[28] Reig M, Forner A, Rimola J, Ferrer-Fàbrega J, Burrel M, Garcia-Criado Á, et al. BCLC strategy for prognosis prediction and treatment recommendation: The 2022 update. Journal of Hepatology 2022;76:681-693.

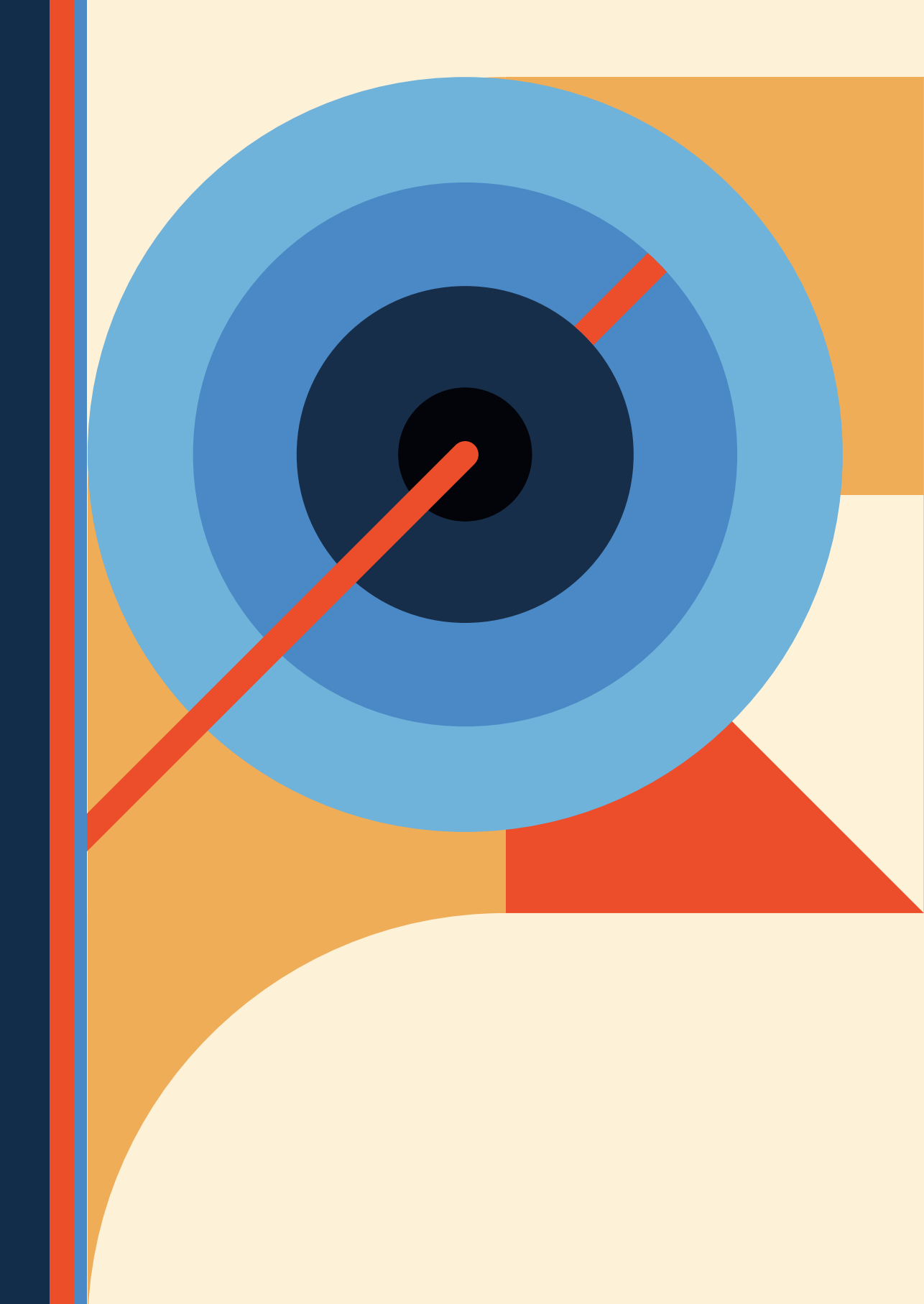

Appendices

NEDERLANDSTALIGE SAMENVATTING

In dit proefschrift worden de resultaten weergegeven van onderzoek naar minimaal invasieve behandelingen van hepatocellulair carcinoom (HCC) bij patiënten voor wie een operatie volgens de richtlijn de beste behandeling zou zijn, maar dit vanwege hun onderliggende leverziekte niet kunnen ondergaan.

HCC is een kwaadaardige levertumor die ontstaat vanuit de meest voorkomende levercellen (hepatocyten). Wereldwijd neemt HCC een 6e plaats in op de lijst van meest gediagnosticeerde soorten kanker en staat het op plaats 4 van meest voorkomende kanker-gerelateerde doodsoorzaken. HCC ontstaat meestal binnen de context van chronische levercirrose, die veelal veroorzaakt wordt door hepatitis B of C, alcohol-gerelateerde leverziekte, of leververvetting. In Nederland werden er in 2021 800 patiënten gediagnostiseerd met HCC, wat een verdubbeling was ten opzichte van 2008. Deze stijging in incidentie wordt voornamelijk toegeschreven aan de vergrijzende bevolking. Implementatie van screeningsprogramma's bij patiënten met levercirrose heeft geleid tot een verbeterde detectie van HCC in een vroeg stadium, en daarmee betere behandeluitkomsten. Echter, aangezien de onderliggende levercirrose ongeneeslijk blijft, wordt de oorzaak van HCC hiermee niet aangepakt en is er risico op de ontwikkeling van nieuwe tumoren na initiële behandeling.

Interventie-oncologische, of minimaal invasieve therapieën spelen een belangrijke rol in de behandeling van HCC. Voor HCC tumoren tot en met 2 cm wordt er volgens de behandelrichtlijnen gekozen voor thermale ablatie. Bij deze behandeling wordt er een naald rechtstreeks in de levertumor geplaatst, onder beeldsturing van echografie of CT. Het uiteinde van deze naald kan door middel van radiogolven of microgolven hitte opwekken waardoor de tumor wordt weggebrand. Deze behandeling wordt onder narcose of diepe sedatie uitgevoerd en vaak kan een patiënt de volgende dag al naar huis.

In het geval van één enkele grotere tumor (>2 cm), of maximaal 3 tumoren van elk maximaal 3 cm bestaat er een grotere kans op onvolledige behandeling na thermale ablatie en heeft chirurgische behandeling vaak de voorkeur. Echter brengt een operatie bij patiënten met onderliggende levercirrose en portale hypertensie een verhoogd complicatierisico met zich mee en wordt er daarom alsnog vaak gekozen voor een minimaal invasieve behandeling. Thermale ablatie wordt in de regel gekozen bij patiënten met tumoren tot een maximale grootte van 3 cm. Bij grotere tumoren wordt er vaak gekozen voor transarteriële chemo-embolisatie (TACE) of transarteriële radio-embolisatie (TARE), of een combinatie van ablatie met TACE. Bij TACE en TARE wordt er onder röntgendoorlichting vanuit de liesslagader met een katheter en voerdraad genavigeerd naar de leverslagader, alwaar kleine chemotherapie-houdende bolletjes of radioactieve bolletjes worden geïnjecteerd in een deel van de lever.

HCC tumoren hebben de eigenschap dat zij voornamelijk slagaderlijk worden voorzien van bloed, in tegenstelling tot gezond leverweefsel dat zijn bloed voornamelijk vanuit de poortader ontvangt. TACE en TARE maken gebruik van dit fysiologische verschil, waardoor de bolletjes hoofdzakelijk in de tumor terecht komen en slechts beperkt in het overige leverweefsel.

Het voornaamste doel van dit proefschrift was om de interventie-oncologische behandelingen te verbeteren voor HCC patiënten. *Deel 1* van dit proefschrift richt zich op de optimalisatie van thermische ablatietechnieken, met als uiteindelijke doel hun effectiviteit bij de behandeling van HCC tumoren >2 cm te verbeteren. In *Deel 2* worden minimaal invasieve combinatietherapieën bestudeerd, gericht op de behandeling van HCC tumoren van 2 tot 5 cm. Ten slotte is *Deel 3* gericht op de langetermijnresultaten na behandeling van HCC met TARE.

Deel 1: Thermale ablatie; reproduceerbaarheid en ablatiemarges

In *Hoofdstuk 2* wordt een vergelijkende studie beschreven waarin twee commercieel verkrijgbare microwave ablatie (MWA) systemen met elkaar werden vergeleken ten aanzien van de afmetingen en sfericiteit van de gecreëerde ablatiezones. De experimenten werden uitgevoerd in ex-vivo varkenslevers die na ablatie gescand werden op een MRI-scanner met hoge veldsterkte. Er werden verschillen gevonden in ablatiegrootte en sfericiteit tussen de twee MWA-systemen bij vergelijkbare instellingen. De ablatieholtes van het Emprint-ablatiesysteem waren consistenter en voorspelbaarder bij herhaalde metingen. Consistentie en voorspelbaarheid in ablatiegrootte en -vorm zijn van groot belang voor nauwkeurige behandelplanning en daarmee uiteindelijk het voorkomen van lokale recidieven.

Betrouwbare bevestiging van volledige tumorablatie op basis van de post-therapeutische CT-scans is cruciaal om lokale tumorrecidieven te voorkomen. *Hoofdstuk 3* geeft een uitgebreid overzicht van de bestaande literatuur over methoden voor kwantificatie van ablatiemarges. In totaal werden er 75 studies opgenomen in de systematische review, waarvan 58 klinische onderzoeken. In de meeste klinische onderzoeken werd er gestreefd naar een minimale ablatiemarge van ≥ 5 mm, wat in overeenstemming is met internationale behandelrichtlijnen. Van alle studies gebruikten er 21 co-registratiesoftware voor de kwantificatie van minimale ablatiemarges, waarbij rigide en niet-rigide registratietechnieken voor de fusie van pre- en post therapeutische scans ongeveer even vaak werden toegepast. De meeste studies maakten hierbij gebruik van semiautomatische segmentatietools. Ook werden er tien studies opgenomen die weefselkrimp na thermische ablatie onderzochten, waarbij de mate van weefselkrimp in de studies aanzienlijk uiteenliep. Het overgrote deel van de beschikbare data komt uit retrospectieve studies. Er is dan ook behoefte aan prospectieve studies naar het verband tussen ablatiemarges en het ontstaan van lokale recidieven.

Hoofdstuk 4 omvat een retrospectieve studie waarin ablatiemarges werden gekwantificeerd met behulp van commercieel verkrijgbare, niet-rigide regisratiesoftware, in 25 HCC patiënten die behandeld werden met thermale ablatie. De beeldregistratie tussen pre- en post-ablatie beeldvorming was in 7/25 patiënten van onvoldoende kwaliteit voor verdere analyse. Bij 8/18 overige patiënten werden lokale recidieven gevonden, waarbij een correlatie werd gevonden tussen negatieve ablatiemarges en het optreden van lokale tumorprogressie. De gemiddelde minimale ablatiemarge was -8,44 mm (SD 4,27) in de groep patiënten die lokale recidieven ontwikkelden, tegenover -0,30 mm (SD: 2,00) in de groep patiënten bij wie dit niet optrad. Er werden geen recidieven gevonden bij patiënten met een minimale ablatiemarge >0 mm. Vanwege de retrospectieve aard van de studie en verschillen in patiëntpositionering tussen diagnostische beeldvorming en behandeling, konden initieel slechts 25/78 patiënten geïncludeerd worden. Gesteund door de bemoedigende resultaten werd de IAMCOMPLETE studie ontworpen om de beperkte toepasbaarheid van ablatiemarge kwantificatie te verbeteren.

In de IAMCOMPLETE studie werd een gestandaardiseerd CT-scanprotocol onderzocht waarbij HCC patiënten tijdens hun ablatieprocedure voorafgaand en na ablatie gescand werden terwijl zij onder narcose waren (eerder gebeurde dit enkel na ablatie). Hierbij werd de beademingstube voor korte tijd losgekoppeld om een ademstop in te lassen en een zo identiek mogelijke positionering van de lever voor en na ablatie te bewerkstelligen. *Hoofdstuk 5* beschrijft de resultaten van de 20 proefpersonen (man: n=13; gemiddelde leeftijd: 67,1 ± 10,8 [SD]; Child-Pugh A: n=12, B: n=8; BCLC very early: n=8, early: n=12, intermediate: n=2). Bij 16/20 patiënten (80%) en bij 84% van alle tumoren leidde dit scanprotocol tot succesvolle beeldregistratie die het mogelijk maakte om de ablatiemarges te kwantificeren. Tumorintekeningen werden gedaan door twee radiologen. Tussen hen werd er een grote overeenstemming gevonden, en ook bij herhaalde intekening van eenzelfde radioloog kwamen de intekeningen nauwkeurig overeen, met 'dice similarity coëfficiënten' van respectievelijk 0.815 en 0.830. Er werd een gemiddelde minimale ablatiemarge gevonden van 0.63 mm (SD: 3,.589). Bij twee tumoren traden er lokale recidieven op, met een gemiddelde minimale ablatiemarge van -4.0 mm. In deze studie werd het optreden van weefselkrimp vermoed, gezien bij slechts 2/9 laesies met een negatieve minimale ablatiemarge daadwerkelijk een lokaal recidief HCC ontstond binnen één jaar.

Deel 2: Behandelcombinaties voor early stage HCC

Patiënten met HCC tumoren 2-5 cm worden vaak behandeld met gecombineerde thermale ablatie en TACE indien zij niet in aanmerking kwamen voor een chirurgische behandeling. In *Hoofdstuk 6* worden de resultaten beschreven van 38 patiënten (man: 34; mediane leeftijd 68.5 (range: 40-84); levercirrose: 33; BCLC early stage HCC: 21, intermediate stage:

17, adjuvante TACE: 27, neoadjuvante TACE: 11) die deze behandelcombinatie ondergingen in het LUMC of Amsterdam UMC locatie AMC. De mediane tijd tot tumorprogressie was 23.6 maanden bij patiënten die behandeld werden met neoadjuvante TACE (voorafgaand aan de ablatie) vs 8.1 maanden na adjuvante TACE (na ablatie) (p = 0.19). Hoewel er geen significant verschil werd gevonden, suggereren de data dat neoadjuvante TACE leidde tot betere lokale ziektecontrole. Dit komt overeen met de behandelvolgorde die tegenwoordig het meest wordt toegepast in de klinische praktijk. De mediane overleving van de totale groep was 52.7 maanden en hierbij werd er geen verschil gevonden tussen de verschillende behandelvolgordes.

Hoofdstuk 7 beschrijft het onderzoeksprotocol van de HORA EST HCC studie. In deze multicenter dosisescalatie cohortstudie werden patiënten met HCC tumoren van 2-5 cm behandeld middels een combinatie van thermische ablatie en adjuvante holmium-166 TARE. De rationale achter dit onderzoek was dat er hyperemie ontstaat in het weefsel direct rondom een ablatieholte, waarbij de verhoogde arteriële weefselperfusie ertoe leidt dat de radio-embolisatie bolletjes hierin ophopen. Dit weefsel direct rondom de ablatieholte correspondeert tevens met de locatie waarin de hoogste kans bestaat op het ontstaan van een lokaal recidief na ablatie, onder andere omdat zich daar micrometastasen kunnen bevinden. Uiteindelijk zou adjuvante behandeling in dit gebied kunnen leiden tot een gereduceerd risico op recidieven. Het doel van de HORA EST HCC studie was om te bepalen aan welke stralingsdosis het behandelvolume blootgesteld zou moeten worden om een geabsorbeerde stralingsdosis van tenminste 120 Gy te bewerkstelligen in het doelvolume (een rand van 1 cm rondom de ablatieholte).

De resultaten van de HORA EST HCC studie worden gepresenteerd in *Hoofdstuk 8*. Twaalf patiënten werden behandeld met thermische ablatie en holmium-166 TARE (mannen: 10; mediaan leeftijd: 66,5 (IQR [64,3-71,7]); mediane tumordiameter: 2.7 cm (IQR [2,1-4,0])). Er werd ophoping van de radio-embolisatie bolletjes waargenomen in het doelvolume. Na 2 patiënten die met 60 Gy holmium-166 waren behandeld werd de dosis verhoogd naar 90 Gy voor alle daaropvolgende patiënten, omdat er nog onvoldoende stralingsdosis in het doelgebied terecht kwam. In het cohort met een toedieningsdosis van 90 Gy werd het eindpunt behaald met een mediaan geabsorbeerde dosis van 138 Gy (IQR: [127-145]). Er traden geen lokale recidieven op binnen een jaar na behandeling bij alle 12 studiepatiënten.

Deel 3: TARE buiten early stage HCC

Tot slot worden in *Hoofdstuk 9* de langetermijnresultaten na TARE beschreven van een retrospectieve cohort studie van HCC patiënten uit drie Nederlandse academische ziekenhuizen. Hierbij werd er in het bijzonder gekeken naar patiënten zonder manifestatie van stralings-geïndiceerde leverziekten (REILD) na de behandeling. In totaal werden er 85

patiënten geïncludeerd, waarvan er 16 REILD ontwikkelden. Van de 69 overige patiënten ontwikkelden er 38 leverdecompensatie gedurende de follow-up. Er werd een verschil gevonden in mediane overleving tussen patiënten die in de follow-up leverdecompensatie ontwikkelden en patiënten die dit niet ontwikkelden: 16 versus 31 maanden. Ten opzichte van een case-matched controlegroep van patiënten die behandeld werden met sorafenib systeemtherapie trad er vaker leverdecompensatie op na TARE. Wel was de mediane overleving na TARE langer: 16 vs 8 maanden. De Albumine-Bilirubine (ALBI) score was een onafhankelijke voorspellende factor voor het ontstaan van leverdecompensatie en voor overleving.

Concluderend draagt dit proefschrift bij aan een verbeterde en meer betrouwbare inzet van minimaal invasieve therapieën bij early stage HCC patiënten. Het onderzoek naar ablatiemarge kwantificatie in dit proefschrift toont aan dat de inzet van beeldregistratie grote potentie heeft om lokale tumorrecidieven te voorkomen. Grotere prospectieve studies, zoals de multicenter PROMETHEUS studie waar het LUMC coördinator van is, zullen moeten uitwijzen hoe de kwantitatieve uitkomstwaarden zoals de minimale ablatiemarge precies geïnterpreteerd zouden moeten worden. Omdat er toenemend wetenschappelijk bewijs is over de superieure voorspelbaarheid van lokale recidieven bij gebruik van beeldregistratie ten opzichte van het naast elkaar beoordelen van diagnostische beeldvorming en post-ablatie CT-scans, zou dergelijke software nu al van klinische meerwaarde zijn in de dagelijkse praktijk. In de HORA EST HCC studie is er aangetoond dat de combinatie van ablatie en TARE technisch mogelijk en veilig is. De combinatie van geoptimaliseerde ablatie en verbeterde combinatiebehandelingen hebben de potentie om uiteindelijk de effectiviteit van chirurgische resectie te evenaren, ook voor grotere early-stage HCC tumoren, maar met lager risico op complicaties, lagere kosten, minder personele inzet en minder verlies van kwaliteit van leven.

CURRICULUM VITAE

Pim Hendriks was born on the 17th of May 1994 in Vianen, the Netherlands. In 2011 he graduated from high school at Cals College Nieuwegein. In the same year he moved to Enschede where he started his bachelor Technical Medicine at the University of Twente, from which he graduated in 2014 on body composition monitoring of dialysis patients at the nephrology department of Medisch Centrum Leeuwarden. Subsequently he started his master in Technical Medicine, focussing on medical imaging and interventions. In 2015 he started a second master in Health Science from which he graduated with distinction in 2016 on his thesis entitled: *'Health economic evaluation of watch and wait policy after clinical complete response to neoadjuvant chemoradiotherapy in locally advanced rectal cancer patients'*. In 2016 he continued his technical medicine mater with internships in various departments and hospitals: Nuclear Medicine (Universtiätsklinikum Münster, Germany), Oral and maxillofacial oncological surgery (Netherlands Cancer Institute, Amsterdam), Trauma Surgery (Isala, Zwolle), and IHU institute for image-guided surgery (Strasbourg, France). During these internships he developed an interest for image guided therapies. Therefore he performed his graduation internship at the department of radiology of the Leiden University Medical Center, investigating ablation margin quantification after radiofrequency ablation of hepatocellular carcinoma.

In July 2018, Pim started his PhD research on interventional oncology treatments for early state hepatocellular carcinoma at the Leiden University Medical Center, which resulted in this thesis. During his PhD he was involved with the technical medicine program at Delft University of Technology, where he supervised and mentored interns, was part of the BSc curriculum update committee, member of the committee of professional behaviour and member of the board of studies. Moreover, he did a clinical fellowship in 2020-2022 in which he further specialized in interventional oncology. In 2023 Pim started as coordinator of 'Leiden Image Guided Therapy': a new build treatment center within the LUMC that will host the interventional radiology department, a hybrid operation room and a high turnover lounge for patients that are treated under local anaesthesia or sedation. For this project he also works closely with the Angio CT team of Philips – Image-guided therapy.

LIST OF PUBLICATIONS

Hendriks P, Rietbergen DDD, Van Erkel AR, Coenraad MJ, Arntz MJ, Bennink RJ, Braat AE, Crobach S, van Delden OM, Dibbets-Schneider P, van der Hulle T, Klümpen HJ, van der Meer RW, Nijsen JFW, van Rijswijk CSP, Roosen J, Ruijter BN, Smit F, Stam MK, Takkenberg RB, Tushuizen ME, van Velden FHP, de Geus-Oei LF, Burgmans MC & Dutch Hepatocellular and Cholangiocarcinoma Group. Adjuvant holmium-166 radioembolization after radiofrequency ablation in early-stage hepatocellular carcinoma patients: a dose-finding study (HORA EST HCC trial). Eur J Nucl Med Mol Imaging, 2024; online ahead of print. DOI: 10.1007/s00259-024-06630-z.

Hendriks P, van Dijk KM, Boekestijn B, Broersen A, van Duijn-de Vreugd JJ, Coenraad MJ, Tushuizen ME, van Erkel AR, van der Meer RW, van Rijswijk CSP, Dijkstra J, de Geus-Oei LF, Burgmans MC. Intraprocedural assessment of ablation margins using computed tomography co-registration in hepatocellular carcinoma treatment with percutaneous ablation: IAMCOMPLETE study. Diagn Interv Radiol, 2024; 105(2):57-65. DOI: 10.1016/j.diii.2023.07.002.

van Erp GCM, **Hendriks P**, Broersen A, Verhagen CAM, Gholamiankhah F, Dijkstra J, Burgmans MC. Computational Modeling of Thermal Ablation Zones in the Liver: A Systematic Review. Cancers, 2023; 15(23):5684. DOI: 10.3390/cancers15235684.

Hendriks P, Boel F, Oosterveer TTM, Broersen A, de Geus-Oei LF, Dijkstra J, Burgmans MC. Ablation margin quantification after thermal ablation of malignant liver tumors: How to optimize the procedure? A systematic review of the available evidence. Eur J Radiol Open, 2023; 11:100501. DOI: 10.1016/j.ejro.2023.100501.

de Reeder A, **Hendriks P**, Plug - van der Plas H, Zweers D, van Overbeeke PSM, Gravendeel J, Kruimer JWH, van der Meer RW, Burgmans MC. Sustainability within interventional radiology: opportunities and hurdles. CVIR Endovasc, 2023; 6(1):16. DOI: 10.1186/s42155-023-00362-1.

Faber R, Burghout K, Bijlstra O, **Hendriks P**, van Erp GCM, Broersen A, Dijkstra J, Vahrmeijer A, Burgmans MC, Mieog JSD. Three-dimensional quantitative margin assessment in patients with colorectal liver metastases treated with percutaneous thermal ablation using semi-automatic rigid MRI/CECT-CECT co-registration, Eur J Radiol, 2022; 156:110552. DOI: 10.1016/j.ejrad.2022.110552.

Hendriks P, Rietbergen DDD, Van Erkel AR, Coenraad MJ, Arntz MJ, Bennink RJ, Braat AE, Crobach S, van Delden OM, van der Hulle T, Klümpen HJ, van der Meer RW, Nijsen JFW, van Rijswijk CSP, Roosen J, Ruijter BN, Smit F, Stam MK, Takkenberg RB, Tushuizen ME, van Velden

FHP, de Geus-Oei LF, Burgmans MC & Dutch Hepatocellular and Cholangiocarcinoma Group. Study Protocol: Adjuvant Holmium-166 Radioembolization After Radiofrequency Ablation in Early-Stage Hepatocellular Carcinoma Patients—A Dose-Finding Study (HORA EST HCC Trial). Cardiovasc Inter Rad, 2022; 45:1057-1063. DOI: 10.1007/s00270-022-03162-7.

Oosterveer TTM, van Erp GCM, **Hendriks P**, Broersen A, Overduin CG, van Rijswijk CSP, van Erkel AE, van der Meer RW, Tushuizen ME, Moelker A, Meijerink MR, van Delden OM, de Jong KP, van der Leij C, Smits MLJ, Urlings TAJ, Braak JPBM, Meershoek-Klein Kranenbarg E, van Duijn-de Vreugd B, Zeijdner E, Goeman JJ, Fütterer JJ, Coenraad MJ, Dijkstra J, Burgmans MC. Study Protocol PROMETHEUS: Prospective Multicenter Study to Evaluate the Correlation Between Safety Margin and Local Recurrence After Thermal Ablation Using Image Co-registration in Patients with Hepatocellular Carcinoma. Cardiovasc Inter Rad, 2022; 45:606-612. DOI: 10.1007/s00270-022-03075-5.

Van Doorn DJ, **Hendriks P**, Burgmans MC, Rietbergen DDD, Coenraad MJ, van Delden OM, Bennink RJ, Labeur TA, Klümpen HJ, Eskens FALM, Moelker A, Vegt E, Sprengers D, Mostafavi N, IJzermans J, Takkenberg RB. Liver Decompensation as Late Complication in HCC Patients with Long-Term Response following Selective Internal Radiation Therapy. Cancers, 2021; 13(21)5427. DOI: 10.3390/cancers13215427.

Hendriks P, Sudiono DR, Schaapman JJ, Coenraad MJ, Tushuizen ME, Takkenberg RB, Oosterveer TTM, de Geus-Oei LF, van Delden OM, Burgmans MC. Thermal ablation combined with transarterial chemoembolization for hepatocellular carcinoma: What is the right treatment sequence?, Eur J Radiol, 2021; 144(1)110006. DOI: 10.1016/j.ejrad.2021.110006.

Hendriks P, Berkhout WEM, Kaanen CI, Sluijter JH, Visser IJ, van den Dobbelsteen JJ, de Geus-Oei LF, Webb AG, Burgmans MC. Performance of the Emprint and Amica Microwave Ablation Systems in ex vivo Porcine Livers: Sphericity and Reproducibility Versus Size. Cardiovasc Inter Rad, 2021; 44:952-958. DOI: 10.1007/s00270-020-02742-9.

Burgmans MC, **Hendriks P**, Rietbergen DDD. Does a Widely Adopted Approach Need Reconsideration: Embolization of Parasitized Extrahepatic Tumor Feeders in Patients Undergoing Transarterial Liver-Directed Therapy? Cardiovasc Inter Rad, 2020; 43:1103-1104. DOI: 10.1007/s00270-020-02478-6.

Hendriks P, Noortman WA, Baetens TR, van Erkel AE, van Rijswijk CSP, van der Meer RW, Coenraad MJ, de Geus-Oei LF, Slump CH, Burgmans MC. Quantitative Volumetric Assessment of Ablative Margins in Hepatocellular Carcinoma: Predicting Local Tumor Progression Using Nonrigid Registration Software. J Oncol, 2019; (5):1-8. DOI: 10.1155/2019/4049287

Sibinga Mulder BG, **Hendriks P**, Baetens TR, van Erkel AR, van Rijswijk CSP, van der Meer RW, van de Velde CJH, Vahrmeijer AL, Mieog JSD, Burgmans MC. Quantitative margin assessment of radiofrequency ablation of a solitary colorectal hepatic metastasis using MIRADA RTx on CT scans: a feasibility study. BMC Med Imaging, 2019; 19(1):71. DOI: 10.1186/s12880-019-0360-2

DANKWOORD

Belangrijke ingrediënten voor dit proefschrift waren de fijne samenwerkingen, onvergetelijke schrijfweken en een dosis gezelligheid. Ik wil graag van deze gelegenheid gebruikmaken om een aantal mensen in het bijzonder te bedanken.

Prof. dr. L.F. de Geus-Oei, beste Lioe-Fee, al sinds mijn afstuderen van gezondheids-wetenschappen in 2016 ben je een mentor voor me. Heel veel dank voor alle kansen en motivatie die je mij gedurende deze tijd hebt gegeven en natuurlijk voor je betrokken begeleiding.

Dr. M.C. Burgmans, beste Mark, jouw energie en positiviteit werken erg aanstekelijk en daarmee heb je mij altijd aangemoedigd voor mijn onderzoek en ontplooiing daarbuiten. Ontzettend bedankt voor je bevlogen begeleiding en alle kansen die ik dankzij jou in het LUMC heb gekregen.

Prof. dr. M.J. Coenraad, beste Minneke, tijdens het zorgpad primaire levertumoren op vrijdagochtend heb ik veel van mijn kennis over HCC opgedaan. Ik heb onze samenwerking erg prettig gevonden en vind het leuk dat ik je hier mag bedanken als lid van mijn promotieteam: heel erg bedankt.

Heel veel dank ook aan alle studiepatiënten die hebben deelgenomen aan de HORA EST HCC en de IAMCOMPLETE studies en daarmee de kern vormden van dit proefschrift.

Veel dank aan alle collega's van de interventieradiologie voor de fijne samenwerking: Carla, Arian, Rutger, Jacob, Dominique, alle laboranten en de administratie.

Bianca en Gerda: bedankt voor de ondersteuning van de studies, hulp bij data invoer, maar ook voor het bieden van een plek om mijn hart te luchten over alle onderzoeksbureaucratie, en natuurlijk voor al het snoep dat er altijd bij jullie op de kamer te vinden is.

Onderzoek doen is ontzettend leuk, maar de collega's van 'the Corner Office' (en alle tijdelijke kantoorruimten die volgden) en van de interventieradiologie op C5-52 maakten het tot een feest. Veel dank aan Wyanne, Willem, Joeri, Dennis, Lisanne, Karin, Alina, Hanneke, Timo, Maaike, Fleur, Marijn, Sietse, Ylva, Gonnie, Coosje, Vesna en Faeze voor de research meetings, schrijfweken, tripjes naar Antwerpen, Texel en Oxford, het congres in Kopenhagen en vooral de muzikale hoogtepunten in stamkroeg Cafe 't Centrum van Melzen!

Onderzoek is het allerleukst op het snijvlak met patiëntenzorg en onderwijs. Ik heb genoten van alle nevenprojecten: het één aanpalend aan mijn onderzoek, het ander stond er juist wat verder vanaf. Ik wil daarom iedereen van de afdeling radiologie en nucleaire geneeskunde bedanken met wie ik heb samengewerkt. Veel dank aan alle studenten die met hun projecten bijdragen leverden aan het onderzoek: ik hoop dat jullie minstens zoveel geleerd hebben van mij als ik van jullie! Ook veel dank aan de curriculumcommissie, met in het bijzonder Tanja en Pleun: ik heb veel opgestoken van de werksessies, het onderwijskundig perspectief en de voor mij nieuwe werkwijzen. Daarnaast wil ik de TG fellows intervisiegroep bedanken voor de fijne bijeenkomsten in Amersfoort. Ook veel dank aan de Philips collega's voor hun interesse in mijn promotieonderzoek.

Heel veel dank ook aan alle vrienden voor het samenzijn met etentjes, borrels, wandelingen, sporten samen op vakantie, of juist klussend in nieuwe huizen. Ik prijs me rijk met zulke fijne mensen om me heen die me inspireren, mij een luisterend oor kunnen bieden, waar ik goede gesprekken mee kan hebben, maar ook juist mee kan lachen!

Bovenal wil ik mijn (schoon)familie heel erg bedanken. Lieve Sjoerd en Nienke, ik ben heel blij om mijn proefschrift te mogen verdedigen met jullie aan mijn zijde als paranimf. Heel erg bedankt voor jullie betrokkenheid bij mijn promotie en bij alles ver daar buiten. Ik ben ontzettend blij met onze goede broers-zus band! Lieve pap en mam, heel erg bedankt voor de onvoorwaardelijke liefde, steun en alle kansen die jullie me geboden hebben. Van jullie heb ik geleerd dat nieuwsgierigheid, hard werken, een goede planning, en een gezonde dosis humor belangrijke ingrediënten zijn in het leven. Een basis die mij ook tijdens het promotietraject zeker heeft geholpen!

Lieve Isabeau, mijn tijd in het LUMC is ook onlosmakelijk verbonden aan jou, en je hebt de afgelopen jaren nog heel veel mooier gemaakt. Samen met jou zijn is mijn grootste geluk en ik kijk uit naar hetgeen de toekomst ons brengt!